Fingerprinting Quaternary Subglacial Processes on Hall Peninsula, Baffin Island, using Multiproxy Data

by

Cassia Lynn Johnson

A thesis

presented to the University of Waterloo

in fulfilment of the

thesis requirement for the degree of

Master of Applied Science

in

Earth Sciences

Waterloo, Ontario, Canada, 2014

Author's Declaration

I hereby declare that I am the sole author of this thesis. This is a true copy of the thesis, including any required final revisions, as accepted by my examiners.

I understand that my thesis may be made electronically available to the public.

Abstract

It is important to study subglacial environments in northern Canada for many reasons, such as to develop a more comprehensive understanding of glacial landscape development and to aid in mineral exploration. The purpose of this research is improve understanding of the Quaternary geology of north central Hall Peninsula, Baffin Island, the subglacial dynamics record in particular, in order to provide industry with new knowledge, maps and interpretations to aid in mineral exploration. The glacial history of north-central Hall Peninsula, Baffin Island is very complex. By studying the subglacial landscape using both remote- and field- based techniques it was possible to develop a subglacial landscape map and a flowset map which highlighted areas with different glacial histories and basal thermal regimes. The subglacial dynamics and how they changed spatially and temporally shaped the landscape to what it is today with a mixture of cold, intermediate, and warm-based ice.

Through mapping using remote sensing and field methods, seven glacial landform and striation directions were found and grouped into four ice flow events. The identified ice flows include regional flows, northern and eastern fjord influenced areas, central deglacial flows, and modern icecap flows. Subglacial erosion was investigated using several proxies including streamlined hill elongation ratios, streamlined hill density, and bedrock controlled lake density studies. These proxies together with the subglacial landscape map were overlaid to select discrete zones, termed glacial terrain zones (GTZs), in an attempt to analyze the subglacial dynamics and how different basal thermal regimes interacted with the landscape.

Five glacial terrain zones (GTZs) were identified, with different spatio-temporal basal ice regimes and landform assemblages. The first zone (GTZ 1) is characterized by an expansive flowset of parallel paleo-flow indicators trending northeast. This zone has the highest degree of areal scour with thin, discontinuous and relatively unweathered till. The second zone, GTZ 2, is an area where the broad northeast flowset is crosscut locally by ice flow indicators that converge into troughs that now form a series of north trending fjords in the north of the study area. This overprinted landscape is found to propagate inland forming a channelized system, leading way to linear erosion. The modern icecap resides in GTZ 3, which inherited the broad northeast flowset, but is overprinted in valleys by eastern flows funneling into the fjords to the east, as well as

western flows flowing from the modern icecap. In the central area, there is a rolling terrain of thicker till (GTZ 4) that is distinguished by its lack of subglacial features. The final contrasting landscape (GTZ 5) is characterized by southeast trending bedrock features (most likely enhanced by southeast flowing ice) and associated perpendicular moraines. GTZ 5 is also characterized by highly weathered bedrock, and locally by landform assemblages recording late deglacial readvances of thin lobes including moraines and striated outcrops.

Geochemical studies for each of these landscapes lead to additional insights, characterizing the five zones further. The geochemical studies took advantage of two till sample databases taken over the study area for exploration purposes by Peregrine Diamonds LTD. The chemical index of alteration (CIA) was applied to compare erosion in the different zones. High CIA values indicate high weathering, where low CIA values low weathering. GTZ 1 is characterized by low CIA values (low weathering footprint), and GTZ 5 is characterized by high CIA value (highly weathered). To study if the GTZs had a distinct geochemical signature, as well as a signature landscape, multivariate geochemical statistics (Principal Component Analysis and Linear Discriminant Analysis) were done over the study area. Interestingly, it was found that the GTZs have geochemical signatures, which reflect the role of underlying bedrock, weathering patterns, glacial dispersal, and the complex relationships between subglacial dynamics and landscape evolution. To determine if the GTZs could be predicted by the till geochemistry, linear discriminant analysis was subsequently applied. The results indicate that the till geochemical data has a predictive capacity with an accuracy of 83.78%, which brings insight into the relationship between glacial landscapes and till composition.

With this multi-proxy approach and building from previous studies, a conceptual model was developed for the study area. During the Last Glacial Maximum (LGM), the study area was inundated by the Laurentide Ice Sheet (LIS), with the Hall Ice Divide parallel to the axis of the peninsula with ice flowing from the divide to the northeast and southwest. As ice thinned, GTZ 1, an area once inundated with warm-based ice, as shown by evidence of areal scour and low CIA values, switched to being cold-based ice preserving an older landscape. Though GTZ 1 was under cold-based ice, warm-based conditions still prevailed within the channelized flow zones, which characterize GTZ 2. Evidence of this is found in the striation record, as well as the low

CIA value indicative of low weathering (or high erosion). This may reflect a transition from LGM (thick-based ice) to thinner, topographically controlled ice, with cold-based ice in interfluves and hilltops, during early deglaciation. The catchment zones of the channelized system locally extend near the central area (GTZ 4) which is reflected in dispersal patterns and the striation record. As the LIS retreated, it went through a series of southeastward readvances and surges (GTZ 5). Though the ice was warm-based near the moraines in GTZ 5, prevailing cold-based conditions prevailed during most of the last glacial cycle, and the late deglacial readvances had limited erosion capacity and did not overprint the cold-based landscape significantly. This is shown by the CIA values indicative of high weathering, and lack of subglacial landforms. Series of pro-glacial lakes also formed in front of the retreating lobe. Ice is needed over GTZ 1 to prevent these lakes from draining northward. This thin ice was most likely cold-based, preserving the older GTZ 1 landscape of areal scouring.

The glacial landscape of Hall Peninsula appears to record a switch from uniform warm-based LGM ice, which was laterally extensive, to localized channel flows in the fjords during deglaciation and intervening cold-based ice. The change in the geometry and basal thermo-mechanical conditions may be the prologue to the separation of the modern day ice cap from the LIS.

Acknowledgements

The project was funded through a Collaborative Research and Development (CRD) grant from the Natural Sciences and Engineering Research Council **(**NSERC) and Peregrine Diamonds LTD to Professors M. Ross (UW) and J.C. Gosse (Dalhousie). Natural Resources Canada (NRCan) and the Canada-Nunavut Geoscience Office (CNGO) provided financial support through the Research Affiliate Program (RAP). Thank you to Peregrine Diamonds LTD for providing all the field logistical support. Several other people also helped in the field including Peregrine staff and Inuit bear monitors and field assistants from Pangnirtung and Iqaluit. I would particularly like to thank the bear monitor Ray Pameolik Ell. I would also like to thank Tommy Tremblay for his expertise in the Quaternary Geology of Hall Peninsula.

I would also like to acknowledge my committee members Dr. Martin Ross, Dr. Jennifer Pell, Dr. Eric Grunsky, and Dr. Isabelle McMartin. I would like to thank my committee for the essential review of my thesis. This thesis was made possible by Dr. Martin Ross's teaching, guidance, and mentorship. I would like to thank Dr. Martin Ross the thesis design, and helping with data interpretation. Dr. Jennifer Pell provided in depth mineral exploration knowledge of the study area expertise which was essential to my thesis. Dr. Eric Grunsky guidance through the statistics portion of my thesis is greatly appreciated. And finally, I would like thank Dr. Isabelle McMartin for sharing her expertise in Quaternary Geology.

I would also like to acknowledge the Quaternary Sciences lab group for their support. Thanks toTyler Hodder for dedicating his undergraduate thesis work on the subglacial erosion index. I would like to give gratitude to Dr. Michelle Trommelen for her guidance. I would also like to thank Ulanna Wityk and Lisa Atkinson for their support and awesomeness.

Lastly, I would like to thank all of the friends I have met during my MSc. Thanks Priscilla, Gerald, Jill, Kelly, Julia and Taylor for being such wonderful house mates. Thanks Lisa, Ryan, Jon and Jess for showing me Ontario. Thank you to Jutta, Lionel, Orin and Heather for GH adventures and more. Thank you mi Mariano for making me smile, quesadillas, my spot, and

for all of the fun and adventures. Te amo. Thank you Ulanna, Lisa, Jen, Pris, Kelly, Eric, Joel, Taylor, Lionel, Sean, Jason, Maddy, Jutta and Mariano for being my family away from home.

Dedication

I would like to dedicate my thesis to my mom, dad, sister, and Grandma Elaine for supporting and encouraging me in my academic endeavours. I would also like to dedicate this to my friends who share a love for science and adventure, in particular my lab group: Ulanna, Lisa, Michelle, Tyler, Ros, Aaron, and Danielle.

Table of Contents

List of Figures

List of Tables

List of Equations

Chapter 1 : Introduction

1.1 Subglacial Landscape of Baffin Island

Canada has been affected by several glaciations in the Earth's recent history (Ehlers and Gibbard 2004), which can be seen in the vast landscape made up of features and materials alluding to its glacial origin. Different parts of Canada were shaped by glaciations to varying degrees. Baffin Island, in the eastern Canadian Arctic, is an area that exemplifies the many ways past glaciations have shaped the landscape (Figure 1.1). The variations in subglacial conditions, whether warm-based (temperatures above the pressure-melting point) or cold based (temperatures below the pressure-melting point), influence subglacial erosion intensity, landform development, and overall glacial landscape evolution through glaciations (Trommelen et al. 2012; Greenwood and Clark 2009; Stokes et al. 2009). The past subglacial conditions can therefore be understood by studying the subglacial landform record (Kleman et al. 2001; Kleman et al. 2010). Baffin Island was covered in cold-based ice for extended periods of time during the Quaternary Period, leading to a terrain of limited glacial erosion, extensive regolith, thin till, and bedrock controlled features (Andrews 1989; Dyke et al. 2002; De Angelis and Kleman 2007). There are fewer areas of Baffin Island where wet-based conditions existed, creating a variety of landforms, complex till sheets and abundant sediment transport patterns (Andrews 1989; Dyke et al. 2002; De Angelis and Kleman 2007; Refsnider and Miller 2010). Due to the temporal and spatial mix of cold- and warm-based ice, Baffin Island has diverse landscapes ranging from terrain which appears to not be affected by glacial erosion to areas drastically sculpted by dynamic ice. There are areas that show inheritance (relict surfaces, older ice-flow indicators, contrasting orientations, old sediment dispersal train directions etc.) and areas that show more intense overprinting by young events which partly or completely obliterated the glacial record of previous events (Trommelen et al. 2012). Because of its geographical location, Baffin Island contains records of landscape evolution over the last glacial cycle, information which can be used academically and also practically for mineral exploration.

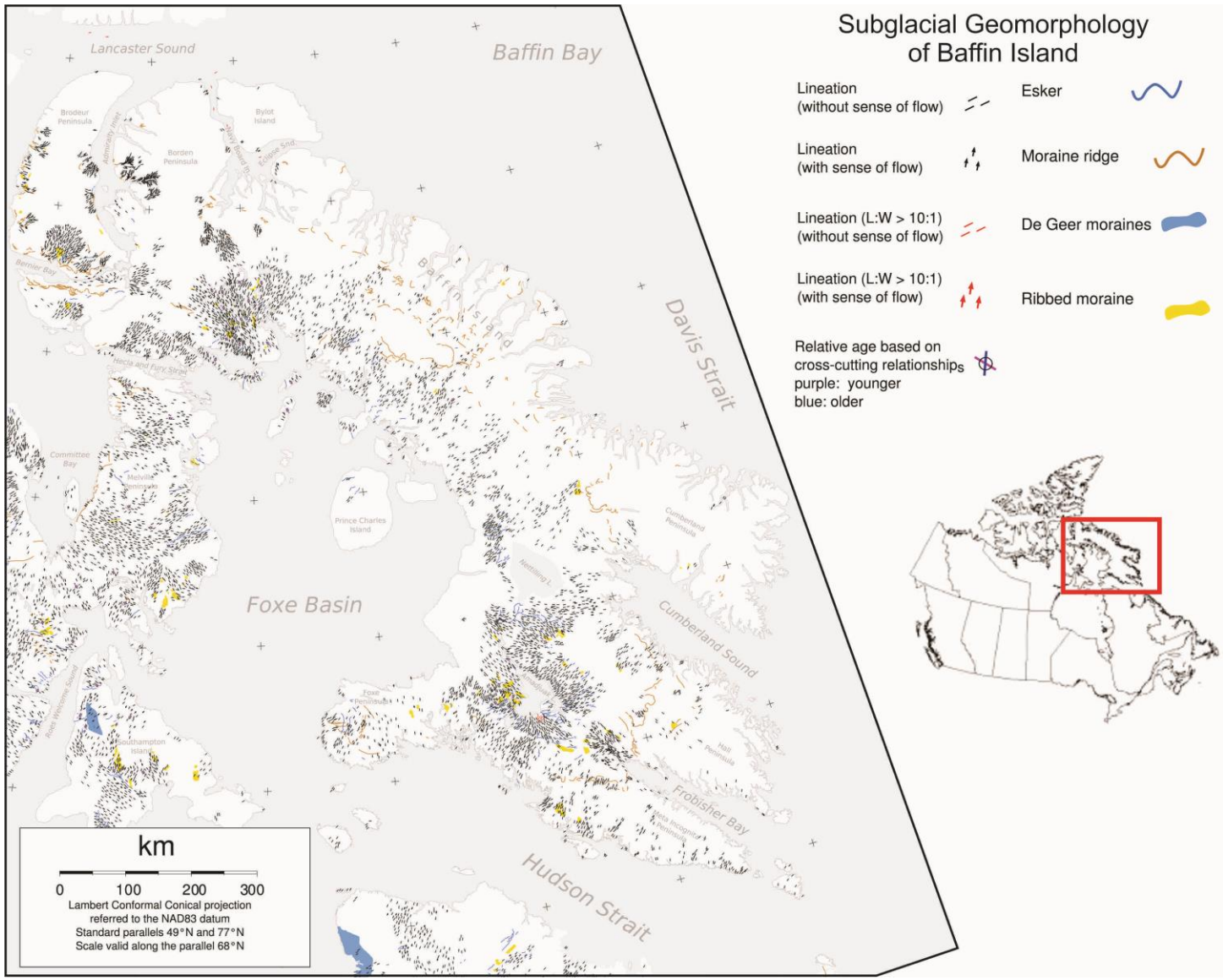

Figure 1-1: The geomorphology of Baffin Island (modified from De Angelis 2007) exemplifying the way past glaciations have shaped the landscape as they differed in time and space.

Baffin Island is the largest island in Canada, and fifth worldwide, and remains largely unexplored for mineral resources. Mineral deposits may be buried underneath glacial sediments, and they may also intersect the bedrock surface over small areas making it difficult for exploration geologists to successfully and cost-effectively vector-in these areas of economic interest. Glacial processes, in particular erosion and sediment transport at the base of glaciers, can leave a traceable signature or footprint in glacial sediment of a mineralized zone over variable distances reaching up to multitudes of kilometres (Dreimanis 1956; Dreimanis and Vagners 1971; DiLabio and Shilts 1979; Shilts 1984; Shilts 1993; Shilts 1996; McClenaghan et al. 2002; Stanley 2009). Consequently, searching for mineral indicators and geochemical pathfinders of economic interest in glacial sediments is a major exploration approach in glaciated regions such as Canada and Scandinavia (Shilts 1984; Paulen and McMartin 2009). This is especially true for diamond exploration. Diamondiferous kimberlite pipes in Canada are vertical structures whose cross-sectional diameter at the bedrock surface is generally sub-kilometre in length. However, they are mineralogically unique and have distinctive mineral and chemical signatures that can be distinguished in glacial sediments over much larger areas (McClenaghan and Kjarsgaard 2001). Consequently, the principal method in exploring for diamonds in Canada involves the search for the distinct mineral assemblages in the glacial sediments and tracing them back to their source based on information about past ice flow dynamics (McClenaghan and Kjarsgaard 2001) as well as on the geophysical signature of potential bedrock source areas. In a nutshell, glaciers have spread the breadcrumbs that lead back to the diamond sources. Drift prospecting methods have played a key role in a number of major diamond discoveries in Canada (Kong et al. 1999; Kirkley, Mogg, and McBean 2003; Rikhotso et al. 2003) such as the highly diamondiferous kimberlites in the Lac de Gras field of the Northwest Territories (Fipke et al. 1995).

In order to utilize drift prospecting methods effectively one has to understand regional glacial dynamics and the subtleties of glacial erosion, sediment production, transportation, and deposition (Klassen 2001). Lack of such knowledge often results in orphaned diamond indicator mineral anomalies in glacial sediments and can adversely affect the decision-making process in prioritizing drilling targets. New and innovative approaches that will improve the knowledge of the dynamic sedimentary and geomorphological processes and history of ice flow are thus

needed to enhance drift exploration strategies, especially in the context of diamond exploration in the Canadian Arctic.

1.2 Study Area and Research Problem

Baffin Island has three southern peninsulas, which are the Meta Incognita, Hall, and Cumberland Peninsulas (Figure 1.1). The focus of this study is north-central Hall Peninsula, Baffin Island (Figure 1.2). Field work was restricted to a smaller area than that of mapping based on remote sensing (Figure 1.2**)**. The larger area is approximately 25,400 km^2.

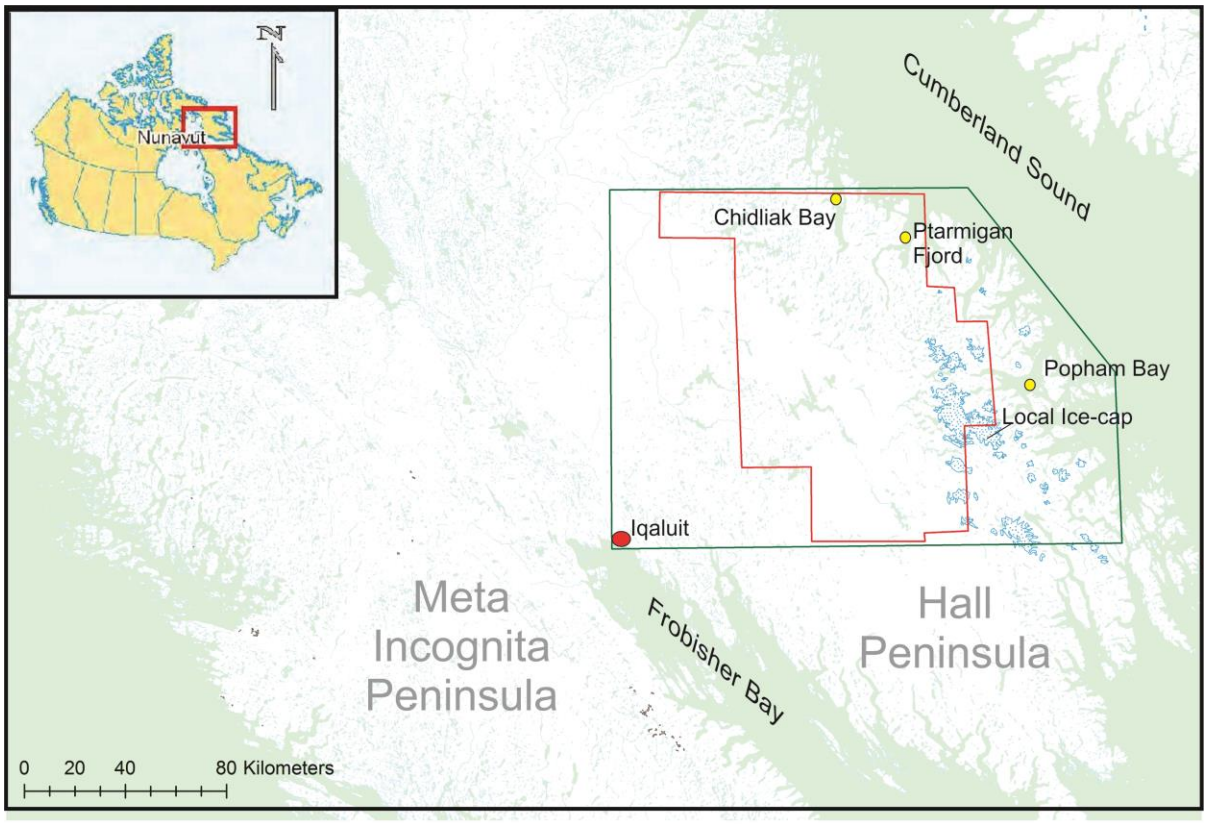

Figure 1-2: The location of the field site on Hall Peninsula, Baffin Island. Focused fieldwork is shown in the red polygon and geomorphology mapping was within the largest, green polygon.

The general goals of this master's thesis are to improve the understanding of the Quaternary Geology on Hall Peninsula through establishing glacial sediment-landform assemblages, investigating relationships with glacial erosion intensity, and determining the net effect on sediment dispersal trains; accomplishing these goals will help build the understanding of past

glacial dynamics on Hall Peninsula, which can in turn be used for research and mineral exploration.

Hall Peninsula lacks geoscience information including geological maps, data, and interpretations. As a result, our understanding of the regional geology is inadequate to meet the needs of researchers and exploration geologists.

This study area encompasses Peregrine Diamond Ltd.'s Chidliak Property. This area has been a highlight of diamond exploration in Canada for the past five years, with more than 60 kimberlites, most of them diamondiferous, being found to date (Pell 2011). The property was discovered using classical drift prospecting combined with airborne and ground-geophysics and targeted drilling surveys. The success of the property was accomplished with minimal understandings of glacial dynamics. Despite the exploration success, many of the indicators recovered from the sampling surveys exhibit extremely complex patterns at surface and some highly interesting anomalies have not been confidently linked to any of the discovered kimberlites. Questions have therefore arisen as to whether more diamondiferous kimberlites have yet to be discovered and whether interpretations about kimberlite indicator mineral (KIM) dispersal patterns are correct. Other problems have arisen as well, with potential geophysical targets appearing to not be associated with a dispersal train and with some discovered kimberlites being without clear geophysical or till compositional signatures.

This combination of complex geological and geophysical factors may hinder exploration effort and significantly raise the cost of exploration. New knowledge about glacial dynamics is critical to take full advantage of the till and geophysical database, which can in turn reduce the risk that is involved in drilling potential targets and resolve some of the unexplained KIM patterns.

1.3 Bedrock Geology

The bedrock geology of Baffin Island has only been mapped at a reconnaissance scale and more research needs to take place for it to be better understood (Pell et al. 2012). Hall Peninsula was mapped at a reconnaissance scale by Blackadar (1967) and revisited by Scott (1996). In 2006, the map was released digitally (St-Onge, Scott, and Henderson) (Figure 2-2). It has been

recognized through previous mapping efforts that Hall Peninsula is divided into three major crustal assemblages,that are (from east to west) a gneissic terrain called the Hall Peninsula Block, an intermediate belt of Paleoproterozoic metasediments and the Cumberland Batholith. (Scott 1996; Scott 1999; St-Onge et al. 2006; Whalen et al. 2010). The Hall Peninsula Block, where the kimberlites are located, consists of Achaean orthogneissic and supracrustal rocks that are approximately 2.92-2.80 Ga, and also includes tectonically reworked younger clastic rocks (Scott 1999; Pell et al. 2012). The central belt of Paleoproterozoic supracrustal rocks is a metamorphosed succession of continental margin correlated with Meta Incognita Peninsula's Lake harbour Group strata, which are <2.01 >1.90 Ga (St-Onge et al. 2006; Whalen et al. 2010). Granulite facies intracrustal granitoids make up the Cumberland Batholith, and are approximately 1.865-1.845 Ga in age (Whalen et al. 2010).

More than 60 kimberlites have been discovered between 2008 and 2012 in the study area. The placement of the kimberlites, which occur in both pipes and steeply dipping sheetsintruded into basement gneisses and overlaying Palaeozoic carbonate, spanned between between approximiately 18 Ma from to 156 Ma (Pell et al. 2012; Heaman et al. 2012). Notable base and precious metal till anomalies have been found suggesting that the area may be prospective for magmatic Ni-Cu-PGE and metamorphosed massive sulphide deposits (Pell 2011). There are two showings of native copper in the study area as well (Pell 2011).

1.5 Thesis Objectives

The main objectives of this thesis are to:

1. Characterize the subglacial geomorphology of north-central Hall Peninsula
2. Map the spatial distribution and relative intensity of subglacial erosion using various proxies
3. Investigate glacial sediment-landform relationships
4. Develop a glacial dynamics evolution model for the study area and analyse the implications within a regional context as well as for mineral exploration on Hall Peninsula

These research goals are designed to contribute to academia and industry, and will bring new insight into the Quaternary geology of north-central Hall Peninsula, which can potentially be used to augment mineral exploration strategies.

1.4 Regional Glacial History

Hall Peninsula has been included in regional studies of the Laurentide Ice Sheet (LIS) (Dyke et al. 2002) and the Quaternary Geology of the north-eastern Canadian Shield (Andrews 1989; Briner et al. 2009; De Angelis 2007; De Angelis and Kleman 2007; Miller et al. 2002; Miller et al. 2005). Few studies have focused on the peninsula itself and they mostly focus on the record of deglaciation and associated late Foxe and Cockburn Substage moraine systems (Miller 1980; Miller 1985).

During the Last Glacial Maximum (LGM), which was approximately 21 k ya, Hall Peninsula and its offshore islands were overwhelmed by ice (Dyke et al. 2002). The portion of the LIS that covered Baffin Island is referred to as the Foxe-Baffin sector, and had an area of .92 x 10 6 km ^{2} (Dredge 2001; Dyke et al. 2002; De Angelis and Kleman 2007) . The Foxe/Baffin sector of the LIS is thought to have largely drained by topographically controlled ice streams and outlet glaciers between the LGM and approximately 7.0 kyr BP (De Angelis and Kleman 2007). The Cumberland Ice Stream filled Cumberland Sound (Figure 1-1) until about 9.0 to 10 ka BP (Jennings 1993; Dyke (2004); De Angelis and Kleman 2007).

Baffin Island is dominated by a landscape reflecting varying thermal regimes as shown through bedrock erosion (Andrews 1989; Refsnider and Miller 2010). There are areas of Baffin Island that show evidence of warm-based erosive ice with areal scour, selective linear erosion, as well as little to no glacial erosion reflecting cold-based ice (Andrews 1989; De Angelis and Kleman 2005; De Angelis and Kleman 2007). During the LGM, an ice divide that paralleled the axis of the Peninsula was active from the LGM to deglaciation (Dyke and Prest 1987; Dyke et al. 2002). Marsella et al. suggest that during deglaciation, the Hall Ice Divide is thought to have run parallel to the axis of the peninsula and to have flowed away from the divide to the northeast and southwest (2000).

The ice divide over Hall Peninsula, as well as the ice streams in Frobisher Bay and Cumberland Sound, controlled ice flow in this area (Dyke and Prest 1987; Dyke et al. 2002; De Angelis 2007). The ice sheet retreated towards Foxe Basin around 8.5 kyr BP, and the ice divide on Hall Peninsula was no longer active. By between 7.0 and 6.0 kyr BP, the Foxe-Baffin sector collapsed promoting thinning ice and further retreat; in the paper presented by De Angelis and Kleman (2007) the study area is completely ice free, with the exception of the local ice cap. By 9 ^{14}C ka BP, the southern portion of the study area was ice free, and is marked by an advance/readvance of the ice sheet (Dyke 2004). The entire study area as presented by Dyke (2004) became ice free by around 7.8 ^{14}C ka BP.

De Angelis and Kleman (2007) described three types of swarms on northwestern Hall Peninsula including ice stream (convergent flow patterns), event (abundant paleo-flow indicators but no eskers) and wet-based deglaciation (directional paleo-flow indicators and aligned melt-water traces). Cold-based zones were also recognized (De Angelis and Kleman 2007). Both a northeast and southwest event were recognized in the northeast and southwest, northwest of the study area respectively, as well as active wet-based deglaciation in the southern portion around moraines. Cold-based ice was also recognized up ice from the moraines (De Angelis and Kleman 2007). It is important to note that these features were mapped and described using remote-sensing, and fieldwork needs to be done to ground-truth some of these observations.

The oldest moraine on the peninsula is the Hall Moraine (Miller 1980; Miller 1985) (Figure 1-3). It trends north-east/south-west across the high part of the Peninsula (Miller 1980; Miller 1985). The Hall Moraine is dated at 10, 760 ± 30 ^{14}C yrs BP, and thus marks a still stand of the margin of the LIS as it retreated to the northwest during the overall deglaciation of the area on Hall Peninsula and Frobisher Bay (Miller 1980; Miller 1985). Dyke et al. (2004) show the first readvance of the ice sheet at 9 ^{14}C ka BP (Hall Moraine).

To the northwest, two major moraine systems younger than the Hall Moraine (Figure 2-3) have been mapped and dated at about 8,000-9,000 ^{14}C yrs BP (the Cockburn Substage) (Miller 1980). The Frobisher Bay Moraine System (Figure 1.3) can be traced from inner Frobisher Bay and up to the north-west where the trace eventually diminishes (Miller 1980; Miller 1985). Drumlinized

till suggests that ice flowed parallel to the axis of the peninsula, flowing from the northwest to the southeast (Figure 1.3) (Miller 1980; Miller 1985). Dyke et al. (2004) suggest that the Frobisher Bay Moraine forms around 7.8 ^{14}C ka BP.

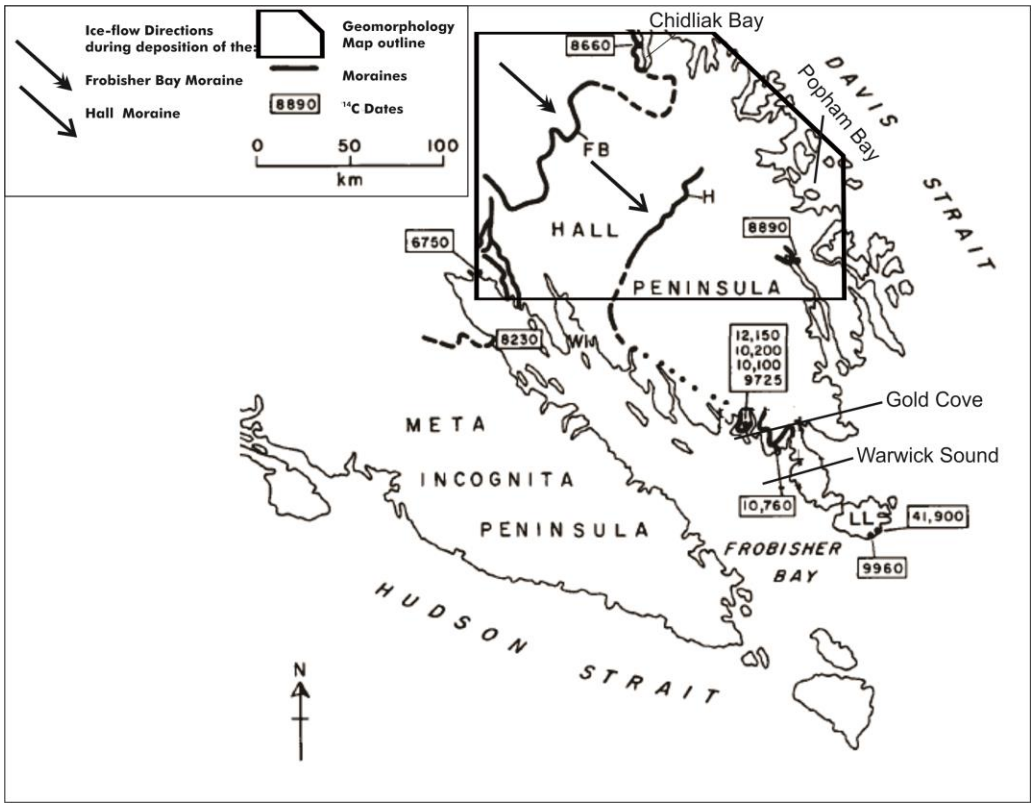

Figure 1-3: Major moraine systems of Southern Baffin Island and their respective radiocarbon ages The dashed lines indicate inferred moraine segments, and the dotted line show interpolated moraine segments. The study area (trapezoid) includes Hall Moraine (H) and Frobisher Bay Moraine (FB). The Chidliak Moraine, mapped by Miller (1985), runs parallel to the east coast and is dated at 8890 and 8660 ^{14}C yrs BP, shown next to Chidliak Bay. Figure modified from Miller (1980).

The Chidliak Moraine runs south-southeast along the east coast of Hall Peninsula to Chidliak Bay (Miller 1985). The ice that deposited this moraine flowed from the plateau of the peninsula and funnelled through the fjords and bays that line the perimeter (Miller 1985). Shell of *Hiatella Arctica* found on the moraine were dated at 8,660 ± 160 ^{14}C yrs BP (GSC-2466), which correlates to the Frobisher Bay Moraine System. East of Chidliak Bay, the drumlins have a north-east trend, which contrasts with the south-east trending features in the centre of the peninsula (Miller 1985).

Previous mapping of a local moraine inland of Popham Bay suggests that it required ice flowing from the east to west (Miller 1985). The local moraine is from the expansion of the local Hall Peninsula ice cap, located within the study area, which formed a terminal moraine that has been dated with *Hiatella* shells gathered from ice-proximal raised marine deltas. These shells yielded an age of 8,890 ±100 ^{14}C yrs (GSC-2586) which is a minimum age for the moraine (Miller 1985). This age correlates the local ice advance to the Frobisher Bay Moraine system (Miller 1985).

Other features of Hall Peninsula are glaciolacustrine shorelines, deltas and overflow channels from proglacial lake systems (Miller 1985). There are two main groups of glacial lakes, one is associated with the Hall Moraine (older) and the other is associated with Frobisher Bay Moraine system (younger) (Miller 1985). There are also well developed ice-contact/proximal deltas where the lakes are against the edge of the moraines (Miller 1985). The older lakes, south of the Hall Moraine, are at 630 m asl and drained south (Miller 1985). The younger lakes, associated with the Frobisher Bay Moraine system, also lie at 630 m asl and are traced to the Frobisher Bay Moraine along the western margin but, to the north-east, the margin is lost (Miller 1985). It has been postulated that the lake could only have existed if a thin residual ice cap remained between Cumberland Sound and the lake, blocking drainage into areas of lower elevation, such as Ptarmigan Fjord (Fig. 1-2) (Miller 1985). Moraine deposits associated to this blockage and inferred ice cap is lacking (Miller 1985). However, since this inferred ice cap was most likely thin and cold-based, it may have not left a clear geomorphic imprint on the landscape.

1.6 Methodology Overview

1.6a Characterizing subglacial geomorphology through mapping

The mapping of subglacial landforms was accomplished using remote-sensing and field-based mapping techniques. Satellite imagery (e.g. Landsat ETM+ band 8; resolution = 15m) and publicly available digital elevation models (DEM) from an online database (http://www.geobase.ca) were used to map glacial landforms, as well as end moraines and u-shaped valleys. Streamlined hills were mapped as straight lines from the Landsat images in

ArcGIS (ESRI). U-shaped valleys and fjords were mapped as polylines also in ArcGIS using both Landsat and a DEM. Targeted field investigation allowed ground-verification of the remote sensing mapping. Paleo-flow indicators, most often in the form of glacial striations, were measured in the field. Glacial striations are often measured to reconstruct the ice flow history of an area (Parent et al. 1995). As summarized by Parent et al. (1995), the direction (or sense) of ice flow on striated outcrops is generally established on the basis of two main sets of criteria: 1) small-scale features such as nail-head striae, rat tails and crescentic marks, and 2) medium-scale features such as rock drumlins, *roches moutonnées,* or stoss-and-lee topography. It is common to find two or more directions of movement on an outcrop. In that case, their relative age can often be determined based on crosscutting relationships and position on the outcrop relative to each other (i.e. McMartin and Paulen, 2009).

1.6b Mapping the spatial distribution and relative intensity of subglacial erosion

An ice sheet's basal thermal regime exercises dominant control over basal sliding and sediment deformation, ice sheet geometry, and the response of the ice sheet to climatic forcing, all of which influence how the landscape is modified by glacial erosion (Refnsider and Miller 2010). Proxies can be used to gain insight into the temporal and spatial variations in the basal thermal regime (Refsnider and Miller 2010; Trommelen et al. 2012). In this study a holistic approach was used, bringing together multiple proxies that were used to develop a more complete understanding of subglacial erosion. The proxies used include the Chemical Index of Alteration or CIA (Nesbitt and Young, 1982; Refsnider and Miller 2010), streamlined hill density and elongation ratios (Stokes and Clark 2002; Stokes et al., 2013), and bedrock-controlled lake density studies (Andrews 1989).

The chemical index of alteration (CIA) approach is sometimes used as a proxy of till weathering or inheritance from a regolith. The CIA is a useful index that reflects the ratio of primary minerals from the upper crust (mainly feldspars) to weathering by-products (neominerals; i.e. clay minerals) in sediments (Nesbitt and Young 1982; Fedo et al. 1995). It is determined according to CIA = $[Al_2O_3/ (Al_2O_3 + CaO^* + NaO + K_2O)]$ X 100, where minerals are expressed as molar proportions and where CaO* represents Ca from silicate-bearing minerals (e.g. non-carbonate sources). The latter assumption is considered to be reasonable for the study area,

which is underlain by igneous and metamorphic rocks with no evidence of carbonate dispersion from sedimentary basins (e.g. Foxe Basin), with the exception of carbonate xenoliths in kimberlites from an eroded platform; which could be a very minor contributor for CaO down ice. For this study, a till geochemistry suite (analysed using Inductively Coupled Plasma Mass Spectrometry (ICP-MS) using total digestion of the size fraction: <180 µm) collected by Peregrine Diamonds Ltd. in 2009 was used (Appendix E). It has been demonstrated that unweathered rocks and minerals ranging in composition from gabbro to K-feldspar have very similar CIA values of about 50 (Fedo et al. 1995). CIA values should thus not vary much due to underlying bedrock lithological changes across the study area. CIA values are thought to mainly reflect weathering of the till or inheritance from a regolith, and therefore can give insight into how erosive the ice was across the study area (Refsnider and Miller 2010).

In the eastern Canadian Arctic, landscapes reflect varying degrees of glacial erosion (Andrews 1989). For example, a high density of small bedrock controlled lakes highlight areas of relatively high glacial scour where areas of surface tors, angular blockfields, and few lakes highlight areas of low glacial scour (Andrews 1989).

Dimensions of streamlined hills of glacial origin are often used as a proxy for relative basal ice flow intensity/velocity (Clark 1993; Hart and Smith 1997; Stokes and Clark 2002). The elongation ratio (E=L/W) is a streamlined hill's length divided by its width. If a streamlined hill has an elongation ratio greater than 10:1, it is generally considered to represent fast basal flow (Clark 1993; King et al. 2009). In the case of bedrock-cored streamlined hills, a case may be made that their elongation ratio also reflects subglacial bedrock erosion intensity.

The elongation ratio and density of lakes were derived using various GIS tools and coupled to combine the proxies to highlight areas of relatively high basal erosion intensity and ice flow, which is referred to as the subglacial dynamics index (Hodder 2012).

1.6c Investigating glacial sediment-landform relationships

The relationship between subglacial erosion, till production, and landform development is

complex (e.g. Boulton 1996). Because of the complexity of the relationships, they are rarely investigated because it requires large and diverse datasets containing both landform and sediment characteristics. It is, however, important to integrate such data in order to understand the evolution of the ice sheet at varying temporal and spatial scales (Trommelen et al. 2012). Information gathered to study subglacial dynamics typically includes subglacial landforms and data concerning their abundance, shape, and orientation (e.g. Clark et al. 2000; Stokes and Clark 2003; Briner 2007; Phillips et al. 2010; Stokes et la, 2013), as well as smaller ice-flow indicators measured in the field (e.g. McMartin and Henderson 2004; Trommelen et al. 2012). In this study, not only subglacial landform characteristics and field-based ice-flow indicators were used, but also bedrock-controlled lake density and extensive till geochemical data. This multi-faceted approach allows the relationships between landform and glacial sediment characteristics to be investigated in order to get more insight into the subglacial dynamics and its effect on landforms and till production and transport.

Landscapes resulting from past glaciations are not homogenous. The glacial record has been shown in many areas as a patchwork of contrasting landscapes (Ross et al. 2009; Trommelen et al. 2012). Each of these areas appears to have a distinct glacial history which may or may not overlap with that of adjacent terrain zones providing distinct or hazy borders respectively, as shown by differentiating subglacial landforms, striation records, etc.; these areas are referred to as glacial terrain zones GTZs (Trommelen et al. 2012). The mosaic landscape can be explained by spatio-temporal changes in subglacial conditions leading to differing amounts of inheritance and overprinting, or varying degrees of landscape preservation (Clark 1999; Trommelen et al. 2012). Following the methodology of Trommelen et al. (2012), streamlined landform flowsets, field-based ice-flow indicator and relative age relationships variation, as well as presence of characteristic types of landforms such as end moraines, topographic characteristics, sediment composition, and the relationship between esker and streamlined landform orientation were all carefully analyzed in order to determine whether the study area contains distinct GTZs or not. In this study, principal component analysis (PCA) was also used to determine whether till could be partitioned into GTZs based on its composition. Results were then combined with CIA results (see above) as well as with the landform record to enhance the GTZ analysis.

Another method used to study the Quaternary geology was multivariate statistics to study the relationship between the landscape, bedrock geology, and till geochemistry. Multivariate methods highlight changes in several properties simultaneously (Davis 2002). Principal component analysis (PCA) is a multivariate method that consists of a linear transformation with x original variables and y new variables, where each new variable is a linear combination of the old variable (Davis 2002). A second till geochemical database of clay-sized sediment (<2 µm) was used to do the multivariate statistics for the study area. The till samples were analysed using the Aqua Regia method. This data contains over 1000 samples with information on 54 elements, making it a complex multivariate database, and was collected by Peregrine Diamonds in 2009.

The objective of PCA is to reduce the number of variables necessary to describe the observed variation within a dataset. In this case, PCA was used to recognize possible trends in the till geochemistry within GTZ, as well as relationship with underlying bedrock geology. Each principal component might be interpreted as describing a geological process such as a differentiation (partial melting, crystal fractionation, etc.), alteration/mineralization (carbonization, silicification, alkali depletion, metal associations and enrichments, etc.) and weathering processes (Grunsky 2010). In areas of thick unconsolidated sediment cover such as till, alluvium or colluvium, the linear combinations of variables and the plots of the loadings may not be so easy to interpret as they may reflect a mixture of several surficial processes, including glacial transport (Grunsky 2010). PCA can be run on a set of data through statistical software such as R Statistical Environment (R Development Core Team, 2013), which was the program utilized for this research.

Maps of principal component scores of the observations can be useful in understanding geochemical processes, as well as surficial processes. If a component expresses underlying lithologies, then a map of that component may outline the major lithological variation of the area. Surficial processes may also affect the resulting component maps. Measure of association, or metric, can have a significant effect on the derivation of principal components. Covariance relationships between the elements reflect the magnitude of the elements and thus elements with large values tend to dominate the variance-covariance matrix (Grunsky 2010). If there is a pattern in the geochemistry of the GTZs, a linear discriminant analysis can be run on the data

through R Environment, to determine if the GTZs could actually be predicted by their geochemistry.

1.6d A holistic approach to developing glacial dynamics evolution model

Delineating GTZs by geomorphological mapping, erosion proxies, and till geochemical groupings, allows for a better understanding of the spatial and relative temporal changes in the glacial record. This is the foundation for a conceptual model of the evolution of subglacial dynamics on north-central Hall Peninsula, Baffin Island. By combining the understanding of the various proxies used to study the subglacial landscape of Hall Peninsula developed through this research and building on Miller (1980), Dyke et al. (2002), and De Angelis and Kleman (2007), a conceptual model has been developed.

1.7 Thesis Structure

The thesis includes a thesis abstract, an introduction chapter (Chapter 1), two chapters designed as publishable papers (Chapters 2-3), and a conclusion chapter.

The first chapter provides the framework for the thesis, explaining the research problem, the main goals and research considerations, and summarizing the relevant geosciences literature specific to the study area.

Chapter 2 was prepared as government publication; specifically an Open File of the Geological Survey of Canada (Johnson et al. 2013). The Open File focuses on field data collected in the summers of 2011 and 2012, as well as remote sensing data of the study area. The second chapter lays the groundwork for the following chapter. The map that was developed from the work done in Chapter 2 is important to industry in the area, as they will use the paleo- flow indicators in prioritizing targets for future drilling.

Chapter 2 is co-authored with supervisor Martin Ross and project collaborator Tommy Tremblay (C-NGO). The research project was designed and supervised by M. Ross, but I was responsible

for data collection, organization, presentation, and interpretation, as well as writing. Tommy Tremblay provided input during project discussions and during the review of earlier versions of the manuscript. Chapter 2 has also been peer-reviewed by Roger Paulen of the Geological Survey of Canada as part of the publication requirements for Open File Reports by Natural Resources Canada.

The third chapter is drafted as a journal manuscript. Chapter three presents a detailed look at the glacial landscape and sediment assemblages, including the geochemistry, which leads to the development of a conceptual model of glacial dynamics evolution from the LGM to final retreat of the LIS and early stages of local ice cap development. Using a holistic approach, GTZs were delineated providing an in-depth understanding of the complex patchwork of glacial landforms and sediments in the study area, which result from different non-coeval ice-flow events. Using a large till geochemical database, the Chemical Index of Alteration (CIA) is calculated over the study area to study weathering. Using another till geochemical database, the possible link between GTZs and till geochemistry is studied using principal component analysis (PCA). The bedrock geology is also considered to see if the geochemistry of the underlying lithologies influences the till more than glacial or perhaps weathering processes. The conceptual model ties the story together with the little research that was done in the past, to what we understand presently.

Chapter 3 is co-authored with Professor Martin Ross, Eric Grunsky, a Research Scientist at Natural Resources Canada (NRCan) and Adjunct Professor at Waterloo, Tyler Hodder, a graduate student at Waterloo, and Tommy Tremblay, also Research Scientist at NRCan. I was responsible for raw data manipulation (chemical index of alteration, streamlined hill mapping, elongation ratio mapping and calculations, preparing raw data for statistical procedures), interpretation, and writing. The streamlined hills and elongation ratio data was given to Tyler Hodder who did a GIS analysis of subglacial erosion using these proxies as well as bedrock-controlled lake density. Tyler Hodder created the subglacial dynamics index. Eric Grunsky was responsible for the principal component analysis and linear discriminant analysis, which was done through R Environment, and aided in interpretation. Tommy Tremblay validated the chemical index of alteration study, and provided input at various stages of the research. I was

also responsible for putting all the results together and for developing the conceptual model as well as for writing the chapter.

The fourth chapter concludes and summarizes the thesis, presenting complications and future research.

Chapter 2 : Glacial geomorphology of north-central Hall Peninsula, Southern Baffin Island

2.1 Introduction

Canada was affected by several glaciations during the Quaternary (Ehlers and Gibbard 2004). Many ore deposits are covered by glacial sediments, which make it difficult to detect the deposits remotely. Currently, an important exploration method in Canada involves the search for distinct mineral assemblages in glacial sediments and tracing them back to their source. To use this method effectively, it is critical to understand regional past glacial dynamics and the subtleties of glacial erosion, sediment production, transportation, and deposition (Klassen 2001). Lack of such knowledge can delay major discoveries and lead to increased exploration costs.

The evolution of ice-flow systems over time has a major effect on the glacial landscape and its sediments. Maps of glacial landforms at various scales, including streamlined hills and striations and other ice flow indicators preserved on glacially abraded outcrops, are necessary to understand the glacial dynamics and ice flow history of an area. Such mapping efforts were undertaken on Hall Peninsula, Baffin Island, because available maps and data were clearly insufficient to meet the needs of mineral exploration in this prospective region. The goal of this report is to present the results of the mapping of large (kilometre scale) subglacial landforms based on remote sensing and of targeted field mapping of meso-scale (sub-kilometre) landforms and outcrop-scale glacial striae and other paleo-ice-flow indicators throughout the study area.

2.2 Location

The study area is located in north-central Hall Peninsula, Baffin Island. Fieldwork was restricted to a smaller area than what was mapped using remotely sensed imagery (Figure 2-1): The location of the field site on Hall Peninsula, Baffin Island. Focused fieldwork is shown in the red polygon and geomorphology mapping was within the largest, green polygon..

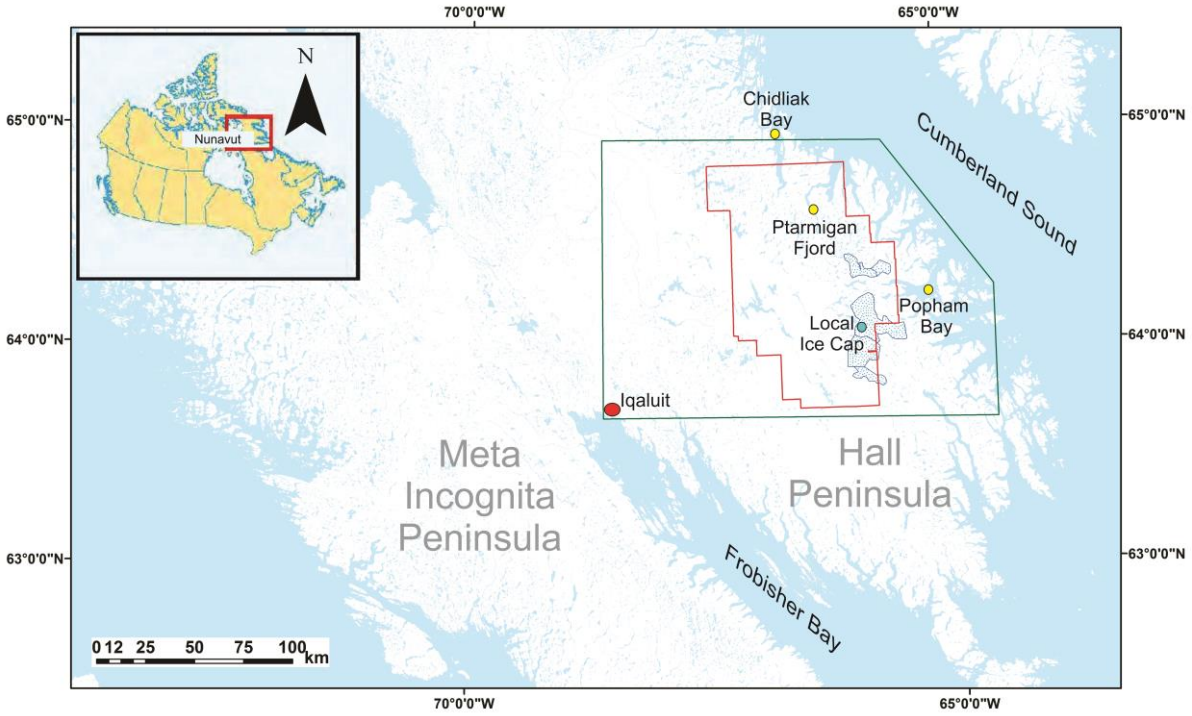

Figure 2-1: The location of the field site on Hall Peninsula, Baffin Island. Focused fieldwork is shown in the red polygon and geomorphology mapping was within the largest, green polygon. The larger area is approximately 25,400 km^2.

2.3 Physiography

Hall Peninsula is the middle of three large peninsulas of southeastern Baffin Island. It is bounded by Frobisher Bay to the south/southwest and Cumberland Sound to the north/northeast (Figure 2-1). Most of central and eastern Hall Peninsula is drained via the McKeand River (Miller 1985), which cuts through the eastern portion of the study area (Pell 2011). Fjords dissect the perimeter of the peninsula, thus directing the drainage. According to the physiographic region maps by Bostock (1970) and Andrews (1989), the physiographic regions of the study area are the stepped plain or dissected upland surfaces to the north and "Baffin Surface" in the south. Baffin Surface is described as an area with few lakes (<5%) with tors and angular blockfields, suggesting that the area has not been intensely scoured by warm-based glacial ice (Andrews, 1989). The land from the coast to approximately 50 km inland consists of abundant lakes, ponds and bedrock-controlled streamlined hills. The central part of the study area is characterized by flat to rolling topography consisting of more continuous till surrounding an area of regolith, and with few ponds and lakes. The central area also contains minor

glaciofluvial and lacustrine deposits. The eastern region is characterized by bedrock hills occupied by the current ice cap, valleys, and fjords.

2.4. Bedrock Geology

The bedrock geology of the study area is summarized by Pell (2011). The bedrock geology of Baffin Island has only been mapped at a reconnaissance scale (Jackson and Berman 2000). Hall Peninsula was mapped by Blackadar (1967) and revisited by Scott (1996). In 2006, the map was released digitally (St-Onge, Jackson, and Henderson) (Figure 2-2).

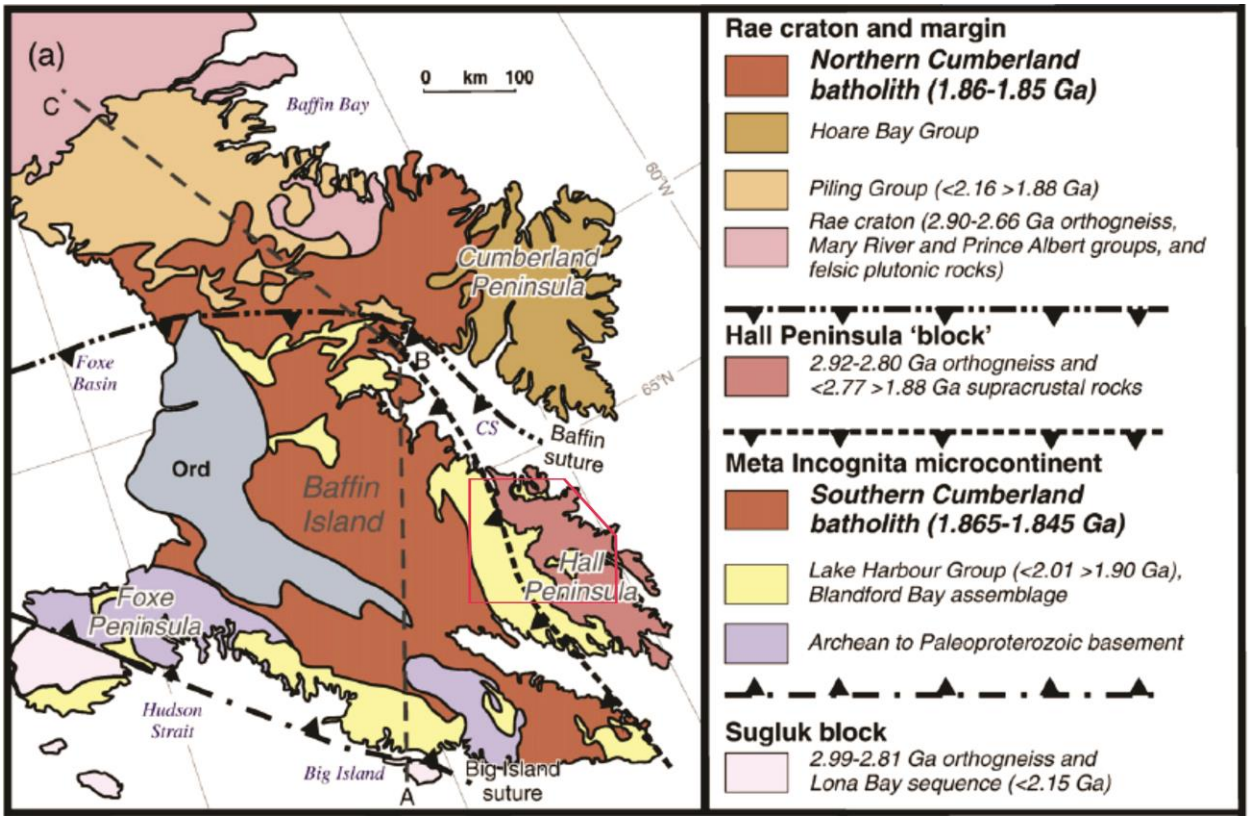

Figure 2-2: A summary of the simplified geology of southern Baffin Island showing tectonostratigraphic assemblages, such as the Hall Peninsula Block located in the study area. As shown, Hall Peninsula is underlain by Hall Peninsula block (orthogneiss and supracrustal rocks) and Lake Harbour Group assemblages (modified from St-Onge et al. 2008 and Whalen 2010).

Hall Peninsula is thought to be underlain by three units. To the east exists a terrain referred to as the Hall Peninsula Block, which is composed of Archean orthognessic and supracrustal rocks (Whalen et al. 2012). Alongside the Hall Peninsula Block is a central belt of intermediate

Paleproterozoic metasediments correlated to the Lake Harbour Group (St-Onge et al. 2006; Whalen et al. 2010). To the west is Cumberland Batholith, which is made up of granulite facies intracrustal granitoids (Scott 1999; Whalen et al. 2012).

More than sixty kimberlite bodies, as well as prospective till anomalies indicative of magmatic Ni-Cu-PGE metamorphosed SEDEX, VMS, and lode gold deposits have been discovered in the study area, and has been the focus of intense diamond exploration since 2005 (Pell 2011; Pell et al. 2012**).** The kimberlite province stretches in a north-south direction for approximately 70 kilometres and in an east-west direction for approximately 40 kilometres (Pell et al. 2012). Most of the kimberlites discovered are hosted in rocks belonging to the Hall Peninsula Block (Pell et al. 2012).

2.5 Surficial Materials

Till throughout Baffin Island is generally thin with the exception of locally thicker deposits in the central region. Small pro-glacial and subaqueous outwash and deltaic sediment bodies also occur attesting of the existence of short-lived proglacial rivers and lakes in the study area (Miller 1985). Based on exploration drill holes, the till in the central plateau area reaches up to 15 m in thickness (Pell 2011). It is thinner in areas proximal to the coasts, where bedrock is discontinuously covered with a thin till veneer about 1-2 m thick. In valley floors and other areas of relatively lower elevation, till is also thicker (Pell 2011). According to Andrews (1989), the till on Baffin Island consists of two types: sandy till with abundant Precambrian clasts (shield type), and a silt-clay matrix-dominated till with abundant Palaeozoic carbonate clasts. The till encountered during field work is from the first "shield" type with a strong local signature characterized by abundant clasts of orthogneisses or Paleoproterozoic metasedimentary rocks found in the study area. Locally, the till can have a strong kimberlitic composition including green matrix, kimberlite and limestone cobbles.

2.6 Previous Studies

Limited research has been done on the Quaternary geology of Hall Peninsula. Hall Peninsula has been included in regional studies of the Laurentide Ice Sheet (LIS) (Dyke et al. 2002) and the

Quaternary Geology of the north eastern Canadian Shield (Andrews 1989; Miller et al. 2002; Miller et al. 2005; De Angelis 2007; De Angelis and Klemen 2007; Briner, et al. 2009). Few studies have focused on Hall Peninsula itself, but have a primary focus on the record of deglaciation and associated late Foxe and Cockburn Substage moraine systems (Miller 1980; Miller 1985). A 1:500 000 scale predictive surficial geology map was released following a remote predictive mapping (RPM) study based on LANDSAT and digital elevation models (DEM) (Harris et al. 2012).

Baffin Island is dominated by a landscape reflecting varying thermal regimes as shown through bedrock erosion (Andrews 1989). The ice sheet velocity and profile were highly controlled by the substrate and thermal regime (Miller et al. 2000). During the Last Glacial Maximum (LGM) (approximately 21 ka ago), the LIS overwhelmed southern Baffin Island, including Hall Peninsula and its offshore islands (Dyke et al. 2002). During early deglaciation, the Hall Ice Divide is thought to have run parallel to the axis of the peninsula and to have flowed away from the divide to the northeast and southwest (Hall et al. 2003).

The oldest moraine on the Peninsula is the Hall Moraine (Miller, 1980; Miller, 1985) (Figure 2-3). About 50 km to the northwest of the Hall Moraine is the inner Frobisher Bay Moraine, which trends northeast/south-west across the high part of the Peninsula. The Hall Moraine was dated with 3 paired valves of *Mya truncata* that averaged 10, 760 ± 70 ^{14}C yrs BP marking the deglaciation from a terminal moraine complex in Warwick Sound (Miller 1980) and thus marks a still stand of the margin of the LIS during the overall deglaciation of the area on Hall Peninsula and Frobisher Bay (Miller 1985). At Gold Cove , shells of *Mya truncata* yielded ages of 10,100 ± 100 ^{14}C yrs BP (GSC-2725), which is considered to date the deglaciation of the cove (Miller, 1980). Other ages for the deglaciation of the cove included the apparent ^{14}C age of 12,150 ± 140 yr (QC-543), which was later re-dated because the initial age was significantly older than GSC-2725; the new analysis yielded an age of 10,200 ± 210 yr B.P. (GSC-2778) which is statistically indistinguishable from the first one (Miller, 1980). A *M. truncata* shell with the age of 9,725 ± 120 yr (QC-450) was also found in marine limit deposits which shows a transition to marine environment after the deglaciation of Gold Cove (Miller 1980).

Further west, two major moraine systems younger than the Hall Moraine (Figure 2-3) have been mapped and dated at about 8,600 ^{14}C yrs BP, equivalent to the Cockburn Substage (Miller 1985). The Frobisher Bay Moraine System (Figure 2-3) was traced from inner Frobisher Bay and up to the northwest where the trace eventually is lost (Miller 1985). Drumlinized till suggests that ice flowed parallel to the axis of the peninsula from the northwest to the southeast (Miller 1985).

Miller (1985) also mapped the Chidliak Moraine, which runs south-southeast along the east coast of Hall Peninsula to Chidliak Bay (Miller 1985). The ice that deposited this moraine flowed northeast from the plateau of the peninsula and funnelled through the fjords and bays that line the perimeter (Miller 1985). Shell of *Hiatella arctica* found on the moraine were dated at 8,660 ± 160 ^{14}C yrs BP (GSC-2466), which correlates to the Frobisher Bay Moraine System. East of Chidliak Bay, the drumlins have a northeast trend, which contrasts with the southeast trending features in the centre of the peninsula (Miller 1985).

Previous mapping of a local moraine inland of Popham Bay (Figure 2-3) suggests that it required ice flowing from the east to west (Miller 1985). The local moraine was deposited by the Hall Peninsula ice cap, located in the study area. *Hiatella arctica* shells gathered from ice-proximal raised marine deltas yielded an age of 8,890 ±100 ^{14}C yrs (GSC-2586) (Miller 1985). This age correlates the local ice advance to the inner continental moraine system in Chidliak Bay and Frobisher Bay (Miller 1985).

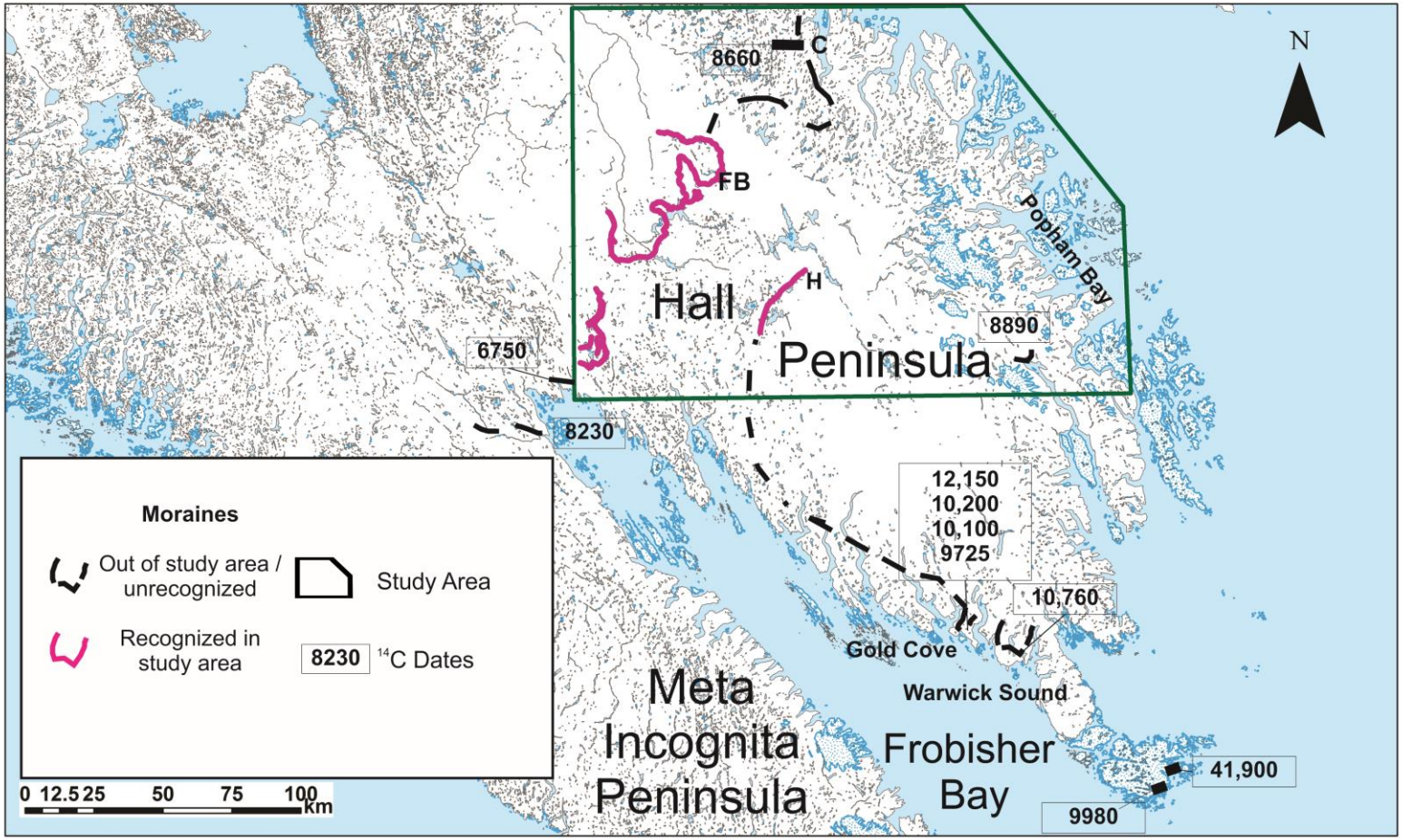

Figure 2-3: Major moraine systems of Southern Baffin Island and their respective radiocarbon ages (Figure modified from Miller 1980). The dashed lines indicate places where the moraines are inferred, and the dotted line is where it is extrapolated. The geomorphology map done in this project is within the trapezoid and includes the Hall Moraine (H) and the Frobisher Bay Moraine (FB). The Chidliak Moraine (C), mapped later by Miller (1985), runs parallel to the east coast and is dated at 8890 and 8660 ^{14}C yrs BP, but was not observed during this study. Figure modified from Miller (1980).

Proglacial features of Hall Peninsula include lacustrine shorelines, deltas and overflow channels from the former proglacial lake systems (Miller 1985). The two main series of the lakes identified are associated with the Hall Moraine (older) and the Frobisher Bay Moraine system (younger) (Miller 1985). There are also well developed ice-contact/proximal deltas where the lakes were against the edge of the moraines (Miller 1985). The older lakes are at 630 m asl and drained south (Miller 1985). The younger lakes also lie 630 m asl and are traced to the Frobisher Bay Moraine along the western margin but, to the northeast, the margin is lost amongst the edge of the largest lake (Miller 1985). Miller (1985) postulated that the only way this large lake could have existed was to be dammed by a thin residual ice cap lying between Cumberland Sound and the large lake. There is no evidence in terms of modern moraine deposits, which would support the existence of such an ice body (Miller 1985). However, this ice cap was most likely thin and perhaps cold-based. Cosmogenic dating of bedrock surfaces and boulders from within the inferred ice cap area could test this late ice cover hypothesis.

2.7 Methods

This study focused on subglacial landforms in order to map and provide information about ice flow dynamics. The mapping of surficial materials (e.g. regolith, till, glaciofluvial and lacustrine deposits) is out of the scope of this report. Remote sensing is frequently used for mapping regional scale glacial features (Clark et al. 2000; De Angelis and Kleman 2007; Kleman and Glasser 2007; Clark et al. 2009; Stokes et al. 2009; Kleman et al. 2010; Trommelen and Ross 2012; Spagnolo et al. 2011; Smith and Knight 2011). Satellite images and air photographs are often used to develop understanding of an area's glacial history, even when little or no previous mapping has been done (Kujansuu 1990). Satellite images can be visually interpreted to highlight specific features of the landscape such as groups of streamlined hills or moraines (Boulton and Clark 1990). Glacial features can thus be reliably mapped by visual interpretation, though it is essential to go through quality checks, such as overlaying geological maps to differentiate glacial features from bedrock features (Clark et al. 2009).

Subglacial landforms often occur in clusters or "fields" that form under certain conditions and different times. These clusters provide insight on glacial dynamics, erosion, transport and deposition. Fields of parallel streamlined ridges thought to have formed by basal ice-flow are

referred to as flowsets (Kleman et al. 1997). It has become clear that because of variable degrees of erosion and preservation, the glacial landscape forms a complex patchwork of glacial landforms and sediments resulting from different non-coeval ice-flow events (Stea and Finck 2001; Clarhäll and Jansson 2003; Ross et al. 2009; Stokes et al. 2009; Trommelen et al. 2012). Some of these "patches", referred to as glacial terrain zones or GTZs (cf. Trommelen et al. 2012), may overlap showing complex crosscutting patterns or may be defined by sharp boundaries separating groups of landforms with contrasting orientation or characteristics (e.g. Ross et al. 2009).

For remote sensing, the study took advantage of LANDSAT 7 with Landsat Enhanced Thematic Mapper Plus (ETM+) satellite imagery, publicly available DEM, airborne magnetics, and topographic maps (Table 2-1). Georeferenced and ortho-rectified air photographs were not used in this study. Satellite images were used to map the study area for meso-and mega-scale subglacial features. A mosaic of available satellite images was created and visualized at a 1:100,000 scale and again at a 1:30,000 scale in order to capture landforms of different sizes. Streamlined ridges (till and bedrock-cored drumlins, mega-flutes, and large *roches moutonnées*) were mapped together as glacial features. There were no distinctions made between different types of streamlined ridges.

Table 2-1: Presented is a summary of the datasets that were used for remote sensing mapping.

Data Source	Spatial Resolution (horizontal)	Technical Properties	Projection	Source
Satellite imagery (ETM+)	15 meters	Panchromatic Band 8	NAD 83, UTM Zone 19	http://www.geobase.ca
DEM	3 arc seconds	1:250,000 NTS tiles	NAD 83, UTM Zone 19	http://www.geobase.ca
Airborne magnetic geophysical survey images	4 meters		NAD 83, UTM Zone 19	Unpublished; Peregrine Diamonds Limited

A crucial component to understanding the Quaternary history of an area is mapping glacial erosional features. Reconstructing ice-flow history is done with measuring glacial striations (Parent et al. 1995; McMartin and Henderson 2004; McMartin and Paulen 2009; Plouffe et al. 2011). As summarized by Parent et al. (1995) the ice-flow direction can be established by two sets of criteria: (1) small-scale features such as nailhead striae, crescentic gouges, and rat-tail ridges and (2) medium sized features such as whaleback forms, and meter-scale *roches moutonnées* (too small to be visible on the LANDSAT images). It is common to have multiple features at one site. When there are two or more ice-flow directions observed in the same location, cross-cutting and stoss-and-lee relationships are studied to determine the relative age of the multiple ice-flows (Parent et al. 1995; McMartin and Paulen 2009). This is achieved by studying the relative positions of the indicators on the outcrop-scale according to the following criteria: a) ice-flow indicators found just on the top parts of an outcrop are usually considered the youngest for that site; b) ice-flow indicators found in depression or lower positions on the same outcrop are typically relatively older (McMartin and Paulen 2009). For example, lower polished surfaces in a down-ice position relative to the ice-flow direction as recorded on top of the outcrop are referred to as "protected surfaces" and the striations on them interpreted as relict or preserved striations from an older ice-flow phase. Also, sometimes deeper grooves or crescentic gouges are crosscut by younger striae superimposed on an angle on top of these features thus giving a clear relative age relationship (Parent et al. 1995; McMartin and Paulen 2009). Quaternary field mapping of striations and other erosional features were used to reconstruct the ice-flow history of the area and to ground-truth the features mapped using remote sensing.

Helicopter-supported fieldwork was based out of camps operated by Peregrine Diamonds Limited during the summers of 2010 and 2011. The data gathered from the field were primarily small-scale ice-flow indicators such as striae, grooves, chattermarks, sculpted outcrops, and in some cases small-medium sized *roches moutonnées* and drumlins. The goal of the 2010 field season was to understand the regional ice-flow in the area. To distinguish the regional flows from the local flows, directional indicators were studied at the tops of bedrock hills as opposed to within valleys. At lower elevations, striation records are often more complex than records of higher elevations, reflecting local topographic influence of ice-flow that developed during late stage deglaciation. The 2011 field season granted more time to investigate these local flows in

high priority areas. The field data is stored in a Microsoft Access database and includes station information (station ID and coordinates), paleo-flow data when observed, sample information and photo identification. The ice-flow indicator measurements collected in the field were also visualized in ArcGIS® (ESRI). The coordinate system used for all of the GIS files is NAD 83, UTM Zone 19.

2.8 Results

2.8.1 Remote Sensing Results

A total of 1293 streamlined hills, one major moraine system, one local moraine, and a series of U-shaped valleys were mapped using remote sensing techniques (Figure 2-4; Appendix A). There are discrete landscapes within the study area recognized on the LANDSAT images which include areas near the coast with relatively high density of lakes (Andrews 1989), ponds, fjord interfluves and streamlined hills, a central area which is relatively featureless and blanketed in till and regolith, and the area dominated by the local ice cap.

Four main orientations of ice-flow were found through analysis of the LANDSAT images. Each flow trajectory was confidently established in the field through analysis of the stoss-lee relations of streamlined hills. These flows can be summarized from relatively oldest to youngest as follows: (1) ice-flow to the northeast in fjord interfluve areas; (2) to the north and northwest in relation to the northern fjords; (3) to the east along the eastern coast (Figure 2-4); and, (4) southeast central to the study area. A southwest flow, which is not strongly represented in the remote sensing results, may be concurrent with the northeast flow (1) flowing on the opposite side of the Hall Ice Divide (Marsella et al. 2000). Fieldwork will be needed in this area to establish the extent of the southwest flow. The southeast flow (5) is found with few striations and the orientation of the late stage moraines. However, most large southeast trending landform features recognized in the satellite imagery are parallel to major bedrock structures visible on the airborne magnetic map and are thus interpreted as bedrock-controlled ridges.

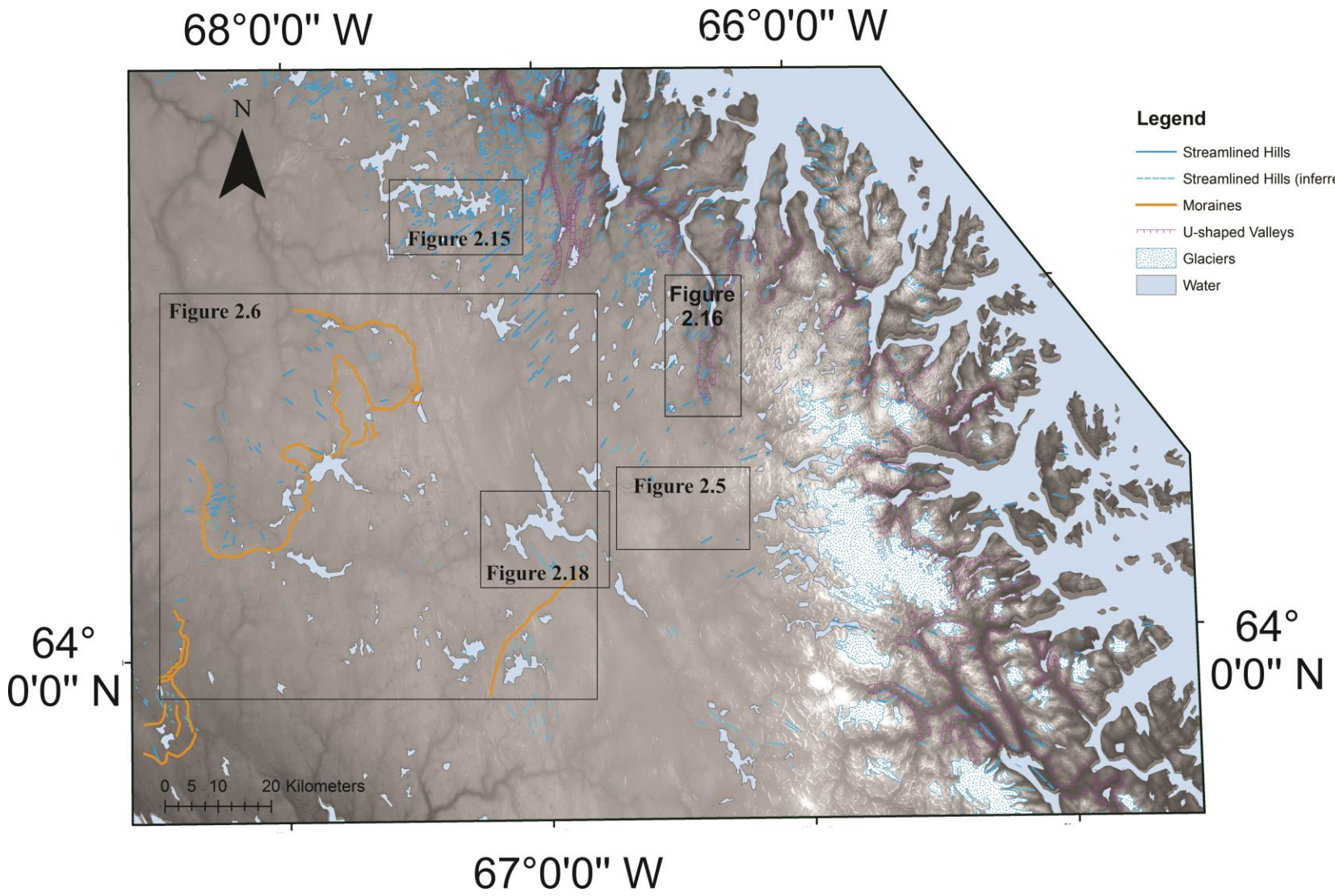

Figure 2-4: Remote-sensing results with moraines, streamlined hills, and u-shaped valleys.

The degree of modification of these northwest/southeast ridges by the southeast-trending ice-flow phase is currently unknown. In the central area, there is rolling topography blanketed with thicker till but no obvious ice-flow indicators at the meso-scale (Figure 2-5).

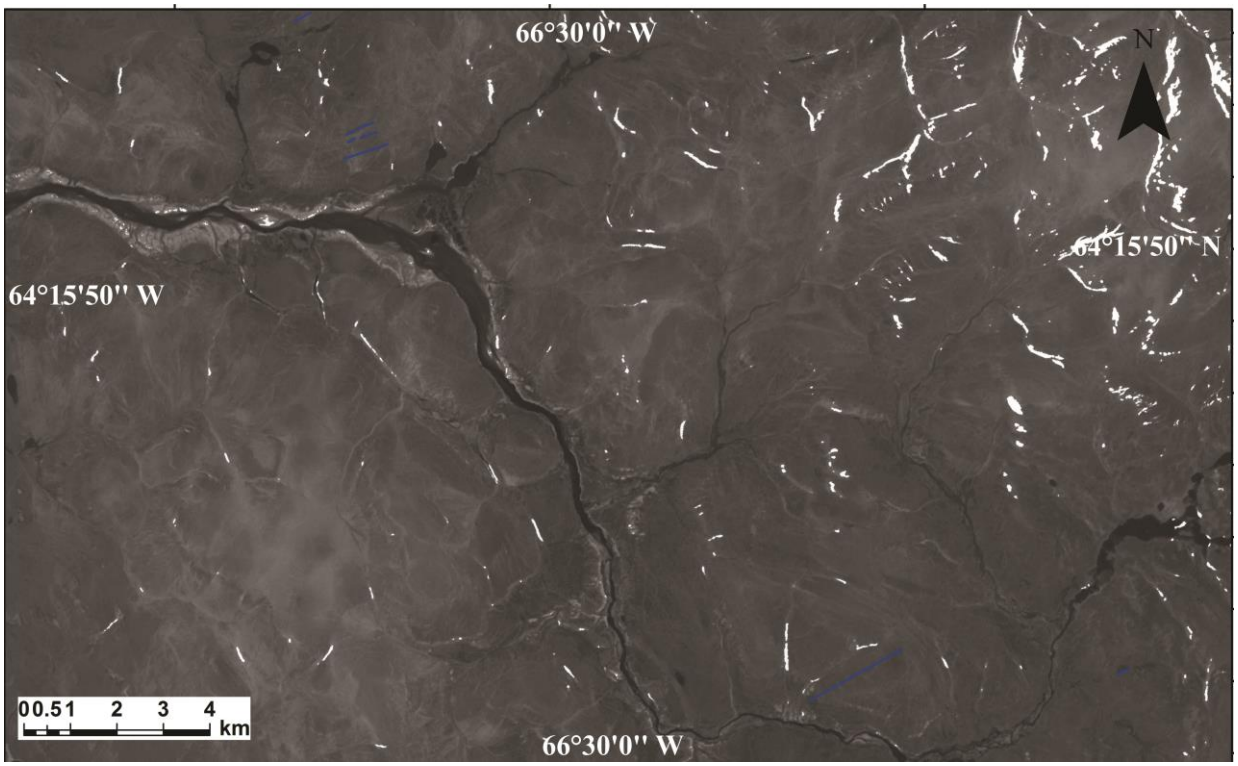

Figure 2-5: Rolling topography covered in till with few streamlined ridges and fewer lakes.

Other potential glacial streamlined hills were mapped as dashed lines. These uncertain features are either outside the fieldwork area and were thus not ground checked or simply too unclear in origin to be mapped under streamlined hills of more certain glacial origin. The dashed lines can be grouped as follow: (1) Streamlined hills generally in a southern direction, found within the lobate Frobisher Bay Moraine perpendicular to each of the lobes; (2) Southeast-trending hills following the fjords in the southeast of the study area and (3) Southeast-trending hills in the centre of the study area. Group 1 and 3 are likely glacial as they are within the lobes of the end moraines. The third group agree with those previously mapped in the central region of the study area (Miller 1985), though it is shown with magnetic data that the bedrock features are striking southeast/northwest. Ice may have been thin enough for basal flow to be controlled by the southeast bedrock features during the ice advances that deposited the moraines.

Two major moraine systems and two local moraines were previously mapped within the study area (Miller 1980; Miller 1985). Components of the Frobisher Bay Moraine system (Figure 2-6a-b) were recognized as well as the local Hall Moraine with analysis of the LANDSAT images. The moraine was hand mapped on the LANDSAT photo below by recognizing the hummocky areas of thicker till, which make up the bulbous portion of the Frobisher Bay Moraine system. The ridges of these moraines are prominent features on the studied images and show that ice flowed approximately from the northwest to the southeast. Parts of the Frobisher Bay Moraine that were not mapped on the LANDSAT include the dashed line segments The Chidliak Moraine that follows the coast and the local moraine showing west flowing ice across from Popham Bay reported by Miller (1985) were not recognized on the LANDSAT images.

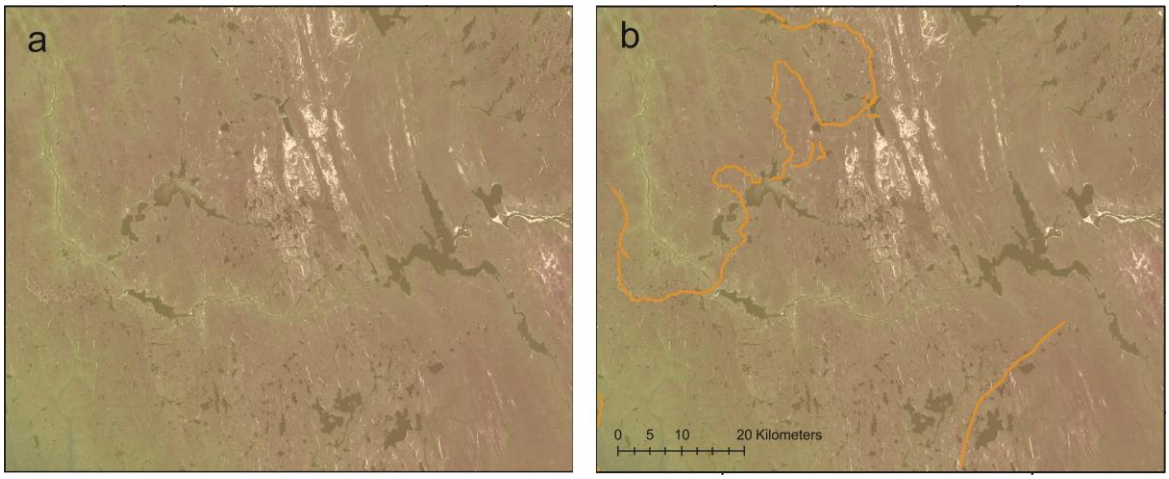

Figure 2-6: A major segment of the Frobisher Bay Moraine system and Hall Moraine (Blake 1966; Miller 1980). a) The ridge is mapped from the LANDSAT image enhanced with DEM; (b) the same image with the mapped outline of the Frobisher Bay Moraine (lobate feature in the northwest) and the Hall Moraine (the more linear feature in the southeast corner). The areas that appear as white tone are areas of regolith lacking evidence of glacial erosion.

With publically available DEM, U-shaped valleys were mapped throughout the study area (Figure 2-7). It is interpreted that many of the valleys extend far inland beyond modern fjords and these troughs contributed to funnelling ice and further eroding the troughs through positive feedbacks.

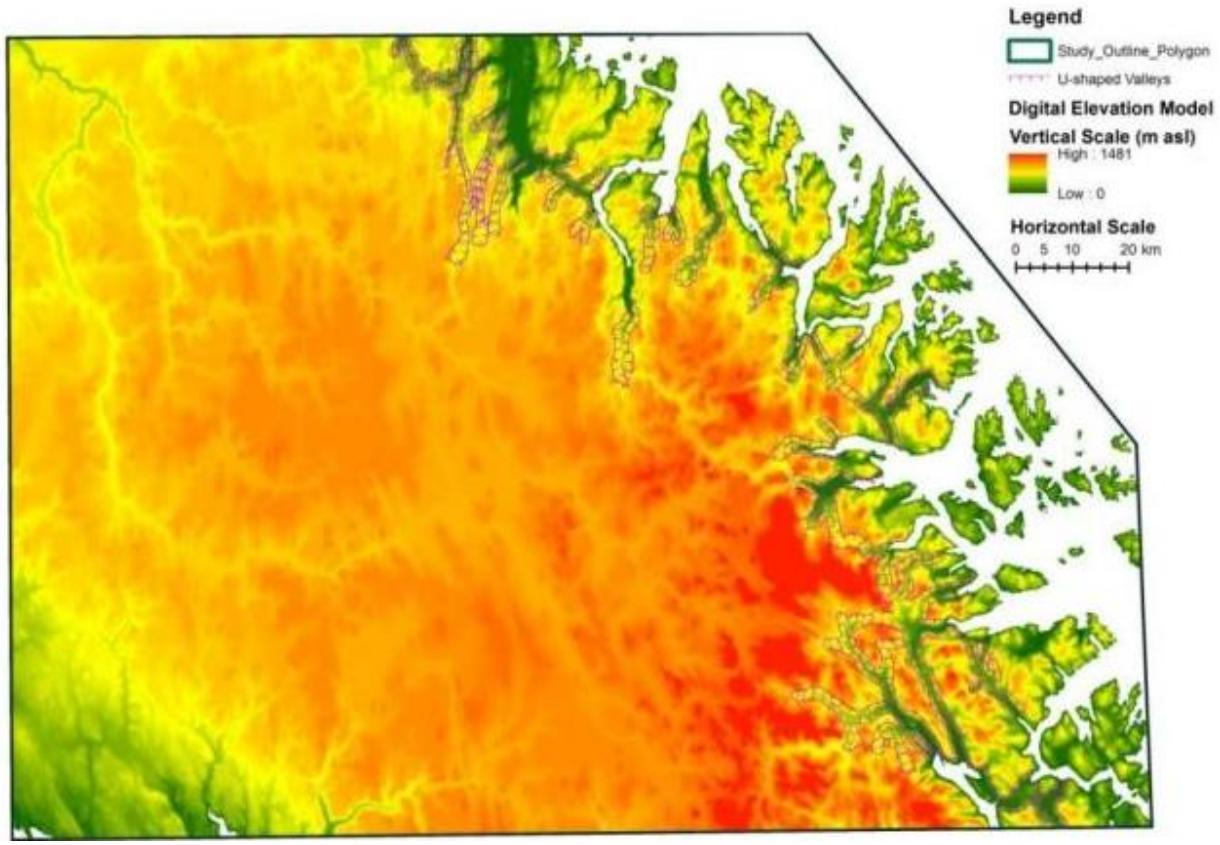

Figure 2-7: U-shaped valleys in purple mapped on a DEM base. The U-shaped valleys start far inland and eventually lead towards the fjords. Cool colours correspond to low elevations (dark green is sea level) and hot colours correspond to high elevation (1095 m asl).

2.8.2 Fieldwork Results

Fieldwork focused on meso- and micro-scale ice-flow indicators. Observations were made at 413 stations (Figure 2-8), with a total of 456 paleo-flow indicators during the summers of 2010 and 2011 from base camps operated by Peregrine Diamonds Limited (Appendix A; Appendix B).

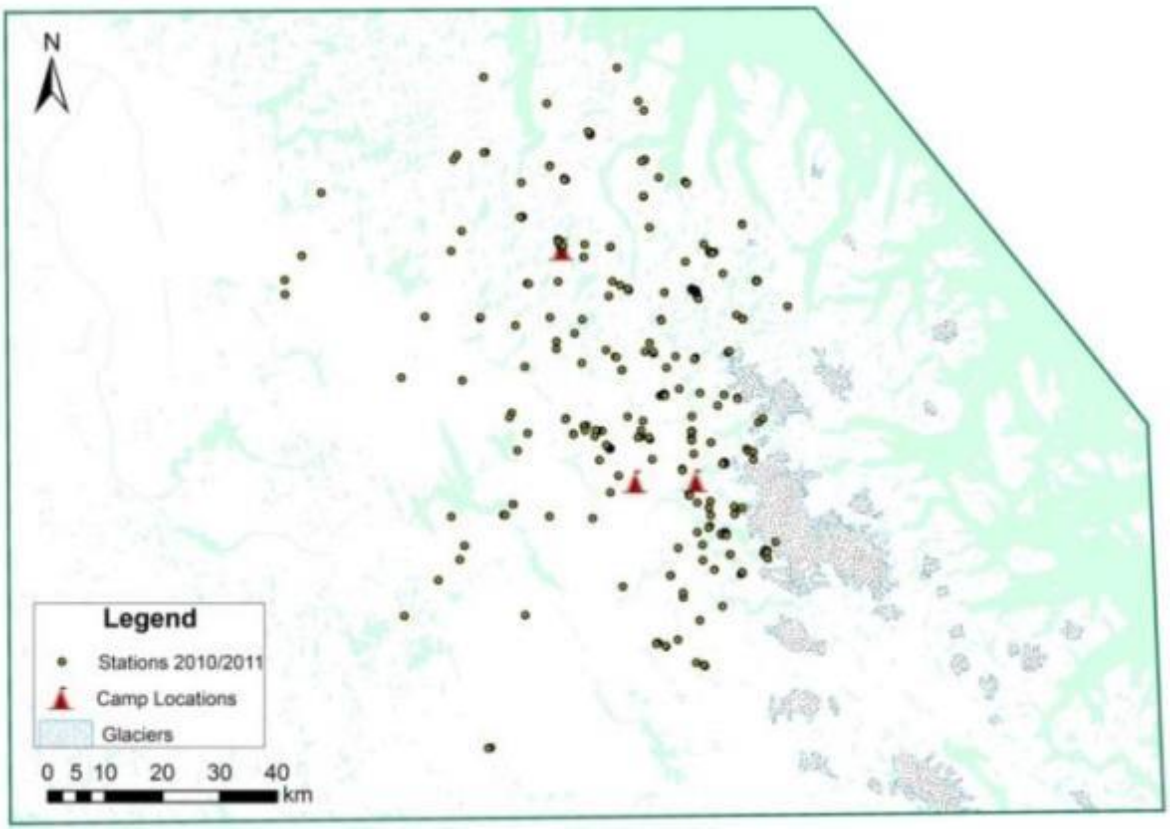

Figure 2-8: Shown are key locations for 2010 and 2011 fieldwork. Black circles show station locations for 2010 and 2011, red triangles show Peregrine Diamond's three base camps, and the yellow polygon denotes Ptarmigan Fjord.

Of the 456 paleo-flow indicators measured, 400 are striations, 48 are chatter marks, and 15 are *roches moutonnées*. A map showing 113 of the 456 features was made to highlight the main azimuths found (Figure 2-9).

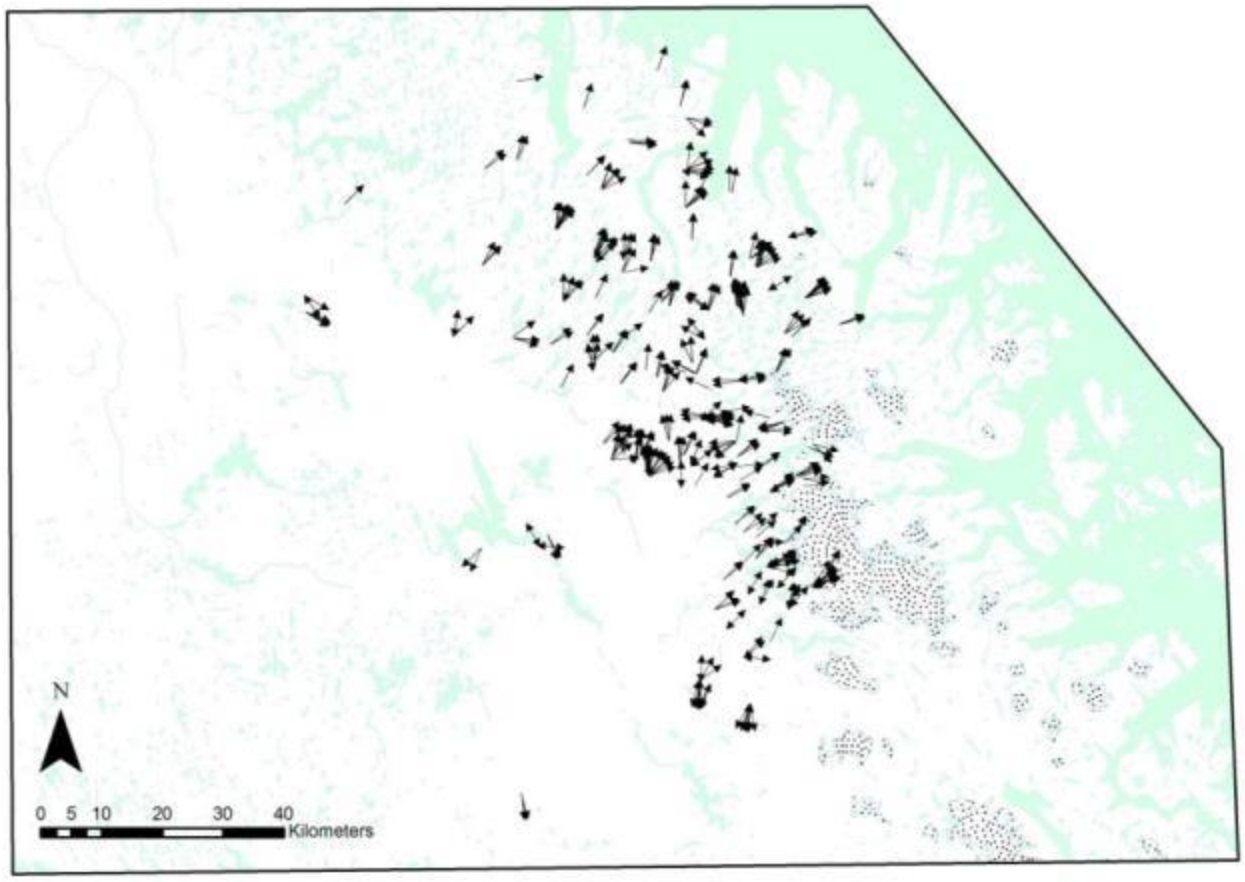

Figure 2-9: The results of the paleo-flow features measured in the field. The local ice cap is shown in stippled blue.

Streamlined bedrock forms were numerous throughout the field study area. Field observations of these landforms were useful to verify the preliminary geomorphological map based on remote sensing. However, measurement of the general orientation of these landforms in the field was done only if there were no smaller scale features found or if there was an evident age relationship with the striation record preserved on them. Out of the 456 paleo-flow indicators, it was possible to get the sense of direction of 375. There are 14 sites where a clear relative age relationship could be established.

Striations make up the bulk of the paleo-flow indicator data (Figure 2-10). Grooves, a slightly larger erosional feature, were grouped into the data as striations. Grooves found throughout the study area were grouped together with striations as a paleo-flow feature. Striations and grooves

are bidirectional, and directional indicators were sometimes needed to confirm ice-flow direction when an obvious stoss-lee relationship was not present. Directional indicators included chatter marks and crescentic gouges (Figure 2-11), which were grouped together under chatter marks. Striations are sometimes found parallel to foliation; special care was thus given to ensure high confidence in the measurement.

Figure 2-10: Striation measurements showing stoss-lee relationship indicating direction of flow.

Figure 2-11: An example of a well striated outcrop showing multiple crescentic gouges indicating the direction (as indicated by the compass). The direction for this station was approximately 183°, showing the southern flow. Note the rough (not polished) surface down-ice (upper left) relative to the abraded/polished surface (lower right).

The field observations agree with the landform-scale patterns based on remote sensing. However, more ice-flow directions were recognized in the field such as the flows with a western direction found in valleys that recorded movement from the Hall Ice Cap, and the northwest valley flows directed into Ptarmigan Fjord.

2.8.3 Relative age relationships

The relative chronology (Figure 2-12) of the flow-sets was established from field observations, some of which are supported by remote sensing data. Tops of ridges were primarily focused on to identify regional flowsets as opposed to local topographically controlled flowsets, though high priority areas with lower elevations were also studied. The ice-flow directions result from a series of glacial events that are thought to span from the LGM to deglaciation, and final retreat to the icecap.

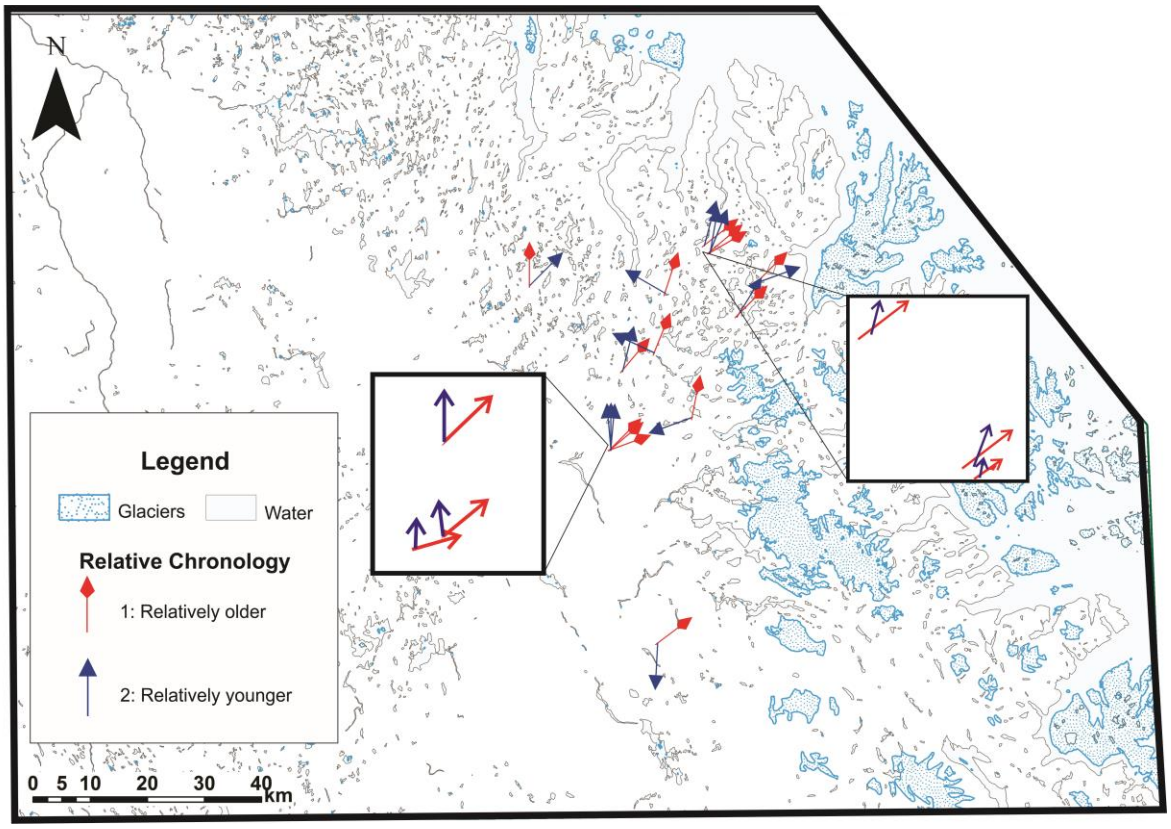

Figure 2-12: Relative chronology relationships documented in the field. A total of 14 relationships were found, with the majority of them documenting an earlier northeast flow overprinted by various other flows.

Through cross-cutting relationships observed in the field, it is possible to put these ice flow events in chronological order. Compared to other paleo-flow features, relatively few age relationships were found in the field. There were 14 sites where relative age relationships were determined, with each of these sites having either a single pair or multiple features showing chronology (Appendix C). The age relationships were studied by observing their relative positions on the outcrop scale, which vary in nature.

The northeast features reflect the oldest flow (Figure 2-13). The majority of the south paleo-flow features, found in the south portion of the study area, are likely to be concurrent and opposite of the northeast flow and separated by the Hall Ice Divide that existed in the area (Marsella et al. 2000). The northeast flows are shown to be relatively older than the north and northwest flows in 11 of the 14 locations studied in the field. The other three sites where a relative age

relationship was observed showed different results. One location showed a relatively older northern flow and younger northeast flow, contrary to what was observed at the bulk majority of the field sites. Another site showed an older north flow, and a relatively younger southwest flow. There was also a single site where there was an older north flow and a relatively younger southwest flow. Many of the relationships studied consisted of younger striae superimposed on or proximal to older northeast features such as chatter marks (Figure 2-13).

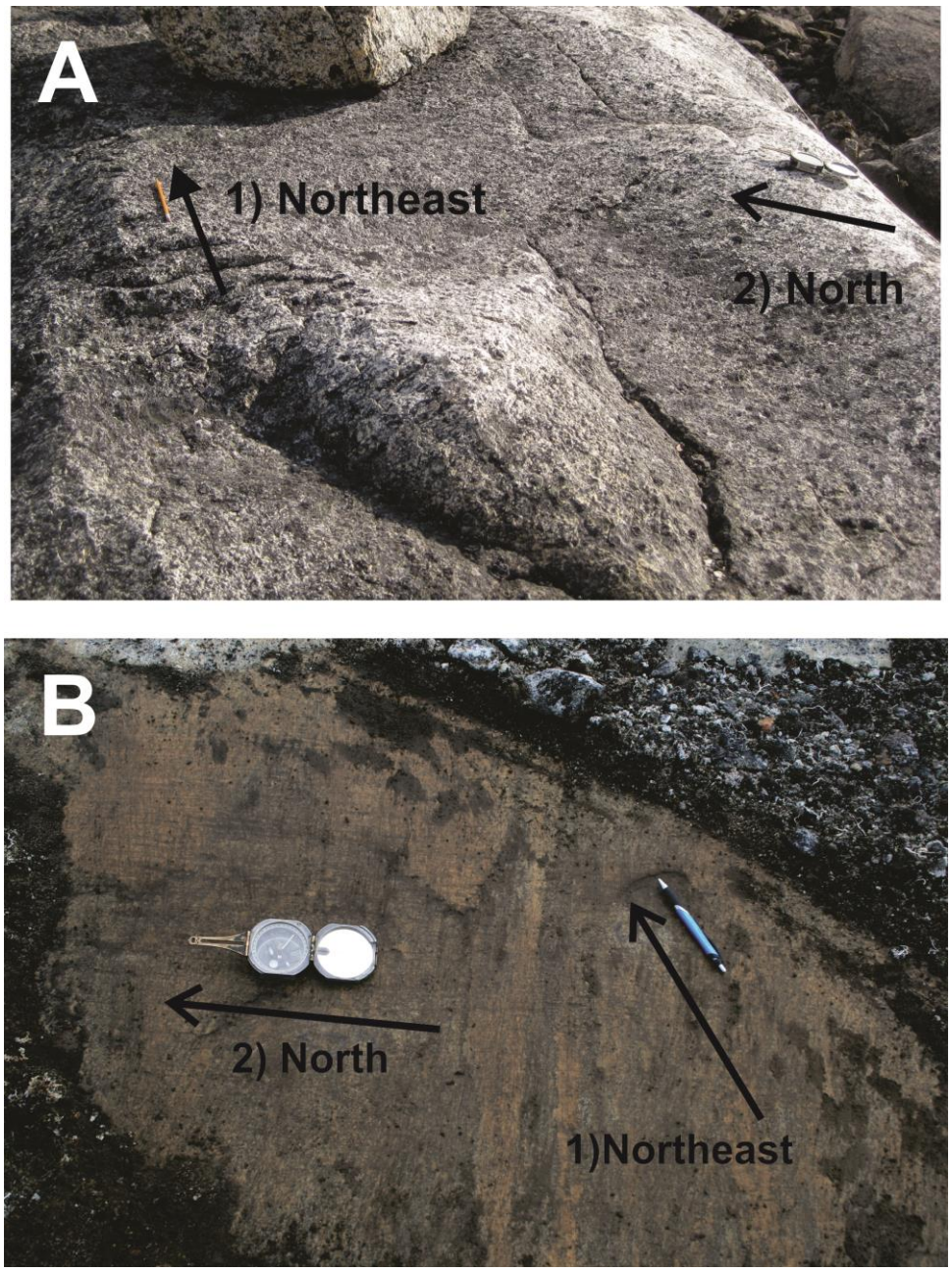

Figure 2-13 A and B: Two examples of the younger (2) striae on abraded surface on top of the outcrop and older crescentic gouges (1). A northward flow direction was determined for the young striations which are ubiquitous at the site on several adjacent outcrops. The rare crescentic gouges found on few rough surfaces are associated to an older northeast flow. These features have a better preservation potential then striations and polished surfaces. They indicate an ice-flow direction parallel to the shape of many individual outcrops suggesting they were primarily moulded by the older flow.

2.9 Interpretation of Ice-flow History

Seven main glacial landform and striation directions were identified and grouped into four phases (Figure 2-14).

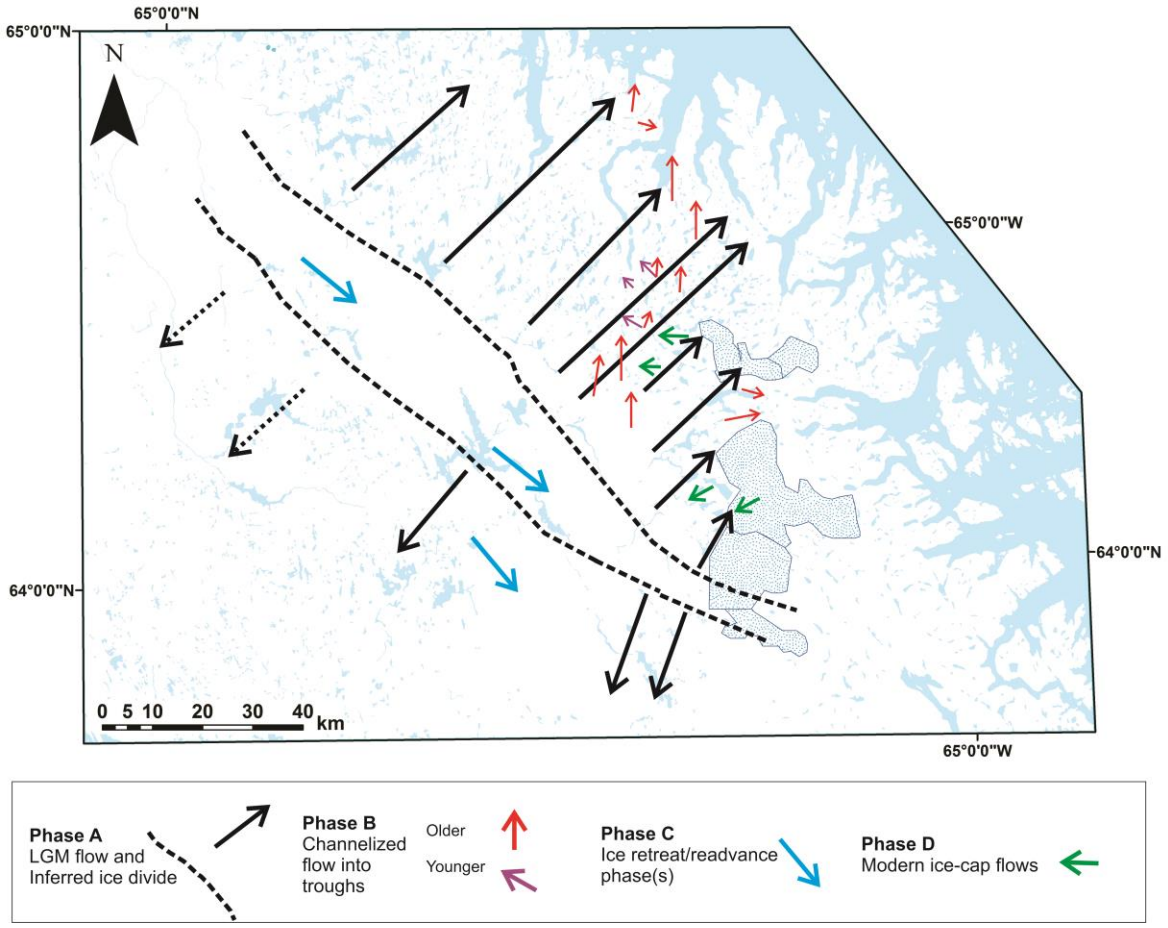

Figure 2-14: Shown is an ice-flow synthesis, in proposed phases A-D. Through field evidence, it is found that phase A is relatively older than phase B and phase D. Phase C, which the moraines are a part of, have been dated

With the relative age indicators in mind, these phases were chronologically ordered. The results of the field and remote sensing based mapping can be summarized and related as such:

a. Regional Flows (Phase A):
    I. Fjord interfluve areas proximal to the coast (between approximately 500 and 850 m asl): Northeast (varies from 20°-70°; average is 43.5°)

II. Southern regions: South (directions between 180°-210°)

b. Fjord influenced areas (between 0 m and 650 m asl) (Phase B):
    I. North (approximately 342°-20°) for northern fjord heads,
        i. Relatively older fjord influenced flow
    II. Northwest (approximately 300°) east side of Ptarmigan Fjord (Figure 2.13)
        i. Relatively younger fjord influenced flow
        ii. Perhaps northeast to the west side of the Ptarmigan Fjord
    III. And east to southeast (72°-112°; 135°) for eastern fjords.
c. Central region (Phase C): Southeast (135°-160°)
d. Hall Ice Cap (Phase D): West (240°-285°) in valleys

The earliest event is the northeast flow interpreted as a regional ice-flow phase (Phase A-I). There is a high degree of parallelism in the orientation of streamlined hills and field-based indicators associated to the northeast flow phase. This suggests that the landscape most likely developed at a time when the ice was relatively thick over that area with ice flow direction being mainly controlled by the ice surface slope. The northeast flows are found throughout the study area, often crosscut by younger flows. The extensive landscape with the strong northeast-trending ice-flow imprint is thus assigned to the LGM. Most of the northeast striations are correlated to this phase, as well as streamlined hills mapped using remote sensing techniques (Figure 2-15). The observations show that the northeast flow was widespread across northern Hall Peninsula. Even proximal to the icecap, northeast flows were found at higher elevations (Figure 15c). Twenty-four southward to south-south-westward ice-flow features are observed in the southern part of the study area (Phase A-II) (Figure 2-11). These indicators are interpreted to be coeval to the northeast features during the LGM reflecting ice-flow on the southern side of a local ice divide.

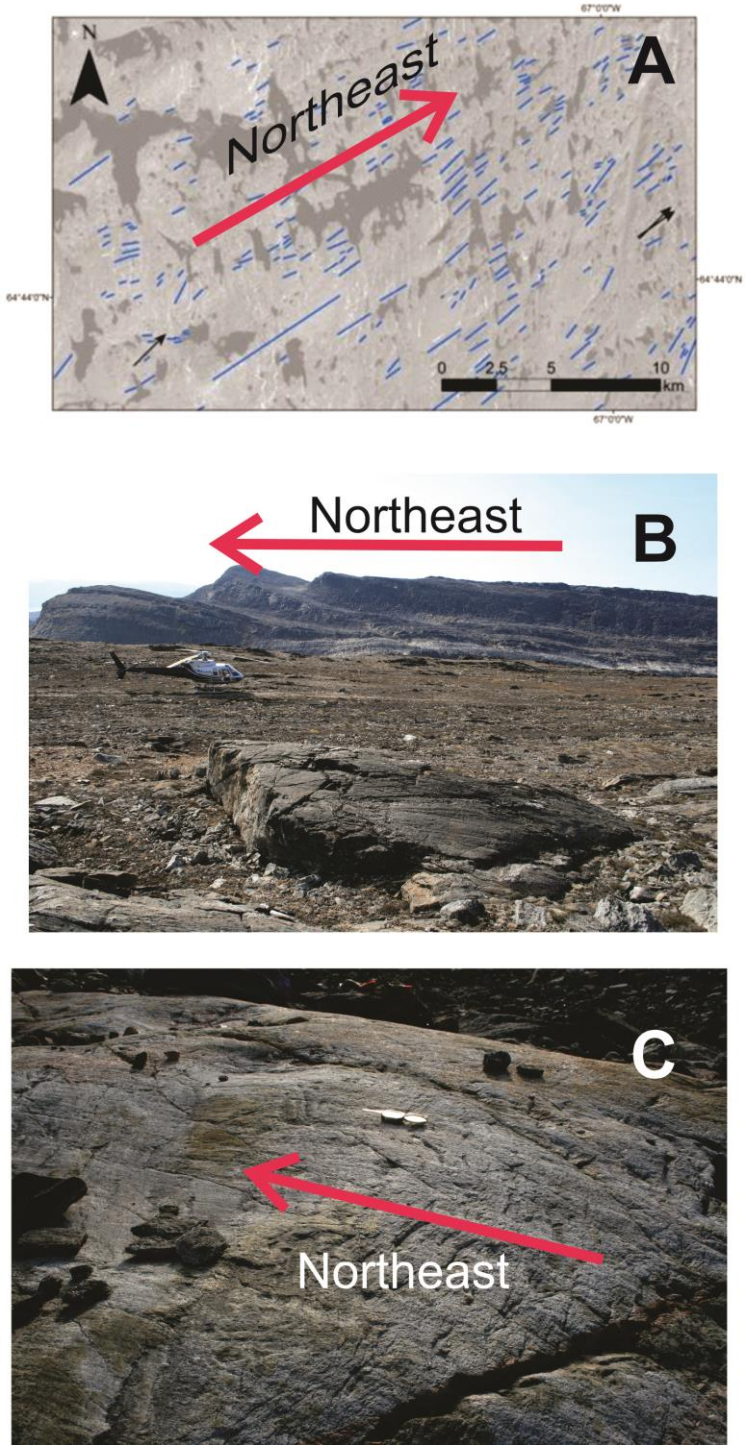

Figure 2-15: (A) Area proximal to the coast showing north-easterly directed streamlined hills (blue lines) and striae (black arrows) and (B) *Roche moutonnée* in the fjord interfluves showing a strong northeast flow near Ptarmigan Fjord and (C) chatter marks and striae showing a northeast flow proximal to the icecap.

During deglaciation, ice-flow became focused into topographical troughs (Phase B). Ice-flow directions associated to that phase are more complex and include multiple directions reflecting convergent ice-flow towards discrete troughs (now forming fjords) (Figure 2-16).

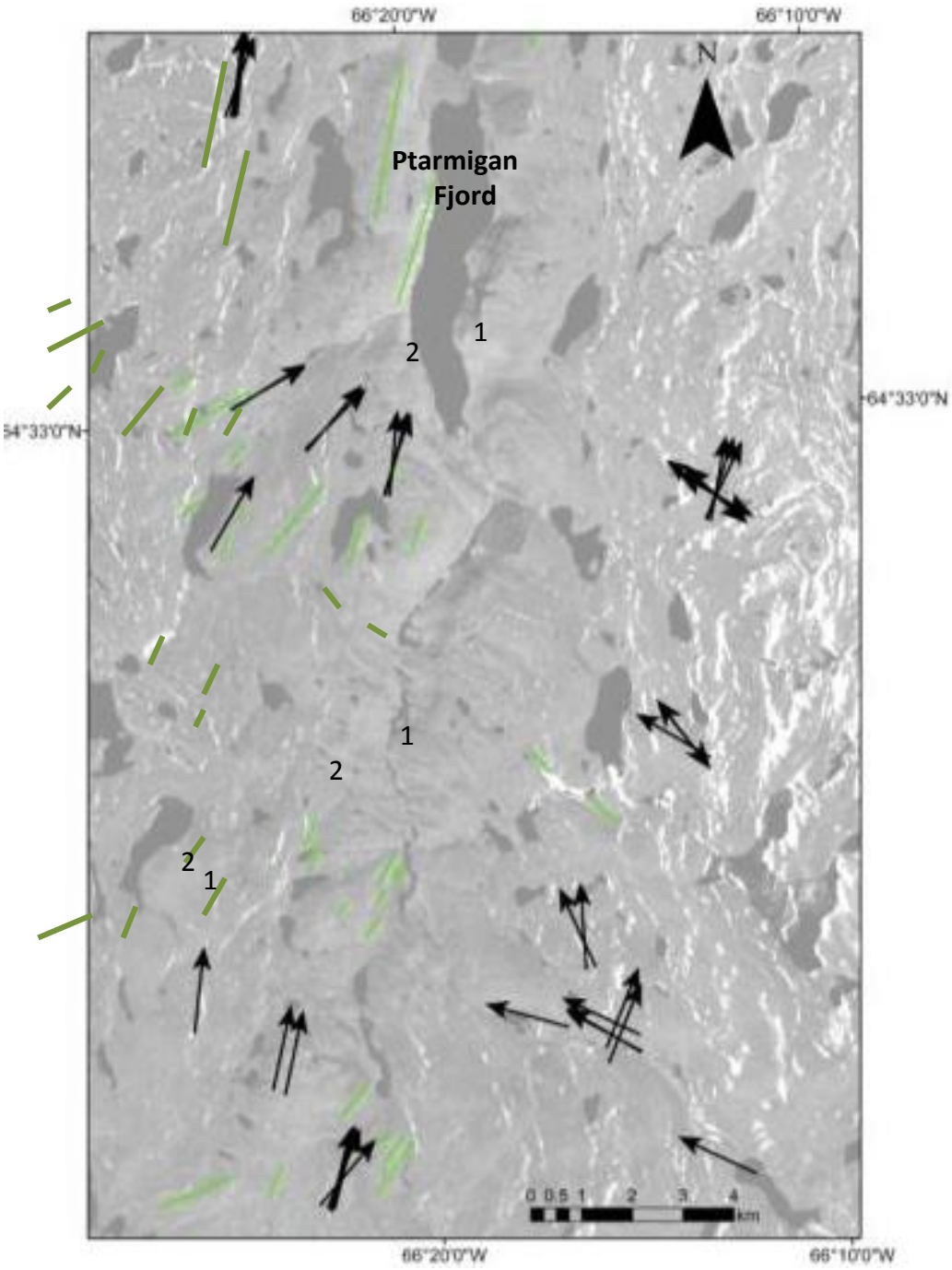

Figure 2-16: Channelized flow as demonstrated by striations (black arrows) and landforms (green lines) showing a span of directions going into the U-shaped valley created by ice draining into Chidliak Bay through Ptarmigan Fjord.

As deglaciation progressed, ice-flow was increasingly topographically controlled. Three sets of striae fall under the earlier deglaciation phase (north, northwest, and east). Some of the northeast flows in the valleys close to the fjords may also be deglacial. The northwest flows, as shown by some of the relative age relationships found, came later as the ice, which is now represented by the local icecap, separated from the LIS. The north flows were found to be older than the northwest flows at two locations. North and east are the best representative directions of that Phase B. Influence of subglacial bed topography on ice flow dynamics increases as ice gets thinner. Erosional forms found in the field demonstrate the effect of the troughs on the ice, as shown by large *roches moutonnées* and drumlins showing north flow, meso-scale northern drumlins, and grooves directed north into the modern fjords (Figure 2-17 a-c).

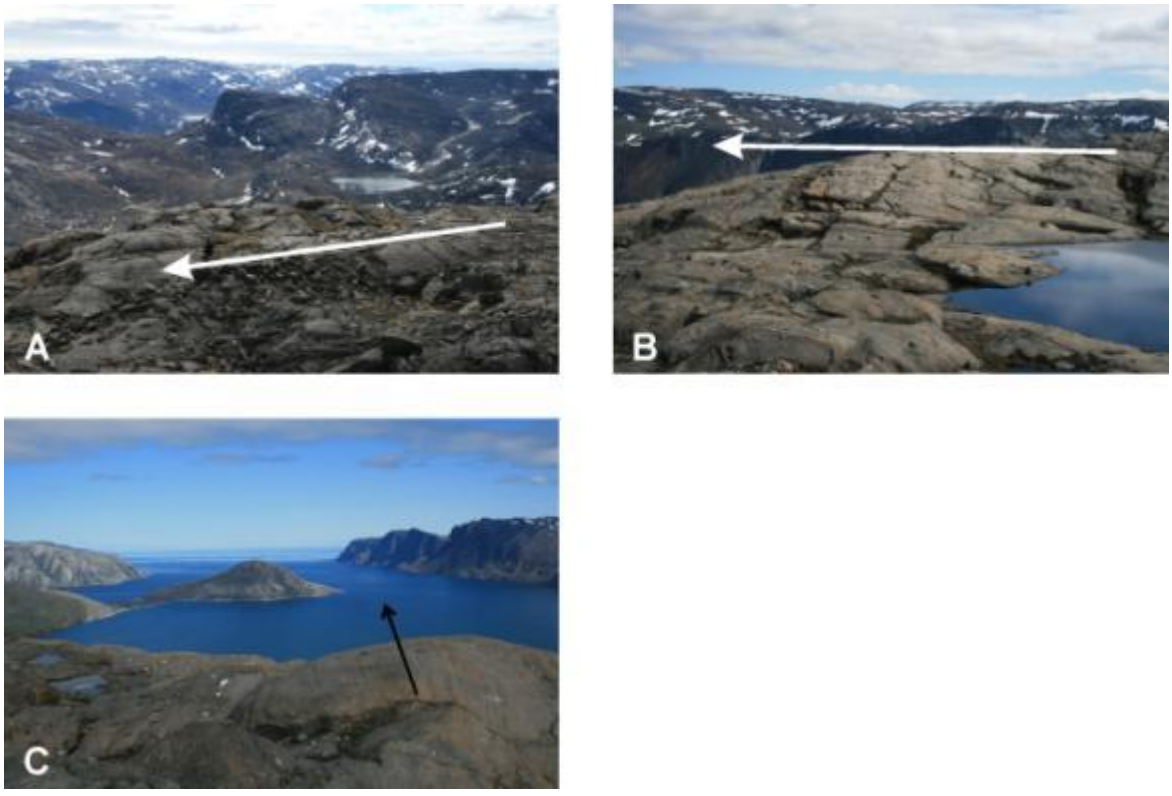

Figure 2-17: Erosional forms demonstrating fjord's topographic effects: a) Large-scale *roches moutonnées*; b) Well-formed grooves; b) Meso-scale drumlins

Southeast striae and possible streamlined hills, amongst the youngest of the flow events, are found in the western portion of the study area (Figure 2-18 a-b). The southeast flows have been

documented previously (Blake 1966; Miller 1980; Miller 1985). The mapped streamlined hills in the area are parallel to bedrock structures seen with geophysical (magnetic) data, and it is unclear whether glaciers have sculpted them. The deposition of Hall Moraine (southeast of the study area) occurred during this deglacial phase (Phase C). The portion of the lobate Frobisher Bay Moraine in the study area is the last local evidence of the LIS.

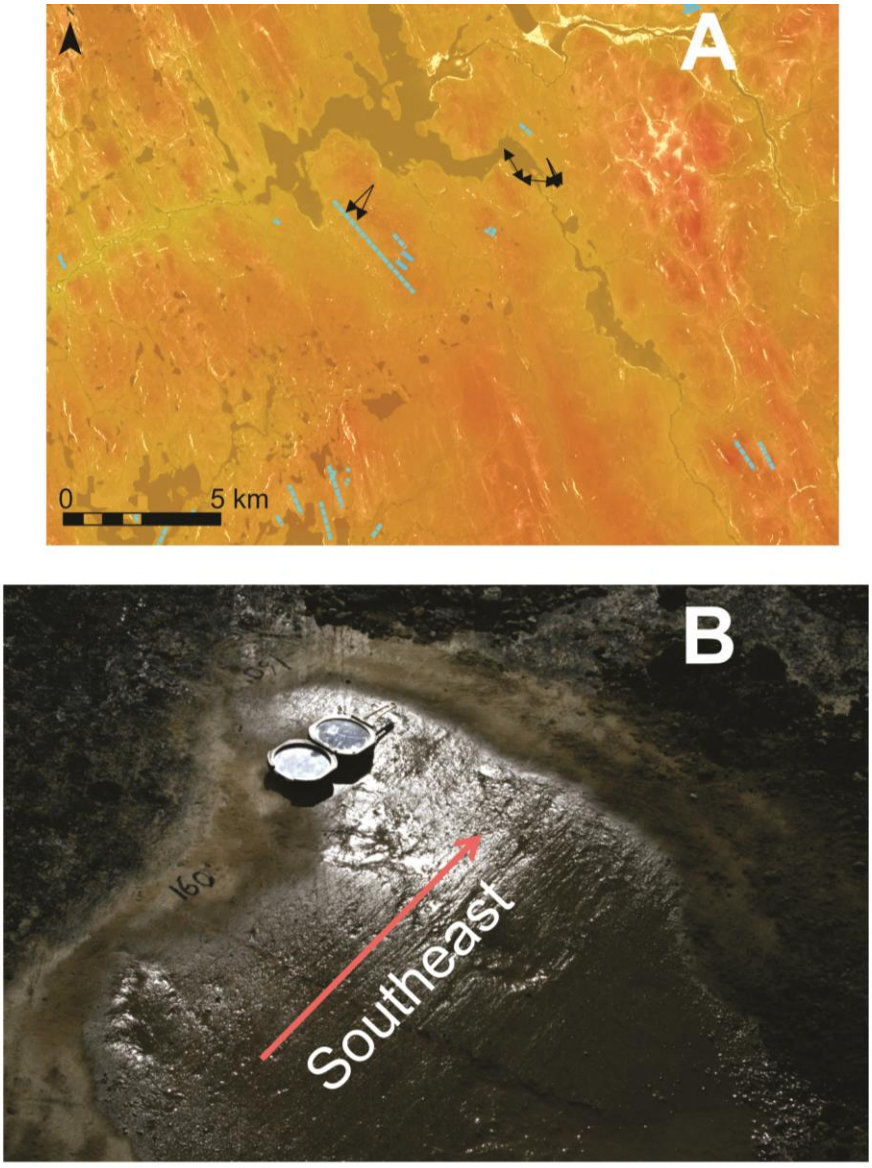

Figure 2-18: Southeast flowing a) streamlined hills and b) striations in the vicinity of the southeast trending bedrock ridges (marked as blue lines on the map). There is a clear southeast ice-flow phase (perpendicular to local moraines). However, the bedrock ridges in A appear to be parallel to prominent bedrock structures as visible on airborne geophysical data as well as in the field. The degree of glacial remoulding of these ridges is unknown, though the bedrock structures are most likely enhanced by glacial abrasion.

The youngest west flows were found in the valleys near the local ice cap, which record movement from the local ice cap (Figure 2-19) (Phase D). West trending paleo-flow features are found in the eastern side of the study area (proximal to the icecap).

Figure 2-19: Late western flows shown with a) striations and b) directional indicators revealing the rounded, up-ice surface and down-ice plucked surface (stoss and lee forms).

For the most part, the higher elevation ridges proximal to the ice cap show the inherited northeastern flow where in the valleys the older flow is overprinted by younger topographically controlled flows (Figure 2-20). There are large scale *roches moutonnées* and micro-scale striations found in valleys proximal to the ice cap (Phase D).

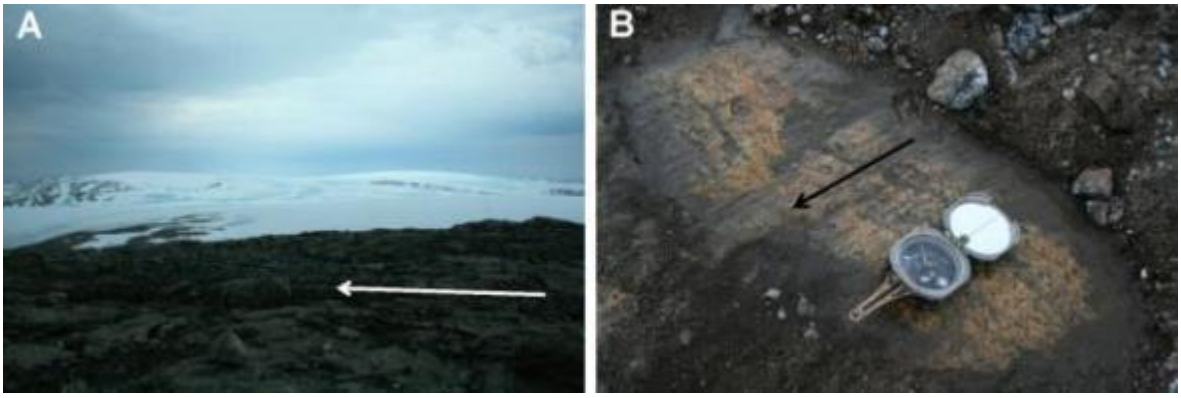

Figure 2-20: a) Northeastern flow (towards the center of the ice cap) associated to the LIS on top of ridges established by b) stoss-lee relationship showing a smooth abraded up-ice surface, and rough down-ice surface.

2.10 Conclusion

With the use of remote sensing and targeted field mapping, a subglacial geomorphological map of Hall Peninsula, Baffin Island, has been completed. Mapping consisted of large, kilometre scale subglacial landforms and sub-kilometre, meso-scale landforms as well as outcrop-scale glacial striae and other paleo-ice-flow indicators throughout the study area. A total of 1293 streamlined hills, one major moraine system, one local moraine, and a series of U-shaped valleys were mapped using remote sensing techniques. A total of 456 paleo-flow indicators were measured in the field (400 striations, 48 chatter marks, and 15 *roches moutonnées*). Such mapping is essential for mineral exploration purposes on Hall Peninsula, Baffin Island, and drift prospecting in northern Canada. It is evident that the glacial history could not have been reconciled from remote sensing alone. Fieldwork was necessary to study discrete flows, as well as directional indicators.

The ice-flow system evolution greatly affects the glacial landscape and sediments, as is shown in southern Baffin Island, and the data reveals a complex glacial landscape mosaic reflecting varying subglacial conditions and ice-flow histories, including four ice-flow phases.

Chapter 3 : Subglacial sediment-landform relationships on Hall Peninsula, Baffin Island: Insights into glacial dynamics evolution

3.1 Introduction

Subglacial landforms often occur in clusters or fields that form under certain conditions. In many areas, landforms with contrasting orientations within the clusters crosscut each other or are found adjacent to each other. Mapping streamlined landforms into flowstages (Boulton and Clark 1990) or flowsets (Kleman and Borgstrom 1996; Clark 1999) have been widely applied as it can lead to the recognition of spatio-temporal shifts in subglacial ice flow dynamics (Kleman et al. 1997, 2008; Clark et al. 2000; Janson et al. 2002; Clark 2009a; Clark 2009b; Trommelen et al. 2012). Flowsets, when analysed in combination with other landform patterns or features of the glacial record, such as the striation record and till compositional data, provide additional insights which can lead to a better understanding of the evolution of subglacial conditions (e.g. thermal regime) and, ultimately, to more comprehensive ice-sheet reconstructions. It has been recognized, through this type of analyses, that glacial landscapes often consist of a mosaic of terrains, or Glacial Terrain Zones (GTZ), where each GTZ has internal characteristics (e.g. sediment-landform relationships) that are distinct from adjacent portions of the landscape (Ross et al. 2009; Trommelen et al. 2012). Through this study, it is also shown that the GTZs also reflect distinctive mineralogy.

GTZ are recognized on the basis of the geomorphic record, but further analysis can also reveal important patterns in till composition that may relate to the GTZ, as till carries the fingerprint of a number of processes that also influence glacial landscape evolution. A number of tools can be used to investigate till composition, and to identify trends and patterns that can then be compared with the geomorphic record to enhance the GTZ analysis and get important insights into subglacial dynamics evolution. On Baffin Island, the Chemical Index of Alteration (CIA) has been used to assess the degree of weathering inheritance in the till (Refsnider and Miller 2010). High CIA values are found in some coastal mountains and in interior plateaus and support the

interpretation that these regions were characterized by low erosion and prolonged periods of cold- based conditions, whereas low values are found at lower elevations, in glacially-scoured troughs (Refsnider and Miller 2010). A number of other proxies such as cosmogenic nuclides and clay mineralogy in tills appear to also show patterns consistent with warm versus cold-based areas derived from the CIA (Staiger et al. 2006; Refsnider and Miller 2013). While these techniques have revealed major contrasts on Baffin Island at the physiographic landscape scale (mountains, high plateaus, and troughs) with clear subglacial thermal zonation and associated erosion record, sediment-landform relationships at the GTZ scale remain poorly understood. This has potential implications for understanding the glacial record and landscape evolution of areas characterized by a wide range of GTZ and ice flow patterns. There are also important implications for mineral exploration in cases where till composition and the ice flow records vary drastically across an area. Hall Peninsula (Figure 3-1) is located on Baffin Island and consists of interior plateaus dissected by several troughs that lead to fjords along the coast. The area is also characterized by a wide range of subglacial terrains and ice flow patterns and is highly prospective making it possible to investigate sediment-landform relationships at a larger scale using extensive industry databases.

In this study we analyse the subglacial landscape of Hall Peninsula, Baffin Island, to develop past subglacial dynamics. In addition, we investigate the degree of spatial relationship of landform assemblages and interpreted subglacial dynamics with subglacial sediment composition. The latter possibly captures the net effect of bedrock geology, topography, basal thermal regime and basal ice flow dynamics and should therefore reveal patterns consistent with the landscape (GTZ) and subglacial dynamics analysis. This study is expected to further advance our understanding of subglacial records (both landforms and sediments), especially the range of GTZ in-between the end-member categories (cold-based and warm-based), as well as to improve understanding of the glacial dynamics history of Hall Peninsula, Baffin Island.

3.2 Location and Geological Setting

3.2.1 Bedrock Geology

The study area is located on north-central Hall Peninsula, Baffin Island. Fieldwork was concentrated within the smaller area represented by the red polygon (Figure 3-1). The larger

area represented by the green polygon shows the limits of remote sensing work (Figure 3.1), and is approximately 25,400 km^2.

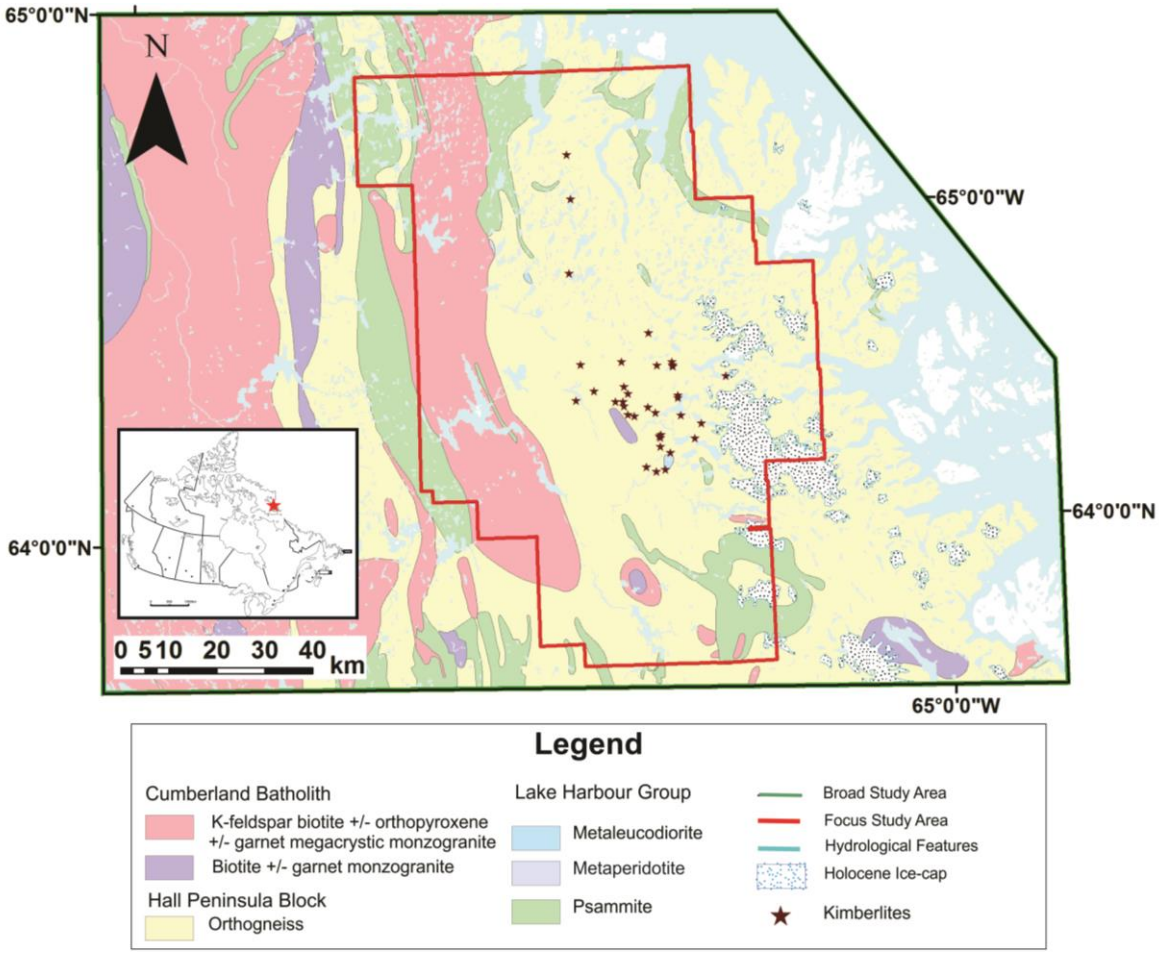

Figure 3-1: Study area and geological map of north-central, Hall Peninsula, Baffin Island, Canada (modified from St-Onge et al. 2006). The majority of this study focuses within the red study area as it is the borders of the field and geochemistry work. Hall Peninsula is underlain by three major crustal units, that include the Cumberland Batholith to the west, a central intermediate belt of Paleoproterozoic metasediments, and an eastern gneissic terrain called the Hall Peninsula Block (Whalen et al. 2010).

In 2006, the bedrock geology map of Baffin Island was released digitally (St-Onge et al.) which compiled previous efforts of reconnaissance scale bedrock mapping by Blackadar (1967) and Scott (1996). Hall Peninsula is thought to be underlain by three major units, that include an eastern Archean Gneiss belt, a central metasedimentary domain that has been correlated to the Paleoproterozoic Lake Harbour Group rocks on Meta Incognita Peninsula, and a western

Cumberland Batholith (Whalen et al. 2012). The bedrock lithologies within the focused study area are as follows (St-Onge et al. 2006):

1. Cumberland Batholith: Located to the west, the Cumberland Batholith is mostly comprised of granulite facies intracrustal (I-type) granitoids which are dated at ~1.865-1.845 Ga in age (Whalen et al. 2010)
2. Intermediate Paleoproterozoic Metasediments (Lake Harbour Group): A central belt consisting of metamorphosed continental margin shelf siliciclastic succession (Whalen et al.2010). This group has been correlated with the Lake Harbour Group strata on Meta Incognita Peninsula (St-Onge et al. 2006).
3. Hall Peninsula Block: The eastern Hall Peninsula Block is a terrain comprised of Archean orthogneissic and supracrustal rocks, which are approximately 2.92-2.80 Ga. It is possible that there are younger clastic rocks that have been reworked to some degree (Scott 1999).

Since 2005, the study area has been the focus of intense diamond exploration and over 60 kimberlite bodies have been discovered (Pell 2011; Pell et al. 2012). The Chidliak kimberlites are located on the Hall Peninsula Block (Pell et al. 2012). The kimberlites found thus far have different morphologies and sizes, ranging from sheet- to larger pipe-like bodies that have plan view sizes of less than one to greater than 50,000 m^2 (Pell et al. 2012). The kimberlites contain mantle-derived xenoliths to variable degrees, which include sodic and chromian garnets, chrome diopside (+/- picroilmenite), and spinel, as well as olivine macrocrysts and phenocrysts (Pell et. al 2012). Some of the kimberlites hold fresh mantle xenoliths, which include websterites, garnet harzburgites, garnet lherzolites, and eclogites that are up to 35 cm in diameter. The dominant groundmass includes spinel, phlogopite, apatite, monticellite, carbonate and serpentine (Pell et. al. 2012). The kimberlites erupted through Paleozoic carbonate rock, which was overlying basement gneisses; the Paleozoic strata have been completely eroded from the area. Carbonate xenoliths are common in the Chidliak kimberlites, and are the only evidence of the Paleozoic strata cover that remain (Pell et al. 2012). Twenty-five of the Chidliak kimberlites have been dated using Perovskite U-Pb technique, which indicated that magnetism took place between 156-138 Ma (Heaman et al. 2012; Pell et al. 2012).

3.2.2 Quaternary Geology

Detailed Quaternary Geology can be found in Chapters 1 and 2. The landscape of Baffin Island shows large spectra of thermal regimes as reflected through bedrock erosion (Andrews 1989 and Miller 2010). The Laurentide Ice Sheet (LIS) inundated Hall Peninsula during the Last Glacial Maximum (LGM), which was from 19-23 ka ago (Dyke et al. 2002). The Hall Ice Divide is thought to have run parallel to the axis of the peninsula flowing from the divide to the southwest and northeast (Marsella et al. 2000).

The study area has been included in regional studies (Andrews 1989; Briner, Davis et al. 2009; De Angelis 2007; De Angelis and Kleman 2007; Dyke et al. 2002 Miller et al. 2002; Miller et al. 2005), but most studies focusing solely on Hall Peninsula look at the deglaciation record (Miller 1980; Miller 1985). The Hall Moraine 10, 760 ± 30 ^{14}C yrs BP (Miller 1980; Miller 1985) is the oldest moraine in the study area, and marks a stable period of the LIS margin as it retreated to the northwest during deglaciation (Miller 1980; Miller 1985). The Frobisher Bay Moraine System is dated at 8,000-9,000 ^{14}C yrs BP (the Cockburn Substage of Miller 1980), and shows that ice flowed parallel to the axis of the margin, so that the ice flowed northwest to southeast (Figure 1.3). Other features of Hall Peninsula include glaciolacustrine shorelines, deltas and overflow channels from proglacial lake systems (Miller 1985). There are two main groups of glacial lakes, one is associated with the Hall Moraine (older) and the other is associated with Frobisher Bay Moraine system (younger) (Miller 1985).

Recent work has also taken place in to the west of the study area (Leblanc-Dumas et al. 2013; Tremblay et al. 2013; Tremblay et al. in press). A zone of regolith has been recognized and studied in detail to the west of the study area (Leblanc-Dumas et al. 2013; Tremblay et al. in press), as well as recognized in previous fieldwork (Chapter 2; Johnson et al. 2013).

The till in the study area is generally thin with locally thicker deposits in the central plateau that reach up to 15 m (Pell 2011). It is thinner in areas proximal to the coasts, where bedrock is covered by a discontinuous thin till veneer. In areas of low elevation such as valley floors the till is also thicker (Pell 2011). The till on Baffin Island consists of either sandy till with abundant

Precambrian clasts (shield type) or a silt-clay rich till with abundant Paleozoic carbonate clasts (Andrews 1989). The till in the study area consists of the shield type of clay with abundant clasts of orthogneisses or Paleoproterozoic metasedimentary rocks, which are found in the study area. Very locally, some till in the study area also has strong kimberlitic composition that includes a green matrix, limestone cobbles, and kimberlite (Johnson et al 2013).

3.2.3 Physiography

Detailed physiography can be found in Chapters 1 and 2. The elevation of the study area ranges from 200 m asl to 700 m asl in a central plateau that decreases towards the northeast to about 200-300 m asl (Miller 1985). Fjords cut into the northern and eastern portions of the study area. The central part of the study area has flat to rolling topography with relatively thicker till (Pell 2012). The western portion of the study area consists of an area of highly weathered bedrock, or regolith. The central area also contains minor glaciofluvial and lacustrine deposits (Miller 1980; Miller 1985). The eastern region contains a Holocene Ice Cap and is characterized by bedrock hills.

3.3 Methodology

In order to understand regional past glacial dynamics, it is essential to decipher the subtleties of glacial erosion, sediment production, transportation and deposition as well as to recognize evidence of distinct subglacial thermal regimes (Trommelen et al. 2012). The subglacial dynamics record is commonly investigated through mapping subglacial landforms and outcrop-scale paleo-flow indicators (Andrews 1989; Kleman and Borgstrom 1996; Clark 1999; Clark et al. 2000; Dyke et al. 2002; Miller et al. 2002; McMartin and Henderson 2004; Kleman and Glasser 2007; De Angelis 2007; McMartin and Paulen 2009; Ross et al. 2009; Ross et al. 2011; Trommelen et al. 2012). Till compositional data also provide important insights into erosion, transport and deposition in the subglacial environment (Klassen and Thompson 1990; Shilts 1984; Shilts 1992) and thus can inform past subglacial dynamics models. Below is a location map outlining the survey and mapping boundaries, as well as locations of select figure (Figure 3-2).

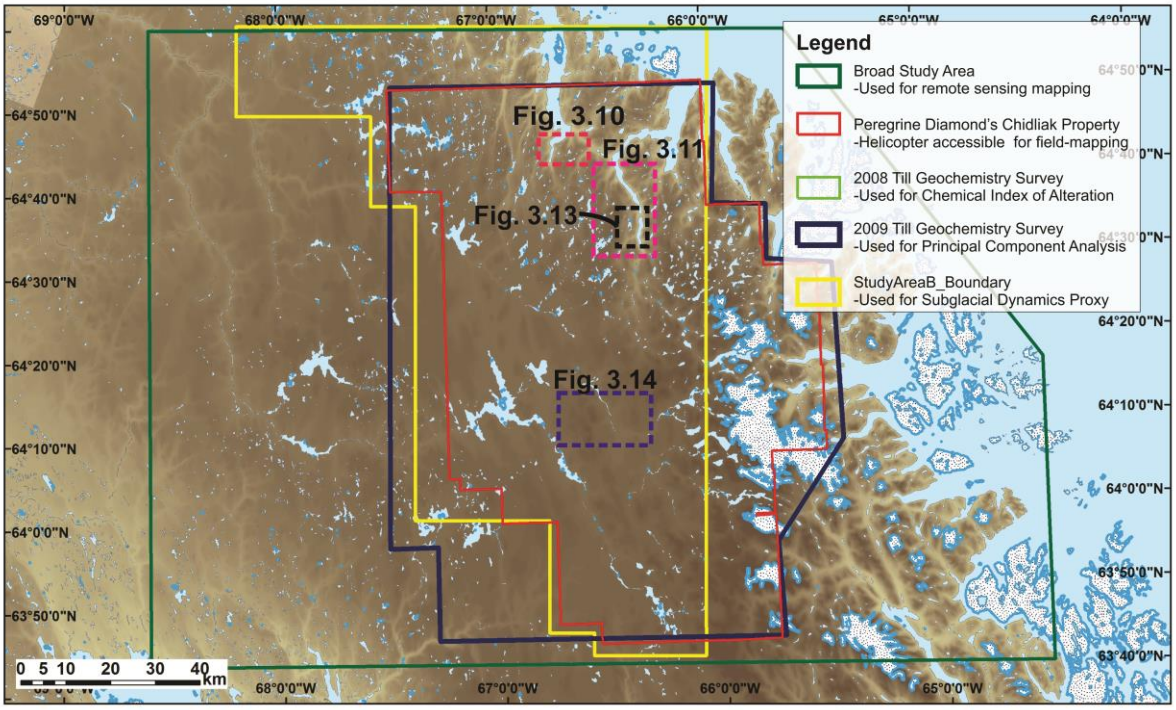

Figure 3-2: Location map showing mapping and survey boundaries, as well as figures highlighting various features.

3.3.1 Remote-sensing based subglacial mapping

The details of the remote-sensing mapping are described in Johnson et al. (2013) [Chapter 2]. Remote sensing was done using LANDSAT7 with Landsat Enhanced Thematic Mapper Plus (ETM+) satellite imagery, publically available digital elevation data obtained from www.geobase.ca, topographic maps and airborne magnetics. The resulting map (Appendix A) was used to identify flowsets, characterize the shape and distribution of glacial landforms, and to outline the GTZ. Unpublished aeromagnetic data provided by Peregrine Diamonds were used to recognize bedrock structural trends, which greatly facilitated the recognition of glacial features that are mainly oblique to these trends. Mapping was done on ArcGIS® (ESRI).

3.3.2 Field based subglacial mapping

The details of the field-based mapping are described in Johnson et al. (2013) [Chapter 2]. Targeted fieldwork took place to map glacial erosional features and to verify the mapping done using remote-sensing techniques. Field based work was done within the red polygon shown in (Figure 3-1). The paleo-flow indicators gathered were primarily small-scale features such as

non-directional indicators like striae, grooves, as well as sculpted outcrops and directional indicators such as chatter marks, crescentic gouges and lee-stoss relationships. Medium-scale features such as drumlins or *roches moutonnées* and whaleback forms were also mapped. If cross-cutting relationships were found in the field, they were documented and analysed to determine, where possible, relative-age relationships. Regional flows were the primary focus, though local flows were studied in high priority areas. As done in Trommelen et al. (2012), the field-based ice flow indicators were studied collectively with and related to the landform record to recognize regional patterns and establish relative age relationships. The coordinate system used for mapping was NAD 83, UTM Zone 19. The full dataset is also available in Johnson et al. (2013) (see also Appendix B).

3.3.3 Flowset Mapping

Flowsets are mapped using the paleoglaciological inversion model (Kleman and Borgstrom 1996), summarizing the geomorphology in independent flow events. For landforms to form a flowset, three criteria are generally met, which are (1) the grouped landforms are parallel, (2) the landforms are of similar morphology and (3) they are within close proximity of each other (Clark 1999; Knight 2010). Generally, if these criteria are met the landforms are interpreted to represent a single and coeval ice flow event. However, isolated paleo-flow indicators are sometimes found in areas of incomplete overprinting, which may have formed from the same ice flow event recorded elsewhere (not proximal) (Trommelen et al. 2012). The flowsets were mapped using traditional remote sensing methods (Boulton and Clark 1990; Kleman and Borgstrom 1996; Clark 1999), but also with the striation record. The flowsets have been studied in terms of their relative chronology (Johnson et al. 2013) where cross-cutting relationship evidence was available.

3.3.4 Subglacial Dynamics Proxies: Coupling bedrock controlled lake and streamlined hill data methodology

The density of bedrock-controlled lakes has been used to gain insights into glacial erosion intensity (Andrew 1989; Hodder 2012). The shape of subglacial landforms has also been used to get insights into subglacial processes (Clark et al. 2000; Stokes and Clark 2002; Stokes and Clark

2003; Clarke 2005) using the assumption that the elongation of drumlins and similar landforms reflects the intensity or velocity of basal ice flow. One parameter that is commonly measured is the elongation of drumlins. The elongation *E* is the ratio of the length *L* to its width *W* (E=L/W), whereby *L* corresponds to the long axis of the landform and *W* is measured across the landform's centroid. Results are often mapped using a grid or raster approach to examine the spatial patterns (Stokes and Clark 2002).

In this study, bedrock-controlled lakes were mapped using a Geographic Information System (GIS). Spatial information which included digital elevation and hydrographic data were obtained from www.geobase.ca, and Landsat images were projected using ArcGIS® (ESRI). A grid was created in ArcToolbox with each cell representing 25 km^2 areas (5 km x 5 km) (Hodder 2012). Lake polygons were created using the hydrographic data, and the centroids of each lake were calculated within each grid cell to study the density of lakes in the region (Hodder 2012). Particular regions in the study area were masked, such as the moraines and the ice cap areas, as the lakes in these areas are not bedrock controlled. Polygons of individual streamlined hills were digitized in ArcGIS, and the elongation ratio calculated from the length and width of each polygon. The length and width of the polygons were calculated following the procedure of Clark et al. (2009). The polygons were hand drawn, and the perimeter and area were exported from ArcGIS into an Excel file, where length and width were calculated from the following two equations (

Equations 3-1 a -b):

Equations 3-1 a - b: Equations used to calculate the length and width from the area and perimeter of streamlined hill polygons mapped in ArcGIS (Clark et al. 2009). The symbol p^i represents the perimeter and A represents the area of a landform polygon.

a) Length, $L = \frac{1}{\pi}\sqrt{P^2 + \sqrt{P^4 - 16\pi^2 A^2}}$

b) Width, $W = \frac{1}{\pi}\sqrt{P^2 - \sqrt{P^4 - 16\pi^2 A^2}}$

The length and width were then used to calculate the elongation ratio (E=L/W) and exported back into ArcGIS.

Streamlined hill elongation ratios were also calculated per grid cell for comparison with lake density results using GIS overlay techniques. The subglacial dynamics index, which includes both the lake density and streamlined hill elongation ratio (Hodder 2012), was applied to classify cells using the Jenks natural breaks. The lake density and streamlined hill elongation ratios were combined to show the spatial distribution of "ice vigor" (Hodder 2012), or areas where the ice was most active. In summary, it outlines areas with a high number of lakes, striations, and streamlined hills. Similar methods utilizing indexes have been used in the Canadian Arctic (Tremblay et al. 2011)

3.3.5 Glacial Terrain Zone Mapping

Due to shifting subglacial conditions and the complex interplay of erosion, transport, and deposition, the record of subglacial landscapes is often fragmentary forming a mosaic of discrete assemblages of landforms and sediments (Clarhäll and Jansson 2003; Ross et al. 2009; Trommelen et al. 2012). Glacial terrain zone mapping (Trommelen et al. 2012) combines classic flowset mapping with field data (paleo-flow indicator data, relative age relationships, terrain observations etc.) to identify, map, and analyse mosaic subglacial landscapes. Glacial terrain zone mapping along with the proxies described above are used to analyse the landscape of north central Hall Peninsula. With this approach, flowsets are first recognized, and then GTZ are delineated and their outline refined by the subglacial dynamics proxies. The map layers displaying the subglacial landform map, subglacial dynamics index, and the directional information of the kimberlite indicator mineral trains were overlain in ArcGIS, and the borders were digitized manually.

3.3.6 Geochemical Studies

3.3.6a Chemical Index of Alteration

Another proxy used to study subglacial dynamics is the Chemical Index of Alteration (CIA), which provides insight into the amount of weathered material in the till which could indicate

inheritance from pre-glacial regolith or interglacial weathering of old till (Nesbitt and Young 1982; Refsnider and Miller 2010). The CIA can thus be viewed as a proxy of erosion intensity because evidence of high inheritance in the surface till is indicative of low erosion. The CIA is a ratio of primary minerals to chemical weathering by-products in sediments, where the minerals are expressed as molar proportions (wt% divided by molecular mass) and the CaO* is the non-carbonate phase (

Equation 3-2) (Nesbitt and Young 1982; Refsnider and Miller 2010).

Equation 3-2 (Nesbit and Young 1982)

$$CIA = [Al_2O_3/ (Al_2O_3 + CaO^* + NaO + K_2O)] \text{ X } 100$$

The till samples from the utilized database were collected in a semi-rectangular grid of approximately 70 km x 120 km, which is shown with the green polygon (Figure 3-2). The actual sample locations are shown in Figure 3-3. The till samples were collected in 2006 and 2008, and analysed using total digestion ICP-MS (Inductively Coupled Plasma Mass Spectrometry) at SRC labs in Saskatchewan, Canada, which combines high temperature inductively coupled plasma source with a mass spectrometer. The atoms of the element in each sample are converted to ions by the ICP source. Once the elements are deduced to ions, the mass spectrometer separates and detects them (www.usgs.com). The (<180 μm size fraction) database contains data for 1591 samples (Appendix E). The calculations leading to the CIA were done in Microsoft Excel (Appendix E), and were displayed in ArcGIS with a NAD83 Zone 19 projection.

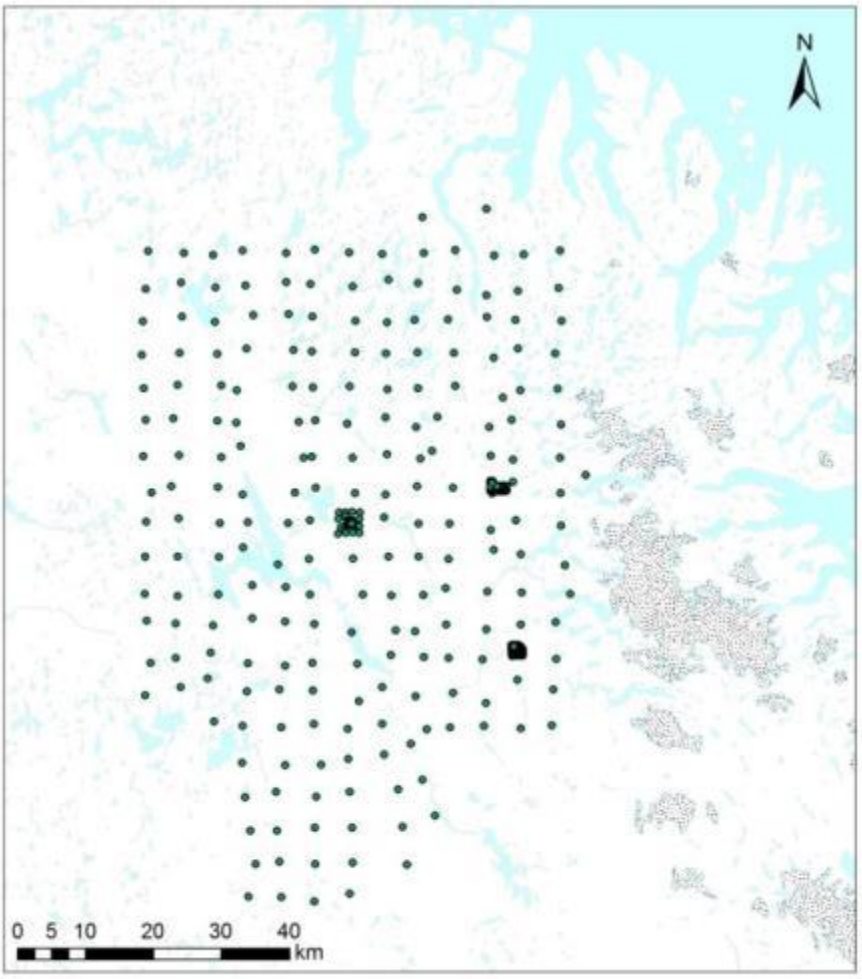

Figure 3-3: Locations of the till geochemical samples used in the chemical index of alteration.

3.3.6b Geochemistry Multivariate Statistics

The hypothesis to test with multivariate statistics is that till characteristics, its composition in particular, might have a signature unique to GTZ. This is because till is generally a mixture of first-cycle sediments (particles derived from direct erosion of fresh or weathered rocks) and reworked (multi-cycle) pre-existing sediments, the proportions of which may vary according to the same processes that led to the development of the mosaic landscape (GTZ). Another factor to consider is bedrock lithological changes: if a GTZ overlaps a major change in bedrock lithology and the till is locally derived, the sediments within the GTZ will have varying composition. This could reveal important insights into the role of bedrock on GTZ development and overall glacial landscape evolution.

A second till geochemistry sampling program was taken over the study area by Peregrine Diamonds Ltd. in 2009. The survey consisted of 1276 till samples, and was collected over a semi-rectangular approximately 70 km x 120 km across (Figure 3-4). The preferred sample medium was frost boils with the approximate depth of 30 cm. A large region in the middle of the property was not sampled as a part of the program. The sample aliquots were tested at Acme lab with partial digestion using Aqua Regia method, which uses a combination of concentrated hydrochloric and nitric acids to leach sulphides, some oxides and some silicates. This database contained results on the clay-sized fraction (< 2 μm), which is the most valuable because many cations are concentrated in the clay fraction due to mineralogical and chemical partitioning (Shilts 1984). Compositional data was analysed using various plots such as bivariate plots, and ternary diagrams in order to recognize different compositional assemblages. However, patterns can be quite complex or subtle and the database contains a wide range of elements. Multivariate analysis is a powerful approach to handle this type of dataset (Grunsky 2010) and Principal Component Analysis (PCA), for example, have been used for the study of tills (Grünfeld 2007; Refsnider and Miller 2013).

Figure 3-4: Locations of the till geochemistry samples used for multivariate statistics.

Several steps were taken to prepare the database for multivariate data analysis. The database contained censored values that are lower than the limit of detection. Elements with high numbers of censored values were removed before applying PCA because these elements do not indicate any obvious process in the study area (Grunsky 2010). The elements dropped because of the high amount of censoring were Sb, Bi, B, W, Tl, S, Hg, Se, Te, Ge, Hf, Ta, In, Re, Be, Pd and Pt. Many elements with fewer censored values were replaced using the imputation of missing values in compositional data using knn methods (impKNNa) function from the robCompositions package software, which is plugged into R-environment statistical software (Hron et al. 2010).

After the censored values were replaced the data was examined in a multivariate context using PCA, which is a dimension-reducing technique (Grunsky 2010). PCA is a method used to describe variation and recognize patterns in large multivariate datasets (Grunsky 2010). By using

PCA, it is possible to view data in a multi-dimensional space, where the first principal component (PC 1) accounts for the majority of the variance in a set of data, and each succeeding component accounts less variance than the preceding component.

Patterns observed from the PCA results can be used as a basis for defining targets or background groups from the till geochemical database. If patterns are found, then techniques such as linear discriminant analysis (LDA) can be used to test the ability to classify and/or categorize sample groups and find which elements have the strongest discriminating power (Grunsky 2010). In other words, the principal components can be tested using linear discriminant analysis to see what elements have the most control over the patterns. LDA tests the accuracy of the PCA by comparing the samples that fell within the GTZs mapped using geomorphology to the samples that were placed in a GTZ by the PCA. Since there were patterns found in the PCA results, linear discriminant analysis was applied to the data to determine if the GTZs could be predicted by their till geochemistry.

Further analyses were conducted by studying two probability estimates to test robustness: posterior probability and typicality probability (Grunsky 2010). These two sets of numbers were output for each sample by R-environment when linear discriminant analysis was completed. Posterior probability forces the samples into one of the GTZ, where the typicality involves the Mahalanobis distance (Grunsky 2010) which estimates the distance of an observation to a centroid or a common point, and is dependent of the covariance and mean of the multivariate. With typicality, it is possible that some of the samples in typicality might not be placed in any class (Grunsky 2010). This analysis shows the predicative capability of the PCA, or the likelihood that a sample would be associated to its GTZ based on geochemistry alone. Posterior probabilities and typicality probabilities for each of the 5 predicted GTZ from the LDA were studied. The results were then interpolated via krigging to study any existing spatial patterns.

In summary, in order to gain insight into the geochemical characteristics of the GTZs, the data was manipulated in the following ways:

1. The values in the database were labelled according to their GTZ (1-5)
2. The values were log-centre transformed

3. The database was ran through a principal component analysis,
    a. Hypothesis: If the GTZs group together in the PCA, there would be a correlation between geochemistry and the GTZ
4. An isometric log-ratio transform was applied to the data and subsequently classified using linear discriminant analysis, based on the GTZs as reference groups.
5. The linear discriminant analysis resulted in posterior probability and typicality results for each of the 5 predicted GTZ. These were visualized in ArcGIS and interpolated via krigging to study any existing patterns.

3.4 Results

3.4.1 Remote sensing mapping

A total of 1293 streamlined hills were mapped using remote sensing and confidently interpreted to be glacial in origin; most ridges have typical glacial landform shapes and are oriented oblique or perpendicular to bedrock structures visible on Landsat or aeromagnetic maps. The Frobisher Bay Moraine (Miller 1980; Miller1985), Hall Moraine (Miller 1980; Miller 1985) and a series of u-shaped valleys were also mapped using remotely-sensed data. To summarize, there were 4 major orientations recognized in the landform record which from relatively oldest to youngest are as follows: (1) ice-flow to the northeast in fjord interfluve regions; (2) to the northwest and north in relation to the northern fjords; (3) to the east along the eastern coast; and, (4) southeast central to the study area (Figure 2-4) (Johnson et. al 2013).

3.4.2 Field-based results

Targeted field based mapping resulted in 456 paleo-flow feature measurements from 413 stations, including small-scale features such as striae and crescentic gouges, and medium-scale features such as rock drumlins and *roches moutonnées*, and cross-cutting relationships. This field-derived data helped recognize and confirm flowsets and their crosscutting relationships (Figure 2-9).

3.4.3 Flowset Mapping Results

The results of both remote sensing and field-based mapping of ice flow indicators were grouped into six distinct flowsets (

Figure 3-5). The flowsets are numbered 1-6, with flowset 1 being subdivided into 1a and 1b (

Figure 3-5). The flowsets are characterized as follows:

- **Flowset 1a** (northeast): This flowset includes laterally extensive fields of parallel streamlined hills oriented to the northeast. Cross-cutting relationships both at the landscape and outcrop scales (Johnsons et al. 2013; Chapter 2) reveal this flowset is the oldest on record in the study area.
    - **Flowset 1b** (southwest)**:** Clear outcrop-scale ice flow features indicate ice flow towards the south and southwest (Johnson et al. 2013; cf. Chapter 2). This flowset is not clearly defined at the landform-scale and is possibly of similar age than 1a
- **Flowset 2** (north): This flowset is spatially associated with a broad valley that extends from fjords along the north coast and indicates more focused north-trending ice flow that crosscuts flowset 1a in 14 locations. This younger flow clearly shows linear erosion which is largely represented by Ptarmigan Fjord.
- **Flowset 3** (northwest): A number of topographically-controlled ice flow indicators show ice flow towards the northwest flowing into Ptarmigan fjord. This flowset could be associated with the same phase as flowset 2 forming a converging pattern. However, the exact relationship with flowset 2 is not clear and flowset 3 could be linked to a time-transgressive shift within flowset 2. Two relative age relationships (Figure 2-12) supporting a flowset 3 as relatively younger than flowset 2 were documented.
- **Flowset 4** (east): The east flows are confined to valleys, and are found near the modern ice cap. The eastern fjords directed these flows. The timing of these flows is not known, but are deglacial flows topographically controlled as the LIS drained through the eastern fjords into Cumberland Sound.
- **Flowset 5** (west): The west flows are also confined to valleys. Flowset 4 and 5 two flows may have been concurrent, flowing on opposite sides of a smaller ice divide. West flows can be found close to the modern day ice cap, and are probably the youngest streamlined landforms in the study area.
- **Flowset 6** (southeast): The southeast flowset includes the flows that are spatially associated with the Frobisher Bay Moraine and the Hall Moraine. They reflect late

deglacial lobate flows which could have formed during short-lived readvances during general ice margin retreat

By mapping these flowsets, it is clear that segments of the landscape have distinct characteristics, and, therefore, subglacial dynamics and histories.

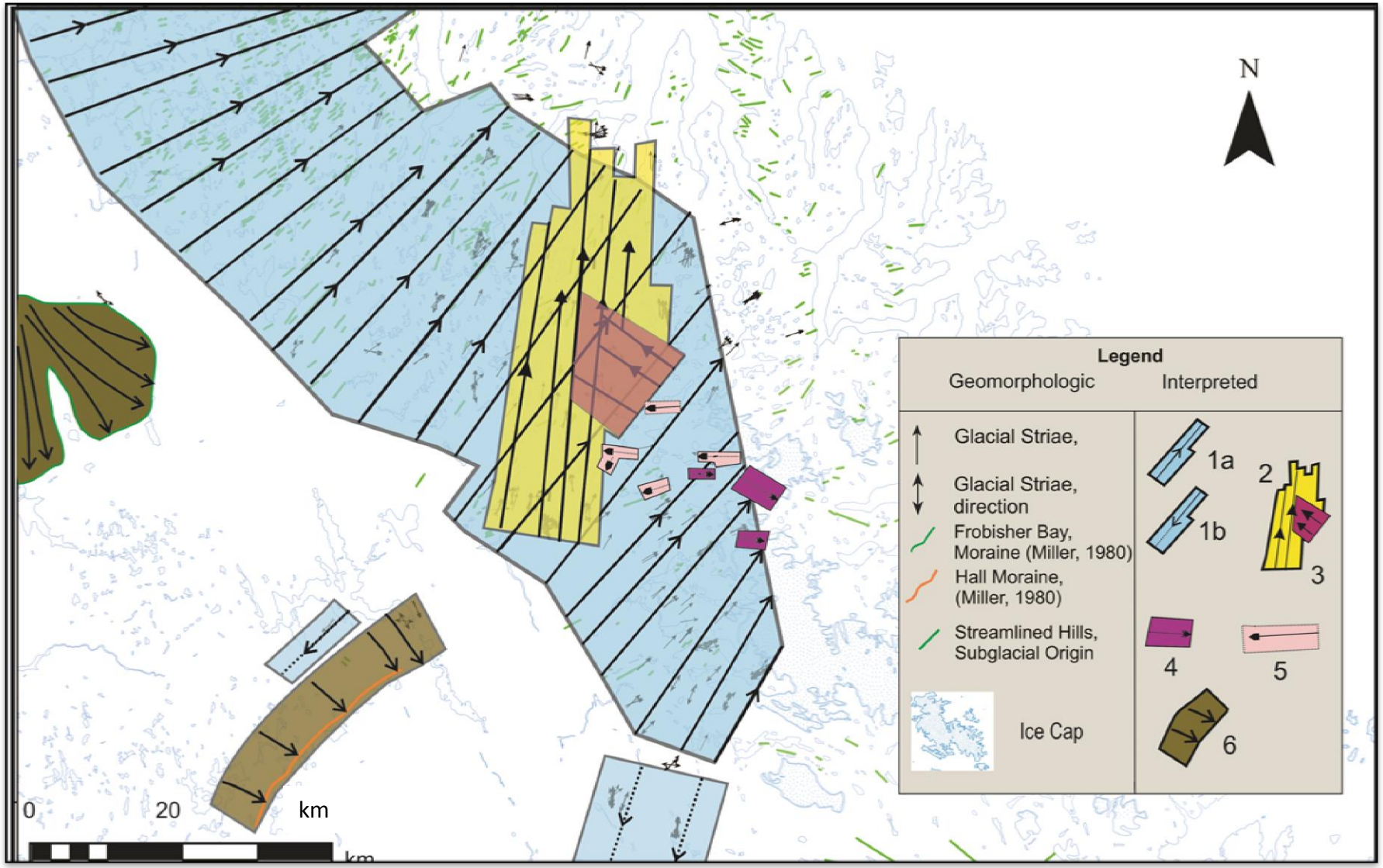

Figure 3-5: Interpreted flowsets based on field and remote observations (Johnson et al. 2013). The southwest flowset (1b) is thought to be contemporaneous with the northeast flowset (1a), with the intervening area between the two flowsets representing the Hall Ice Divide. The fjord directed flowsets are found locally around Ptarmigan Fjord, with striae azimuths going north (yellow-2) and northwest (red-3). To the east near the ice cap, northeast flows are found on the tops of ridges (blue-1a), but east fjord-directed flows (purple-4) and the inferred ice cap westward flows (pink-5) are found locally within the valleys. The southeast flows (brown-6) are based on outcrop-scale ice flow indicators and moraines.

3.4.4 Subglacial dynamics proxy results

3.4.4a Coupling bedrock controlled lake and streamlined hill proxy results

The density of bedrock controlled lakes and elongation ratios of streamlined bedrock hills highlight areas of higher and lower areal scour in the study area. The resulting index values (Table 3-1) were used to produce maps highlighting the differences of scour throughout the study area.

Table 3-1: Subglacial Dynamics Indexed Values and Streamlined Hills Density Classes. The total number of cells in the study area was 348. The lake density and elongation ratio indexes were combined to produce a final index which went into the Subglacial Dynamics Index, creating a comprehensive view of subglacial dynamics. For example, if a pixel had 12 lakes giving it a value of 1, and an elongation ratio of 1.75 giving it a value of 2, the Subglacial Dynamics Value would be 3 (Modified from Hodder 2012).

Lake Density			Streamlined Hill Elongation Ratio			Streamlined Hill Density	
Class	Number of Cells	Indexed Value	Class	Number of Cells	Indexed Value	Class	Number of Cells
0-13	176	1	No Hills	192	--	0	192
14-30	92	2	1.37 - 1.69	25	1	1 - 3	70
31-47	39	3	1.70 - 1.88	52	2	4-9	51
48-66	25	4	1.89 - 2.10	58	3	10 - 15	22
67-91	16	5	2.11 - 2.50	18	4	16 - 21	6
			2.51- 3.20	3	5	22-30	7

A higher density of elongated streamlined hills characterizes the northwest portion of the study area, along with more bedrock controlled lakes. The central area by comparison is relatively featureless (Figure 3-6; Figure 3-7**).** Though this method highlights areas of high areal scour in the northwest, areas of high linear erosion around Ptarmigan Fjord found in the north are not accentuated.

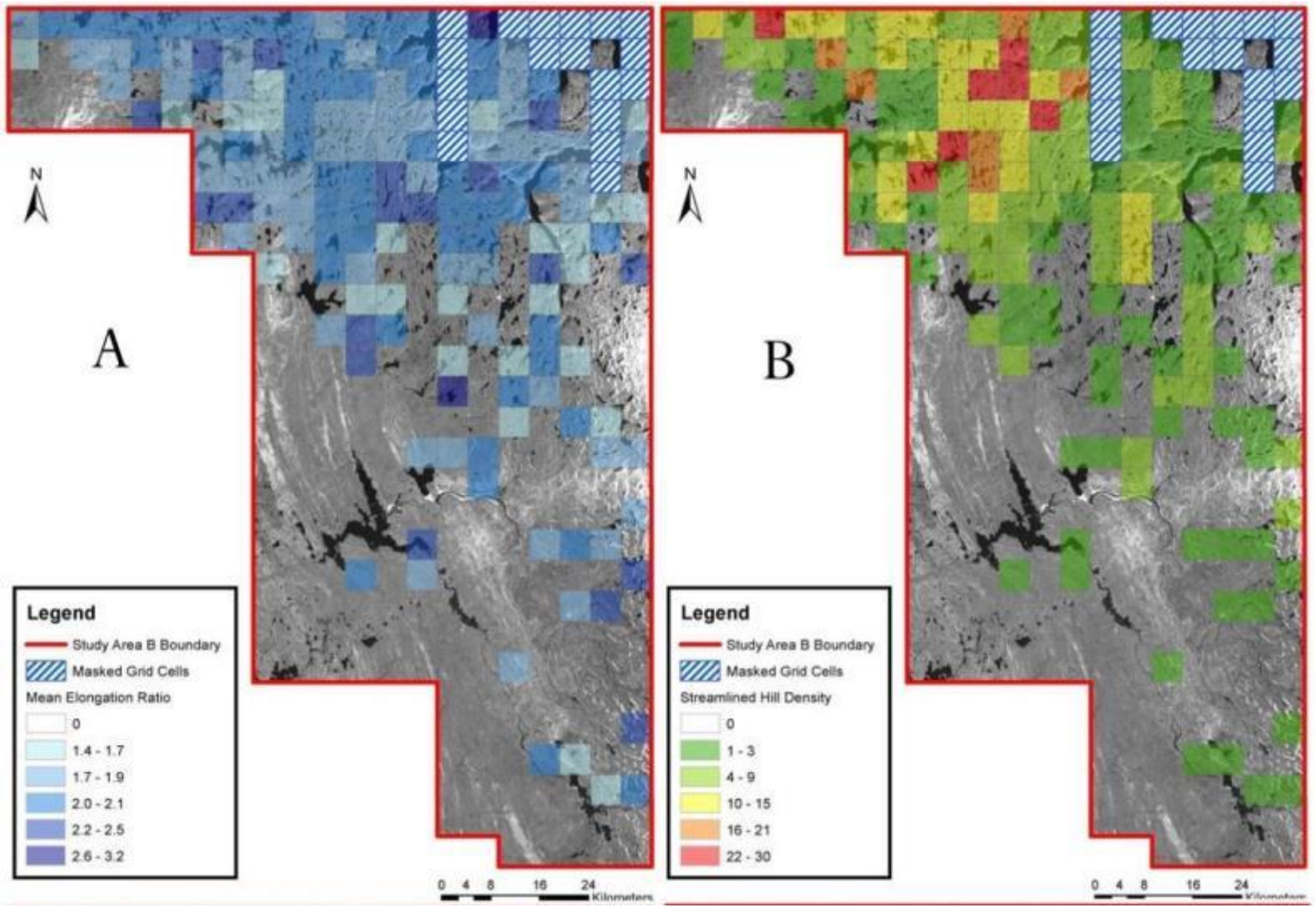

Figure 3-6: These two maps and the two maps shown on the following page (Figure 3-7) show some of the proxies of subglacial dynamics over the study area: A) Elongation ratios of streamlined hills; B) Streamlined hill density. Figure modified from Hodder (2012).

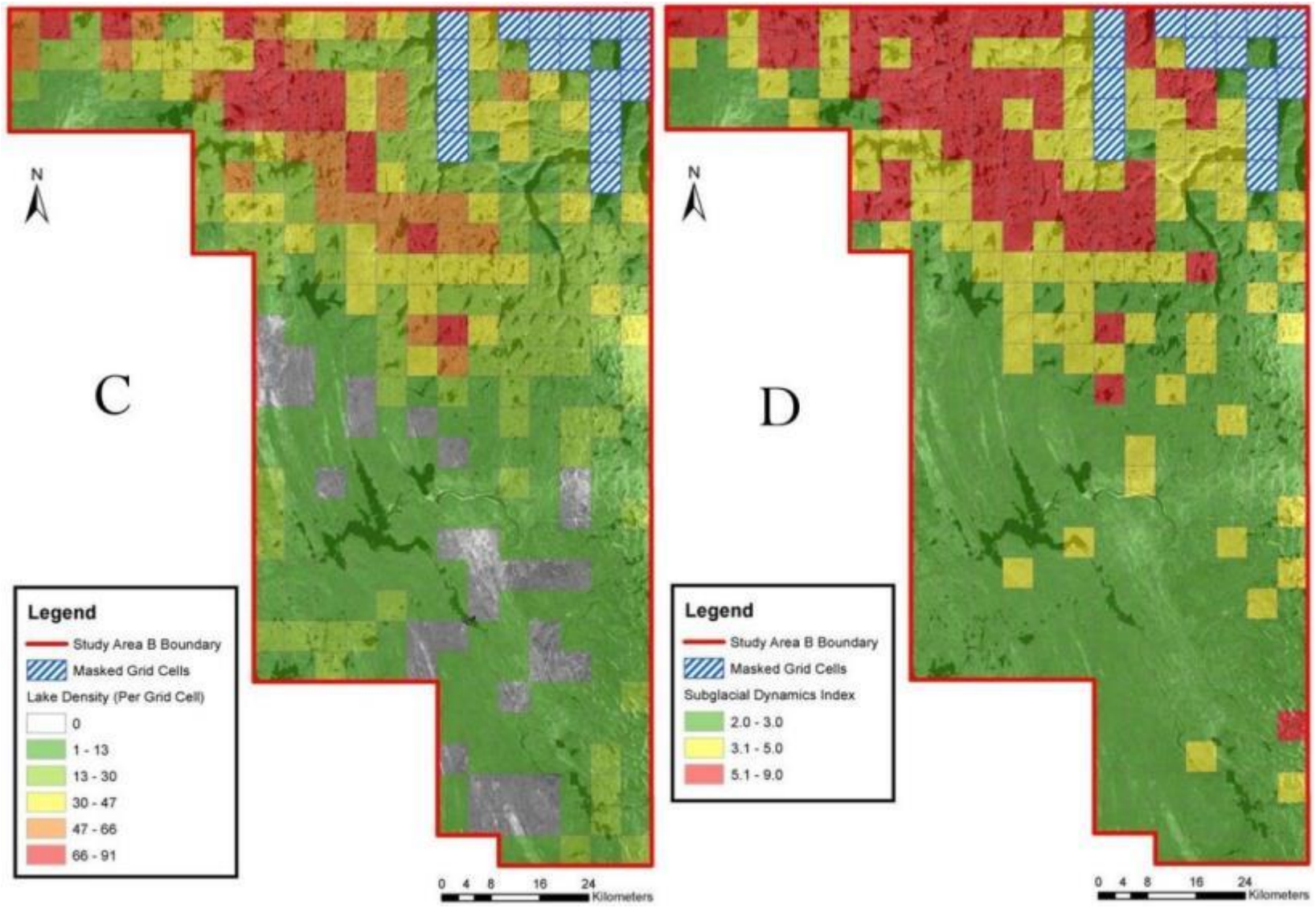

Figure 3-7: These maps, and the maps shown on the previous page (Figure 3-6) show some proxies of subglacial dynamics over the study area: C) Bedrock controlled lake density and D) Subglacial dynamics index made by combining lake density (B) and streamlined hill elongation ratio (A) following Hodder (2012) methodology. Figure modified from Hodder (2012).

3.4.5 Glacial Terrain Zone Mapping

Five distinct GTZs were delineated based on the multifaceted results presented above (Figure 3-8). The degree of landscape inheritance and overprint varies across the GTZs, each recording a portion of the glacial dynamics history over the study area. Some zones are better defined than others because of the extent of fieldwork done throughout the property. By piecing together the records in each of the zones, a more complete paleoglaciologic reconstruction is achieved. The five GTZs are briefly summarized as:

GTZ 1: Preserved northeast ice-flow system and moderate to high areal scouring
GTZ 2: Channelized flow system (linear erosion)
GTZ 3: Local ice cap and valley flows (linear erosion in valleys; cold-based on hill tops)
GTZ 4: Relatively featureless with more continuous till cover
GTZ 5: Southeast trending features, perpendicular moraine and areas of felsenmeer/regolith

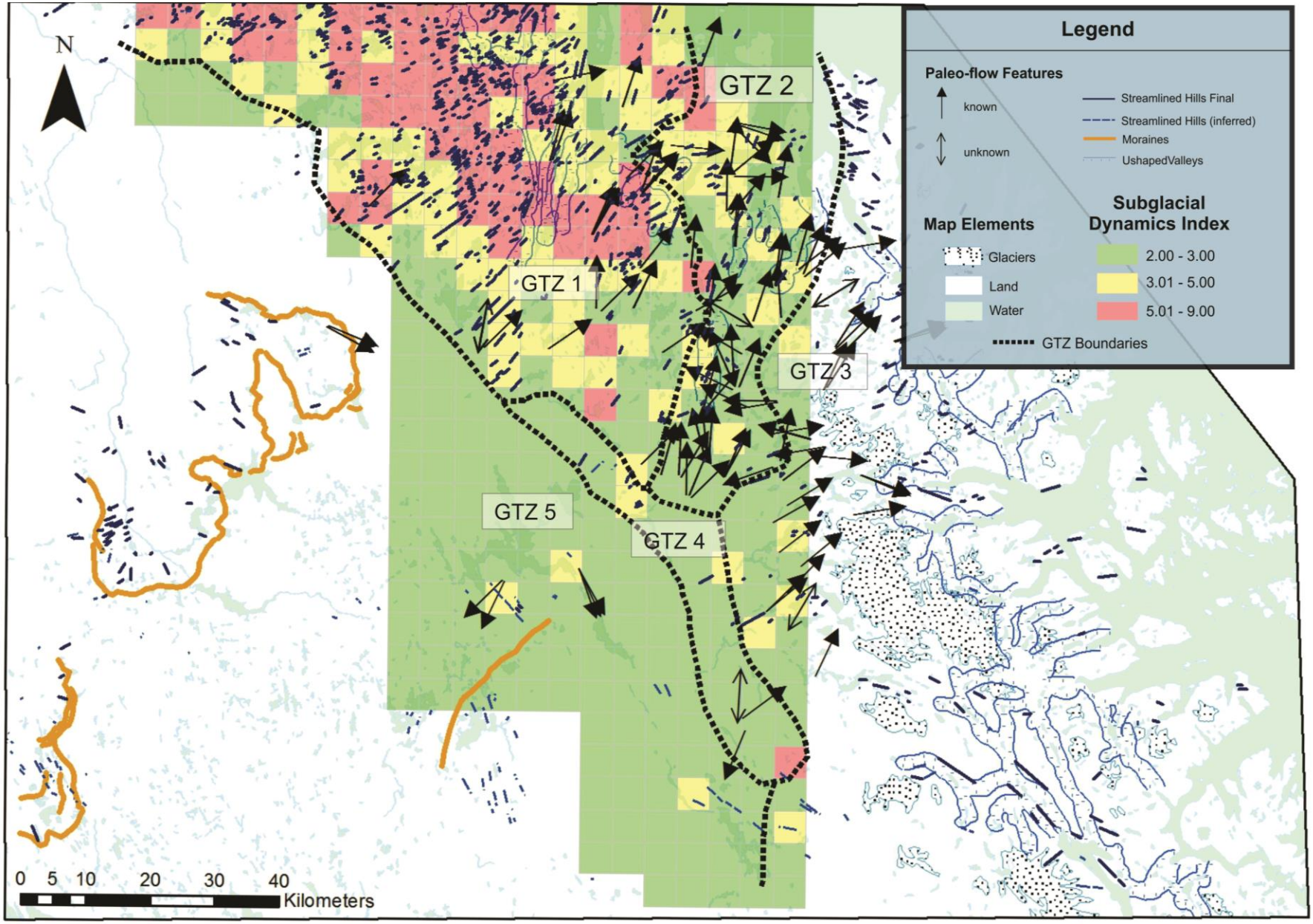

Figure 3-8: Delineation of GTZs was based primarily on the subglacial feature map (Johnson et al. 2013), and fine-tuned with the subglacial dynamics index and available indicator mineral train data (not shown). These proxies overlay the subglacial feature map showing a unique set of subglacial landscape characteristics in each zone.

Paleo-flow indicators and their azimuths largely distinguish the GTZs. Rose diagrams were made with the azimuths of paleo-flow indicators for each GTZ zone to visually assess the differences between the GTZs (
Figure 3-9).

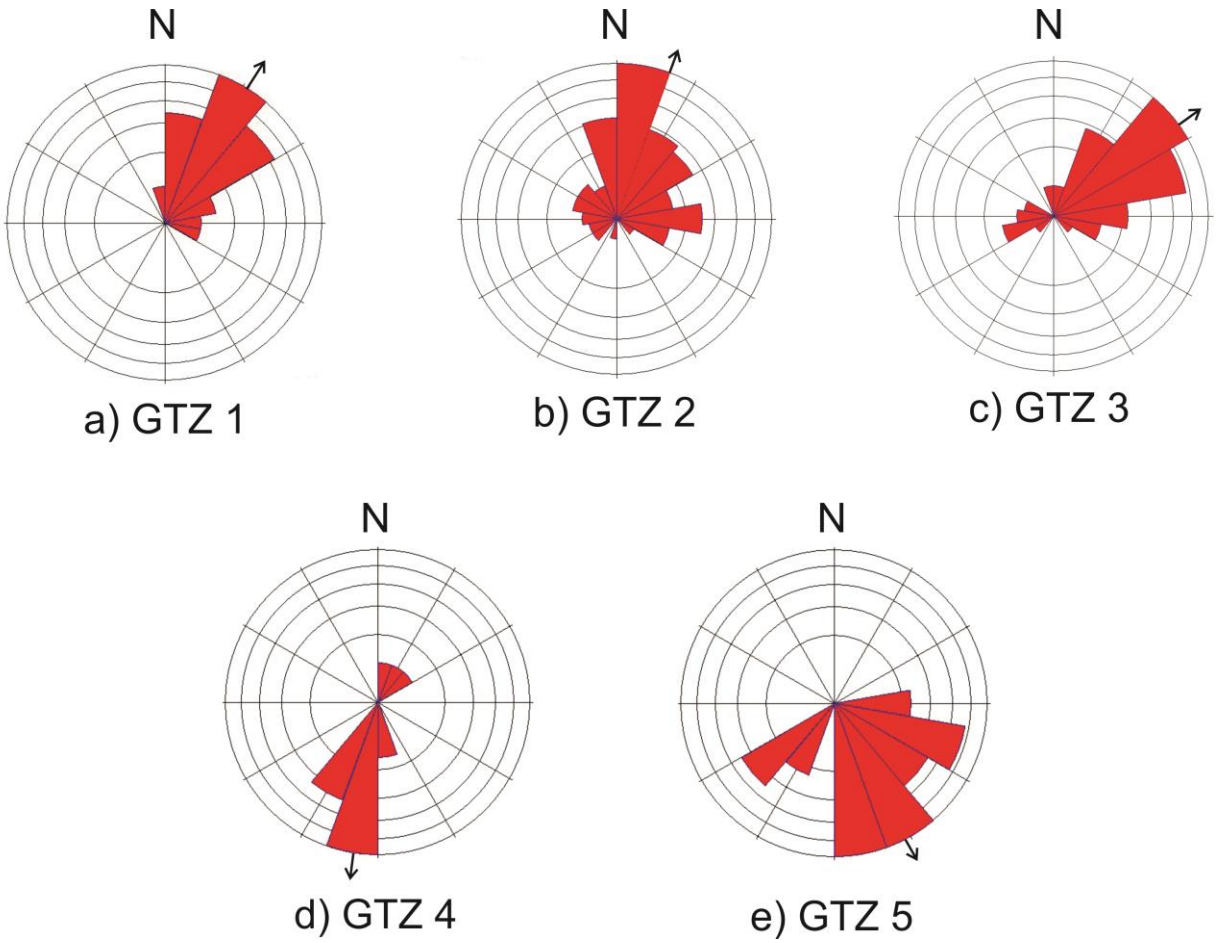

Figure 3-9: Rose diagrams for GTZs 1 to 5: a) GTZ 1 has a resultant vector of 32° (north-northeast), and the data range from 348° to 108°. The total number of points is 89. b) GTZ 2 has a resultant vector of 20° (north-northeast), and that data range from 0° to 346°. There are 180 data points. C) GTZ 3 has a resultant vector of 54° (northeast), and the data range from 10° to 355°. There are 144 data points; d) GTZ 4 has a resultant vector of 189° (south), and the data range from 3° to 210°. There are 27 data points; e) GTZ 5 has a resultant vector of 152° (south-southeast), and the data range from 95° to 330°. There are 17 data points.

3.4.5a GTZ 1

The GTZs are differentiated based on a variety of characteristics, including geomorphology and the subglacial erosion intensity proxies described. GTZ 1 is characterized by a broad flowset of

northeast trending streamlined hills (Figure 3-10) and parallel paleo-flow indicators, with dominant azimuth of 32° (Figure 3-9).

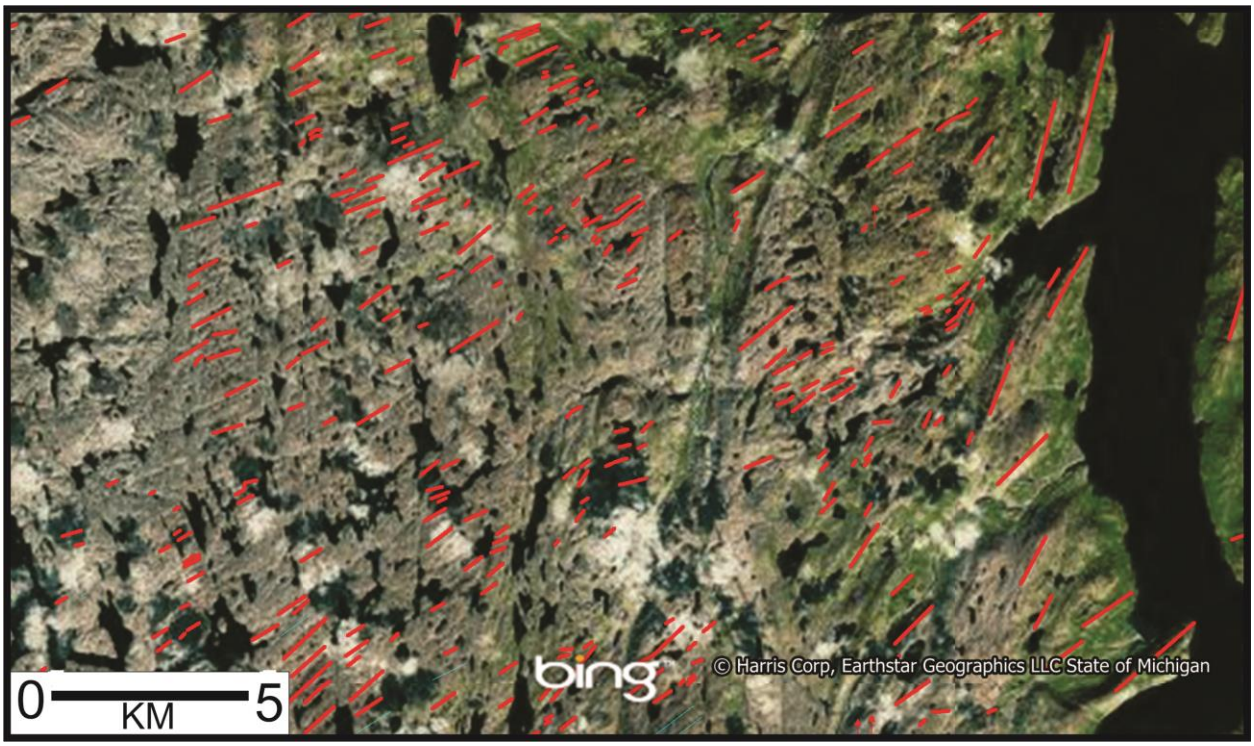

Figure 3-10: GTZ 1 is characterized by strong northeast pattern of streamlined hills (red lines). The streamlined hills crosscut the bedrock structures striking north/south.

GTZ 1 also has the highest streamlined hill density longest elongation ratios and the highest lake density of the study area. Therefore, the highest subglacial dynamics index values occur in GTZ 1 (Figure 3-8). The spatial zoning of subglacial dynamics index values could lead to further partitioning of GTZ 1. In an area such as GTZ 1, dispersal patterns of mineral indicators are predicted to be oriented to the northeast, and be relatively parallel to the landforms in that GTZ (Figure 3-10). Two such dispersal trains from known kimberlite sources are indeed oriented to the northeast, with lengths of 6.5 and 18.0 km, respectively (Figure 3-11). The dispersal trains are shown through garnet pie diagrams which display garnet composition for selected kimberlites (Figure 3-12) (Neilson et al. 2012).

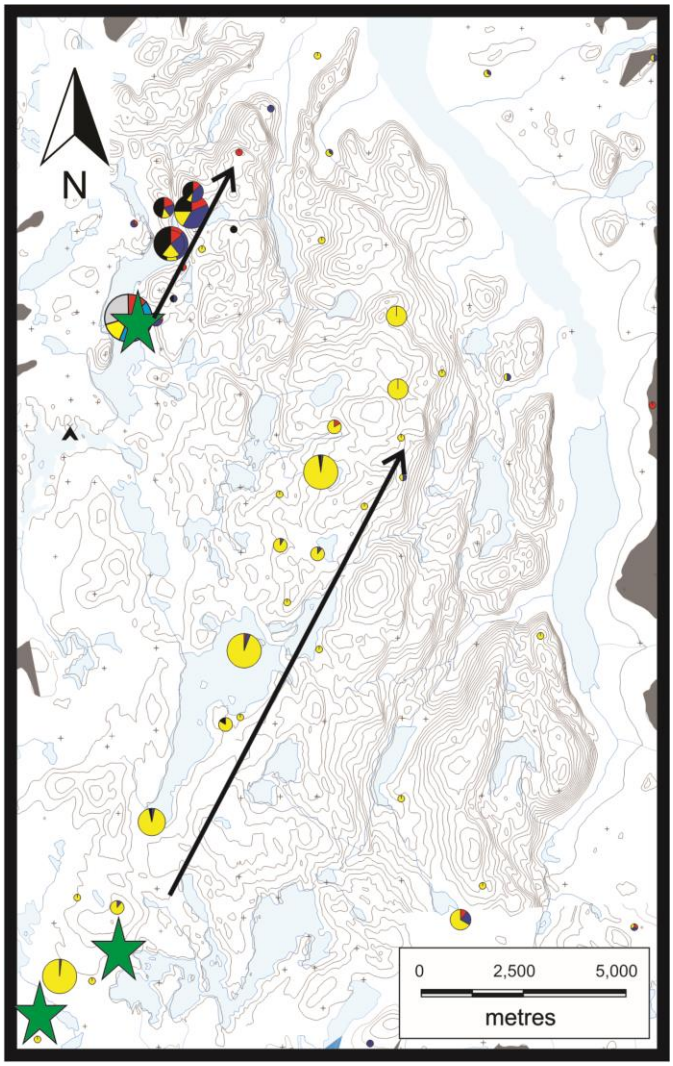

Figure 3-11: Northeast indicator mineral trains in part characterize GTZ 1. The short mineral train to the north is approximately 6.55 km long, and the train to the south is approximately 18.0 km. The green stars represent the kimberlites, and the arrows show the direction of the trains, as demonstrated by the garnet pies (see Figure 3-12 for legend) (modified from Neilson et al. 2012).

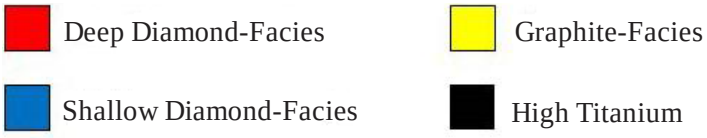

Figure 3-12: The garnet pies in Figure 3-11 represent the mantle tenor of selected kimberlites (figure modified from Neilson et al. 2012).

3.4.5b GTZ 2

The northeast flowset within GTZ 1 is clearly crosscut locally by ice-flow indicators that converge into troughs that form a series of fjords. The orientation of ice flow indicators overprinting the northeast-trending indicators is shown in Figure 3-9. The resultant vector, which is 20°, indicates the dominant ice flow direction.

The troughs and associated ice flow indicators forming GTZ 2 clearly crosscut the regular landscape of GTZ 1 and are thus younger. Landforms and ice flow indicators of this younger GTZ can be traced inland suggesting propagation of a channelized flow system towards the central portion of Hall Peninsula (Figure 3-13a).

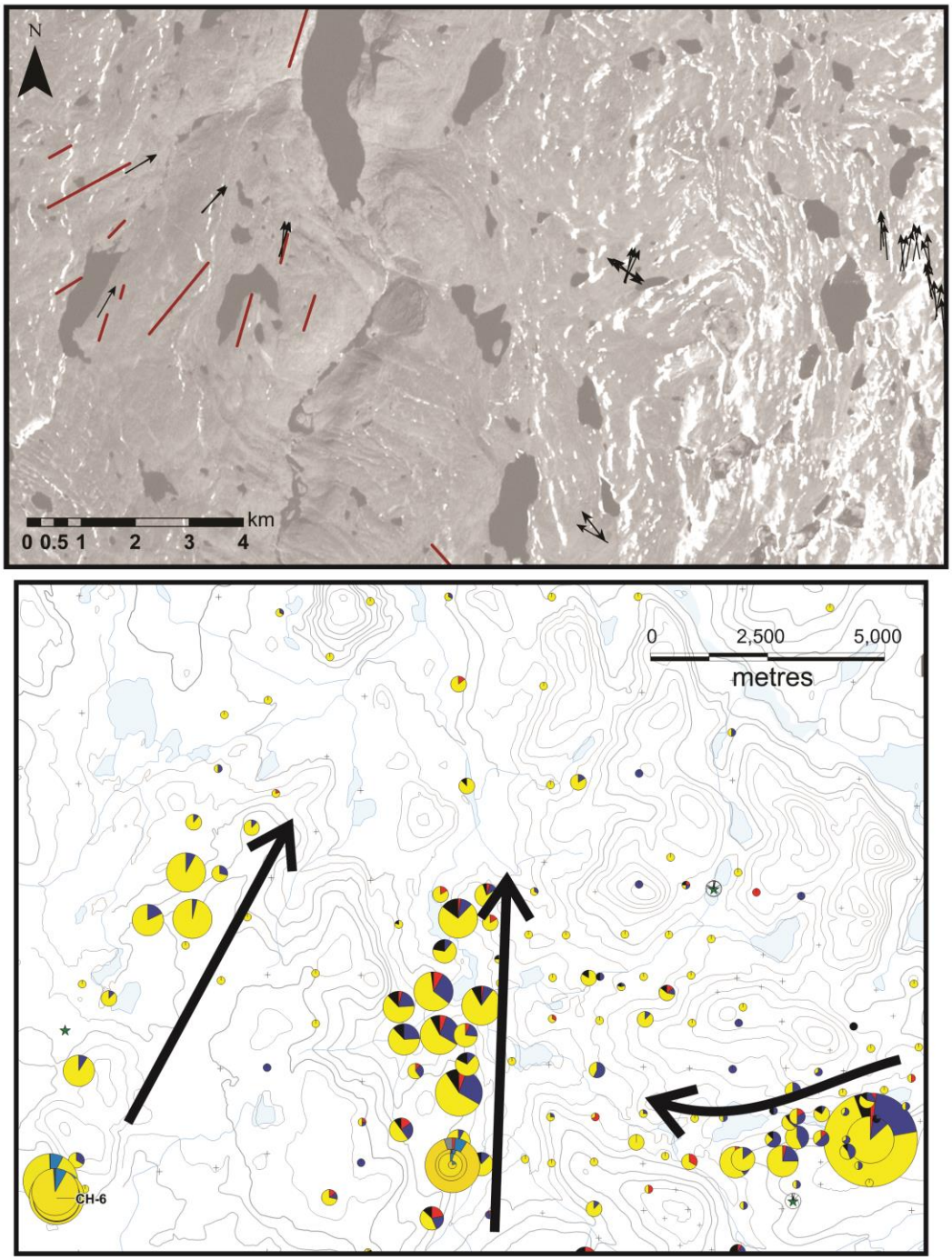

Figure 3-13 GTZ 2 is defined by the channelized flow system directed by Ptarmigan Fjord. Flows are found far inland going north into Ptarmigan Fjord, crosscutting the older northeast flow set. Flows are also going northwest into the fjord from its eastern side. This zone was delineated by a) the paleo-flow indicators (black arrows) and streamlined hills (red lines) funnelling into the fjord as well as by b) indicator mineral trains funnelling into the fjord. The legend for the garnet pie diagrams is shown in Figure 3-12.

The trough that now forms Ptarmigan Fjord (Figure 3-2) had a strong influence over the ice once the ice sheet thinned, with north flows propagating far inland, with evidence of the northern pull found 40 km south of the fjord's head. The landforms and striations near the inland tip of the fjord propagate towards it (Figure 3-13**)**. There are also more northern striations to the east of the longer extension of Ptarmigan Fjord, propagating north to the shorter extension (Figure 3-13a). The pull of Ptarmigan Fjord is found in the indicator mineral trains as well, with trains funnelling into Ptarmigan Fjord developing converging dispersal trains (Figure 3-13b). The trains in GTZ 2 are more complicated than in GTZ 1, with this zone having a higher degree of overprinting.

3.4.5c GTZ 3

The most complicated landscape is arguably GTZ 3. GTZ 3 potentially has the youngest landscape features shaped by the modern icecap and its past extensions, but also has significant inheritance as well as overprinting in the valleys. GTZ 3 is similar to GTZ 2, as it shows inheritance of the older northeast flow set in areas of higher elevation, and overprinting in the valleys where ice was directed into the eastern fjords, or linear erosion. Eastern flows were not found propagating far inland like the northern flows were. West-trending ice flow indicators were also found in GTZ 3, but only in valleys proximal to the modern ice cap (Figure 2-19), indicating that small valley lobes once extended into these valleys from the ice cap. The paleo-flow directions are summarized with a rose diagram (Figure 3-9), showing a dominant northeast flow (54°), but with directions ranging mainly from northeast to southeast, with minor indicators in the southwest and northwest quadrants.

This area was not included in the bedrock-controlled lake and streamlined hill density study as it is partly covered by the modern ice cap, which would have led to erroneous GIS results. Generally, this area reflects the influence of the local icecap and how it evolved after the retreat of the LIS.

3.4.5e GTZ 4

Central to the property is GTZ 4; a zone that is defined by its relative lack of glacial streamlined landforms. This central area of the peninsula contains relatively thick till and rolling topography

(Figure 2-5). Low densities of streamlined hills characterize this GTZ and bedrock controlled lakes. Subglacial erosional features are scarce in this central part of the study area, and the kimberlite indicator minerals in this study area occur in high densities reflecting the many kimberlites found in this area. The KIMs are found in more of a smear or cloud and have not been defined into trains by the exploration company, and cannot be shown for confidentiality purposes.

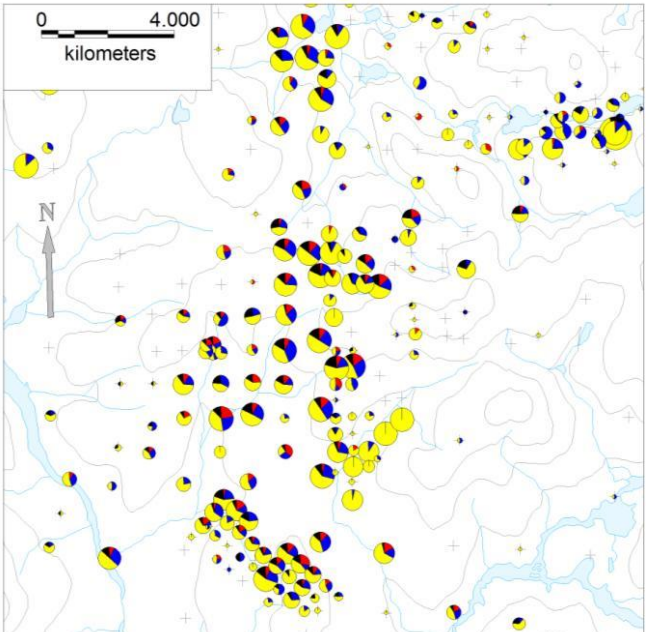

Figure 3-14: KIMs shown in garnet pie graphs (see table 3.2 for legend) showing smear over GTZ 4.

A total of 27 paleo-ice flow indicators, mainly outcrop-scale indicators, were measured in the south of the GTZ, showing a south to southwest flow (Figure 3-9). However, there are a few northeast-trending ice flow indicators in the GTZ. Altogether, these characteristics suggest that GTZ 4 could have been under the Hall Ice Divide for some time, which may show evidence of migration.

3.4.5e GTZ 5

Further south, another distinct landscape is found, which has been denoted GTZ 5. This area has the highest elevation, and lowest subglacial dynamics index. Few striations indicating ice flow towards the southeast (Figure 3-9) were found on a limited number of outcrops. This area also contains frontal moraines (Figure 2-6) that are consistent with a southeast ice flow dynamics, as well as paleo-shorelines of proglacial lakes, mapped by Miller (1980). The bedrock structures

within GTZ 5 are striking southeast, making it uncertain to map bedrock ridges as glacial landforms. This area is also characterized by regolith zone (Tremblay et al. 2013) (Figure 3-15).

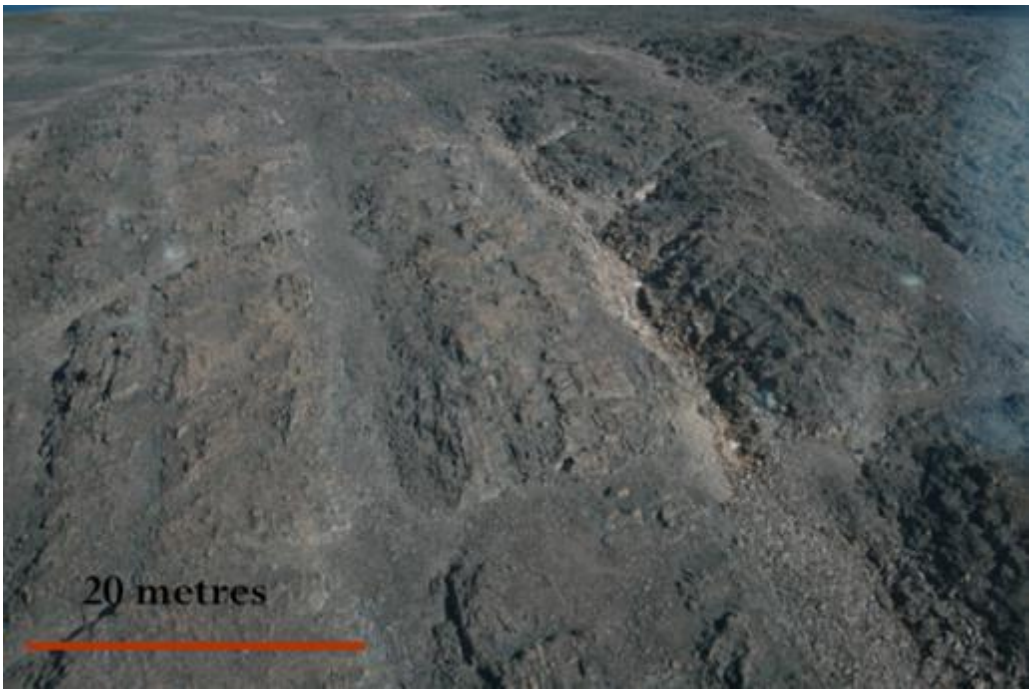

Figure 3-15: Highly weathered bedrock typical of GTZ 5.

A summary of the main GTZ characteristics is shown in Table 3-2. The CIA data is included in the table, which are explained in the following section.

Table 3-2: Summary of the main GTZ characteristics.

	Discriminating Characteristics	Flow-set comments	Dispersal Trains Characteristics	StereoStat Rose diagram Resultant (#samples)	Mean CIA (standard deviation)	Mean subglacial dynamics Index	Subglacial Dynamics Style
GTZ 1	Preserved NE system	Laterally extensive NE flowset	NE ribbon shaped	32 (89)	51.65 (5.68)	4.75	Erosive areal scouring followed by cold-based ice to preserve the landscape
GTZ 2	Channelized Flow System	NE flowset crosscut by convergent channelized flows	NE, N, and W converging ribbon shaped	20 (180)	66.67 [1] (7.93) 51.91[2] (4.56)	3.33	Selective linear erosion; cold-based ice in the intervening highlands
GTZ 3	Local Ice Cap	NE flowset crosscut by channelized and local ice cap flows	NE ribbon shaped	54 (144)	61.84 (6.86)	2.86[3]	Complicated areal- linear erosion at different times
GTZ 4	Relatively thick till; rolling topography	Perhaps under an ice divide	Amoeboid shaped fans	189 (27)	56.22 (6.76)	2.60	till blanket; possibly stagnant (meltout) conditions
GTZ 5	SE trending bedrock, Perpendicular hummocky Moraines and Regolith	SW flows corresponding to the laterally extensive NE flows, as well as later SE flows	No data	152 (17)	60.62 (4.67)	2.26	Mostly cold-based ice, with limited areas of erosion and ice-marginal moraine deposition.

[1] There are two results for GTZ 2 mean CIA. The first result includes a very dense sample suite from a site with a relatively high elevation of 700 m.
[2] The second result for the CIA of GTZ 2 is 52; this value better reflects the subglacial erosion conditions of most of GTZ 2.
[3] Most of this GTZ 3 has been masked out due to the local icecap in the mean subglacial dynamics index exercise.

3.4.6 Geochemical Studies Results

3.4.6a Chemical Index of Alteration Results

The CIA values were calculated from the fine fraction of till (<180 um), and results range from 37 to 79.41 (Figure 3-16) (Appendix E). The lowest CIA values (higher erosion) are generally closer to the coast, whereas the higher values (lower erosion) are further inland (Figure 3-16). High CIA values appear to occur in the central and southwestern parts of the grid on plateaus and ridges. On areas of regolith (Leblanc-Dumas et al. 2013), the CIA values are also higher; samples taken from the regolith zone show a weathering signal. Low CIA values are found mostly in the east part of the property, and at the head of the northern fjords. A portion of GTZ 5 to the southwest also has a lower CIA, which may correspond to the south/southwest flows from the Hall Ice Divide. Ideally, the CIA would likely show a stronger signal using the clay sized fraction as opposed to a general fine fraction as used in this study. Nonetheless, it is assumed that the patterns are unaffected by this.

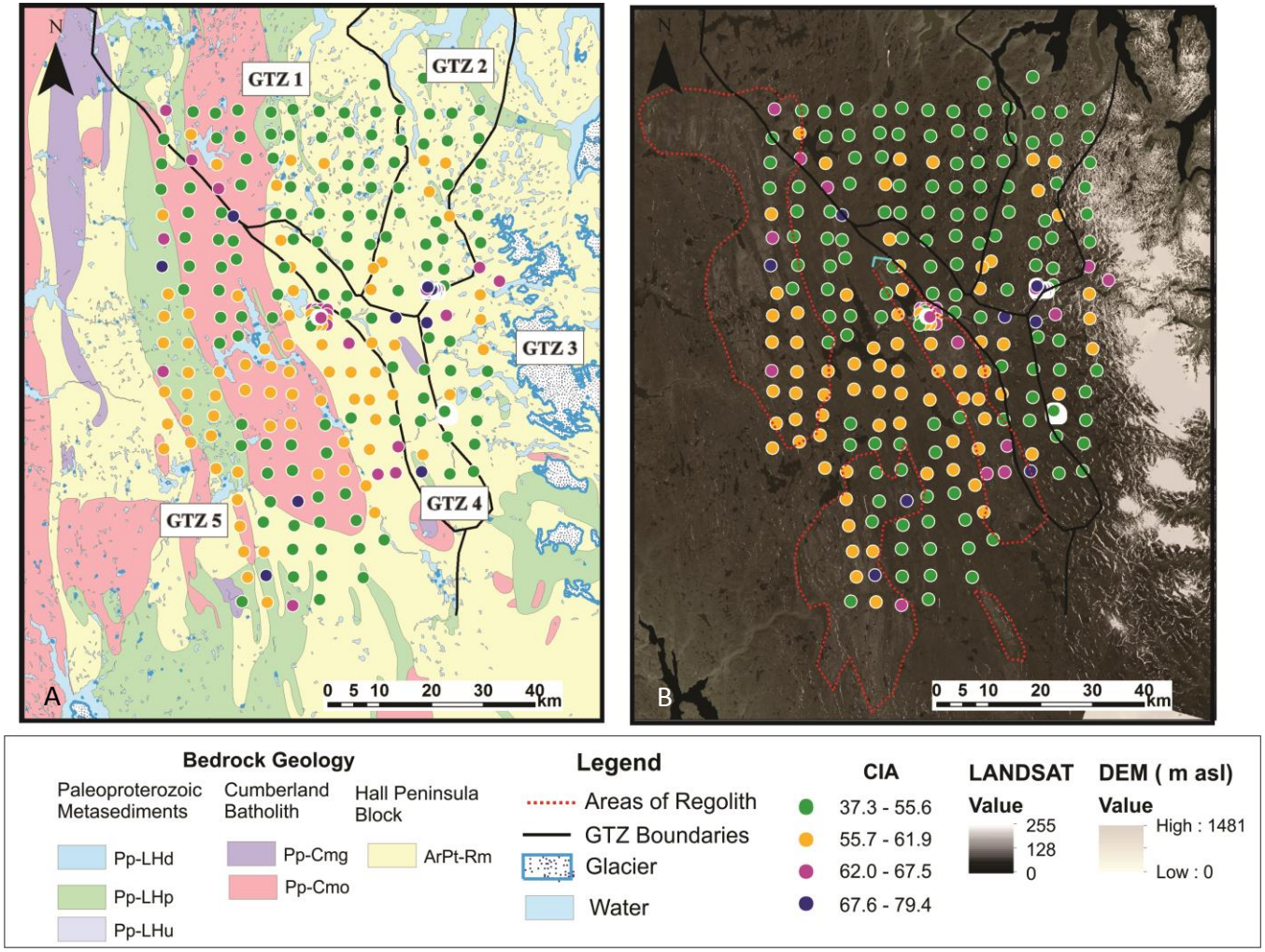

Figure 3-16: The spatial distribution of the CIA values overlaying (A) bedrock geology and (B) DEM and LANDSAT imagery, with areas of regolith outlined with a stippled red line. The figures show the distribution of weathering fingerprint in the till, with low values corresponding to low weathering inheritance (generally to the east, green and dark yellow) and high values representing areas of higher weathering fingerprint (purple and blue). CIA results displayed in graduated colours separated into four classes by natural breaks (jenks) in ArcGIS overlying DEM data.

The CIA is displayed on a LANDSAT combined with a transparent DEM image, and there is a broad trend of increasing CIA with elevation (Figure 3-16b). When plotting elevation against CIA, it becomes clear that values close to 50 have no clear relationship with elevation and these probably reflect the normal value of fresh rocks in the study area (Figure 3-17). However, the graph shows that CIA values greater than 65 are all above 600 m elevation. This means that weathering inheritance in the till is greater above 600 m asl. However, a wide range of CIA values occur at these higher elevations, which suggest that weathering inheritance is heterogeneous above 600 m, and even above 700 m asl.

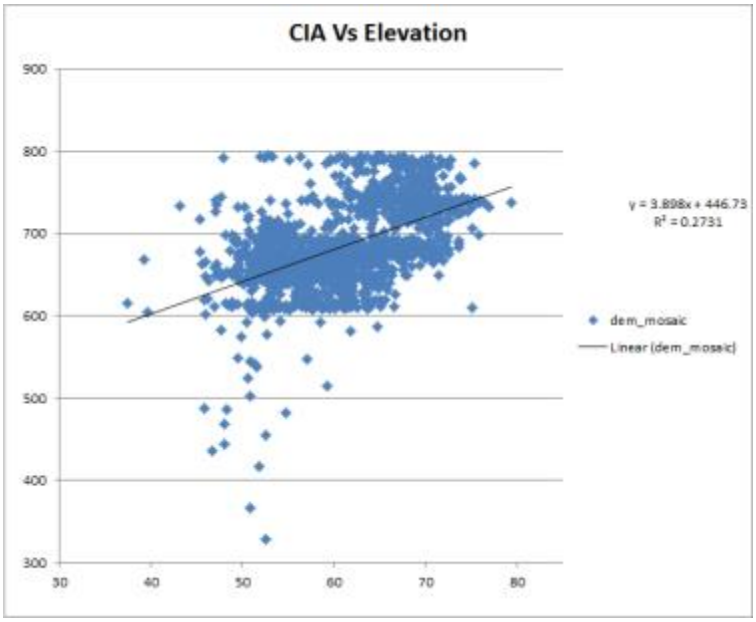

Figure 3-17: Graph showing the CIA (x axis) versus elevation m asl (y axis) to study the relationship between elevation and CIA. According to the R^2 value, there is no linear relationship. There does appear to be two groupings, being between 700 and 800m asl and those between 600 and 700 m asl.

To see if bedrock played a critical role in controlling the CIA results, a plot was made by pairing the CIA results for each sample with its bedrock (Figure 3-18). The CIA seems to be independent from the bedrock type, as each bedrock type shows a similar spread of CIA values, with the exception of the biotite +/- garnet monzogranite because of the small sample number.

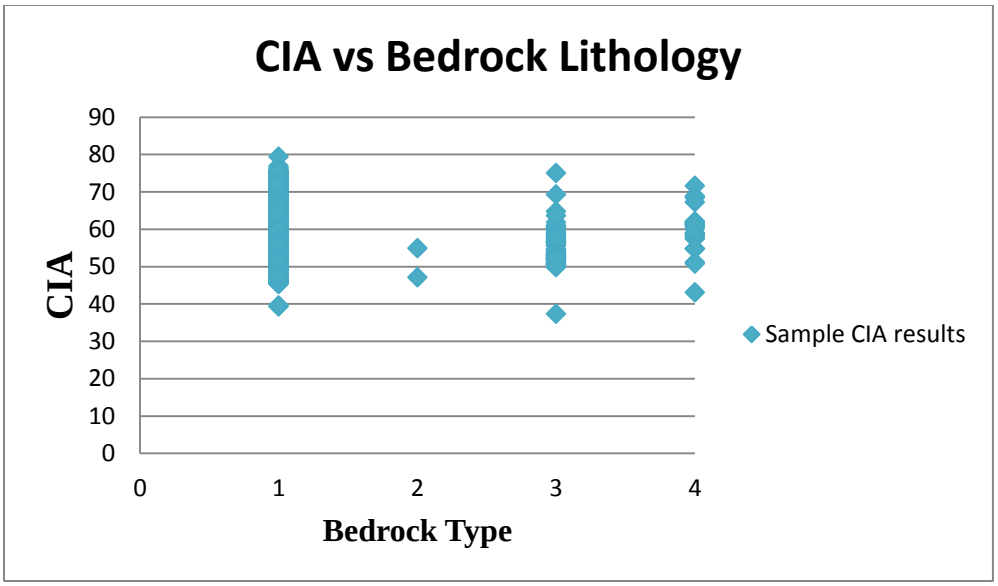

Figure 3-18: Till sample CIA results compared to their bedrock type: 1) Orthogneiss (Hall Peninsula Block) with a mean CIA of 61.95 and a standard deviation of 6.76; 2) Biotite +/- garnet monzogranite (Cumberland Batholith) with a mean CIA of 49.15 and standard deviation of 2.98; 3) K-feldspar biotite +/- orthopyroxene monzogranite (Cumberland Batholith) with a mean CIA of 55.38 and standard deviation of 5.30; and 4) Psammite (Lake Harbour Group) with a mean CIA of 59.69 and standard deviation of 5.83. The four bedrock types do not to have a dominant control over the CIA, as the means are comparable within their standard deviations, with the exception of 2, which is likely explained by the small sample suite.

The CIA results for samples falling over each rock type shown, and regardless of the rock type, the samples seem to have comparable data spread. It appears as that bedrock does not have major control over the CIA.

The statistics for the CIA are shown in Table 3-3. The CIA seems to further characterize each of the five zones. The CIA highlights not only the northwestern portion of the study area as high erosion, but also areas around the coast in general, which is not captured by the subglacial dynamics index method. To develop a comprehensive understanding of erosion, the CIA was able to pick up linear erosion, where the subglacial dynamics index method was sensitive only to areas of relatively high areal scour.

Table 3-3: Statistics for the CIA results for each GTZ. A thick cluster of till sample points near the border of GTZ 2 and GTZ 3 was taken out of the GTZ 2 results. The GTZ 2 boundary was likely drawn too far east.

CIA Statistics	GTZ 1	GTZ 2	GTZ 2 (corrected)	Extra Data (GTZ 3?)	GTZ 3	GTZ 4	GTZ 5
Mean	51.65	66.66	51.91	69.51	61.83	56.22	60.62
Max	64.75	79.41	61.58	79.41	75.95	70.03	75.05
Min	37.33	45.81	45.81	53.00	45.27	39.27	43.08
Standard Deviation	5.68	7.93	4.56	4.57	6.86	6.76	4.67
Count	43	167	27	140	867	20	484

The CIA results for GTZ 1 area have a mean value of 51.65 (Table 3-3), which is the lowest result with respect to the other 4 GTZs, suggesting that this area underwent more bedrock erosion than the other zones. This is also consistent with the subglacial dynamics index. However, as explained in section 3.4.6b , the CIA results for GTZ 1 are not aligned with the PCA interpretation for GTZ1, which shows an overlap with GTZ 5 and a weathering assemblage.

The mean CIA for GTZ 2 is 66.66 (Table 3-3). The mean CIA value is the highest out of the calculated means, as it includes CIA samples from high elevations in the study area, where cold-based ice would have developed during deglaciation. The mean CIA without these high values is 51.86, which is comparable to GTZ 1, and probably representative of fresh rock values. This lower value is more fitting to the expected CIA value of GTZ 2, as there is evidence of linear erosion. These results also suggest that the boundaries drawn for GTZ 2 may have gone too far inland, and suggest some adjustment to the outline may be needed. The removed values are likely more representative of GTZ 3.

The mean CIA value for GTZ 3 is 61.83 (Table 3-3). The high CIA indicates little erosion. The samples were collected inland, near the border of the GTZ, where elevations are highest for that GTZ, which may bias the outcome. The mean CIA could be lower if more data from lesser elevations would have been available.

The mean CIA value is 56.22 for GTZ 4 (Table 3-3). This shows a gradual increase in CIA values proceeding inland, or an increase in weathering, but it is still low and close to typical values for fresh rocks (Fedo et al. 1995). However, the subglacial dynamics index suggests little subglacial erosion for this area.

GTZ 5 has high CIA values, with a mean value of 60.62 (Table 3-3). Extensive evidence of regolith has been found during recent mapping by the government (Tremblay et al. in press), which shows this area was subject to very limited glacial erosion. GTZ 5 is thus interpreted to have been cold-based for most of the last glacial cycle and was probably located underneath a persistent local ice divide until late in the deglaciation, This area was, however, affected during ice retreat by some warm-based ice-marginal processes, as evidenced by the few SE-trending ice flow indicators and perpendicular moraines, which complicate the overall subglacial dynamics footprint of the GTZ. Nevertheless, the subglacial processes during deglaciation seem to have been insufficient to overprint the ice divide and cold-based footprint of that area.

3.4.6b Multivariate Statistical Evaluation of Multi-element Geochemical Data

The Eigenvalues versus Eigenvalue numbers produced from the clay dataset produce Eigenvectors or principal components (PCs) (Figure 3-19). Eigenvalues and Eigenvectors are key concepts in linear algebra (matrix algebra). PCs are the variables that have most control over the data. It is shown that PCs 1-5 have significant control over the data (Figure 3-19). Essentially, the higher the Eigenvector (EV), the more control the component has over the variability of the samples. PC1 controls most of the variability. PC2 and 3 have similar controls, and the data show a break in slope at PC3 indicating increased control of PC3, 2, and 1, relative to 4 and 5.

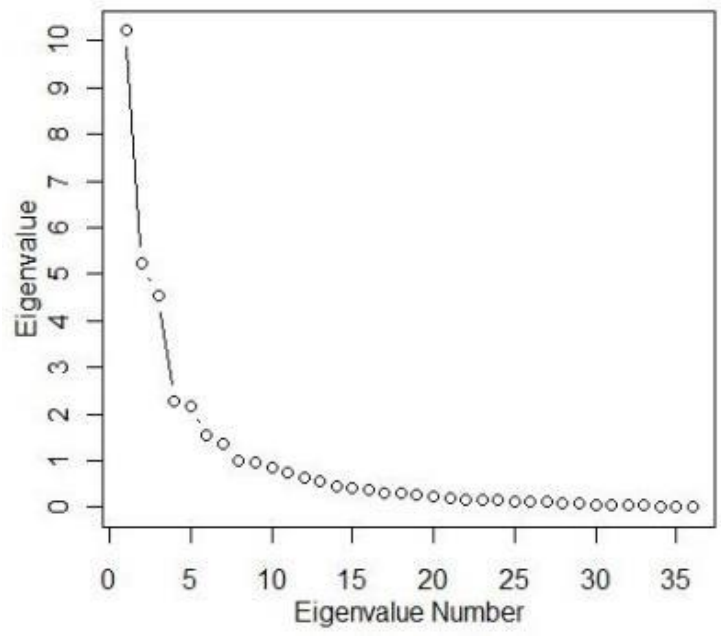

Figure 3-19: Eigenvalue vs. Eigenvalue number for the clay sized till fraction. PC1 (highest Eigen value and lowest Eigenvalue Number) shows it has the most control over the data. PC 2 and 3 also have significant control, as do 4 and 5. The data 'elbows' at 3 and 5, showing a change in the significance of the impact.

The plot of PC1 versus PC2 (Figure 3-20) shows a striking pattern on the positive and negative sides of the x axis, or PC1. According to the PCA, the till in GTZ 1 and 5 is distinct from that of GTZ 2 and 3. The positive axis of PC1 contains GTZ 1 and 5, with a relative enrichment in Fe-Al-Ga-V-Sc, reflecting mafic group assemblages and/or weathering. GTZ 2 and 3 are concentrated on the negative axis of PC 1, with a relative enrichment of C-Th-U-Li-K-Rb, reflecting a felsic assemblage. GTZ 4 has significantly less geochemical samples than the other GTZs, but it plots somewhere in between the other four not fitting to either extreme. As shown with the CIA and field mapping results, GTZ 5 has undergone weathering, which would strongly impact till composition. While Al, Fe, and V could well come from mafic rocks, an enrichment in Ga suggests weathering may best explain that assemblage. Ga is indeed used as a tracer of weathering processes and tends to be more abundant in bauxites derived from granitic rocks (Kabata-Pendias 2001). Enriched Al-Fe-Ga-V in the till on Hall Peninsula could therefore be a fingerprint of regolith mixed in the till more than increased amount of mafic minerals. The Canada-Nunavut Geoscience Office has found extensive areas of regolith during recent mapping (Tremblay et al. 2013) and they seem to correspond with the white-toned areas on Landsat imagery (Figure 2-6). The Al association also speaks strongly for a weathered componenent

(bauxite). Ga is also s associated with sphalerite. Co, Sc, Ni, Mn, Zn and Cr area also on the negative axis of PC 1 which could be related to supracrustal rocks. Till in GTZ 1 is located down-ice from the weathered zone (GTZ 5) and would thus contain a weathering signature, albeit diluted compared to GTZ 5. However, the CIA results (Section 3.4.6a) does not show inheritance in GTZ 1, or the CIA for GTZ 1 indicates erosion, which is contrary to the PCA results.

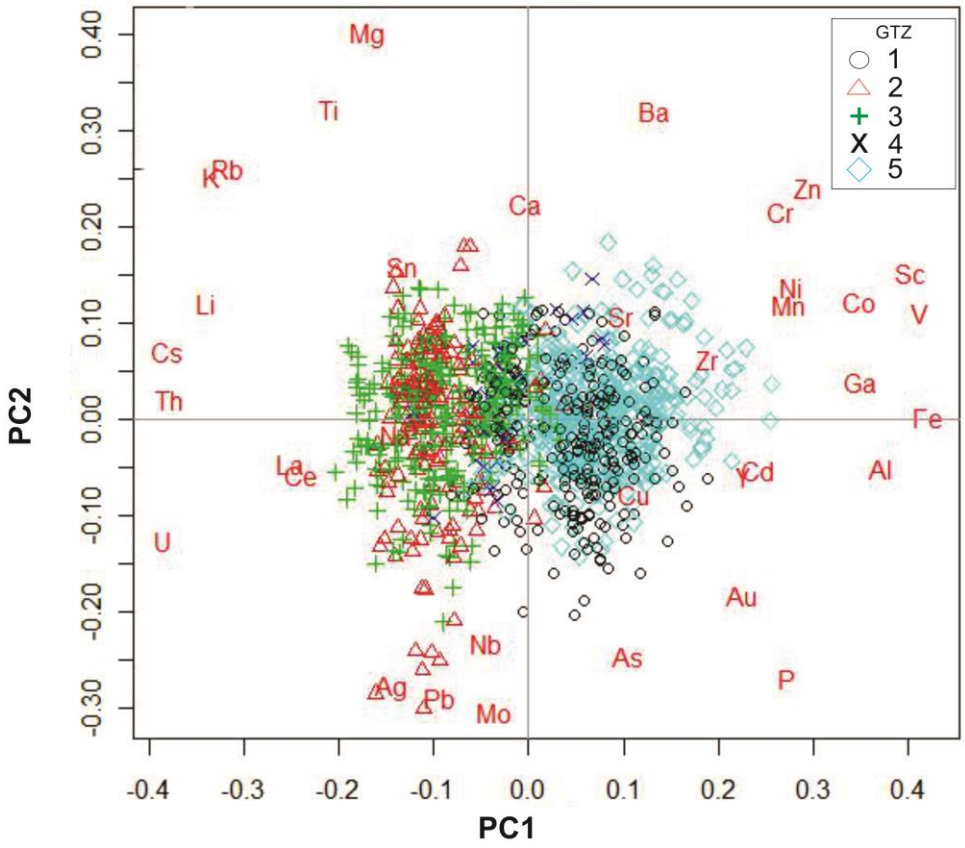

Figure 3-20: PC1 VS PC2 of the clay sized till geochemistry samples. There is a clear distinction between GTZs 1/ GTZ 5 and GTZs 2 and 3. GTZ 4 has a significantly less number of samples, and plots somewhere in the middle.

PC 2 does not show as strong of a pattern with the GTZs as PC1 does (Figure 3-20). The positive axis of PC2 has a thicker cluster of samples from GTZ 2 (red triangles), and the negative axis as a thicker cluster of samples from GTZ 1 (black circles). PC 2 does have an interesting spread of geochemistry, which could relate to the kimberlites in the study area. The pathfinder elements for kimberlites include, but are not limited to Ni, Mg, Cr, Co, Ca, Fe, Ti and Ba (Rose

et al. 1979), which are found on the positive axis of PC 2. The pathfinders are dependent on the compositions of kimberlites, and a more in depth look into the kimberlite geochemistry would have to be done to confirm the potential kimberlitic footprint.

When overlaying PC 1 scores over a geological map, there are significant overlaps with the PC 1 scores with the available bedrock geology map (Figure 3-21). The PC 1 scores are negative on the east side (green) and more positive on the west side (red).

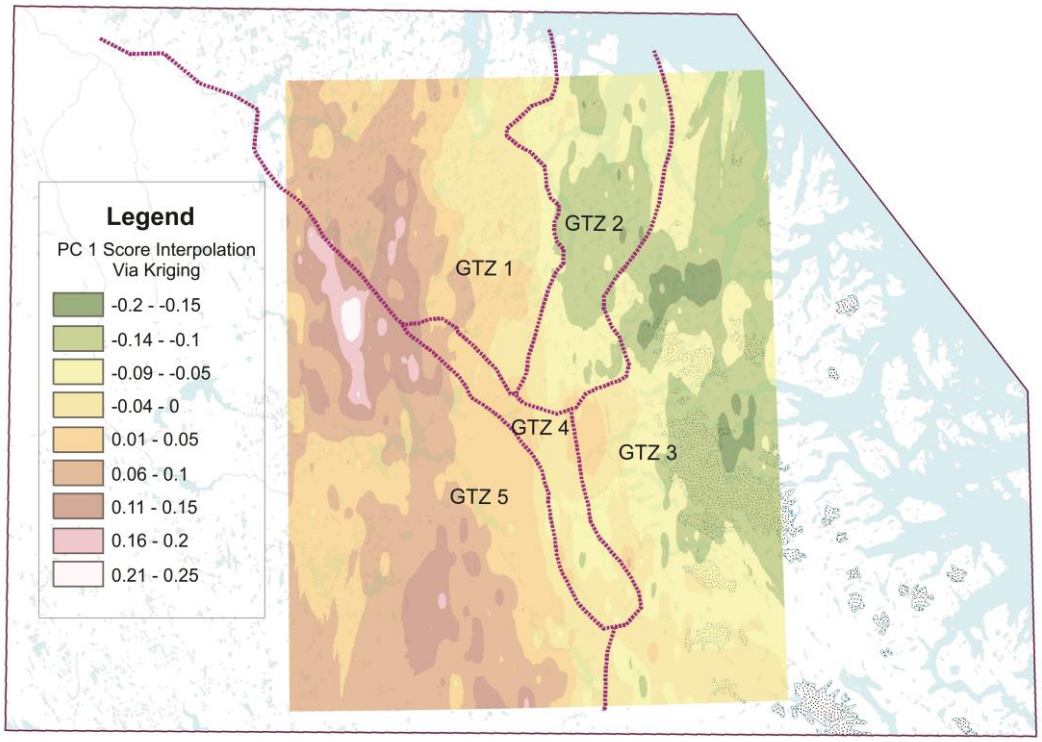

Figure 3-21: Figure 3-21A shows PC scores interpolated over the study area via krigging. There are clear patterns with the GTZs and the PC 1 scores, which suggests that PC 1 and the GTZs are correlated, which is likely related to bedrock and regolith signature.

Though the GTZs were mapped primarily on geomorphology, PC 1 is likely related to bedrock geology and regolith in the study area, which is shown in the similarities between the interpolated PC 1 results (Figure 3-21) to a bedrock map overlaid with striations accentuating its geomorphological characteristics (Figure 3-22).

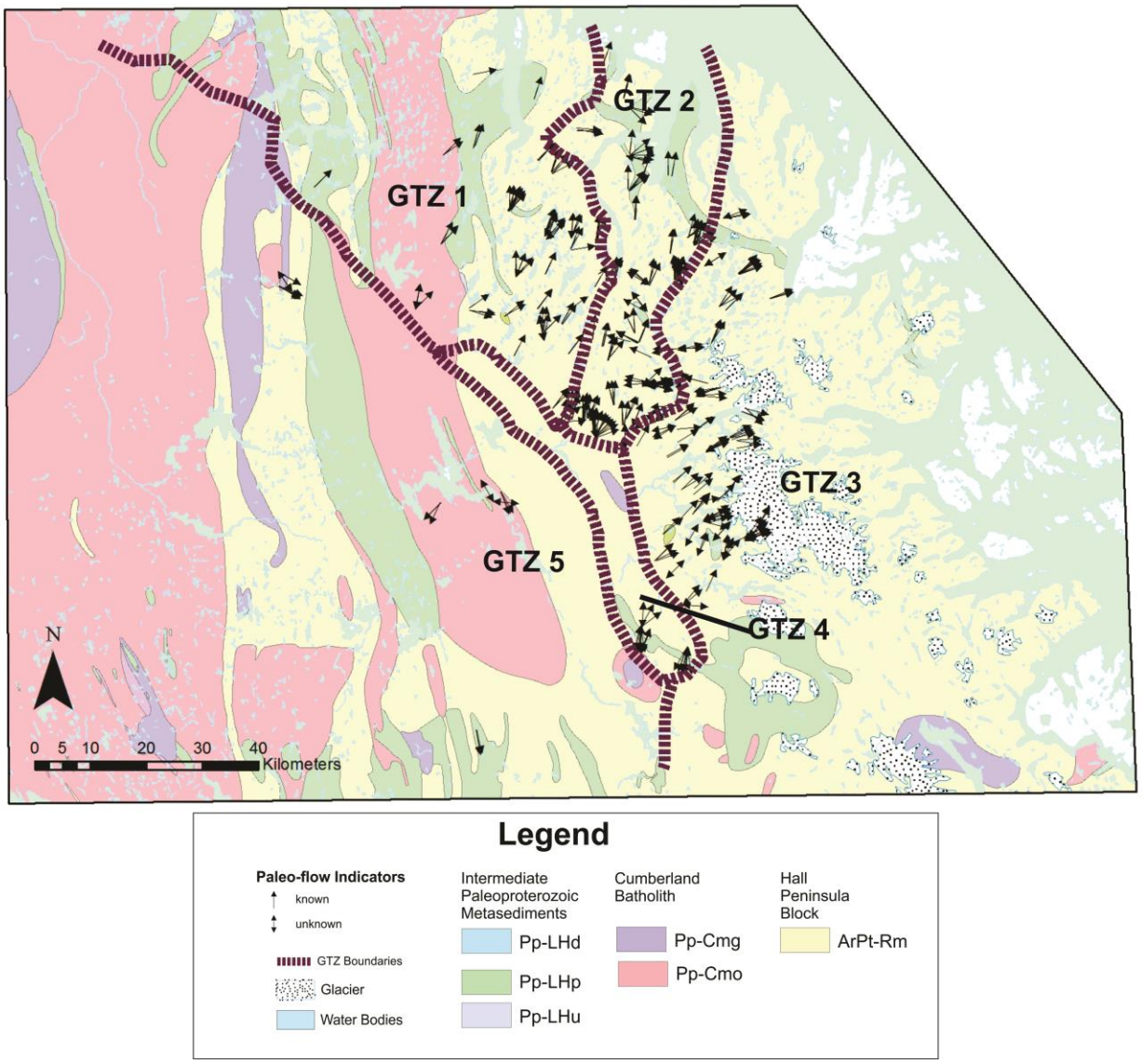

Figure 3-22: The GTZs overlaying the bedrock geology map (Whalen 2010). The paleo-flow indicators are included to demonstrate the primary proxy used to separate the GTZ. There is a strong relationship between the GTZ and bedrock, but there are more factors to consider.

To study the relationship between the bedrock and glacial geology, streamlined hill polygons were overlaid on top of the bedrock map to see if any relationships could be made (Figure 3-23). The streamlined hill polygons (red polygons) in the north are largely found within the northern portion of the Cumberland Batholith (pink). Though the formation of the streamlined hills is related to factors such as elevation and basal thermal conditions, it does appear that the body of Cumberland Batholith does exert partial control over the formation of the streamlined hills.

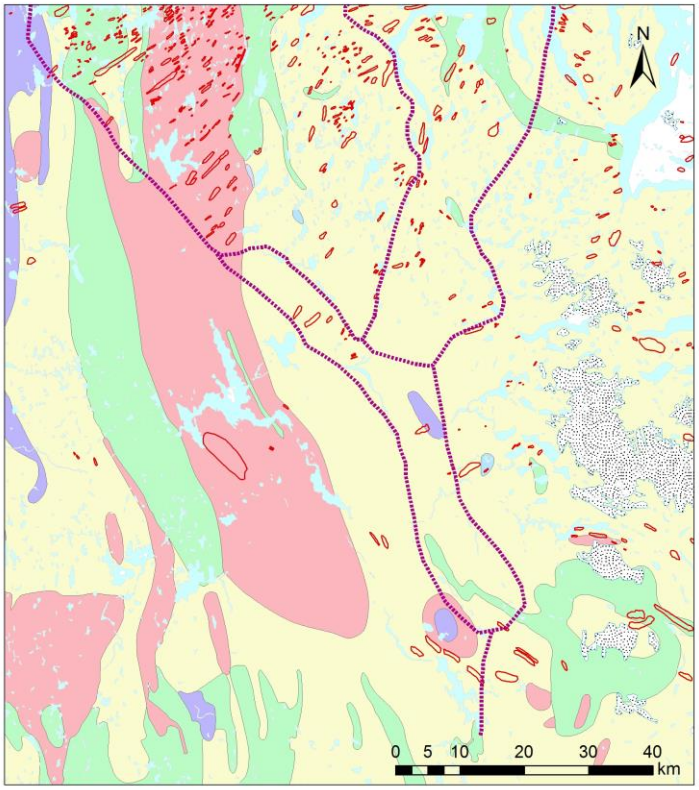

Figure 3-23: Streamlined hill polygons over bedrock geology map (See Figure 3-1 or Figure 3-22 for legend). In the north, the density of the streamlined hills is higher in the Cumberland Batholith than the Hall Block or the metasediments.

To determine if the GTZs could be predicted by the till geochemistry, a linear discriminant analysis was subsequently applied to the data. Results show that the linear discriminant analysis predicts the correct GTZ 83.78 % of the time (Table 3-4**).**

Table 3-4: Predictive Accuracy Matrix. There is an overall accuracy of 83.78%, which is calculated by dividing the diagonals line (bold numbers) by the row sums of each class and multiplied by 100%.

GTZS	1 LDA	2 LDA	3 LDA	4 LDA	5 LDA
GTZ 1	**84.36**	2.55	.73	0	12.36
GTZ 2	4.02	**70.11**	24.71	.57	.57
GTZ 3	1.19	9.25	**84.78**	4.48	.30
GTZ 4	6.25	0	12.5	**65.63**	15.63
GTZ 5	6.3	0	.87	13.70	**89.13**

Three GTZ are chemically distinct (Figure 3-24). The overlap between GTZ 1 and 5 is probably due to the fact that GTZ 1 is located down-ice from GTZ 5. Hence, a certain proportion of detritus in till within GTZ 1 likely have their source in GTZ 5, whereas GTZ 5 has one of the lowest subglacial dynamics index and, therefore, should have a predominantly local provenance (short sediment transport if any). These two situations best explain the compositional overlap between GTZ 1 and 5. Furthermore, there is probably a transition zone at the boundary between GTZ 1 and 5 and adjusting the position of that boundary could lead to reduced overlap and increased predictability of GTZ based on composition. GTZ 2 and 3 are similar chemically and this probably reflects the similarity in the underlying bedrock, which may be more homogeneous and lacking chemical changes due to weathering. As shown in Table 3-4, GTZ 4 is geochemically most similar to GTZs 3 and 5. Given that most of the samples from GTZ 4 come from an area in between GTZ 3 and 5, and that this is interpreted as a sluggish ice divide area, it makes sense that this GTZ would reflect similarities.

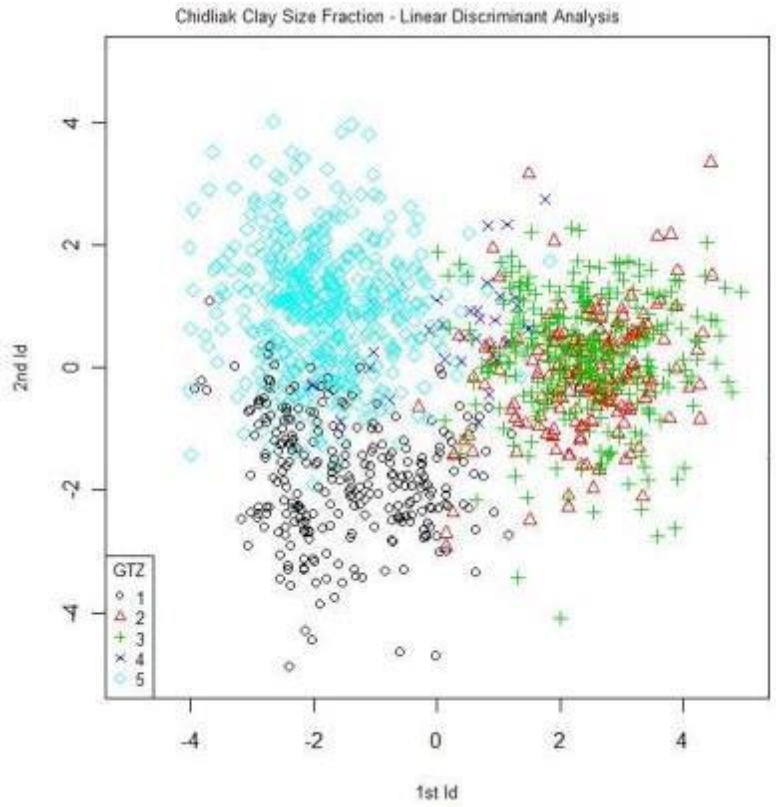

Figure 3-24: Shown above are the linear discriminant scores for the first two linear discriminant functions (LD1 and LD2). The distinctiveness of the GTZs 3, 1 and 5 are clearly shown in this projection of the discriminant function scores. Significant overlap between GTZs 2,3 and 4 are also notable. The distinctiveness and overlap of the groups is also expressed in Table 3-5, where row GTZ 2 shows confusion with prediction of GTZ 3. Note that the predictive accuracy for row GTZ 3 is more distinctive.

PCA shows that bedrock and weathering is the primary component controlling the till geochemical data, which also correlates with the GTZs which are separated on their subglacial characteristics. Linear discriminant analysis shows that there is a strong spatial relationship between till composition and GTZs, with the accuracy ranging from 65.3-89.1, with an overall accuracy of 83.78%.

Predicted probability and typicality probability are two values that describe different types of classification, and are output for each till sample by R-environment when running LDA from the package "MASS" and the package "rgr" (Venables and Ripley 2002; Garret 2013). Posterior probability considers new information to revise original probability, or priori probability (Tatsuoka 1970). Typicality measures how likely a random sample is to be a part of certain

group and is calculated on the variability between all of the groups in the analysis (Tatsuoka 1970). Typicality probabilities are calculated based on absolute distances, where posterior probabilities are calculated of relative distances, which makes posterior probabilities inherently biased as they force samples into a group, where when calculating typicality probabilities, a sample may belong to none, one or more groups (Tatsuoka 1970) (Figure 3-25).

Maps showing the interpolation of the typicality and posterior probabilities are shown in Figure 3-25 and Figure 3-26. If the posterior probability and typicality probability scores fall within the GTZs than it suggests that the GTZs could be roughly delineated based on the till geochemistry alone. The results show that the mapped probabilities do indeed show evidence that the data has a predictive capacity, as the posterior and typicality probability scores for each sample do fall within the allotted GTZs. The predicted probabilities generated by the linear discriminant analysis show that the chemical suite for each GTZ is distinct with some overlap.

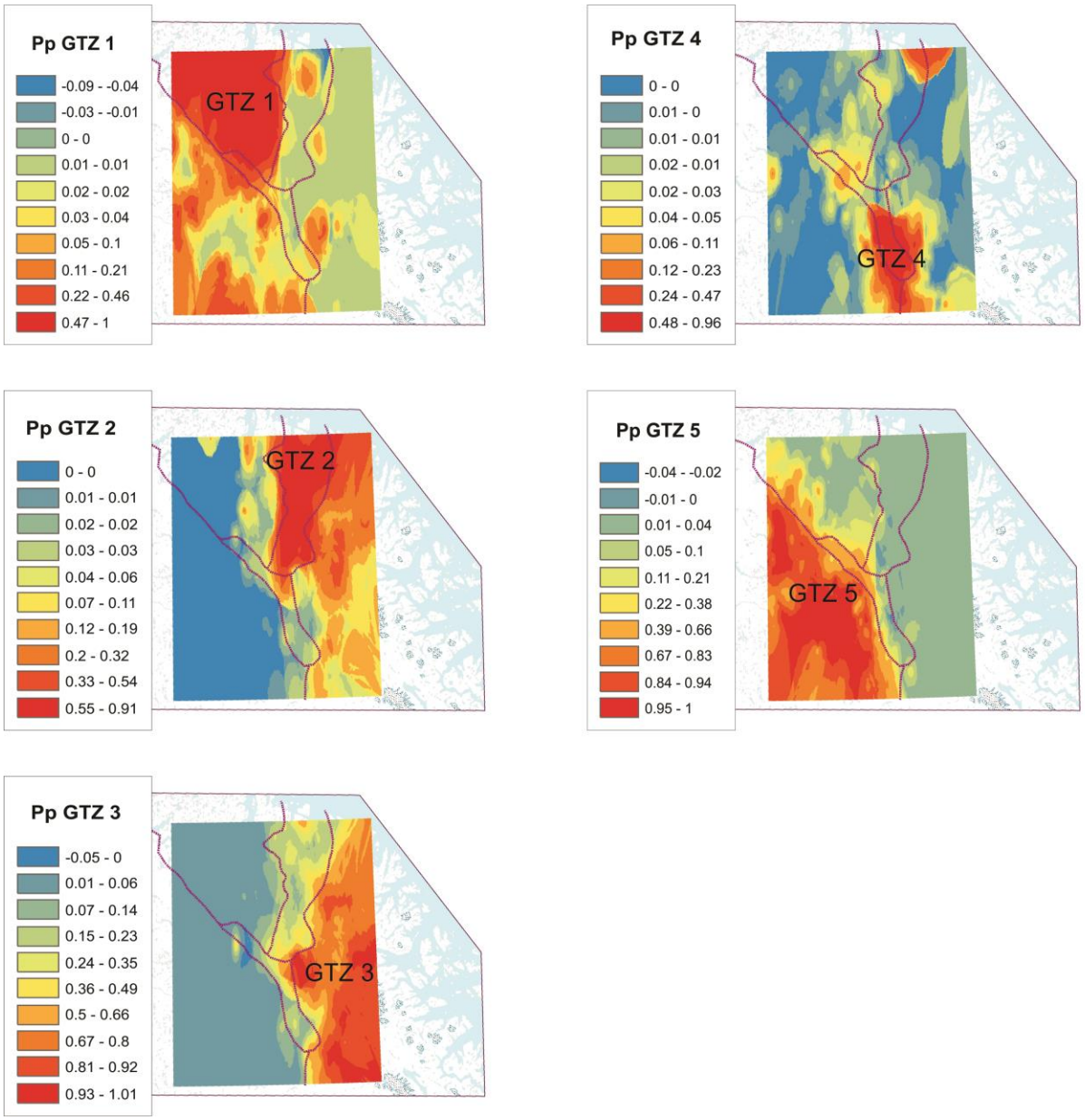

Figure 3-25: The posterior probability (Pp) results of each GTZ show the predictive capacity of the data. As shown, the geochemistry is fairly accurately predicted for each GTZ.

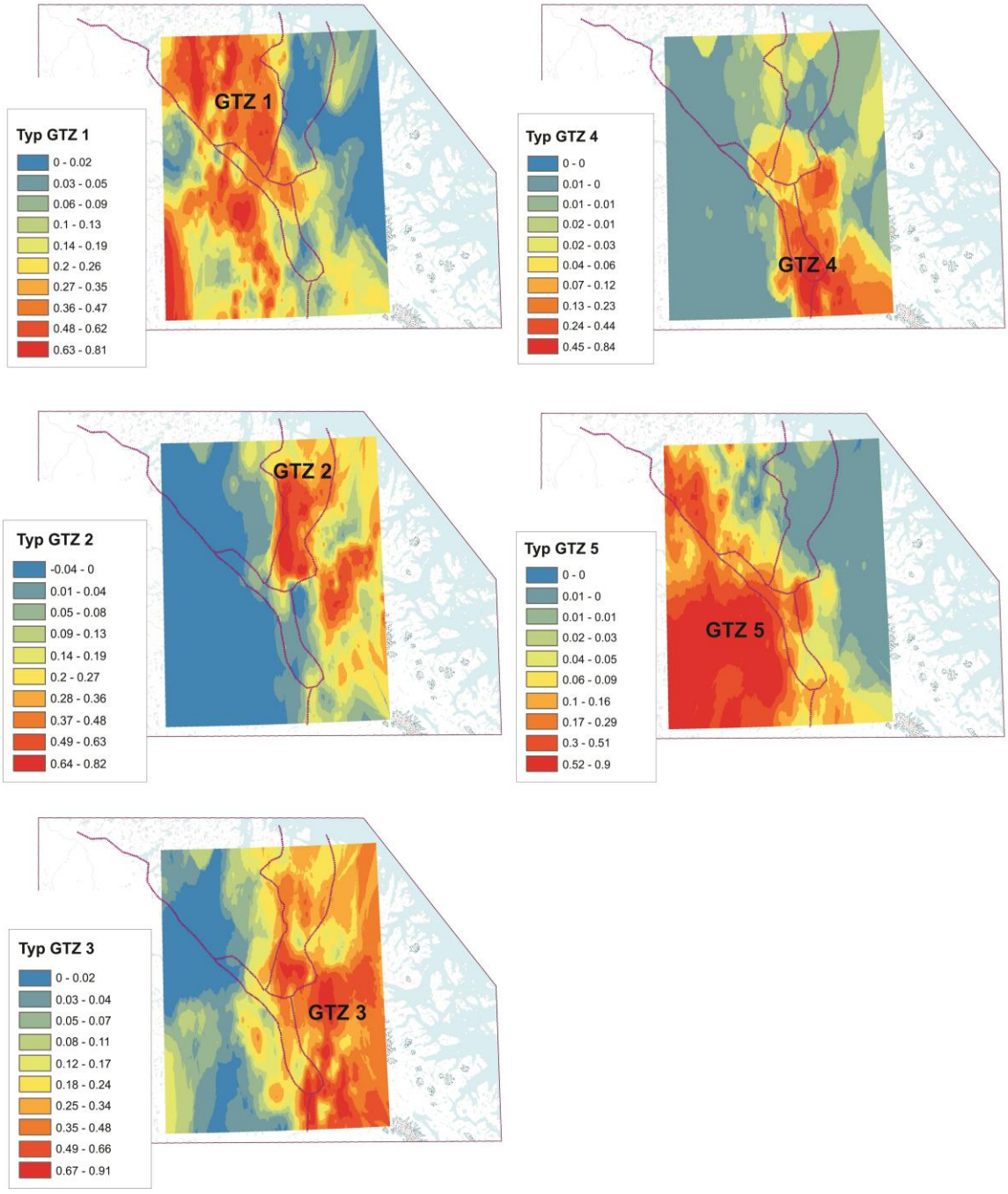

Figure 3-26: Typicality results for each GTZ. Considering that both of these probability analyses show strong patterns for each GTZ, it would seem that we have a strong predictive tool for fine tuning, or maybe even pre-defining, the GTZ based of their geochemistry.

3.5 Interpretation and discussion

The multi-faceted approach used in this study highlighted a mosaic landscape, with each zone having a distinct glacial record. Flows are preserved to various degrees in different zones. Each of the proxies highlights different aspects of the subglacial history of the area. Remote sensing mapping highlighted large features, which would be difficult to map in the field, where field-mapping lead to the recognition of subtle yet critical later flows, such as the northern flows found inland beneath Ptarmigan Fjord. As shown in previous studies (Andrews 1989), mapping bedrock controlled lake densities allowed areas of high areal erosion to be described quantitatively. Combining this proxy with elongation ratio data, and therefore ice velocity, gave an in depth look at the sum of the subglacial environment or the ice-vigour (Hodder 2012). The CIA quantitatively described differences in weathering, which shows the dramatic contrast between GTZ 1 and 5, for example. Each proxy described a useful aspect of the subglacial history. As discussed by Trommelen et al. (2012) and Kleman et al. (1997), a multi-proxy set of tools was necessary to capture the timeline of events.

When comparing to other similar and recent studies on Cumberland Peninsula, east of Hall Peninsula, there are many similarities. Like Cumberland Peninsula, Hall Peninsula has been influenced by cold- and warm-based ice, reflecting variable spatial and temporal conditions in basal thermal regimes (Refsnider and Miller 2010; Refsnider and Miller 2013). Also, Hall Peninsula has similar landscapes to Cumberland Peninsula; warm-based erosion in fjord onset zones and the fjords themselves and less erosive cold-based ice fjord interfluves and the interiors (Refsnider and Miller 2010). The high CIA values found in the silt fraction in the interior of the Hall Peninsula are similar to those found in the silt fraction in the interior of Cumberland Peninsula shown by Refnsider and Miller (2010). It was also found that like on Cumberland Peninsula, the basal thermal regime on Hall Peninsula switched from a large flow event flowing from the Hall Ice Divide to the northeast and southwest, and switching to preferential funnelling into fjords, which developed a complex landscape partially preserved by cold-based ice and partially undergoing linear erosion.

The Cumberland Peninsula till CIA study was done using both clay and silt sized fractions (Refsnider and Miller 2010). The two till databases used to calculate the CIA were originally collected by Dredge (2004) and Utting et al (2008) from 20 to 50 cm depth. The samples from both sets of data were analysed using Inductively Coupled Plasma Emission Spectroscopy (ICP-ES) techniques, and digested with aqua-regia (Dredge et al. 2004; Utting et al. 2008). The CIA values for the clay fraction were divided by 100. The CIA values on Cumberland Peninsula ranged from 20 to 90, with some samples in this study also showing an inherited weathering signal (Refsnider and Miller 2010). According to Fredo et al. (1995), rocks and minerals that are not weathered, which range from K-feldspar to gabbro, have similar CIA values of 50. The resulting values fit within the range found in this study, which show a range of 10 to 100 (Fredo et al. 1995). Though the CIA study done here is comparable to other studies, the results do not agree with the PCA results. This is likely because of the rock types in the study area. The CIA for this study area may be inadequate, as the PCA results in this case show weathering across a wider spectrum of rock types. The contrasting results may have also resulted from the differing size fractions used, as well as the differences in sample coverage. Overall, the PCA analysis is a better proxy for weathering in this study.

The clay-sized geochemical database used for the PCA as a part of this study was not suitable for CIA analysis, as some minerals were only partially digested resulting in elements K, Ca and Na to be extremely underrepresented, and thus the CIA too high. The clay sized geochemical database had undergone partial digestion using Aqua Regia. A possible future exercise is to test the viability of the CIA would be to test the CIA of bedrock, both fresh and weathered, to study the variations of the CIA in the different bedrock types (including regolith). Another proxy that is going to be studied is cosmogenic radionuclide (CRN) data, similar to what was done on Cumberland Peninsula (Refsnider and Miller 2010). Samples have been collected across the five GTZs and are hypothesized to correspond to the GTZs described above. For example, the interior of the study area (GTZ 5) that has undergone little erosion and has high CIA is likely to correspond with CRN concentrations that will show complex burial-exposure histories.

The PCA shows that weathering in GTZ 5 most likely created a geochemical footprint assemblage (Al-Fe-Ga-V) that has been dispersed down-ice affecting the geochemical make-up

of the till in GTZ 1 (Figure 3-27). The compositional overlap between GTZ 5 and 1 show that areal scouring does not seem to produce large volumes of tills through erosion of fresh rocks, which is consistent with the low erosion models of shield terrains (Sudgen and John 1976). Linear erosion, however, is much more efficient at eroding down into fresh rocks, which probably explains the geochemistry of GTZ 2. GTZ 3 and 4 are less clear. The landscape signature of these zones is also less clearly defined than the other GTZs. GTZ 3, in particular, includes a landscape of areal scouring and evidence of linear erosion, as well as possibly cold-based spots around the high terrain of the ice cap. Overall, this zone is weakly defined compared to the others and this could explain the considerable geochemical overlap with GTZ 2 and 4. More detailed work is needed in that area to test and/or better define the outline of GTZ 3.

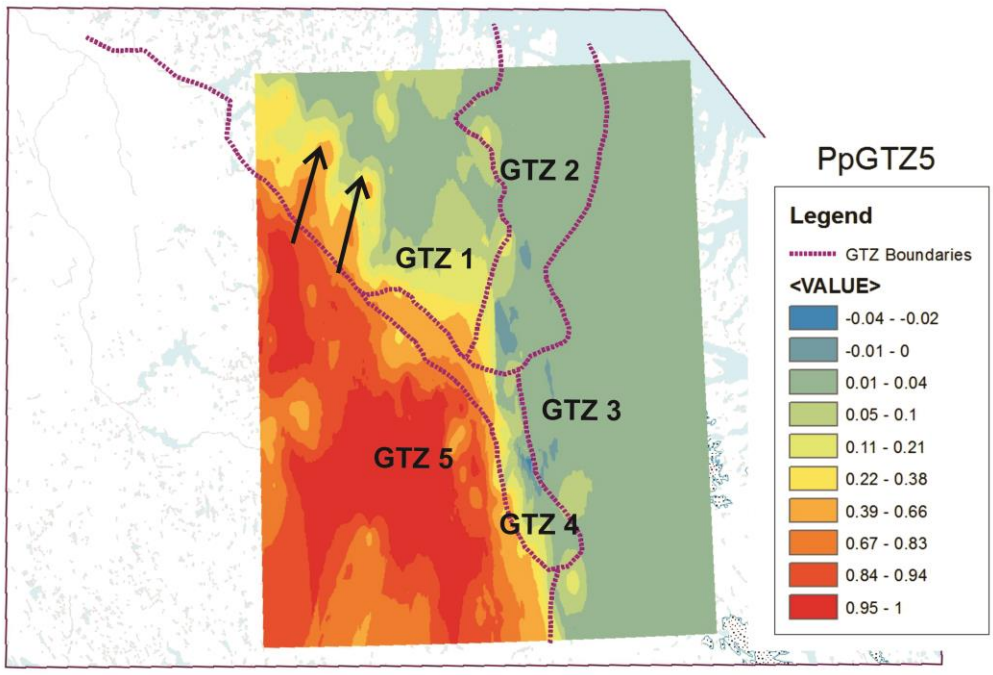

Figure 3-27: Posterior probability figure for GTZ 5 showing overlap with GTZ 1. This indicates that the till in the southwest corner of GTZ 1 is very similar to that of GTZ 5, which is expected in this area because GTZ 1 is located down-ice from GTZ 5. The GTZ 5/1 boundary was determined based on the landform record, but the till compositional boundary is more gradational.

Linear discriminant analysis shows that there is a strong spatial relationship between the till composition and the GTZs, which were initially defined mainly on the basis of the

geomorphological record. It is known that the nature of the bedrock geology can exert a control on basal ice flow dynamics (Anandakrishnan et al. 1998; Bamber et al. 2006). In addition, the basal thermal regime also is a primary controlling factor on basal flow dynamics (Graham et al. 2009). The two factors together will influence erosion and the degree of weathering inheritance (or freshness) of the bedrock over subglacial terrain. It will also influence the degree of overprinting and dilution from up-ice sources. Therefore, by partitioning the landscape into zones that are internally consistent in terms of erosional and basal ice flow intensity records, we integrate bedrock and thermal regime factors. For example, GTZ 5 was defined as an area of low erosion and low basal ice flow dynamics (possibly a cold-based ice divide). GTZ 2 was recognized by its clear linear erosion characteristics. The degree of preservation of rock surfaces that were exposed to weathering processes is thus much higher in GTZ 5 than GTZ 2 and this is shown in the multivariate statistics, whereby trace element assemblages consistent with weathering processes were identified as one characteristic of GTZ 5, but not for GTZ 2. Transport distances are also probably much shorter in GTZ 5 than GTZ 2. Overprinting and dilution effects in GTZ 5 are thus expected to be low or inexistent compared to the other zones. The composition of the till on Hall Peninsula thus appears to represent the net effect of several factors that also control subglacial landscape evolution. Hence, there is a strong relationship between till composition and GTZ, or there is glacial process consistent with GTZ characteristics to explain most overlaps, such as the one between GTZ 5 and 1.

In summary, areas where cold-based conditions prevailed led to the production of material with high regolith inheritance and the till from areas of linear subglacial erosion does not have that inheritance. The geochemical make-up of the till in GTZ 2 probably reflects that of fresh rocks from the catchment area. Areas that were affected by moderate subglacial erosion and basal flow intensity may also be distinguishable as their geochemical signature reflects both inheritance and overprinting. Therefore, the integration of geomorphology and till geochemistry reveals patterns that relate to past subglacial conditions. In addition, the combination of GTZ mapping, the subglacial dynamics index, CIA mapping, and PCA analysis, could help constrain estimates of sediment transport distances, with important implications for subglacial processes as well as drift prospecting. Estimating sediment transport distances from till data is always a challenge in mineral exploration. This study shows, for example, that till within GTZ 1 has a signature that

overlaps with that of GTZ 5 located up-ice. Therefore, it is likely that part of the till matrix in GTZ 1 has a source in GTZ 5. If our interpretation that GTZ 5 was predominantly cold-based and located under an ice divide, then we can further assume that particles in GTZ 1 till are unlikely to come from farther away than GTZ 5.

Cosmogenic isotopes, ^{10}Be and ^{26}Al in particular, have been used as proxies to identify areas of high pre-glacial exposure inheritance and areas where erosion has removed that signal (Refsnider and Miller 2010). This approach could be used on Hall Peninsula to further characterize the GTZ. However, thanks to the large number of samples and good spatial coverage of the till geochemical database, the multivariate statistical analysis of till geochemistry reveals spatial patterns and assemblages, which would be difficult to capture with other methods. A multi-faceted approach integrating glacial geomorphology and till geochemistry thus seems to be powerful for capturing complex, and sometimes subtle, patterns which give insights into past subglacial conditions.

3.6 Reconstructing the glacial dynamics of Hall Peninsula

Four distinct glacial styles were recognized, which are 1) cold-based ice divide; 2) uniform areal scouring and NE-trending streamlined hills, 3) channelized flow crosscutting ubiquitous northeast flow and 4) late deglacial southeast flow. Delineating these zones has led to an understanding of the spatial and temporal pattern changes, building the foundation for a conceptual model of the evolution of subglacial dynamics (Figure 3-29 to Figure 3-32) and has gained insight into the transition between the LIS to the Holocene Ice Cap on Hall Peninsula. The conceptual models are based off of Johnson and Ross (2012) and then modified with Tremblay et al. (2013). The legend for the four conceptual models is shown in Figure 3-28.

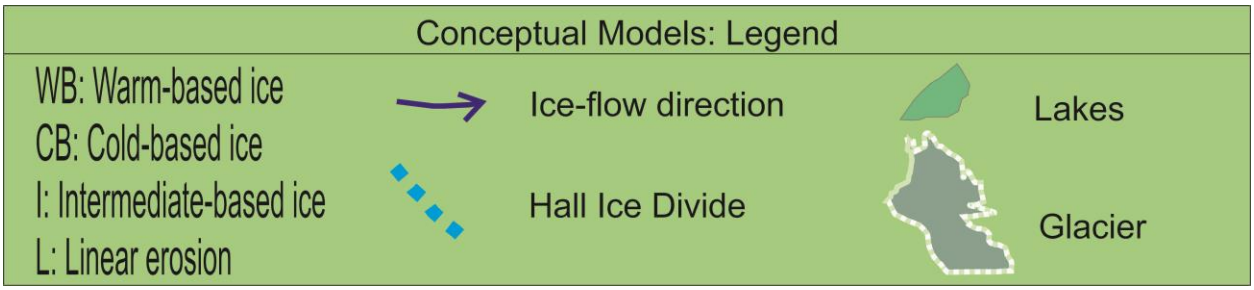

Figure 3-28: Legend for the conceptual models Figure 3-29 to Figure 3-32.

The LGM ice was a large, uniform system that was controlled by ice surface slope and thickness (Figure 3-29). The Hall Ice Divide running parallel to the long central axis of the peninsula had ice flowing northeast and southwest away from the centre and towards the coast (Marsella et al. 2000). Ice in the middle of the peninsula was likely cold-based, as suggested by field evidence (tors, felsenmeer, deep weathering etc.), the GIS analysis (subglacial dynamics index), and till geochemistry showing high inheritance. Radiating from that, the ice was warm-based, as shown by ubiquitous northeast landforms. Southwest and south features have also been documented in the study area, showing flow from the other side of the ice divide.

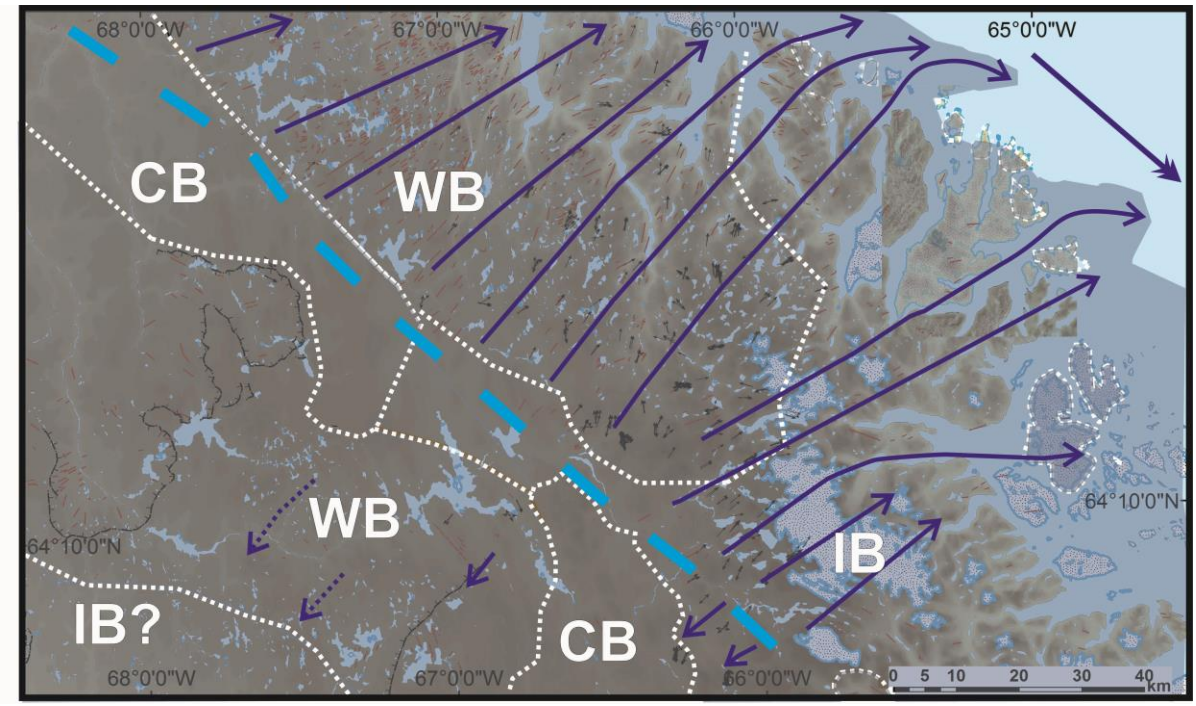

Figure 3-29: The white dotted lines, based off of the GTZ boundaries, show the possible configuration of the subglacial environment at the LGM. Massive ice from the LGM covered Hall Peninsula and its surrounding islands. The surrounding islands were likely covered in cold based ice. Ice is thought to have flown from the Hall Ice Divide (HID) running parallel to the axis of the peninsula. The Cumberland Ice Stream (CIS) may have been flowing parallel to the peninsula in Cumberland Sound at the time. Around the HID, the ice was either cold (CB) or intermediate based (IB). The lack of landforms, highly weathered bedrock, and high CIA alludes to these conditions. Warm based ice (WB) conditions likely existed in the northern part of the study area, shown by the areal scouring and low CIA. Intermediate based ice with sticky spots [IB (SP)] may have existed near the present-day ice cap., which is supported by a higher CIA as compared to GTZ 1. Warm based ice may have existed to the west, but more field work needs to be done to confirm this. (Figure modified from Tremblay et al. 2013).

During deglaciation, the area of cold-based conditions expanded due to ice thinning, and warm-based ice became more focused along troughs, forming a channelized flow system (Figure 3-30). Linear erosion in the troughs is found crosscutting the ubiquitous northeast paleoflow indicators. Flow was directed north and east. The down-ice portion of these troughs now forms a series of fjords.

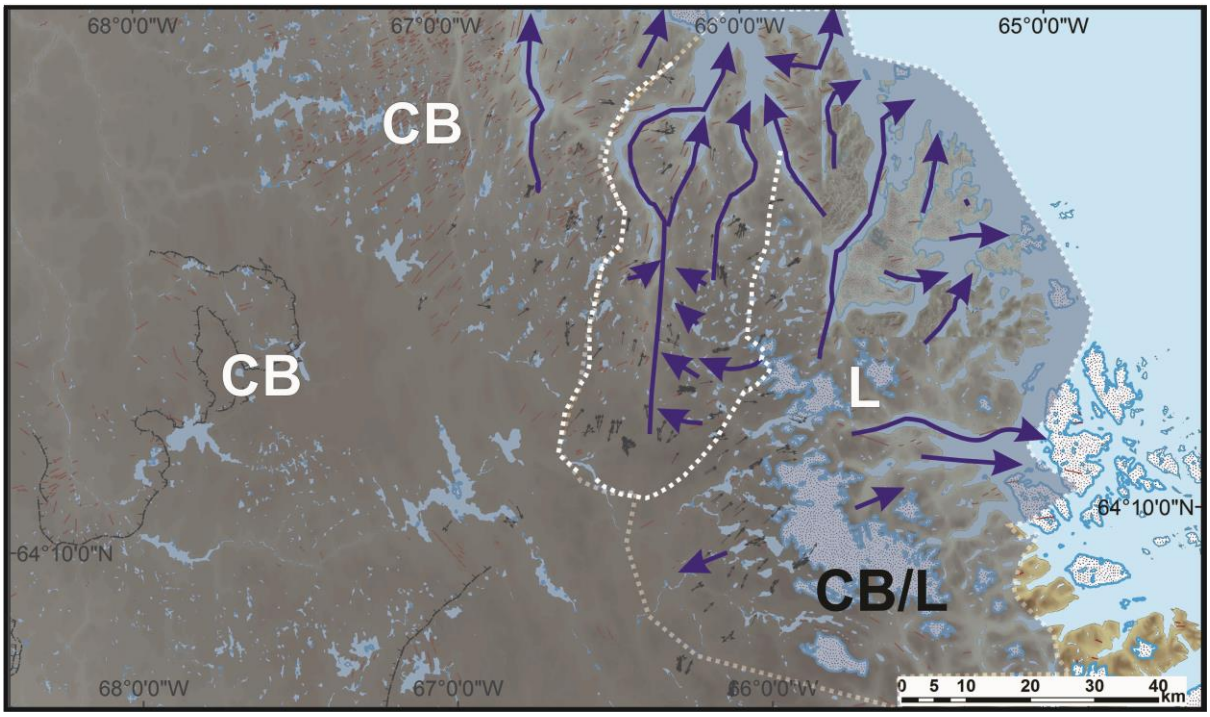

Figure 3-30: During deglaciation, as ice receded and thinned, flow dominated in the troughs where ice was thicker and heavily erosive, which lead to the creation of the northern and eastern fjords. Large areas of cold based (CB) ice existed preserving the pristine LGM landscape, and on the other regions of higher elevation. Ice drawdown over Ptarmigan Fjord could be one of the reasons why the ice mass eventually split forming a local ice cap which separated from the LIS. The portion of ice indicated with an L implies intense linear erosion, which characterizes GTZ 2. Further east in the study area, there was a mix of cold-based (CB) ice with linear erosion (CB/L) taking place as ice funneled through the fjords, which characterizes GTZ 3. (Figure modified from Johnson et al. 2012).

Ice continued to retreat to the position of Hall Moraine, dated at 11 ka (Miller 1980), which indicates a dynamic ice margin (Figure 3-31). The ice that deposited the Hall Moraine was not heavily erosive. Very little evidence of erosion was observed in the field, which is also supported by the GIS analysis (subglacial dynamic index), the CIA and multivariate geochemical analysis. In the central part of the peninsula, felsenmeer and weathered bedrock are found, and very few paleo-erosional features. The Hall Moraine is one of the few features that exist that suggests warm-based ice existed there. The lobes that created these late glacial moraines were

probably very thin and had low erosive capacity. Our interpretation is that these thin lobes readvanced quickly (perhaps through surges) to form these terminal moraines without eroding much across the area affected by the readvance. The material forming these moraines could come from farther inside the catchment, but further studies are needed on these moraines to determine provenance of sediments. Nonetheless, it is quite clear that the bedrock outcrops up-ice of these moraines show little sign (if any) of glacial erosion. It is also hypothesized that ice persisted to the north of these readvancing lobes. This would explain why the landscape there (GTZ 1) is preserved without widespread crosscutting and overprinting. Due to its characteristics, this GTZ 1 landscape is interpreted as LGM in age and was preserved almost intact, probably under cold-based ice. This could be tested later through boulder dating. However, this remnant ice is also required to form the short-lived glacial lakes that have been recognized and mapped by Miller (1980).

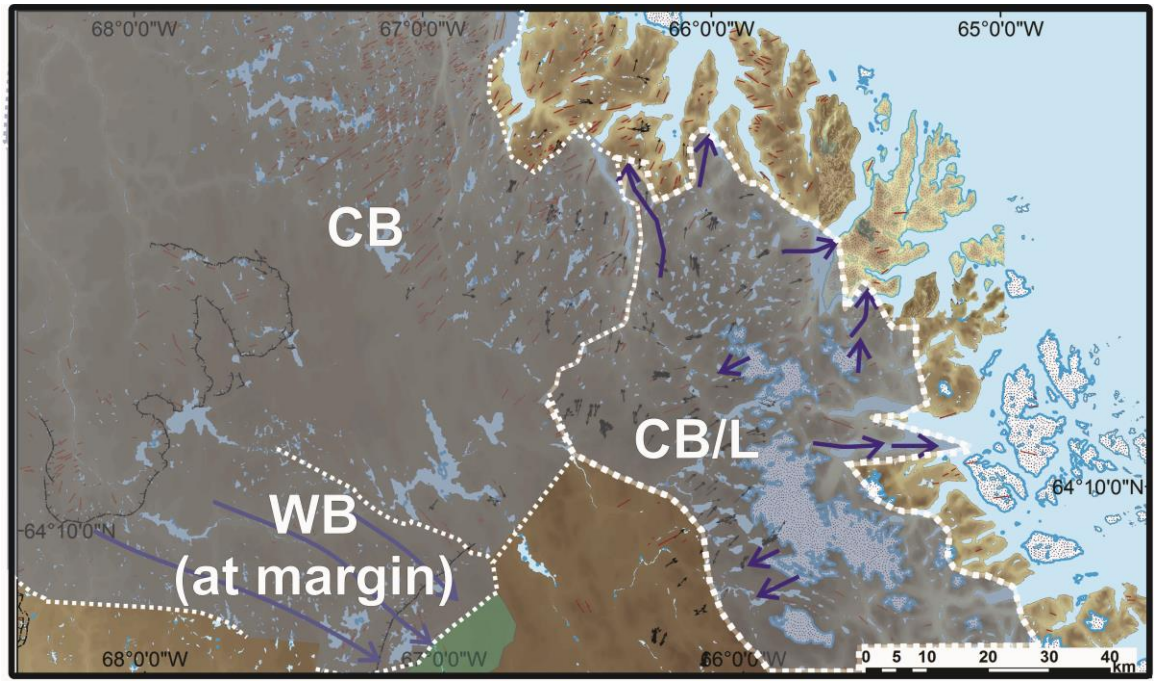

Figure 3-31: The white dotted lines show conceptual ice boundaries during the represented time. The light green areas represent ice-dammed lakes. Hall Moraine (11 ka ago) is shown solid blue, and indicating dynamic ice margin during retreat (Miller 1980). The ice mass is still present in the southeastern part of study area. (Figure modified from Johnson et al. 2012).

One of the last evidence of LIS dynamics in the area is the Frobisher Bay Moraine dated at 8-9 ka (Miller 1980) (Figure 3-32).

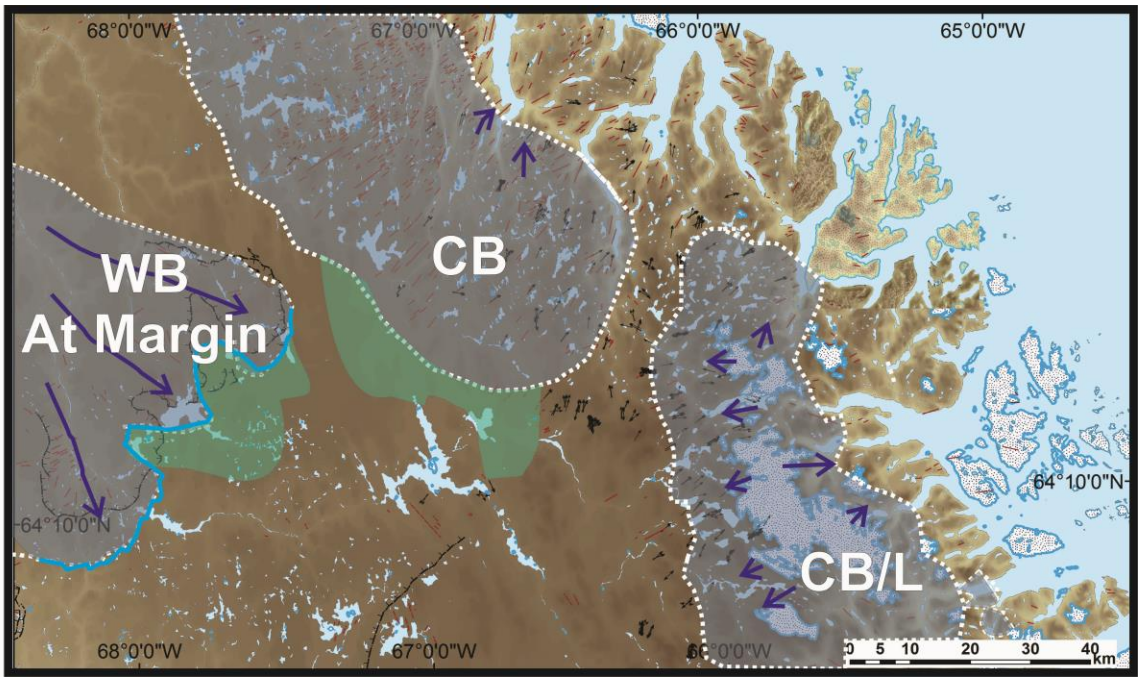

Figure 3-32: This map shows the approximate ice margin and Frobisher Bay Moraine (shown with solid blue line) from Miller (1980) which has been dated at 8-9 ka ago. The topography between the cold-based where the lakes are thought to have resided and cold-based/linear erosion areas is approximately 100 m, preventing lake drainage. (Figure modified from Johnson et al. 2012).

3.7 Conclusions

The field-based mapping and remote sensing analysis show a complex glacial history for the study area, which is comprised of 6 different flowsets, which from oldest to youngest are: 1a)Northeast; 1b) Southwest; 2) North; 3) Northwest; 4) West; 5) East; and 6) Southeast. These six flows, as well as the study on streamlined hill elongation ratio, streamlined hill density, and bedrock controlled lake density were overlaid and grouped based on internal consistencies outlining five GTZs. Therefore, a mosaic was recognized, with each zone having a distinct glacial record. Delineating these zones has led to an understanding of the spatial and temporal pattern changes, building the foundation for a conceptual model of the evolution of subglacial dynamics.

To further this study, geochemical studies including CIA and statistics using PCA and LDA surprisingly showed that there is a strong relationship between the landform based GTZ analysis and their internal geochemistry. This shows that the multi-faceted approach can be used to

determine inheritance and overprinting which are related to proxies of basal dynamics (at the heart of GTZ). Altogether this leads to a powerful comprehensive analysis of the subglacial record. We have gained important insights into subglacial dynamics evolution of the study area, which led to a robust reconstruction.

Three distinct dynamic styles were recognized, which are 1) Uniform with areal scouring and streamlining of landforms, 2) Channelized flow during deglaciation with intervening cold-based zones and 3) Late deglacial southeast flow. Flows were preserved to various degrees in different zones. PCA shows bedrock as the principal component controlling the till geochemical data. LDA shows there is a strong spatial relationship between the till composition and the GTZs, with an accuracy of 83.78%. In other words, the till geochemistry for each GTZ is distinct and could be placed within the correct zone using multivariate statistics 83.78% of the time. There was a switch from uniform warm-based ice during the LGM to a channelized flow during deglaciation with intervening cold-based zones, and cold-based zones inland and in the northwest. These changes within the LIS occurred during deglaciation and the channelized system, in particular, initiated the separation of the Hall Ice Cap from the LIS.

Chapter 4: Conclusions

4.1 An in depth understanding of glacial processes of north central Hall Peninsula

This project is the first comprehensive study of the subglacial record of north central Hall Peninsula looking into glacial landforms, glacial sediments, their relationships, and overall significance for glacial dynamics and drift prospecting. This research provides new insights into the transition of the Laurentide Ice Sheet to the modern ice cap, and into the subglacial dynamics and spatial-temporal changes of the ice sheet over time. Evidence gathered from the field and remote-sensing based research shows evidence of a fragmented landscape, where each fragment has a unique subglacial record. Delineating these zones has led to an understanding of temporal and spatial pattern changes, building the foundation for a conceptual model of the evolution of subglacial dynamics over Hall Peninsula. Four distinct glacial dynamics styles were recognized, which are 1) Uniform with areal scouring and glacial streamlining radiating from a central cold-based zone, 2) channelized flow in glacial troughs crosscutting ubiquitous northeast flow, 3) Limited Late deglacial southeast flow in the central area, and 4) ice cap flows within valleys extending beyond the modern ice cap. Flows were preserved to various degrees in different zones,which controls the different dispersal patterns. There was a switch from uniform warm-based ice during the LGM to a channelized flow during deglaciation with intervening cold-based zones in the highlands between troughs, as well as cold-based zones inland and in the northwest. These changes within the LIS occurred during deglaciation and the channelized system, in particular, initiated the separation of the Hall Ice Cap from the LIS, or from a larger ice cap covering Baffin Island.

4.2 Thesis Contributions

The thesis provided more knowledge and understanding of the Quaternary Geology of north central Hall Peninsula, Baffin Island. The most significant contributions of this thesis are as follows:

1) There is now a 1:500,000 map of the subglacial landscape of north-central Hall Peninsula, Baffin Island, Nunavut. Mapping subglacial features is crucial to understanding the Quaternary History of a glaciated area, and Hall Peninsula was lacking such geomorphological information and knowledge. A total of 1293 streamlined hills have been mapped, 456 paleo-flow indicators and 14 crosscutting relationships determined, and previously mapped features have been integrated with the newly mapped landforms in a common GIS format. This map was used to create a flowset map and reconstruction summarizing ice flow shifts recorded for the study area.

2) Relative glacial erosion intensity and the relationship between landscape and glacial erosion intensity has been established in the study area using multiple proxies including bedrock controlled lake density, streamlined hill elongation ratio and density, and a Chemical Index of Alteration from 1591 till samples. The results have been analysed in a GIS providing new georeferenced maps of all these proxies for the study area.

3) A landscape analysis has been done on the study area, which brought insight into subglacial dynamics and basal thermal conditions and how they change across the study area. A mosaic landscape has been recognized on the basis of sediment-landform assemblages as established from the analysis of the different data obtained in 1 and 2, which lead to the partitioning of the study area into 5 Glacial Terrain Zones (GTZs); each GTZ being internally consistent in terms of glacial record and subglacial dynamics, and, consequently, also in terms of glacial sediment dispersal patterns.

4) The geochemical composition of the till was studied using a principal component analysis (PCA) in an attempt to study patterns in the chemical composition of the till, and compare with the ones established through geomorphology. A linear discriminant analysis was applied to the data. Results show that most GTZ have a till composition that is consistent with their glacial dynamics record which leads to a strong relationship between till composition and the landscape. Specifically, there is a high predictability of

GTZ based on till composition. Furthermore, the glacial dynamics record of certain GTZ (e.g. GTZ 5 and 1) seems to explain most of the compositional characteristics and overlap. This is a very interesting and promising finding which gives insights into the complex interrelationships between the nature of the subglacial bedrock and the subglacial conditions and overall glacial dynamics. This analysis could be further refined once new bedrock maps become available. GTZ boundaries could be adjusted based on till compositional groupings to map with more accuracy the areas where there is strong relationship between glacial landscapes and till compositional characteristics, and underlying bedrock types. This type of analyses is also a way to enhance the GTZ methodology of Trommelen (2012).

5) An innovative, multi-faceted approach was used combining mapping of glacial landforms using targeted fieldwork and remote sensing, with analysis of multiple subglacial dynamics proxies such as Chemical Index of Alteration and streamlined landform elongation, as well as a till compositional analysis to study possible geochemical patterns. The integration of multiple datasets in a GIS has allowed development of a "constrained" subglacial understanding that has highlighted previously unrecognized patterns and relationships. This type of approaches is still uncommon, but is promising and could be applied in other study areas.

6) A conceptual model was proposed displaying the shift between LGM ice to the local Holocene Ice Cap, which was developed through the research of this project and building on Blake (1966), Miller (1980; 1985), Dyke (2002), and De Angelis and Kleman (2007).

4.3 Implications of Work

Prior to this study, Hall Peninsula was lacking geosciences information at the scale and resolution needed to reconstruct subglacial dynamics and landscape evolution. As a result, our understanding of the regional ice sheet evolution and its net effect on till composition and dispersal patterns was inadequate to meet the needs of researchers and exploration geologists. Most of Canada has been greatly shaped by the Quaternary glaciations, and therefore Quaternary

Mapping is essential for many mineral exploration programs. The mapping, which comprises a large portion of my research project, is useful for Canadian geosciences both for economic and academic reasons.

4.3a Quaternary Geology: Mapping and Landscape Analysis

This thesis has shown that the glacial landscape forms a mosaic of internally distinct or unique assemblages each recording a portion of the overall glacial history of the area. For example, older ice-flow phases appear to have been well preserved in some areas (high inheritance), while they have been partly or completely overprinted and obliterated in others. Till composition and dispersal patterns are controlled by subglacial conditions which can be determined by the proxies of erosion and other related subglacial conditions (basal thermal regime, relative ice-flow velocity). The degree of landscape inheritance versus overprinting probably affects the spatial patterns significantly. This thesis explores these types of relationships and has led to new insights on glacial landscape and ice-sheet evolution of Hall Peninsula. The GTZ analysis also allows to understanding, explaining, and perhaps predicting dispersal patterns across a region. The research presented herein thus provides ways to enhance exploration programs that utilize ice flow records and till composition to vector-in buried targets, especially in areas where the glacial record is complex and spatially variable such as is the case on Hall Peninsula.

4.3b Till Geochemistry

Till geochemistry was studied for two reasons: 1) to calculate a chemical index of alteration (CIA) which is used as an erosion proxy as part of the GTZ analysis, and 2) to study the resulting GTZs in terms of their overall geochemistry to explore the relationship between glacial landforms and other erosion proxies, bedrock lithologies and till compositional patterns. Though more research should be done on the chemical index of alteration and how CIA values for fresh rocks vary with different bedrock lithologies, it did successfully highlight areas of linear erosion on Hall Peninsula which were not highlighted using other proxies, such as streamlined hill elongation ratios and bedrock controlled lake density. The latter only showed areas of areal scour versus areas of little erosion (possibly indicative of prevailing cold-based conditions). The

principal component analysis gave interesting results, showing that the GTZs do have characteristic geochemical properties that can be explained consistently using both bedrock geology and glacial dynamics records. Principal component analysis shows bedrock as the principal component controlling the data, but with some assemblages reflecting weathering in areas where glacial dynamics record predict weathering to be preserved or present in till. Linear discriminant analysis shows that there is a strong spatial relationship between the till composition and the GTZs, with an accuracy of 83.78%.

4.3c Mineral Exploration Implications

This project is of importance to industry. As mentioned previously, the Chidliak Property is an area prospective for diamonds. The mapping and interpretations done as a part of my thesis is needed to understand the multi-million-dollar sampling surveys taken and to answer questions about kimberlite indicator mineral (KIM) trains and geophysical anomalies. The mapping thus far has been useful to industry aiding in understanding the KIM trains. It also allowed previous understanding of the glacial geology of the property to be confirmed, further questioned, or rejected. The map enhances the knowledge of the glacial history for industry, as well as for government and academic scientists. When my project is finished, the industrial partner will be able to use the maps to decipher glacial dynamics from the mapped subglacial record. A better understanding of the glacial dynamics could lead to new discoveries including diamondiferous kimberlites and other economic deposits.

The study I conducted also highlights how geochemical sampling survey data can be utilized. As shown here, the CIA and PCA used can inform industry about complex geochemical assemblages which can enhance the way till geochemical databases can be used by the mineral exploration industry.

References

Andrews JT. 1989. Quaternary geology of the northeastern Canadian Shield. In: *Quaternary Geology of Canada and Greenland*. Fulton RJ, editor. 1st ed. Ottawa: Geological Survey of Canada. 276 p.

Anandakrishnan, S., Blankenship D.D., Alley, R.B., and Stoffa P. L. (1998), Influence of subglacial geology on the position of a West Antarctic ice stream from seismic observations, *Nature*, 394: 62– 65.

Bamber, J.L., Ferraccioli, F., Joughin, I., Shepherd, T., Rippin, D.M., Siegert, M.J., Vaughan, D.G., 2006. East Antarctic ice stream tributary underlain by major sedimentary basin. *Geology* (34): 33–36.

Blackadar, R.G. 1967. Geological Reconnaissance, Southern Baffin Island, District of Franklin. Geological Survey of Canada Paper 66-47; Maps 16-1966, 17-1966, 18-1966.

Blake, W. J. 1966. End moraines and deglaciation chronology in Northern Canada with special reference to Southern Baffin Island. Geological Survey of Canada, Paper 66-26, 31 p.

Boulton GS. 1996. Theory of glacial erosion, transport and deposition as a consequence of subglacial sediment deformation. *Journal of Glaciology*, 42 (140): 43-62.

Boulton GS and Clark CD. 1990. A highly mobile Laurentide Ice Sheet revealed by satellite images of glacial lineations. *Nature* 346 (6287): 813-817.

Bostock, H.S. 1970: Physiographic regions of Canada. Geological Survey of Canada, Map 1254A.

Briner, J.P., Gosse, J.C., and Bierman, P.R. 2006, Applications of cosmogenic nuclides to Laurentide Ice Sheet history and dynamics. In: Application of cosmogenic nuclides to the

study of Earth surface processes: The practice and the potential. Siame, L.L., Bourlès, D.L., and Brown, E.T., eds. Geological Society of America Special Paper 415, p. 29–41

Briner J.P., Davis P.T., andMiller G.H. 2009. Latest Pleistocene and Holocene glaciation of Baffin Island, arctic Canada: Key patterns and chronologies. *Quaternary Science Reviews* 28: 2075-87.

Clarhall A. and Jansson K.N. 2003. Time perspectives on glacial landscape formation - glacial flow chronology at Lac Aux Goelands, northeastern Quebec, Canada. *Journal of Quaternary Science* 18(5): 441-52.

Clark C.D. 1999. Glaciodynamic context of subglacial bedform generation and preservation. *Annals of Glaciology* 28: 23-32.

Clark C.D., Knight J.K., Gray J.T. 2000. Geomorphological reconstruction of the Labrador sector of the Laurentide Ice Sheet. *Quaternary Science Reviews* 19(13): 1343-66.

Clark C.D., Hughes A.L.C., Greenwood S.L., Spagnolo M., Ng F.S.L. 2009. Size and shape characteristics of drumlins, derived from a large sample, and associated scaling laws. *Quaternary Science Reviews* 28(7-8): 677-92.

Davis J.C. 2002. *Statistics and Data Analysis in Geology* 3rd ed. New York: John Wiley & Sons, Inc.

De Angelis, H. 2007. Glacial geomorphology of the east-central Canadian arctic. *Journal of Maps*: 323.

De Angelis, H. and Kleman, J. 2005. Palaeo-Ice Streams in the Northern Keewatin Sector of the Laurentide Ice Sheet. *Annals of Glaciology*, *42(*42): 135-144.

De Angelis H and Kleman J. 2007. Paleo-ice streams in the Foxe/Baffin sector of the Laurentide Ice Sheet. *Quaternary Science Reviews* 26(9-10): 1313-31.

DiLabio, R. N. W. and Shilts, W. W. 1979. Composition and Dispersal of Debris by Modern Glaciers, Bylot Island, Canada. In *Moraines and Varves: Origin, Genesis and Classification*, edited by C. Schluchter, 145-155. Rotterdam: A.A. Balkema.

Dredge, L.A. 2001. Late Pleistocene and Holocene Glaciation and Deglaciation of Melville Peninsula, Northern Laurentide Ice Sheet. *Géographie Physique Et Quaternaire* 55 (2): 159-170.

Dredge, L. A. (2004), Till geochemistry results, central Baffin Island,Nunavut (NTS 37A, 37D, 27B, 27C), Open File 4543, Geological Survey of Canada, Ottawa.

Dreimanis, A. 1956. Steep Rock Iron Ore Boulder Train. *Proceedings Geological Association of Canada* 8: 27-70.

Dreimanis, A. and Vagners, U. J. 1971. Bimodal Distribution of Rock and Mineral Fragments in Basal Tills. In *Till, a Symposium*, edited by R. P. Goldthwait, 237-250. Columbus, Ohio: Ohio State University Press.

Dyke, A.S. and Prest, V.K. 1987. Late Wisconsinan and Holocene History of the Laurentide Ice Sheet. *Géographie Physique Et Quaternaire* 41 (2): 237-263.

Dyke A.S., Andrews J.T., Clark P.U., England J.H., Miller G.H., Shaw J., Veillette J.J. 2002. The Laurentide and Innuitian Ice Sheets during the Last Glacial Maximum. *Quaternary Science Reviews* 21(1-3): 9-31.

Dyke, A.S. 2004. An Outline of North American Deglaciation with Emphasis on Central and Northern Canada. In *Quaternary Glaciations—Extent and Chronology, Part II: North America*, edited by J. Ehlers and P. L. Gibbard, 337-424: Elsevier Amsterdam.

Ehlers, J. and Gibbard, P.L. (editors). 2004. Quaternary Glaciations - Extent and Chronology, Part II: North America. *Developments in Quaternary Science*, Vol. 2b. Amsterdam, Elsevier.

Fedo, C.M., Nesbitt, H.W. and Young, G.M. 1995. Unraveling the effects of potassium metasomatism in sedimentary rocks and paleosols, with implications for paleoweathering

conditions and provenance. *Geology* 23, 921-924.

Fipke, C.E., Gurney, J.J., Moore, R.O. 1995. Diamond exploration techniques emphasizing indicator mineral geochemistry and Canadian examples. Geological Survey of Canada, Bulletin 423: 80.

Garret, R.G.,The 'rgr' package for the R Open Source statistical computing and graphics environment - a tool to support geochemical data interpretation *Geochemistry: Exploration, Environment, Analysis*, November 2013, v. 13, p. 355-378, First published on November 15, 2013, doi:10.1144/geochem2011-106

Graham, A.G.C., Larter, R.D., Gohl, K., Hillenbrand, C.L., Smith, J.A., and Kuhn, G. 2009. Bedform signature of West Antarctic paleo-ice stream reveals a multi-temporal record of flow and substrate control. *Quaternary Science Reviews*, 28

Greenwood, SI, and Clark, C.D., 2009. Reconstructing the last Irish Ice Sheet 2: a geomorphologically driven model of ice sheet growth, retreat and dynamics. *Quaternary Science Reviews*, 28.

Grunsky E. 2010. The interpretation of geochemical survey data. Geochemistry Exploration, Environment Analysis 10 (1):27-74.

Hall, A.M. and Glasser, N.F. 2003. Reconstructing the basal thermal regime of an ice stream in a landscape of selective linear erosion: Glen Avon, Cairngorm Mountains, Scotland. *Boreas:* 32, 191-207.

Harris, J.R., Parkinson, W., Dyke, A., Kerr, D., Russell, H., Eagles, S., Richardson, M. and Grunsky, E., 2012. Predictive surficial geological mapping of Hall Peninsula and Foxe Basin Plateau, Baffin Island using LANDSAT and DEM data; Geological Survey of Canada Open File 7038.

Hart J.K. and Smith B. 1996. Subglacial deformation associated with fast ice flow, from the Columbia Glacier, Alaska. *Sedimentary Geology* 111: 177-197.

Heaman, L.M, Grutter, H.S., Pell, J., Holmes, P., and Grenon, H. U-Pb Geochronology, Sr- and Nd- Isotope Compositions of Groundmass Perovskite from the Chidliak and Qilaq Kimberlites, Baffin island, Nunavut. 10th International Kimberlite Conference, Bangalore. 10IKC—193

Hodder, T. 2012. A GIS analysis of subglacial erosion intensity of Hall Peninsula, Baffin Island, Nunavut. BSc Thesis. University of Waterloo, Waterloo, Ontario, Canada.

Jackson, G.D. and Berman, R.G. 2000. Precambrian metamorphic and tectonic evolution of northern Baffin Island, Nunavut, Canada. *Canadian Mineralogist* 38: 399-421.

Jennings, AE. 1993. The Quaternary History of Cumberland Sound, Southeastern Baffin-Island - the Marine Evidence. *Geographie Physique Et Quaternaire* 47 (1): 21-42.

Johnson, C. L. and Ross, M. 2012. Glacial landscape evolution on Hall Peninsula, Baffin Island, since the Last Glacial Maximum: insights into switching glacial dynamics and thermo-mechanical conditions. Abstract EP53D-1071. Presented at 2012 Fall Meeting, AGU. San Francisco, California., 3-7 Dec.

Johnson, C.L., Ross, M. and Tremblay, T. 2013. Glacial geomorphology of north-central Hall Peninsula, Southern Baffin Island. Geological Survey of Canada, Open File 7413.

Kabata-Pendias, A., 2001. Trace Elements in Soils and Plants, third ed. CRC Press, NY

King E.C., Hindmarsh R.C.A., and Stokes C.R. 2009. Formation of mega-scale glacial lineations observed beneath a west Antarctic ice stream. *Nature Geoscience* 2(8): 585-588.

Kirkley M., Mogg T., and McBean D. 2003. Snap Lake field trip guide, in Slave Province and northern Alberta field trip guidebook: Vlllth International Kimberlite Conference: 67-78.

Klassen RA. 2001. A Quaternary geological perspective for geochemical exploration in glaciated terrain. In: Drift exploration in glaciated terrain. McClenaghan MB, Cook SJ,Bobrowsky PT, editors. Special Volume 185 ed. London: Geological Society of London. 1-17 p.

Kleman, J., Hattestrand, C., Borgstrom, I., and Stroeven, A., 1997. Fennoscandian palaeoglaciology reconstructed using a glacial geological inversion model. *Journal of Glaciology* 43: 283-299.

Kleman J. and Glasser N.F. 2007. The subglacial thermal organization (STO) of ice sheets. *Quaternary Science Reviews* 26(5-6): 585-97.

Kleman J., Jansson K., De Angelis H., Stroeven A.P., Hättestrand C., Alm G., Glasser N. 2010. North American ice sheet build-up during the last glacial cycle, 115–21kyr. *Quaternary Science Reviews* 29(17-18): 2036-51.

Kong, J.M., Boucher, D.R. and Scott Smith, B.H., 1999. Exploration and geology of the Attawapiskat kimberlites, James Bay Lowland, Northern Ontario, Canada. In: *Proceedings of the VIIth InternationalKimberlite Conference*, Cape Town. Vol. 1, pp 452– 467.

Kujansuu R., 1990. Glacial flow indicators in air photographs. In: *Glacial Indicator Tracing*, R. Kujansuu and M. Saarnisto (editors). Rotterdam, Netherlands: A.A. Balkema.

Leblanc-Dumas, J., Allard, M. and Tremblay, T. 2013. Quaternary geology and permafrost characteristics in central Hall Peninsula, Baffin Island, Nunavut. *in* Summary of Activities 2012, Canada-Nunavut Geoscience Office, p. 101-106.

Marsella K.A., Bierman P.R., Davis P.T., Caffee M.W. 2000. Cosmogenic 10Be and 26Al ages for the Last Glacial Maximum, eastern Baffin Island, arctic Canada. Geological Society of America Bulletin 112(7): 1296-312.

McClenaghan, M.B., Bobrowsky P.T., Hall G.E.M., and Cook, S.J., (editors) 2001. Geological Society Special Publication 185 ed. Bath, UK: The Geological Society Publishing House. 83 p.

McClenaghan, M.B. and Kjarsgaard, B.A. 2001. Indicator mineral and geochemical methods for diamond exploration in glaciated terrain in Canada. *Drift Exploration in Glaciated Terrain.*

McClenaghan, M. B., Ward, B. C., Kjarsgaard, I. M, Kjarsgaard, B. A., Kerr, DE and L. A. Dredge. 2002. Indicator Mineral and Till Geochemical Dispersal Patterns Associated with the Ranch Lake Kimberlite, Lac De Gras Region, NWT, Canada. *Geochemistry: Exploration, Environment, Analysis* 2 (4): 299-319.

McMartin, I. and Paulen, R.C. 2009. Ice-flow indicators and the importance of ice-flow mapping for drift prospecting. In: Application of till and stream sediment heavy mineral and geochemical methods to mineral exploration in western and northern Canada. GAC Short Course Notes 18 ed. Ottawa: Geological Association of Canada. 15 p.

McMartin, I. and Henderson, P. 2004. Evidence from Keewatin (central Nunavut) for paleo-ice divide migration. *Géographie Physique Et Quaternaire* 58(2-3):163-86.

Miller G.H., Wolfe, A.P., Steig, E.G., Sauer, P.E., Kaplan, M.R., and Briner J.P. 2002. The Goldilocks dilemma: Big ice, little ice, or "just-right" ice in the eastern Canadian arctic. *Quaternary Science Reviews* 21:33-48.

Miller, G.H., Wolfe, A.P., Brine,r J.P., Sauer, P.E., and Nesje, A. 2005. Holocene glaciation and climate evolution of Baffin Island, Canada. *Quaternary Science Reviews* 24:1703-21.

Miller, G. H., Wolfe, A. P., Steig, E. G, Sauer, P. E., Kaplan, M. R., and. Briner, J. P. 2002. The Goldilocks Dilemma: Big Ice, Little Ice, Or "just-Right" Ice in the Eastern Canadian Arctic. *Quaternary Science Reviews* 21: 33-48.

Miller G.H. 1985. Moraines and proglacial lake shorelines, Hall Peninsula. In: *Quaternary Environments: The eastern Canadian Arctic, Baffin Bay and West Greenland*. Andrews JT, editor. Boston: Allen and Unwin. 546 p.

Miller G.H. 1980. Late Foxe Glaciation of southern Baffin Island, N.W.T., Canada. Geological Society of America Bulletin 91(Part 1): 399-405.

Nesbitt H.W. and Young G.M. 1982. Early Proterozoic climates and plate motions inferred from major element chemistry of lutites. *Nature* 299(5885): 715-717.

Paulen, R.C. 2009. Drift prospecting in northern Alberta- A unique glacial terrain for

exploration. R.C. Paulen and I. McMartin (eds.), *Application of Till and Stream Sediment Heavy Mineral and Geochemical Methods to Mineral Exploration in Western and Northern Canada*; Geological Association of Canada, GAC Short Course Notes 18, p. 185-205.

Paulen, R. C. and I. McMartin, eds. 2009. *Application of till and stream sediment heavy mineral and geochemical methods to mineral exploration in western and northern Canada*. GAC Short Course Notes 18 ed. St. John's Nfld.: Geological Association of Canada.

Parent, M., Paradis S, Boisvert, E. 1995. Ice-flow patterns and glacial transport in the eastern Hudson Bay region: Implications for the late Quaternary dynamics of the Laurentide Ice Sheet. *Canadian Journal of Earth Science* 32(12): 2057-70.

Pell J. 2011. 2011 Technical Report on the Chidliak property, 66° 21' 43" W, 64° 28' 26" N Baffin Region, Nunavut. Peregrine Diamonds LTD.

Pell, J., Grutter, H., Grenon, H., Dempsey, S., and Neilson, S. 2012. Exploration and discovery of the Chidliak kimberlite province, Baffin Island, Nunavut: Canada's newest diamond district. 10th International Kimberlite Conference, Bangalore. 10IKC—40

Pell, J., Clements, B., Grutter, H., Neilson, S., and Grenon, H. 2013. Following kimberlite indicator minerals to source in the Chidliak kimberlite province, Nunavut. New Frontiers for Exploration in Glaciated Terrain. in, *New frontiers for exploration in glaciated terrain*; Paulen, R C (ed.); McClenaghan, M B (ed.). Geological Survey of Canada, Open File 7374: 47-52.

Philips, E., Everest, J., and Diaz-Doce, D. 2010. Bedrock controls on subglacial landform distribution and geomorphological processes: Evidence from the Late Devensian Irish Sea Ice Stream. Sedimentary Geology, 232: 98-118.

Plouffe A, Bednarski JM, Huscroft CA, Anderson RG, and McCuaig SJ. 2011. Late Wisconsinan glacial history in the Bonaparte Lake map area, south-central British Columbia: Implications for glacial transport and mineral exploration. *Canadian Journal of Earth Science* 48(6): 1091-111.

R development core team, 2011. R: A language and environment for statistical computing. Vienna, http://www.r-project.org.

Refsnider K.A. and Miller G.H. 2010. Reorganization of ice sheet flow patterns in arctic Canada and the mid-Pleistocene transition. *Geophysical Research Letters* 37:L13502.

Refsnider, K.A. and Miller, G.H. 2013. Ice-sheet erosion and the stripping of Tertiary regolith from Baffin Island, eastern Canadian Arctic. *Quaternary Science Reviews* 67: 176-189.

Rikhotso C.T., Poniatowski B.T., and Hetman C.M. 2003. Overview of the exploration, evaluation of geology of the Gahcho Kue kimberlites, Northwest Territories, in Slave Province and northern Alberta field trip guide. Vlllth International Kimberlite Conference :79-86.

Ross M., Campbell J.E., Parent M., and Adams R.S.. 2009. Palaeo-ice streams and the subglacial landscape mosaic of the North American mid-continental prairies. *Boreas* 38(3): 421-39.

Rose, A. W., Hawkes, H. E., and Webb, J. S. (Eds.). (1979). *Geochemistry in mineral exploration* (2nd ed.). London: Academic Press Inc.

Scott, D.J. 1996. Geology of the Hall Peninsula east of Iqaluit, southern Baffin Island, Northwest Territories; in Current Research 1996-C; Geological Survey of Canada, p.83-91.

Scott, D. J. 1999. "U–Pb Geochronology of the Eastern Hall Peninsula, Southern Baffin Island, Canada: A Northern Link between the Archean of West Greenland and the Paleoproterozoic Torngat Orogen of Northern Labrador." *Precambrian Research* 93 (1): 5-26.

Shilts, W. W. 1996. Drift Exploration." In *Past Glacial Environments: Sediments, Forms and Techniques,* edited by J. Menzies. Glacial Environments: Volume 2 ed., 411-438. Oxford: Butterworth-Heinemann Ltd.

Shilts, W. W. 1993. Geological Survey of Canada's Contributions to Understanding the Composition of Glacial Sediments. *Canadian Journal of Earth Sciences* 30 (2): 333-353.

Shilts W.W. 1984. Till Geochemistry in Finland and Canada. *Journal of Geochemical Exploration* 21 (1-3): 95-117.

Smith M.J. and Knight J. 2011. Palaeoglaciology of the last Irish Ice Sheet reconstructed from striae evidence. *Quaternary Science Reviews* 30(1-2):147-60.

Smith M.J. and Wise S.M. 2007. Problems of bias in mapping linear landforms from satellite imagery. *International Journal of Applied Earth Observation and Geoinformation* 9(1):65-78.

Stanley, C.R. 2009. Geochemical, mineralogical and lithological dispersal models in glacial till: physical process constraints and application in mineral exploration. R.C. Paulen and I. McMartin (eds.), *Application of Till and Stream Sediment Heavy Mineral and Geochemical Methods to Mineral Exploration in Western and Northern Canada; Geological Association of Canada*, GAC Short Course notes 18, 35-48.

Spagnolo, M., Clark, C.D., Hughes, A.L.C., Dunlop, P. 2011. The topography of drumlins; assessing their long profile shape. *Earth Surface Process Landforms* 36(6):790-804.

Stea, R. and Fink, P. 2001. An evolutionary model of glacial dispersal and till genesis in maritime Canada. In: *Drift Exploration in Glaciated Terrain*. McClenaghan MB, Bobrowsky PT, Hall GEM, editors. 185th ed. London: The Geological Society of London. 237 p.

Stokes, C.R. and Clark, C.D. 2002. Are long subglacial bedforms indicative of fast ice flow? *Boreas* 31:239-49.

Stokes, C.R., Clark, C.D., and Storrar, R. 2009. Major changes in ice stream dynamics during deglaciation of the north-western margin of the Laurentide Ice Sheet. *Quaternary Science Reviews* 28(7-8):721-38.

St-Onge, M.R., Jackson, G.D. and Henderson, I. 2006. Geology, Baffin Island (south of 70^{o} N and east of 80^{o} W), Nunavut. Geological Survey of Canada, Open File 4931, scale 1:500 000.

Sudgen D.E. and John B.S., editors. 1976. *Glaciers and Landscape: A Geomorphological Approach*. New York: Wiley.

Tatsuoka, M.M. 1970. Discriminant Analysis: The Study of Group Differences (Selected Topics in Advanced Statistics: An Elementary Approach, Number 6). Champaign, Illinois: Institute for Personality and Ability Testing, Inc.

Tremblay, T., Lamothe, M. and Paulen, R. C. 2011. A spatial analysis of the geomorphology and geochemical alteration of cold-based zones transitional with warm-based zones, Melville Peninsula, Nunavut GACMAC 2011, conference abstract, Arctic landscape evolution: large scale geomorphic response to regional climatic, oceanographic, and geodynamic processes, Ottawa.

Tremblay, T., Leblanc-Dumas, J., Allard, M., Gosse, J.C., Creason, C.G., Peyton, P., Budkewitsch, P. and LeBlanc, A-M. 2013. Surficial geology of southern Hall Peninsula, Baffin Island, Nunavut: summary of the 2012 field season. *in* Summary of Activities 2012, Canada- Nunavut Geoscience Office, p. 93-100.

Tremblay, T., Leblanc-Dumas, J., Allard, M., Ross, M. and Johnson, C., in press: Surficial geology of central Hall Peninsula, Baffin Island, Nunavut: summary of the 2013 field season; *in* Summary of Activities 2013, Canada-Nunavut Geoscience Office.

Trommelen M.S., Ross M., and Campbell J.E. 2012. Glacial terrain zone analysis of a fragmented paleoglaciologic record, southeast Keewatin Sector of the Laurentide Ice Sheet. *Quaternary Science Reviews* 40:1-20.

Utting, D. J., Little, E.C.,Young, M.D., McCurdy, M.W., Dyke, A.S., and, Girard, I. 2008. Till, stream-sediment and bedrock analyses, North Baffin Island, Nunavut (NTS 37E, F, G, H and 47E), Open File 5742.Geological Survey of Canada, Ottawa.

Whalen, J.B.,Wodicka, N, Taylor, B.E. and Jackson, G.D. 2010. Cumberland batholith, Trans-Hudson Orogen, Canada: Petrogenesis and implications for Paleoproterozoic crustal and orogenic processes *Lithos*, 117, 1–4, 99-118

Venables, W.N., Ripley, B.D., 2002. Modern Applied Statistics with S (fourth ed.). Springer, Berlin.

Appendix A: Glacial Landform and Ice Flow Indicator Map

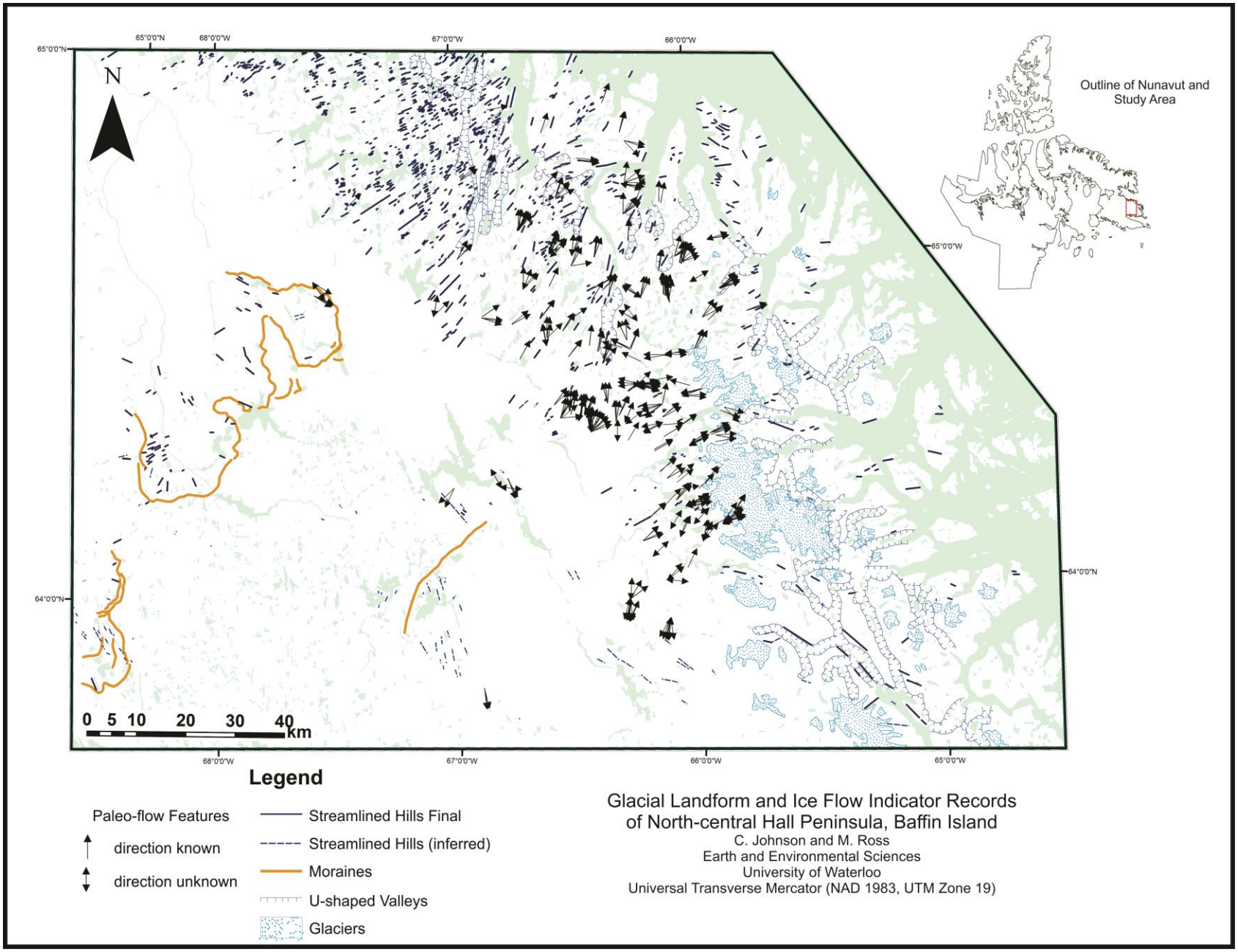

Appendix B: Paleo Ice-flow Data

Station ID	Date	Easting	Northing	Paleoflow Features	Paleoflow Sense	Azimuth
10TIAC001	04/08/2010	619504	7154764	striations	known	55
10TIAC002	04/08/2010	609916	7161045	striations	known	42
10TIAC003	04/08/2010	625480	7148200	striations	known	12
10TIAC003	04/08/2010	625243	7148301	striations	known	12
10TIAC004	04/08/2010	633105	7141454	striations	unknown	45
10TIAC005	04/08/2010	633286	7141491	striations	unknown	80
10TIAC006	04/08/2010	633354	7141461	striations	unknown	72
10TIAC007	04/08/2010	633420	7141461	striations	unknown	90
10TIAC008	04/08/2010	633669	7141719	striations	unknown	81
10TIAC009	04/08/2010	633688	7141738	striations	unknown	105
10TIAC010	04/08/2010	633746	7141872	striations	unknown	80
10TIAC011	04/08/2010	633880	7141700	striations	unknown	80
10TIAC012	04/08/2010	633944	7141716	striations	unknown	85
10TIAC013	04/08/2010	633957	7141527	striations	unknown	105
10TIAC013	04/08/2010	633957	7141527	striations	unknown	91
10TIAC013	04/08/2010	633957	7141527	striations	unknown	86
10TIAC014	05/08/2010	626404.61	7145949.69	striations	known	22
10TIAC015	05/08/2010	626472.63	7145962.21	striations	known	14
10TIAC016	05/08/2010	626414.85	7145915.42	striations	known	14
10TIAC017	05/08/2010	626392.75	7145925.11	roches moutonnées	known	40
10TIAC018	05/08/2010	626391.07	7145921.24	striations	known	14
10TIAC019	05/08/2010	626391.72	7145923.17	striations	known	14
10TIAC020	05/08/2010	616671.61	7137485.54	striations	known	36
10TIAC021	05/08/2010	616597.1	7137361.91	chatter marks	known	45
10TIAC022	05/08/2010	617935.96	7134849.46	striations	known	30
10TIAC023	05/08/2010	617936.47	7134849.92	chatter marks	known	85
10TIAC024	05/08/2010	617952.63	7134774.48	striations	known	32
10TIAC025	05/08/2010	617983.68	7134709.53	chatter marks	known	20
10TIAC025	05/08/2010	617983.68	7134709.53	chatter marks	known	14
10TIAC025	05/08/2010	617983.68	7134709.53	chatter marks	known	50

10TIAC027	05/08/2010	636417.81	7142674.05	chatter marks | striations	known	80
10TIAC028	06/08/2010	643805.06	7117203.96	striations	known	105
10TIAC029	06/08/2010	643796.42	7117229.57	striations	unknown	80
10TIAC030	06/08/2010	643740.82	7117399.82	striations	unknown	62
10TIAC031	06/08/2010	643742.56	7117409.39	striations	unknown	62
10TIAC032	06/08/2010	644413.26	7117686.68	striations	unknown	65
10TIAC033	06/08/2010	644407.9	7117639.68	striations	unknown	75
10TIAC034	06/08/2010	644692.21	7117512.58	striations	known	55
10TIAC035	06/08/2010	644558.58	7117437.94	striations	known	65
10TIAC036	06/08/2010	644649.72	7117098.29	striations	known	74
10TIAC037	06/08/2010	651453.83	7114592.98	striations	known	240
10TIAC038	06/08/2010	651415.17	7114523.79	striations	known	35
10TIAC039	06/08/2010	651202.78	7113966.58	striations	unknown	62
10TIAC040	06/08/2010	651181.33	7113961.29	striations	unknown	55
10TIAC041	06/08/2010	651238.03	7113855.03	striations	unknown	68
10TIAC042	06/08/2010	651372.12	7113713.15	striations	unknown	65
10TIAC045	07/08/2010	607487.37	7122535.85	striations	known	160
10TIAC046	07/08/2010	607427.68	7122547.93	striations	known	155
10TIAC047	07/08/2010	607395.25	7122535.99	striations	known	150
10TIAC050	08/08/2010	641606.14	7121942.31	roches moutonnées	known	50
10TIAC051	08/08/2010	641953.17	7120608.33	chatter marks	known	80
10TIAC052	08/08/2010	641780.79	7118703.67	roches moutonnées	known	40
10TIAC053	08/08/2010	641807.67	7118698.21	striations	known	40
10TIAC054	08/08/2010	641561.17	7118382.52	sriations	known	45
10TIAC055	08/08/2010	641548.81	7118397.35	striations	known	35
10TIAC057	08/08/2010	640595.91	7112757.75	striations	unknown	30
10TIAC058	08/08/2010	642582.43	7111148.03	striations	unknown	20
10TIAC059	08/08/2010	642596.68	7111160.84	striations	known	25
10TIAC060	08/08/2010	644013.18	7104743.51	striations	known	25
10TIAC061	08/08/2010	640757.97	7094428.64	striations	unknown	192
10TIAC062	08/08/2010	640734.99	7094520.43	striations	unknown	185
10TIAC063	08/08/2010	640812.21	7094439.12	striations	unknown	194
10TIAC064	08/08/2010	640926.61	7094307.94	striations	unknown	190

10TIAC065	08/08/2010	640799.98	7094372.74	chatter marks	known	185
10TIAC066	08/08/2010	634150.78	7097705.74	striations	unknown	202
10TIAC067	08/08/2010	634150.92	7097721.82	striations	unknown	202
10TIAC068	08/08/2010	634150.89	7097736.43	chatter marks	known	202
10TIAC069	08/08/2010	634070.22	7097824.33	chatter marks	known	202
10TIAC070	08/08/2010	632733.16	7098356.14	striations	known	192
10TIAC071	08/08/2010	632732.44	7098354.55	striations	known	185
10TIAC072	08/08/2010	632738.32	7098348.88	striations	known	188
10TIAC073	08/08/2010	632643.22	7098334.02	striations	known	187
10TIAC074	08/08/2010	634983.47	7110090.83	striations	known	70
10TIAC075	08/08/2010	634919.58	7110106.69	striations	known	45
10TIAC076	08/08/2010	634897.45	7110096.91	striations	known	65
10TIAC077	08/08/2010	634894.61	7110095	striations	known	47
10TIAC078	08/08/2010	638105.57	7124190.73	striations	known	52
10TIAC080	09/08/2010	629591.71	7134371.44	striations	unknown	180
10TIAC082	09/08/2010	638651.23	7135258.34	striations	known	47
10TIAC083	09/08/2010	638655.75	7135253.52	striations	known	60
10TIAC084	09/08/2010	638541.19	7135250.14	striations	known	52
10TIAC085	10/08/2010	640707.03	7167890.24	striation	known	52
10TIAC086	10/08/2010	640708.07	7167881.24	chatter marks	known	52
10TIAC087	10/08/2010	640708.78	7167927.92	chatter marks	known	15
10TIAC088	10/08/2010	640710.62	7167864.62	striations	known	55
10TIAC089	10/08/2010	640727.17	7167872.2	striations	known	62
10TIAC090	10/08/2010	640728.05	7167868.78	striations	known	52
10TIAC091	10/08/2010	641675.97	7166551.64	striations	known	60
10TIAC091	10/08/2010	641675.97	7166551.64	roches moutonnées	known	10
10TIAC092	10/08/2010	641683.86	7166549.1	chatter marks	known	70
10TIAC093	10/08/2010	641691.95	7166570.69	striations	known	15
10TIAC094	10/08/2010	641651	7166718.98	roches moutonnée | striations	known	50
10TIAC094	10/08/2010	641651	7166718.98	striations	known	22
10TIAC095	10/08/2010	638525.5	7160093.26	striations	known	0
10TIAC096	10/08/2010	638558.06	7160161.92	striations	known	355

10TIAC097	10/08/2010	638625.12	7159913.03	chatter marks | striations	known	355
10TIAC098	10/08/2010	638927.69	7159716.28	chatter marks	known	355
10TIAC099	10/08/2010	638916.86	7159704.29	striations	known	10
10TIAC100	10/08/2010	639023.9	7159790.19	striations	known	10
10TIAC101	10/08/2010	639152.84	7159889.82	striations	known	10
10TIAC102	10/08/2010	639205.52	7159925.71	striations	known	350
10TIAC103	10/08/2010	639416.8	7159732.3	striations	known	355
10TIAC104	10/08/2010	639417.42	7159629.67	striations	known	342
10TIAC105	10/08/2010	639429.94	7159228.76	striations	known	355
10TIAC106	10/08/2010	639433.03	7159187.62	striations	known	348
10TIAC107	10/08/2010	639484.6	7159144.24	striations	known	345
10TIAC108	10/08/2010	639539.33	7158862.53	striations	known	355
10TIAC109	10/08/2010	639563.63	7158801.95	striations	known	10
10TIAC110	10/08/2010	639674.69	7158531.65	striations	known	355
10TIAC111	10/08/2010	639796.3	7158336.49	striations	known	355
10TIAC112	10/08/2010	639265.09	7148119.05	striations	unknown	85
10TIAC113	10/08/2010	639235.32	7147960.59	striations	unknown	90
10TIAC114	10/08/2010	639085.59	7147824.89	striations	unknown	75
10TIAC115	10/08/2010	639078.62	7147819	striations	known	260
10TIAC116	10/08/2010	639081.89	7147826.73	chatter marks	known	270
10TIAC117	11/08/2010	644433.84	7129570.26	striations	unknown	58
10TIAC118	11/08/2010	644360.61	7129547.85	striations	unknown	58
10TIAC119	11/08/2010	644346.67	7129747.72	striations	unknown	62
10TIAC120	11/08/2010	644404.16	7129870.94	striations	known	52
10TIAC121	11/08/2010	644230.49	7129785.9	chatter marks	known	62
10TIAC122	11/08/2010	644230.47	7129765.49	striations	known	60
10TIAC123	11/08/2010	644220.85	7129734.68	chatter marks	known	60
10TIAC124	11/08/2010	644161.22	7129843.48	chatter marks	known	55
10TIAC125	11/08/2010	643977.29	7129634.23	striations	known	68
10TIAC126	11/08/2010	648207.7	7132183.56	striations	known	60
10TIAC127	11/08/2010	648239.15	7132148.58	chatter marks	known	80
10TIAC128	11/08/2010	648241.08	7132150.01	striations	known	70
10TIAC129	11/08/2010	648239.16	7132111.2	Chatter marks| striations	known	70

10TIAC130	11/08/2010	648236.9	7132102.72	striations	known	65
10TIAC131	11/08/2010	648483.62	7131778.05	striations	known	70
10TIAC132	11/08/2010	649291.42	7131695.06	striations	known	85
10TIAC133	11/08/2010	649336.14	7131710.62	striations	known	100
10TIAC134	11/08/2010	641972.86	7133307.41	striations	known	56
10TIAC135	11/08/2010	641997.36	7133302.4	striations	known	52
10TIAC136	11/08/2010	650271.01	7136850.21	striations	known	112
10TIAC137	11/08/2010	650274.62	7136849.72	striations	known	110
10TIAC138	11/08/2010	650985.38	7137430.9	striations	known	105
10TIAC139	11/08/2010	651089.93	7137524.54	striations	known	135
10TIAC140	11/08/2010	643159	7139724.77	striations	known	87
10TIAC141	11/08/2010	643151.97	7139714.73	striations	known	95
10TIAC142	11/08/2010	644255.46	7141653.45	striations	known	285
10TIAC143	11/08/2010	644237.56	7141635.31	striations	known	285
10TIAC145	11/08/2010	638958.86	7131325.75	chatter marks	known	58
10TIAC147	12/08/2010	636951.61	7128693.66	striations	known	60
10TIAC148	12/08/2010	637016	7128411.11	striations	known	60
10TIAC149	12/08/2010	624308.17	7132152.15	striations	unknown	350
10TIAC150	12/08/2010	624302.81	7132168.33	striations	known	0
10TIAC150	12/08/2010	624302.81	7132168.33	striations	known	5
10TIAC151	12/08/2010	624302.75	7132166.43	chatter marks	known	70
10TIAC152	12/08/2010	624335.57	7132181.37	striations	known	355
10TIAC152	12/08/2010	624335.57	7132181.37	chatter marks	known	50
10TIAC153	12/08/2010	624418.72	7132231.36	chatter marks	known	355
10TIAC154	12/08/2010	624445.13	7132246.93	chatter marks	known	355
10TIAC155	12/08/2010	624451.04	7132243.26	chatter marks	known	44
10TIAC156	12/08/2010	624454.68	7132244.19	chatter marks	known	30
10TIAC156	12/08/2010	624454.68	7132244.19	chatter marks	known	25
10TIAC156	12/08/2010	624454.68	7132244.19	chatter marks	known	60
10TIAC157	12/08/2010	624336.93	7132292.74	chatter marks	known	45
10TIAC157	12/08/2010	624336.93	7132292.74	chatter marks	known	22
10TIAC157	12/08/2010	624336.93	7132292.74	striations	known	0
10TIAC158	12/08/2010	624159.62	7132340.57	striations	known	355
10TIAC159	12/08/2010	624034.33	7132545.12	striations	known	350

10TIAC160	12/08/2010	623840.15	7132715.22	striations	known	22
10TIAC160	12/08/2010	623840.15	7132715.22	striations	known	3
10TIAC161	12/08/2010	623858.95	7132741.63	striations	known	350
10TIAC161	12/08/2010	623858.95	7132741.63	striations	known	355
10TIAC161	12/08/2010	623858.95	7132741.63	striations	known	8
10TIAC162	12/08/2010	623865.16	7132739.98	striations	known	45
10TIAC163	12/08/2010	623721.24	7132853.54	striations	known	8
10TIAC164	12/08/2010	622910.48	7135335.85	striations	known	0
10TIAC165	12/08/2010	622889.04	7135355.07	striations	known	22
10TIAC166	12/08/2010	622881.11	7135325.98	striations	known	30
10TIAC167	12/08/2010	622946.53	7135361.28	chatter marks	known	2
10TIAC168	12/08/2010	622970.54	7135338.03	striations	known	22
10TIAC169	12/08/2010	622170.26	7135318.81	striations	known	5
10TIAC170	12/08/2010	622132.89	7135314.09	striations	known	0
10TIAC170	12/08/2010	622132.89	7135314.09	striations	known	0
10TIAC171	12/08/2010	622004.32	7135301.39	striations	known	13
10TIAC172	12/08/2010	621875.55	7135464.72	striations	known	10
10TIAC173	12/08/2010	620244.71	7136295.78	striations	known	12
10TIAC174	12/08/2010	619788.39	7136158.71	striations	known	12
10TIAC174	12/08/2010	619788.39	7136158.71	striations	known	4
10TIAC174	12/08/2010	619788.39	7136158.71	striations	known	350
10TIAC174	12/08/2010	619788.39	7136158.71	striations	known	14
10TIAC175	12/08/2010	619803.39	7136112.89	chatter marks	known	350
10TIAC176	12/08/2010	619991.36	7135422.87	striations	known	15
10TIAC177	13/08/2010	625562.89	7198686.57	striations	known	20
10TIAC178	13/08/2010	629262.42	7192837.54	striations	known	16
10TIAC178	13/08/2010	629262.42	7192837.54	striations	known	13
10TIAC179	13/08/2010	630237.98	7191181.35	roches moutonnées | striations	known	108
10TIAC179	13/08/2010	630237.98	7191181.35	roches moutonnées |striations	known	100
10TIAC179	13/08/2010	630237.98	7191181.35	striations	known	135
10TIAC180	13/08/2010	620915.87	7187275.51	striations	known	100
10TIAC181	13/08/2010	620991.38	7187030.56	striations	known	96

10TIAC182	13/08/2010	620865.33	7186946.85	striations	known	87
10TIAC183	13/08/2010	620761.54	7187098.86	striations	known	92
10TIAC184	13/08/2010	620532.05	7187560.97	striations	known	95
10TIAC185	13/08/2010	624360.89	7167369.06	striations	known	20
10TIAC186	13/08/2010	624392.8	7167408.42	striations	known	7
10TIAC186	13/08/2010	624392.8	7167408.42	striations	known	10
10TIAC187	13/08/2010	624453.8	7167409.8	striations	known	7
10TIAC188	13/08/2010	624472.76	7167450.97	striations	known	5
10TIAC189	13/08/2010	624420.89	7167430.09	striations	known	6
11TIAC002	21/07/2011	615647.46	7167564.93	striations	unknown	45
11TIAC003	21/07/2011	615588.4	7168077.63	striations	known	22
11TIAC003	21/07/2011	615588.4	7168077.63	striations	known	42
11TIAC004	21/07/2011	615389.44	7168594.66	striations	known	22
11TIAC005	21/07/2011	615287.57	7168714.04	striations	known	22
11TIAC006	22/07/2011	615231.21	7168744.61	striations | roches moutonnées	known	20
11TIAC007	22/07/2011	615345.87	7168198.7	striations	unknown	28
11TIAC008	22/07/2011	630150.93	7176212.53	striations	known	50
11TIAC009	22/07/2011	630173.46	7176273.37	chatter marks	known	38
11TIAC009	22/07/2011	630173.46	7176273.37	chatter marks	known	40
11TIAC009	22/07/2011	630173.46	7176273.37	chatter marks	known	55
11TIAC010	22/07/2011	630197.23	7176268.63	chatter marks	known	0
11TIAC011	22/07/2011	630251.19	7176257.94	striations	known	45
11TIAC013	22/07/2011	629881.48	7182411.84	striations	known	98
11TIAC013	22/07/2011	629881.48	7182411.84	striations	unknown	105
11TIAC014	22/07/2011	630271.35	7182499.15	striations	known	98
11TIAC015	22/07/2011	630369.5	7182645.28	striations	known	7
11TIAC016	22/07/2011	630362.29	7182672.3	striations	known	50
11TIAC016	22/07/2011	630362.29	7182672.3	striations	known	70
11TIAC017	22/07/2011	630402.49	7182648.38	striations	known	90
11TIAC018	22/07/2011	630448.38	7182669.14	striations	known	70
11TIAC019	22/07/2011	632885.77	7179524.88	striations	known	20
11TIAC020	22/07/2011	637425.96	7178816.82	chatter marks	known	0
11TIAC021	22/07/2011	637747.79	7178532.45	striations	known	10

11TIAC022	22/07/2011	641971.62	7166291.9	striations	known	20
11TIAC023	22/07/2011	642044.24	7166339.94	striations	known	21
11TIAC024	22/07/2011	642528.92	7166557.22	striations	known	0
11TIAC024	22/07/2011	642528.92	7166557.22	striations	known	5
11TIAC025	22/07/2011	642216.68	7166324.21	striations	known	0
11TIAC027	22/07/2011	644055.69	7162796.06	striations	unknown	58
11TIAC028	23/07/2011	609057.09	7172691.09	striations	known	28
11TIAC029	23/07/2011	609083.71	7172721.61	striations	known	35
11TIAC030	23/07/2011	609089.36	7172710.66	striations	known	5
11TIAC031	23/07/2011	609082.38	7172696.65	striations	known	22
11TIAC032	23/07/2011	609082.13	7172699.06	striations	known	22
11TIAC033	23/07/2011	609032.55	7172669.2	striations	known	0
11TIAC033	23/07/2011	609032.55	7172669.2	striations	known	22
11TIAC035	23/07/2011	608845.22	7172602.6	striations	known	23
11TIAC035	23/07/2011	608845.22	7172602.6	striations	known	25
11TIAC036	23/07/2011	608728.56	7172670.34	striations	known	30
11TIAC036	23/07/2011	608728.56	7172670.34	striations	known	45
11TIAC036	23/07/2011	608728.56	7172670.34	striations	known	45
11TIAC037	23/07/2011	608747.24	7172673.62	striations	known	14
11TIAC038	23/07/2011	608709.49	7172655.72	striations	known	32
11TIAC038	23/07/2011	608709.49	7172655.72	striations	known	37
11TIAC039	23/07/2011	608696.17	7172656.17	striations	known	30
11TIAC042	24/07/2011	647372.4	7171412.27	striations	unknown	70
11TIAC042	24/07/2011	647372.4	7171412.27	striations	known	78
11TIAC042	24/07/2011	647372.4	7171412.27	striations	known	80
11TIAC044	24/07/2011	649832.29	7161522.69	striations	known	55
11TIAC045	24/07/2011	649816.41	7161511.86	striations	known	58
11TIAC046	24/07/2011	649831.2	7161590.34	striations	known	52
11TIAC046	24/07/2011	649831.2	7161590.34	striations	known	60
11TIAC048	24/07/2011	649883.34	7161375.28	chatter marks	known	45
11TIAC048	24/07/2011	649883.34	7161375.28	chatter marks	known	70
11TIAC049	24/07/2011	644916.54	7149039.94	striations	known	22
11TIAC049	24/07/2011	644916.54	7149039.94	striations	known	25
11TIAC050	24/07/2011	645216.58	7149205.95	striations	known	32

11TIAC052	24/07/2011	647553.31	7154899.62	striations	known	45
11TIAC053	24/07/2011	647551.98	7154935.46	striations	known	45
11TIAC055	24/07/2011	655360.17	7157043.44	striations	known	68
11TIAC055	24/07/2011	655360.17	7157043.44	striations	known	72
11TIAC055	24/07/2011	655360.17	7157043.44	striations	known	74
11TIAC056	24/07/2011	637484.08	7164841.43	striations	known	6
11TIAC056	24/07/2011	637484.08	7164841.43	striations	known	10
11TIAC061	26/07/2011	650037.59	7161522.96	striations	known	42
11TIAC061	26/07/2011	650037.59	7161522.96	striations	known	54
11TIAC062	26/07/2011	650049.39	7161530.43	striations	known	42
11TIAC063	26/07/2011	650069.82	7161483.07	striations	known	55
11TIAC064	26/07/2011	650069.79	7161483.63	striations	known	65
11TIAC065	26/07/2011	649922.01	7161430.39	striations	known	45
11TIAC065	26/07/2011	649922.01	7161430.39	chatter marks | striations	known	70
11TIAC065	26/07/2011	649922.01	7161430.39	chatter marks	known	70
11TIAC067	26/07/2011	646433.12	7155523.17	striations	known	32
11TIAC067	26/07/2011	646433.12	7155523.17	striations	known	45
11TIAC067	26/07/2011	646433.12	7155523.17	striations	known	45
11TIAC067	26/07/2011	646433.12	7155523.17	striations	known	62
11TIAC067	26/07/2011	646433.12	7155523.17	striations	known	62
11TIAC068	26/07/2011	633873.34	7159469.88	striations	known	25
11TIAC069	26/07/2011	633843.55	7159492	striations	known	18
11TIAC069	26/07/2011	633843.55	7159492	striations	unknown	120
11TIAC069	26/07/2011	633843.55	7159492	chatter marks	unknown	312
11TIAC070	27/07/2011	633846.96	7159476.34	striations	known	10
11TIAC070	27/07/2011	633846.96	7159476.34	striations	known	305
11TIAC071	27/07/2011	633218.33	7154783.01	striations	unknown	322
11TIAC071	27/07/2011	633218.33	7154783.01	striations	unknown	322
11TIAC072	27/07/2011	633306.76	7154585.11	striations	known	300
11TIAC074	27/07/2011	631941.44	7148804.5	striations	known	22
11TIAC074	27/07/2011	631941.44	7148804.5	striations	known	298
11TIAC074	27/07/2011	631941.44	7148804.5	striations	known	300
11TIAC075	27/07/2011	631896.62	7149105.65	striations	known	22

11TIAC075	27/07/2011	631896.62	7149105.65	striations	known	295
11TIAC076	27/07/2011	631272.6	7150683.84	striations	known	335
11TIAC076	27/07/2011	631272.6	7150683.84	striations	known	356
11TIAC077	27/07/2011	630454.2	7149172	striations	known	285
11TIAC079	28/07/2011	573959.37	7176847.44	striations	known	45
11TIAC079	28/07/2011	573959.37	7176847.44	roches moutonnées	known	45
11TIAC081	28/07/2011	567589.89	7161651.62	roches moutonnées	known	120
11TIAC081	28/07/2011	567589.89	7161651.62	striations	unknown	145
11TIAC082	28/07/2011	567666.51	7159135.11	striations	known	112
11TIAC082	28/07/2011	567666.51	7159135.11	striations	known	115
11TIAC082	28/07/2011	567666.51	7159135.11	striations	known	118
11TIAC082	28/07/2011	567666.51	7159135.11	striations	known	123
11TIAC084	28/07/2011	633808.00	7141838.09	striations	unknown	85
11TIAC084	28/07/2011	633808.00	7141838.09	striations	unknown	105
11TIAC084	28/07/2011	633808.00	7141838.09	striations	unknown	264
11TIAC084	28/07/2011	633808.00	7141838.09	striations	known	275
11TIAC084	28/07/2011	633808.00	7141838.09	striations	known	285
11TIAC086	29/07/2011	627475.73	7159963.49	striations	known	5
11TIAC086	29/07/2011	627475.73	7159963.49	striations	known	15
11TIAC086	29/07/2011	627475.73	7159963.49	striations	known	18
11TIAC087	29/07/2011	646600.79	7141101.38	striations	known	248
11TIAC087	29/07/2011	646600.79	7141101.38	striations	known	255
11TIAC088	29/07/2011	646612.62	7140941.62	striations	known	255
11TIAC088	29/07/2011	646612.62	7140941.62	striations	known	260
11TIAC089	29/07/2011	649395.88	7130349.44	striations	known	80
11TIAC096	01/08/2011	632586.77	7098362.51	chatter marks	known	30
11TIAC096	01/08/2011	632586.77	7098362.51	roches moutonnées	known	53
11TIAC096	01/08/2011	632586.77	7098362.51	striations	unknown	183
11TIAC096	01/08/2011	632586.77	7098362.51	striations	unknown	183
11TIAC096	01/08/2011	632586.77	7098362.51	striations	known	184
11TIAC096	01/08/2011	632586.77	7098362.51	chatter marks	known	188
11TIAC097	01/08/2011	647146.89	7110366.85	striations	unknown	25
11TIAC099	01/08/2011	647182.47	7110354.59	striations	unknown	10

11TIAC100	01/08/2011	647187.11	7110351.09	striations	unknown	14
11TIAC103	01/08/2011	601664.57	7154951.66	roches moutonnées	known	95
11TIAC103	01/08/2011	601664.57	7154951.66	striations	known	100
11TIAC103	01/08/2011	601664.57	7154951.66	striations	known	108
11TIAC104	01/08/2011	601761.93	7155120.7	striations	known	55
11TIAC105	01/08/2011	592063.67	7155235.18	striations	unknown	10
11TIAC105	01/08/2011	592063.67	7155235.18	striations	known	45
11TIAC106	01/08/2011	607835.57	7153716.41	striations	known	50
11TIAC106	01/08/2011	607835.57	7153716.41	striations	known	60
11TIAC108	02/08/2011	603132.64	7080001.32	striations	known	165
11TIAC108	02/08/2011	603132.64	7080001.32	striations	known	170
11TIAC108	02/08/2011	603132.64	7080001.32	striations	known	173
11TIAC112	02/08/2011	596656.7	7120363.38	striations	known	25
11TIAC112	02/08/2011	596656.7	7120363.38	striations	known	45
11TIAC112	02/08/2011	596656.7	7120363.38	striations	known	225
11TIAC113	02/08/2011	606052.63	7120659.01	striations	unknown	95
11TIAC114	02/08/2011	621683.63	7134410.06	striations	unknown	12
11TIAC114	02/08/2011	621683.63	7134410.06	striations	known	15
11TIAC113	02/08/2011	606052.63	7120659.01	striations	unknown	330
11TIAC117	03/08/2011	631226.23	7170829.62	striations	known	2
11TIAC117	03/08/2011	631226.23	7170829.62	striations	known	4
11TIAC121	03/08/2011	646105.88	7120790.37	striations	known	45
11TIAC121	03/08/2011	646105.88	7120790.37	striations	known	45
11TIAC124	03/08/2011	638239.89	7124056.38	striations	known	45
11TIAC129	05/08/2011	637104.34	7107092.84	striations	unknown	45
11TIAC132	05/08/2011	645370.32	7113794.51	striations	known	42
11TIAC133	05/08/2011	645369.56	7113795.21	striations	unknown	43
11TIAC136	05/08/2011	647412.3	7110698.23	striations	unknown	42
11TIAC137	05/08/2011	651778.46	7114360.59	striations	unknown	45
11TIAC137	05/08/2011	651778.46	7114360.59	striations	unknown	50
11TIAC137	05/08/2011	651778.46	7114360.59	striations	unknown	55
11TIAC138	05/08/2011	651731.23	7114237.93	striations	unknown	70
11TIAC138	05/08/2011	651731.23	7114237.93	striations	unknown	75

11TIAC139	05/08/2011	653270.7	7115954.86	striations	known	30
11TIAC139	05/08/2011	653270.7	7115954.86	striations	known	30
11TIAC139	05/08/2011	653270.7	7115954.86	striations	known	32
11TIAC139	05/08/2011	653270.7	7115954.86	striations	known	32
11TIAC140	05/08/2011	647406.86	7121877.15	striations	known	35
11TIAC140	05/08/2011	647406.86	7121877.15	striations	known	35
11TIAC140	05/08/2011	647406.86	7121877.15	striations	known	40
11TIAC141	08/08/2011	639575.79	7117654.61	striations	known	43
11TIAC142	08/08/2011	636261.68	7114876.05	striations	known	45
11TIAC142	08/08/2011	636261.68	7114876.05	striations	known	50
11TIAC144	08/08/2011	640042.16	7102275.08	striations	unknown	50
11TIAC145	08/08/2011	640042.25	7102276.76	striations	known	40
11TIAC145	08/08/2011	640042.25	7102276.76	striations	unknown	95
11TIAC146	11/08/2011	619924.39	7167892.67	striations	unknown	4
11TIAC146	11/08/2011	619924.39	7167892.67	striations	known	20
11TIAC146	11/08/2011	619924.39	7167892.67	striations	known	26
11TIAC147	11/08/2011	619762.8	7165659.03	roches moutonnées | striations	known	20
11TIAC147	11/08/2011	619762.8	7165659.03	striations	known	30
11TIAC148	11/08/2011	619728.95	7165636.31	striations	known	80
11TIAC149	11/08/2011	615291.42	7161381.33	striations	known	25
11TIAC149	11/08/2011	615291.42	7161381.33	striations	known	25
11TIAC151	11/08/2011	613852.63	7155147.78	striations	known	35
11TIAC151	11/08/2011	613852.63	7155147.78	striations	known	38
11TIAC152	11/08/2011	614995.35	7149604.35	striations	known	10
11TIAC152	11/08/2011	614995.35	7149604.35	striations	unknown	348
11TIAC152	11/08/2011	614995.35	7149604.35	striations	unknown	350
11TIAC153	11/08/2011	609517.2	7146553.81	striations	known	28
11TIAC154	11/08/2011	619443.75	7147182.28	striations	known	36
11TIAC154	11/08/2011	619443.75	7147182.28	striations	known	38
11TIAC155	12/08/2011	626127.81	7160728.73	striations	known	40
11TIAC155	12/08/2011	626127.81	7160728.73	striations	known	45
11TIAC156	12/08/2011	624753.62	7161412.57	striations	known	58
11TIAC156	12/08/2011	624753.62	7161412.57	striations	known	60

11TIAC157	12/08/2011	624167.08	7158825.02	striations	known	30
11TIAC158	12/08/2011	618191.1	7152345.21	striations	known	30
11TIAC158	12/08/2011	618191.1	7152345.21	striations	known	35
11TIAC159	12/08/2011	615026.04	7150972.95	striations	known	0
11TIAC159	12/08/2011	615026.04	7150972.95	striations	known	7
11TIAC159	12/08/2011	615026.04	7150972.95	striations	known	45
11TIAC159	12/08/2011	615026.04	7150972.95	striations	known	45
11TIAC160	12/08/2011	623644.18	7149430.5	striations	known	6
11TIAC161	12/08/2011	634189.37	7146378.13	striations	known	295
11TIAC162	12/08/2011	638597.59	7137845.59	striations	known	230
11TIAC162	12/08/2011	638597.59	7137845.59	striations	known	235
11TIAC162	12/08/2011	638597.59	7137845.59	striations	known	250
11TIAC162	12/08/2011	638597.59	7137845.59	striations	known	255
11TIAC162	12/08/2011	638597.59	7137845.59	striations	known	265
11TIAC162	12/08/2011	638597.59	7137845.59	striations	known	11
11TIAC163	12/08/2011	638551.66	7134100.65	striations	unknown	238
11TIAC163	12/08/2011	638551.66	7134100.65	striations	unknown	243
11TIAC163	12/08/2011	638551.66	7134100.65	striations	unknown	258
11TIAC164	13/08/2011	627454.85	7137799.44	striations	known	4
11TIAC164	13/08/2011	627454.85	7137799.44	striations	known	345
11TIAC164	13/08/2011	627454.85	7137799.44	chatter marks	known	345
11TIAC164	13/08/2011	627454.85	7137799.44	striations	known	354
11TIAC165	13/08/2011	629222.75	7134170.37	striations	known	0
11TIAC165	13/08/2011	629222.75	7134170.37	striations	known	9
11TIAC165	13/08/2011	629222.75	7134170.37	striations	known	355
11TIAC166	13/08/2011	638597.5	7133696.58	striations	known	85
11TIAC171	14/08/2011	640757.61	7094440.34	striations	known	170
11TIAC171	14/08/2011	640757.61	7094440.34	striations	known	185
11TIAC171	14/08/2011	640757.61	7094440.34	striations	known	190
11TIAC171	14/08/2011	640757.61	7094440.34	striations	known	200
11TIAC171	14/08/2011	640757.61	7094440.34	striations	known	200
11TIAC171	14/08/2011	640757.61	7094440.34	striations	known	210
11TIAC172	14/08/2011	632421.61	7098189.08	striations	unknown	170
11TIAC172	14/08/2011	632421.61	7098189.08	striations	unknown	195

11TIAC173	14/08/2011	639605.06	7122795.86	striations	known	45
11TIAC173	14/08/2011	639605.06	7122795.86	striations	known	59
11TIAC174	14/08/2011	641848.85	7123101.24	striations	known	49
11TIAC176	12/07/2011	616372.24	7179419.85	striations	known	18
11TIAC176	12/07/2011	616372.24	7179419.85	roches moutonnées	known	40
11TIAC176	12/07/2011	616372.24	7179419.85	striations	known	20
11TIAC176	12/07/2011	616372.24	7179419.85	striations	known	18
11TIAC177	15/07/2011	616370.56	7179147.99	roches moutonnées	known	62
11TIAC177	15/07/2011	616370.56	7179147.99	roches moutonnées	known	42
11TIAC178	18/07/2011	610157	7160977	striations	unknown	22
11TIAC178	18/07/2011	610157	7160977	chatter marks	known	0
11TIAC178	18/07/2011	610157	7160977	striations	known	45
11TIAC178	18/07/2011	610157	7160977	chatter marks	known	0
11TIAC179	18/07/2011	596624	7166694	striations	known	45
11TIAC179	18/07/2011	596624	7166694	striations	known	42
11TIAC179	18/07/2011	596624	7166694	striations	known	28
11TIAC180	18/07/2011	597047	7182653	striations	known	55
11TIAC180	18/07/2011	597047	7182653	striations	known	45
11TIAC181	18/07/2011	613832	7181504	striations	known	42
11TIAC181	18/07/2011	613832	7181504	striations	known	44
11TIAC182	20/07/2011	616192	7167667	striations	known	38
11TIAC183	20/07/2011	602289	7197015	striations	known	78
11TIAC184	20/07/2011	602653	7183960	striations	known	20
11TIAC185	20/07/2011	602309	7183847	striations	known	15
11TIAC186	20/07/2011	613305	7192444	striations	known	18
11TIAC187	20/07/2011	629753	7135407	striations	known	28
11TIAC188	20/07/2011	629753	7135407	striations	known	23
11TIAC189	20/07/2011	631322	7133864	striations	unknown	52
11TIAC190	20/07/2011	631132	7134232	striations	unknown	22
11TIAC191	20/07/2011	631700	7130372	striations	known	30

Appendix C: Relative Age Relationships

Station ID	Paleoflow Features	Paleoflow Sense	Azimuth	Relative Age	Nature of Relationship
10TIAC017	roches moutonnées	known	40	1	Superimposed Striae
	striations	known	14	2	
10TIAC085	striation	known	52	1	
	chatter marks	known	52	1	
	chatter marks	known	15	2	
10TIAC094	striations	known	15	2	Superimposed Striae
	roches moutonnées | striations	known	50	1	
	striations	known	1	2	
10TIAC150	striations	known	0	2	Superimposed Striae
	striations	known	5	2	
	chatter marks	known	70	1	
10TIAC152	striations	known	355	2	Protected surface | Superimposed striae
	chatter marks	known	50	1	
10TIAC157	chatter marks	known	45	1	Superimposed striae
	chatter marks	known	22	1	
	striations	known	0	2	
11TIAC065	striations	known	45	1	Unpolished chatter marks
	chatter marks | striations	known	70	2	
	chatter marks	known	70	2	
11TIAC067	striations	known	32	2	Positions on outcrop
	striations	known	45	1	
	striations	known	45	1	
11TIAC069	striations	known	18	1	Superimposed striae
	striations	unknown	120	2	
	chatter marks	unknown	312	2	

11TIAC074	striations	known	22	1	Superimposed striae
	striations	known	298	2	
	striations	known	300	2	
11TIAC075	striations	known	22	1	Superimposed striae
	striations	known	295	2	
11TIAC096	chatter marks	known	30	1	Superimposed striae
	roches moutonnées	known	53	1	
	striations	unknown	183	2	
	striations	unknown	183	2	
	striations	known	184	2	
	chatter marks	known	188	2	
11TIAC178	chatter marks	known	0	1	Superimposed striae
	striations	known	45	2	
	chatter marks	known	0	1	
11TIAC162	striations	known	230	2	Protected surface
	striations	known	235	2	
	striations	known	250	2	
	striations	known	255	2	
	striations	known	265	2	
	striations	known	11	1	

Appendix D: Streamlined Hill and Bedrock Controlled Lake Density Study Details

- The first step in the spatial analysis was to develop a raster file (grid) for the study area. A cell size of 5km X 5km or 25 km^2 was used. Care was taken to eliminate hydrographic features that were not lakes (rivers or streams) from the hydrographic database, and include lakes that were not mapped by comparing the hydrographic database to the LANDSAT imagery. Centroid points were created from lake polygons (Hodder 2012). The lakes are classified based on which grid cell the centroids are located in. The total number of lakes per cell, or centroids per cell, was calculated in the GIS. Care was given to ensure the lakes mapped were bedrock controlled; not lakes on hummocky till which generally are not indicative of basal erosion. Areas with thick till and other sediment containing lakes, such as the moraines, were thus masked. Polygons containing fjords were also masked because they reflect linear erosion as opposed to areal scouring. Linear erosion is not accounted for by the lake density approach and has to be mapped and considered separately.

- The elongation ratios (E=L/W) of streamlined bedrock landforms can also be correlated to glacial erosion intensity (Stokes and Clark 2002). As indicated above, streamlined hills were mapped as polygons in ArcGIS, which allowed the perimeter and the area of the streamlined hills to be calculated. Elongation ratios of the streamlined hills were calculated in Excel using the methodology outlined in Clark et al. (2009). The streamlined hills elongation ratios were then converted to points and classified using the same method as for the lake data.

Appendix E: Chemical Index of Alteration

This till database was collected by Peregrine Diamonds Limited in 2008. The size fraction displayed is fines, which is anything <180 µm. The coordinate system used was NAD 83 Zone 19.Total digestion was used to analyse the till samples.

Sample Number	Easting	Northing	Al_2O_3 wt%	CaO wt%	Na_2O wt%	K_2O wt%	CIA
BE-06-001	594343.6	7170110.6	15.3	10.9	3	0.86	37.33
BE-06-002	620194.42	7129913.9	10.6	7.08	1.52	0.94	39.27
BE-06-003	614875.77	7169607	13.5	8.71	2.24	0.99	39.60
BE-06-004	594983.46	7105225.3	13	6.06	2.08	2.53	43.08
BE-06-005	356808	7147862	14.6	6.46	2.88	1.56	44.55
BE-06-006	642585	7119602	16.1	6.28	3.78	1.69	45.27
BE-06-007	640495.37	7110013.9	15.9	7.04	2.99	1.34	45.34
BE-06-008	635060	7111654	19	9.83	2.47	0.75	45.51
BE-06-009	632621	7148515	14.5	5.69	3.19	1.44	45.81
BE-06-010	619885.76	7144133.5	16.4	6.24	4.19	1.06	45.83
BE-06-011	603269	7139661	16.7	7.71	3.09	0.53	45.91
BE-06-012	633915.42	7145239	14.9	5.97	3.05	1.53	45.95
BE-06-013	615597.6	7159551.3	16	6.18	3.82	1.18	45.98
BE-06-014	615428.33	7155002.6	15.2	6.28	2.78	1.58	46.20
BE-06-015	615603.19	7140130.3	16.3	6.07	4.04	1.09	46.36
BE-06-016	625657.87	7170184.8	15	5.12	3.71	1.6	46.66
BE-06-017	620152.5	7165312.9	16.5	5.59	4.54	1	46.86
BE-06-018	635438.73	7111064.3	16.9	6.48	3.22	1.91	46.88
BE-06-019	635555	7111101	16.4	6.06	3.41	1.74	46.98
BE-06-020	635428.59	7119782.7	15.2	6.41	2.45	1.33	47.02
BE-06-023	625271.33	7135240.6	15	5.97	2.72	1.41	47.09
BE-06-024	595138.42	7075050.5	16.8	6.52	2.2	3.14	47.09
BE-06-025	634851.58	7155715.4	15.7	5.05	3.5	2.42	47.20
BE-06-026	620149.12	7149878.8	16	5.07	4.21	1.4	47.53
BE-06-027	610039.51	7169825.9	15.4	6.04	2.55	1.63	47.62
BE-06-028	635446.6	7111403.2	17.6	6.7	2.96	2.13	47.62
BE-06-029	634159.64	7139331.1	16.7	5.46	3.88	1.89	47.64
BE-06-030	360497	7163302	15.8	4.32	4.32	2.1	47.83
BE-06-031	631258	7126075	17.2	7.05	2.69	1.37	47.88
BE-06-032	635254.29	7111682.1	16.3	6.04	2.9	1.79	47.95
BE-06-033	624580.91	7160019.6	15.7	4.66	4.16	1.57	47.99
BE-06-034	620768.88	7175021.5	15.9	4.92	4.06	1.48	48.00
BE-06-035	634950	7110908	18.4	8.12	2.39	1.02	48.17
BE-06-036	610073.92	7150125.7	15.8	5.52	3.33	1.37	48.17
BE-06-037	620980.2	7169788.4	16	4.78	4.19	1.49	48.20
BE-06-038	635453.62	7111163.6	16.6	6.31	2.93	1.43	48.20
BE-06-039	630620.39	7144170.4	16.3	5.11	3.43	2.2	48.49
BE-06-040	635147	7111161	16.4	6.35	2.56	1.43	48.66
BE-06-041	634951	7110860	17.8	7.64	2.31	0.9	48.81
BE-06-042	604673	7149992	17.1	5.18	4.18	1.5	48.83
BE-06-043	630841.64	7139961.7	15	4.66	3.08	2	48.85
BE-06-044	635450.45	7111264.8	17.3	6.41	2.85	1.61	48.89

BE-06-045	635446.17	7111116.6	16.4	5.7	2.9	1.82	48.95
BE-06-046	635057	7111010	16.5	6.31	2.62	1.28	49.01
BE-06-047	619651.48	7159885.9	16.1	4.44	4.36	1.35	49.08
BE-06-048	635046	7110910	16.5	5.93	3	1.22	49.20
BE-06-049	635058	7110967	17.4	6.85	2.54	1.17	49.29
BE-06-050	635049	7111055	17.2	6.85	2.51	0.97	49.38
BE-06-051	635549	7111157	16.9	5.62	3.1	1.84	49.40
BE-06-052	640444.87	7115480.9	16.8	4.87	3.39	2.55	49.42
BE-06-053	610854.86	7155143	15.6	4.82	3.47	1.37	49.44
BE-06-054	615673.05	7149688.1	16.3	4.74	4.02	1.32	49.45
BE-06-055	635051	7111553	15.9	5.24	3.08	1.51	49.49
BE-06-056	640863	7164625	15.8	4.08	4.01	1.94	49.51
BE-06-057	635451.47	7111667.1	16.4	5.34	3.19	1.61	49.55
BE-06-058	358654	7158565	15.4	3.96	3.71	2.19	49.56
BE-06-059	635552	7111004	16.4	4.83	3.59	1.84	49.58
BE-06-060	635151	7111308	17.5	5.99	3.06	1.73	49.58
BE-06-061	635352	7111163	16.1	5.95	2.54	1.24	49.63
BE-06-062	605017	7145124	15.7	5.13	3.16	1.28	49.67
BE-06-063	635143	7111414	16	5.03	3.26	1.53	49.74
BE-06-064	584938.29	7139971	17.9	4.74	4.34	2.11	49.80
BE-06-065	635348	7111760	17	5.34	3.25	1.92	49.80
BE-06-066	615775.27	7165848.4	16.8	4.77	4.07	1.42	49.84
BE-06-067	594712.62	7164999.5	18.2	4.55	4.31	2.7	49.88
BE-06-068	362016	7170160	16	4.3	3.19	2.73	49.97
BE-06-069	620098.38	7155135	16.6	4.79	3.93	1.3	50.03
BE-06-070	635143	7111258	17.2	6.12	2.54	1.7	50.08
BE-06-071	354821	7130922	16.7	4.36	3.97	1.98	50.15
BE-06-072	639875.64	7100234.4	18.1	3.88	5.39	1.91	50.15
BE-06-073	357970	7153596	16.4	4.08	3.87	2.31	50.18
BE-06-074	635048	7111102	16.7	5.97	2.58	1.35	50.21
BE-06-075	635146	7111209	17.6	5.76	3.11	1.72	50.21
BE-06-076	635151	7111107	17.2	6.38	2.37	1.35	50.35
BE-06-077	641279	7159756	14.4	3.62	3.38	1.9	50.35
BE-06-078	579614.03	7159727.7	19.6	4.05	5.2	3.14	50.36
BE-06-079	595907.98	7160642.1	17.7	4.51	4.09	2.3	50.40
BE-06-080	635149	7111054	16.9	6.12	2.41	1.4	50.44
BE-06-081	635147	7111361	17	5.53	2.88	1.72	50.51
BE-06-082	635148	7111755	16.2	5.51	2.47	1.64	50.54
BE-06-083	594891.46	7155709	18	5.02	3.97	1.8	50.55
BE-06-084	641208	7144497	16.4	4.47	3.44	2.08	50.56
BE-06-085	594059.13	7141326	16.8	4.46	4.16	1.35	50.58
BE-06-086	625434.05	7155089.8	15.2	3.98	3.46	1.75	50.63
BE-06-087	635353	7111555	17.1	5.77	2.6	1.76	50.63
BE-06-088	640689	7149776	16.5	4.01	3.66	2.52	50.71
BE-06-089	590285.27	7164715.1	19.9	5.71	4.24	1.82	50.73
BE-06-090	635254	7110512	16.6	4.54	3.51	1.93	50.74
BE-06-091	635255.78	7111345.2	17	4.85	3.54	1.71	50.76
BE-06-092	634844	7110916	18.4	7.28	2.08	1.1	50.76
BE-06-093	631353.11	7169395.2	13.9	3.57	2.97	1.93	50.79
BE-06-094	610481.29	7164831.1	15.3	4.11	3.13	2.02	50.82

BE-06-095	604947	7170254	15.2	4.3	3.19	1.52	50.82
BE-06-096	635051	7112005	17	4.69	3.47	2.04	50.83
BE-06-097	635353	7111788	17.5	5.09	3.18	2.24	50.86
BE-06-098	635259.62	7111154.9	17.3	5.98	2.66	1.35	50.87
BE-06-099	590790.73	7125012.1	17.1	4.08	4.09	2.18	50.88
BE-06-100	610507.02	7080079.1	16.7	3.67	4.24	2.27	50.91
BE-06-101	635347	7111251	18.3	6.04	2.92	1.7	50.94
BE-06-102	617881.3	7085322.1	15.1	4	3.38	1.56	50.98
BE-06-103	634455	7111956	17.1	4.72	3.73	1.59	50.99
BE-06-104	634752	7110708	18.2	6.76	2.44	1.1	50.99
BE-06-105	635253.97	7111297.5	18.5	6.24	2.8	1.66	51.04
BE-06-106	609455	7131077	13.6	3.84	2.7	1.5	51.04
BE-06-107	635548	7111311	17.5	4.86	3.25	2.39	51.06
BE-06-108	609693.4	7144658	17.4	4.74	3.86	1.57	51.07
BE-06-109	600757	7165482	16.4	4.06	3.64	2.16	51.08
BE-06-110	610091.71	7075470.4	17.3	3.43	4.46	2.76	51.09
BE-06-111	635261.63	7111043.7	17.6	5.77	2.91	1.4	51.17
BE-06-112	609808	7130381	13.5	3.29	3.01	1.78	51.21
BE-06-113	590638.85	7135316.7	17.8	3.79	4.12	3.03	51.23
BE-06-114	580007.46	7164463.5	19	4.35	4.51	2.54	51.24
BE-06-115	610510.78	7139676.9	17.2	4.31	4.16	1.55	51.25
BE-06-116	630231.86	7163568.6	15.3	3.81	3.2	2.16	51.29
BE-06-117	634950	7111859	16.9	5.1	2.84	1.94	51.30
BE-06-118	608390	7128423	14.1	3.77	2.86	1.68	51.31
BE-06-119	599226.43	7090484	16.9	4.54	3.56	1.75	51.36
BE-06-120	635350	7110905	17.8	5.08	3.43	1.82	51.37
BE-06-121	356792	7173998	15	3.58	3.4	1.9	51.44
BE-06-122	635451.29	7110715.2	16.9	4.35	3.62	1.92	51.46
BE-06-123	635450.37	7111463.4	17.1	5.05	2.95	1.92	51.49
BE-06-124	634141	7111805	16	4.24	3.38	1.65	51.52
BE-06-125	630194.72	7176268.5	15.9	4.04	3.43	1.82	51.53
BE-06-126	635261.22	7111118	17.6	6.27	2.39	1.13	51.53
BE-06-127	610464.69	7085177.5	16	3.72	3.62	2.12	51.59
BE-06-128	635551	7110906	17	4.54	3.44	1.87	51.61
BE-06-129	635148	7111453	17	5.25	2.7	1.79	51.63
BE-06-130	609855.55	7095318.6	16.5	3.83	3.77	2.1	51.66
BE-06-131	635150	7110969	17.1	5.53	2.6	1.51	51.71
BE-06-132	634653	7110505	17	4.94	2.95	1.87	51.74
BE-06-133	590979.19	7130035.8	18	3.7	4.39	2.61	51.76
BE-06-134	635260	7110815	18	5.36	3.09	1.78	51.79
BE-06-135	635445.55	7111364	17.7	5.27	2.76	2.17	51.80
BE-06-136	635146	7111707	16.4	5.34	2.24	1.72	51.81
BE-06-137	625847.35	7164334.4	14.9	3.85	3.1	1.62	51.82
BE-06-138	609709	7130384	14.8	3.63	3.11	1.88	51.84
BE-06-139	635353	7110953	17.3	4.96	3.15	1.73	51.84
BE-06-140	634950	7111906	16.4	4.81	2.61	2	51.89
BE-06-141	635550	7110857	17.4	4.54	3.57	1.85	51.89
BE-06-142	635349	7111100	18.2	6.2	2.57	1.26	51.90
BE-06-143	632470	7135043	16.4	5.18	1.35	3.28	51.92
BE-06-144	585052.93	7155096.4	18.6	3.73	4.48	2.82	51.95

BE-06-145	635452.21	7110966.6	17.2	4.42	3.64	1.74	51.95
BE-06-146	615133.99	7095960.6	16.4	4.08	3.48	1.86	51.97
BE-06-147	635251.91	7110852.3	17.8	5.17	3.16	1.71	51.97
BE-06-148	600558.31	7094386.6	18.2	4.31	4.28	1.78	51.99
BE-06-149	634651	7110712	16.3	4.93	2.74	1.45	52.01
BE-06-150	635549	7110500	17.2	4.29	3.52	2.1	52.02
BE-06-151	610088	7130211	14.7	3.82	2.82	1.82	52.03
BE-06-152	635145	7111661	17.1	5.23	2.62	1.8	52.03
BE-06-153	634855	7110613	16.6	4.51	3.1	1.85	52.03
BE-06-154	604824.95	7100469.6	15.7	3.29	3.66	2.26	52.07
BE-06-155	584127.01	7145458.4	20.6	4.12	4.97	3.04	52.08
BE-06-156	634855	7110766	16.5	4.96	2.67	1.62	52.11
BE-06-157	610500	7130390	13.1	3.4	2.57	1.5	52.12
BE-06-158	635448.23	7111708.7	17.3	4.51	3.37	1.96	52.16
BE-06-159	634452	7111763	15.9	3.99	3.25	1.82	52.18
BE-06-160	608774	7129363	14	3.58	2.72	1.68	52.23
BE-06-161	605160.94	7089776.9	17.8	4.1	4.13	1.87	52.24
BE-06-162	634851	7110663	16.9	4.73	3.08	1.64	52.25
BE-06-163	593410.91	7144792.5	17.1	4.14	3.88	1.57	52.28
BE-06-164	584720.56	7150332	19.4	4.2	4.74	2.1	52.28
BE-06-165	635360	7110506	17.8	4.54	3.52	2.03	52.29
BE-06-166	595084.56	7130125	16	4.44	2.97	1.51	52.30
BE-06-167	635055	7110561	16.2	4.2	3.26	1.64	52.30
BE-06-168	635242.58	7111851.8	17	4.24	3.23	2.29	52.31
BE-06-169	601122	7160805	17.7	4.06	3.8	2.3	52.33
BE-06-170	635443.23	7110814.2	18	4.8	3.39	1.93	52.34
BE-06-171	585661.94	7169780.8	17.1	3.72	3.62	2.63	52.35
BE-06-172	634850	7110506	18.7	5.23	3.54	1.55	52.37
BE-06-173	635254	7110704	17.4	4.43	3.63	1.66	52.37
BE-06-174	635441.94	7111561.3	16.9	4.81	2.72	1.98	52.38
BE-06-175	635553	7110810	17.2	4.26	3.48	2	52.38
BE-06-176	632471	7134894	17.3	5.42	1.2	3.58	52.42
BE-06-177	635048	7110715	15.7	4.23	3	1.5	52.42
BE-06-178	635241	7110745	17	4.15	3.56	1.87	52.43
BE-06-179	635251.62	7111642.1	17	4.82	2.71	2.02	52.46
BE-06-180	611460.66	7103826.8	15.7	3.67	3.33	1.92	52.46
BE-06-181	634451	7112010	15.2	4.84	2.24	1.19	52.46
BE-06-182	635551	7110708	17.3	4.18	3.52	2.11	52.46
BE-06-183	635047	7110499	16.3	4.17	3.17	1.81	52.49
BE-06-184	600985	7129978	16.6	3.67	3.62	2.21	52.50
BE-06-185	625628.46	7150239.4	15.8	3.76	3.15	2.09	52.53
BE-06-186	641049	7170104	13.4	2.96	3.01	1.64	52.53
BE-06-187	635055	7110760	17.1	4.95	3.09	1.26	52.54
BE-06-188	635150	7110660	17.2	4.86	3.07	1.5	52.58
BE-06-189	601650	7150150	17.2	4.11	3.57	1.98	52.62
BE-06-190	635447.1	7110906.9	17.8	4.33	3.74	1.85	52.62
BE-06-191	635044	7111210	16.7	5.07	2.54	1.47	52.70
BE-06-192	635727.31	7169525.1	15.5	3.36	3.36	2.09	52.72
BE-06-193	635446.78	7111016.4	16.5	4.48	2.87	1.77	52.74
BE-06-194	635149	7111958	17.7	4.25	3.41	2.32	52.76

BE-06-195	635288.29	7099786.4	18.5	4.35	4.12	1.73	52.77
BE-06-196	635044	7111757	14.9	4.19	2.43	1.59	52.77
BE-06-197	634455	7111850	15.6	3.81	3.13	1.74	52.77
BE-06-198	640085.14	7105521.3	17.5	3.96	3.99	1.75	52.78
BE-06-199	640343	7154957	17.5	4.18	3.71	1.8	52.79
BE-06-200	634949	7112056	17.1	4.37	2.84	2.47	52.79
BE-06-201	590581.79	7145104.7	18.8	3.71	4.59	2.31	52.81
BE-06-202	635353	7111206	17.3	4.52	2.74	2.52	52.82
BE-06-203	635554	7110760	16.8	3.91	3.41	2.11	52.83
BE-06-204	635148	7111508	16.8	4.9	2.6	1.67	52.84
BE-06-205	635543	7110566	16.6	3.8	3.54	1.92	52.85
BE-06-206	635446.65	7111511	17.1	4.72	2.73	2	52.88
BE-06-207	634952	7111060	17.2	5.37	2.34	1.58	52.88
BE-06-208	610363	7130391	14.6	3.29	3.03	1.87	52.92
BE-06-209	634751	7110504	17.2	4.99	2.73	1.6	52.93
BE-06-210	635545	7111268	17.3	4.41	2.99	2.26	52.93
BE-06-211	634754	7110607	17	4.74	2.96	1.5	52.94
BE-06-212	583846.83	7135441.2	18.6	3.42	4.68	2.39	52.98
BE-06-213	631258	7135306	15.4	3.94	2.44	2.29	53.00
BE-06-214	635045	7111503	17.1	3.92	3.7	1.79	53.02
BE-06-215	635254	7110603	16.6	4.08	3.35	1.64	53.03
BE-06-216	634354	7111957	15.2	3.87	2.88	1.56	53.03
BE-06-217	602034	7134491	17.3	4.23	3.83	1.22	53.05
BE-06-218	635051	7111902	17.4	4.5	2.8	2.41	53.05
BE-06-219	634946	7110508	17.2	4.36	3.26	1.78	53.06
BE-06-220	635354	7111000	16.9	4.51	2.89	1.84	53.07
BE-06-221	599766.95	7105523.2	15.9	3.35	3.36	2.25	53.08
BE-06-222	579452.62	7154790.7	18.8	3.21	4.43	3.22	53.09
BE-06-223	635156	7111864	17.1	4.27	2.82	2.48	53.13
BE-06-224	635049	7112058	17.2	4.07	3.2	2.3	53.16
BE-06-225	634158.41	7136066.2	15.9	4.11	2.16	2.75	53.17
BE-06-226	635452.11	7111209.4	17.1	5	2.64	1.48	53.21
BE-06-227	634151	7111860	14.1	3.53	2.7	1.41	53.24
BE-06-228	634956	7111159	17	4.95	2.48	1.71	53.24
BE-06-229	624218.45	7120447.3	15.8	4.3	2.63	1.6	53.24
BE-06-230	632475	7134991	17	5.18	1.21	3.25	53.25
BE-06-231	634947	7110657	17.4	5.31	2.62	1.21	53.25
BE-06-232	635549	7111362	17.8	4.67	2.98	2.04	53.29
BE-06-233	635049	7111702	16	4.35	2.65	1.62	53.29
CHG-08-001	635454.47	7110498.6	17.5	3.92	3.64	2.05	53.30
CHG-08-002	594397.87	7126434.2	16.2	3.56	3.45	1.89	53.30
CHG-08-003	635451.38	7110609.5	17.9	3.98	3.66	2.24	53.30
CHG-08-004	611212.13	7109324	15.7	3.55	3.1	2.03	53.31
CHG-08-005	635252.4	7110892.9	18.2	4.97	3.06	1.72	53.32
CHG-08-006	634856	7110706	17.2	4.79	2.72	1.73	53.32
CHG-08-007	634848	7111505	17.3	4.43	2.94	2.08	53.32
CHG-08-008	635349	7110611	18.6	4.32	3.85	1.93	53.33
CHG-08-009	635353	7110750	16.8	4.29	3.07	1.7	53.35
CHG-08-010	635542	7110954	17.1	4.17	3.28	1.82	53.36
CHG-08-011	634818.33	7164183.2	15.9	3.22	3.09	2.73	53.37

CHG-08-012	589985.33	7169516.1	18.5	3.91	3.76	2.64	53.39
CHG-08-013	635153	7110810	16.2	4.12	2.97	1.63	53.39
CHG-08-014	635550	7110610	17.2	3.88	3.43	2.11	53.45
CHG-08-015	635257.05	7111185.1	17.7	4.88	2.86	1.69	53.46
CHG-08-016	635042	7111398	16.8	4.68	2.65	1.62	53.47
CHG-08-017	634850	7112053	17.3	4.71	2.64	1.98	53.48
CHG-08-018	635148	7111907	16.9	3.94	2.96	2.46	53.49
CHG-08-019	635049	7111856	17.6	4.26	3.08	2.3	53.49
CHG-08-020	635441.26	7111316.4	17.1	4.32	2.8	2.22	53.50
CHG-08-021	635249	7110659	17	4.25	3.14	1.71	53.55
CHG-08-022	635153	7110909	17.9	4.84	2.88	1.83	53.56
CHG-08-023	634750	7110757	18	4.9	2.79	1.94	53.57
CHG-08-024	635153	7110758	17.2	4.18	3.22	1.85	53.58
CHG-08-025	634652	7110553	17.5	4.82	2.74	1.73	53.61
CHG-08-026	610886.84	7134446.2	16.8	2.35	3.96	3.46	53.62
CHG-08-027	635549	7111207	16.3	4.09	2.88	1.77	53.64
CHG-08-028	634753	7110901	17.4	5.11	2.4	1.66	53.64
CHG-08-029	634849	7111760	16.9	4.21	3.06	1.76	53.66
CHG-08-030	634950	7111809	16.5	4.57	2.3	1.98	53.68
CHG-08-031	591167.97	7139748.7	16.7	3.66	3.59	1.7	53.70
CHG-08-032	629651.32	7109977.1	16.4	3.8	3.1	1.97	53.70
CHG-08-033	634854	7110965	17.4	4.68	2.62	2	53.73
CHG-08-034	635148	7110855	17.8	4.63	2.95	1.9	53.73
CHG-08-035	622611	7087003.4	14.9	3.37	3	1.63	53.74
CHG-08-036	624639.78	7110158.4	15.2	3.74	2.81	1.53	53.75
CHG-08-037	610097.02	7090479.7	16.2	3.05	3.45	2.49	53.79
CHG-08-038	615176.5	7130831.1	15.5	3.52	2.92	1.92	53.85
CHG-08-039	634750	7110807	18.1	5.49	2.18	1.79	53.86
CHG-08-040	634751	7110663	18	5.55	2.42	1.24	53.87
CHG-08-041	609768	7129786	15.3	3.39	2.82	2.1	53.92
CHG-08-042	634952	7110559	17.8	4.18	3.46	1.77	53.93
CHG-08-043	623016.92	7145615.2	14.8	3.32	2.74	1.94	53.93
CHG-08-044	635353	7110558	17.7	3.98	3.51	1.94	53.95
CHG-08-045	635348	7110811	17.6	4.24	3.28	1.77	53.95
CHG-08-046	634956	7110807	17.5	4.86	2.76	1.44	53.95
CHG-08-047	634952	7111110	17.1	5.02	2.25	1.62	53.97
CHG-08-048	610090	7130132	16.3	3.77	2.97	1.99	53.98
CHG-08-049	634948	7111012	17.3	5.15	2.27	1.52	53.99
CHG-08-050	635353	7110860	17.6	3.96	3.6	1.72	54.01
CHG-08-051	635155	7110609	19.1	3.86	3.91	2.59	54.02
CHG-08-052	635145	7111569	17.5	4.47	2.75	2.05	54.06
CHG-08-053	605043.81	7079833.5	18.3	3.58	3.96	2.33	54.07
CHG-08-054	635154	7110509	19	4.37	3.77	1.84	54.07
CHG-08-055	635454.6	7110648.3	17.7	3.86	3.54	2.02	54.08
CHG-08-056	635347	7111054	16.6	4.56	2.54	1.5	54.08
CHG-08-057	634049	7111714	16.3	4.04	2.8	1.73	54.11
CHG-08-058	634661	7110615	17.1	4.36	2.76	1.88	54.11
CHG-08-059	635355	7110708	18.6	4.09	3.78	1.94	54.14
CHG-08-060	609760	7130385	15.1	3.29	2.78	2.06	54.15
CHG-08-061	591149.08	7150280.4	17.8	3.96	3.66	1.7	54.17

CHG-08-062	634796.41	7106960.3	17.7	3.91	3.57	1.84	54.17
CHG-08-063	635051	7111808	17.2	4.68	2.4	1.93	54.18
CHG-08-064	630198.64	7114396.6	16.5	3.84	2.97	1.9	54.23
CHG-08-065	634656	7112010	17.7	4.37	2.57	2.52	54.29
CHG-08-066	634652	7110664	16.4	4.54	2.48	1.35	54.31
CHG-08-067	635257.89	7111800.7	17.5	4.47	2.61	2.12	54.32
CHG-08-068	635260.99	7110944.2	17.8	4.52	2.91	1.81	54.33
CHG-08-069	634948	7112005	17.8	4.32	2.78	2.34	54.33
CHG-08-070	634951	7111956	17.5	4.87	2.3	1.9	54.36
CHG-08-071	634354	7112055	15.8	4.18	2.43	1.54	54.36
CHG-08-072	610182	7130184	15.2	3.32	2.8	1.94	54.40
CHG-08-073	634951	7111598	17	4.18	2.72	2.01	54.40
CHG-08-074	635053	7110860	17.8	4.63	2.82	1.7	54.44
CHG-08-075	634951	7111309	15.5	4.26	2.11	1.58	54.53
CHG-08-076	609709	7130336	14.5	3.12	2.74	1.76	54.54
CHG-08-077	635230.09	7111898.1	17.4	3.97	3.09	2.03	54.55
CHG-08-078	610109	7129982	15.4	3.36	2.73	2.06	54.55
CHG-08-079	635348	7110659	18.2	3.93	3.61	1.91	54.57
CHG-08-080	634751	7111059	16.8	4.91	2.06	1.54	54.58
CHG-08-081	634748	7110559	17.7	4.75	2.59	1.69	54.58
CHG-08-082	600052.55	7099936.6	17	3.44	3.37	2.16	54.60
CHG-08-083	635260.85	7111740.4	18.4	4.6	2.75	2.22	54.61
CHG-08-084	634152	7111659	15.7	3.57	2.82	1.77	54.62
CHG-08-085	634546	7110502	19.2	5.16	2.7	1.96	54.63
CHG-08-086	635254	7110556	18.1	4.08	3.43	1.82	54.63
CHG-08-087	595070.24	7109370.9	14.9	2.86	2.75	2.44	54.65
CHG-08-088	604634	7105359	15.1	2.88	2.9	2.32	54.67
CHG-08-089	600732	7169750	16.2	3.16	3.02	2.5	54.69
CHG-08-090	609854	7130380	15.3	3.3	2.72	2.03	54.70
CHG-08-091	634846	7110558	17.3	4.4	2.74	1.67	54.72
CHG-08-092	604919.36	7085209.9	17.8	2.92	4.07	2.51	54.73
CHG-08-093	635447.22	7110764.8	18.3	3.95	3.43	2.11	54.78
CHG-08-094	635046	7111601	17.1	5.12	2.07	1.29	54.79
CHG-08-095	618534.46	7079753	15.8	3.44	3.07	1.6	54.79
CHG-08-096	634348	7111859	15.6	3.62	2.75	1.63	54.79
CHG-08-097	609715	7129778	15.3	3.32	2.66	2.04	54.80
CHG-08-098	634952	7111461	16.1	4.37	2.08	1.76	54.81
CHG-08-099	634750	7111554	16.9	3.96	2.84	1.89	54.84
CHG-08-100	609863	7129737	15.4	3.25	2.74	2.07	54.89
CHG-08-101	630378.45	7119923.1	16.3	4.24	2.35	1.68	54.89
CHG-08-102	631073	7135044	15.3	3.89	2.06	1.94	54.91
CHG-08-103	635054	7110609	16.5	4.23	2.57	1.5	54.92
CHG-08-104	635355	7111706	17.5	4.53	2.44	1.95	54.93
CHG-08-105	634247	7111847	16.4	3.77	2.87	1.73	54.94
CHG-08-106	615372.25	7134185.9	12.8	4.17	0.77	1.51	54.98
CHG-08-107	616159	7110564.4	16.8	3.25	3.36	2.14	54.99
CHG-08-108	634856	7111715	15.4	3.87	2.51	1.31	55.03
CHG-08-109	635290.35	7125423.8	16.2	4.2	1.94	2.22	55.04
CHG-08-110	604495	7155269	16.6	3.64	3.26	1.45	55.06
CHG-08-111	632473	7134793	17	4.46	1.08	3.67	55.09

CHG-08-112	634249	7111755	17.3	3.75	3.06	2.07	55.11
CHG-08-113	634352	7112103	17.2	3.98	2.57	2.35	55.11
CHG-08-114	635554	7110654	18.2	3.68	3.38	2.36	55.14
CHG-08-115	634856	7111906	17.1	4.24	2.5	1.93	55.14
CHG-08-116	615365.46	7145584.3	19	3.57	3.91	2.33	55.16
CHG-08-117	610142	7130216	15	3.2	2.61	1.92	55.17
CHG-08-118	635149	7110998	17.6	4.95	2.51	1.07	55.19
CHG-08-119	634154	7111707	16.7	3.64	2.95	1.92	55.21
CHG-08-120	634949	7111360	15.3	3.93	2.07	1.72	55.21
CHG-08-121	604289	7165169	15.8	3.15	2.76	2.34	55.24
CHG-08-122	634851	7111006	17.7	4.62	2.46	1.74	55.26
CHG-08-123	635055	7110800	17.3	4.1	2.95	1.56	55.28
CHG-08-124	634852	7112097	17.4	4.22	2.48	2.14	55.29
CHG-08-125	635450.25	7110869.3	17.9	3.96	3.21	1.84	55.29
CHG-08-126	634142	7111559	16.3	4.05	2.33	1.83	55.30
CHG-08-127	609969	7130209	15.1	3.05	2.66	2.11	55.30
CHG-08-128	635349	7111657	17.7	4.66	2.38	1.76	55.32
CHG-08-129	635256.94	7110992	17.5	4.51	2.63	1.48	55.33
CHG-08-130	609806	7130335	14.8	3.06	2.55	2.02	55.34
CHG-08-131	634849	7112007	17	4	2.54	2.09	55.35
CHG-08-132	635251.84	7111399.3	18.2	4.61	2.71	1.7	55.35
CHG-08-133	633960	7111900	16	3.83	2.43	1.79	55.37
CHG-08-134	635545	7111462	16.3	4.12	2.39	1.58	55.38
CHG-08-135	609964	7130188	15	3.1	2.61	1.96	55.45
CHG-08-136	635151	7110712	16.8	3.54	3.13	1.73	55.52
CHG-08-137	633972	7110896	15.6	3.98	1.98	1.85	55.52
CHG-08-138	617195.2	7090807.2	17	3.49	3.3	1.66	55.61
CHG-08-139	634954	7110704	19	5.6	2.18	1.29	55.61
CHG-08-140	634950	7110610	17.6	3.87	2.98	1.93	55.65
CHG-08-141	634750	7110859	18.5	4.98	2.28	1.77	55.69
CHG-08-142	609761	7129886	14.6	2.74	2.44	2.41	55.72
CHG-08-143	609712	7130283	15.5	3.08	2.64	2.19	55.73
CHG-08-144	624279.76	7115112.1	16.9	3.39	3.23	1.8	55.73
CHG-08-145	633953	7111602	16.7	3.69	2.88	1.68	55.73
CHG-08-146	609957	7130381	15.4	2.93	2.72	2.24	55.74
CHG-08-147	634945	7111557	16.7	4.25	2.07	1.95	55.77
CHG-08-148	634752	7111956	17.5	4.16	2.4	2.18	55.78
CHG-08-149	610014	7130142	16.2	3.17	2.8	2.27	55.81
CHG-08-150	614876.93	7100428.1	15.2	2.92	2.76	2.01	55.83
CHG-08-151	635547	7111066	16.9	4.04	2.55	1.68	55.85
CHG-08-152	609981	7130233	15.3	3.04	2.6	2.11	55.86
CHG-08-153	609705	7130139	15.4	3.07	2.6	2.13	55.87
CHG-08-154	635051	7111303	17	4.3	2.43	1.47	55.91
CHG-08-155	634949	7111756	17.3	4.54	2.28	1.51	55.91
CHG-08-156	610184	7130065	14.5	2.79	2.54	2	55.95
CHG-08-157	609705	7129997	14.7	2.86	2.47	2.12	55.98
CHG-08-158	609912	7129782	15.4	3.03	2.66	2.03	56.04
CHG-08-159	609858	7130274	15.8	3.08	2.63	2.28	56.04
CHG-08-160	634951	7112109	17.4	3.62	2.74	2.36	56.05
CHG-08-161	634848	7111155	16.3	3.98	2.05	1.98	56.11

CHG-08-162	634254	7111799	17.1	3.62	2.92	1.84	56.11
CHG-08-163	609449	7129587	15	2.96	2.41	2.18	56.17
CHG-08-164	620765.46	7092273.4	15.1	3.05	2.57	1.85	56.18
CHG-08-165	632571	7135107	17.5	4.27	1.2	3.57	56.27
CHG-08-166	634951	7111208	17.7	4.5	2.32	1.62	56.28
CHG-08-167	634255	7111705	15.5	3.34	2.4	1.86	56.29
CHG-08-168	635151	7110556	19	3.97	3.15	2.17	56.30
CHG-08-169	585203.05	7105861.2	15.5	2.25	2.4	3.68	56.32
CHG-08-170	634453	7111899	17.7	3.97	2.53	2.16	56.34
CHG-08-171	604561	7109460	15.6	2.9	2.76	2.1	56.35
CHG-08-172	610111	7130380	15.9	2.94	2.75	2.26	56.35
CHG-08-173	635351	7111354	17.7	4.3	2.48	1.66	56.38
CHG-08-174	609945	7130208	16.6	3.21	2.85	2.14	56.38
CHG-08-175	609714	7129836	15	2.51	2.55	2.62	56.40
CHG-08-176	634802.02	7111082.6	17.3	4.25	2.12	1.99	56.41
CHG-08-177	610006	7130331	14.5	2.76	2.44	2	56.43
CHG-08-178	604203	7130414	15.4	2.77	2.7	2.23	56.43
CHG-08-179	631171	7135349	17	3.7	2.19	2.57	56.46
CHG-08-180	610108	7130107	14.6	2.82	2.44	1.95	56.47
CHG-08-181	635148	7111810	17.6	3.92	2.52	2.07	56.57
CHG-08-182	635351	7111503	18.2	4.69	2.16	1.74	56.58
CHG-08-183	609765	7130283	15.6	2.86	2.64	2.23	56.61
CHG-08-184	609811	7129785	14.6	2.33	2.47	2.67	56.61
CHG-08-185	594255	7094751	15.4	2.34	2.67	2.9	56.65
CHG-08-186	600598	7115532	15.7	2.58	2.7	2.66	56.65
CHG-08-187	600694	7120594	15.7	2.56	2.72	2.66	56.66
CHG-08-188	604516	7139763	17	3.44	2.64	2.21	56.69
CHG-08-189	610107	7130278	15.2	2.94	2.51	1.97	56.70
CHG-08-190	579972.78	7104668.1	15.6	2.3	2.34	3.58	56.71
CHG-08-191	634146	7111758	15.5	3.42	2.29	1.7	56.72
CHG-08-192	635253.71	7111494.3	18.5	4.34	2.69	1.65	56.74
CHG-08-193	635313.58	7115114.5	18.2	3.86	2.75	2.15	56.75
CHG-08-194	634448	7112059	18	3.93	2.45	2.34	56.77
CHG-08-195	634950	7111412	15.3	3.66	1.88	1.76	56.77
CHG-08-196	610535	7128624	14.9	2.98	2.39	1.84	56.78
CHG-08-197	634953	7110955	17.7	4.94	1.86	1.31	56.80
CHG-08-198	609860	7129784	15.3	2.74	2.59	2.17	56.90
CHG-08-199	605057	7135243	17	2.79	3.35	2.12	56.90
CHG-08-200	634450	7111704	16.4	3.42	2.64	1.72	56.90
CHG-08-201	595772.37	7120882.3	15.7	2.33	2.64	3.06	56.90
CHG-08-202	620537.37	7139521.9	12.3	1.97	2.13	2.06	56.90
CHG-08-203	611528	7129570	14.8	2.56	2.42	2.35	56.97
CHG-08-204	609762	7130338	14.3	2.68	2.38	1.86	56.97
CHG-08-206	631170	7135401	16.8	3.4	2.28	2.54	56.98
CHG-08-207	610001	7130279	14.6	2.7	2.35	2.07	57.00
CHG-08-208	633951	7111649	17.6	3.97	2.43	1.9	57.01
CHG-08-209	610064	7130013	15.2	2.7	2.44	2.34	57.02
CHG-08-210	630280.88	7160326.8	14.5	2.52	2.25	2.43	57.06
CHG-08-211	634654	7111956	18	3.73	2.5	2.45	57.06
CHG-08-212	609767	7130085	14.4	2.55	2.44	2.01	57.08

CHG-08-213	609961	7130165	15.4	2.79	2.51	2.19	57.10
CHG-08-214	634457	7111660	18	3.77	2.79	1.92	57.10
CHG-08-215	610352.7	7113958.5	15.5	2.48	2.6	2.64	57.10
CHG-08-216	632276	7134794	18.1	3.98	1.27	3.93	57.13
CHG-08-217	634852	7111857	17.2	3.71	2.42	2.01	57.14
CHG-08-218	634649	7112103	18	3.75	2.35	2.58	57.18
CHG-08-219	634749	7112058	18	3.75	2.53	2.3	57.20
CHG-08-220	609763	7130183	15.6	2.84	2.6	2.06	57.20
CHG-08-221	634854	7111103	16.7	4.32	1.72	1.67	57.21
CHG-08-222	610009	7130087	15.9	3.06	2.53	2	57.21
CHG-08-223	604857	7115162	14.9	2.34	2.54	2.5	57.22
CHG-08-224	609759	7129836	15.4	2.65	2.51	2.35	57.27
CHG-08-225	609887	7130208	15.7	2.77	2.55	2.29	57.28
CHG-08-226	635045	7111955	17.5	3.09	2.9	2.46	57.28
CHG-08-227	609761	7130229	15.6	2.82	2.52	2.18	57.28
CHG-08-228	634652	7110803	16.5	3.98	2.03	1.59	57.30
CHG-08-229	609915	7129740	15.4	2.41	2.49	2.77	57.30
CHG-08-230	635047	7111252	17.6	4.45	2.1	1.43	57.34
CHG-08-231	634655	7111860	17.3	4.16	1.79	2.17	57.37
CHG-08-232	634252	7111952	16.9	3.37	2.39	2.31	57.37
CHG-08-233	619075.55	7097500	15	2.54	2.52	2.19	57.40
CHG-08-234	634469	7111806	16.2	4.64	1.48	1.06	57.41
CHG-08-235	632879	7135187	16.4	3.64	1.14	3.39	57.42
CHG-08-236	609933	7130164	15.8	2.95	2.52	2.04	57.42
CHG-08-237	609754	7130138	15.3	2.74	2.48	2.11	57.42
CHG-08-238	604562	7160392	16.1	2.94	2.74	1.92	57.44
CHG-08-239	633978	7110607	16	3.51	2.15	1.79	57.44
CHG-08-240	601783	7155507	16.3	3.17	2.65	1.8	57.45
CHG-08-241	610208	7130186	14.6	2.49	2.33	2.26	57.47
CHG-08-242	589195.85	7107153.5	15.6	2.11	2.32	3.59	57.48
CHG-08-243	633955	7112004	16.9	3.56	2.37	1.96	57.50
CHG-08-244	600585	7109023	15.4	2.27	2.56	2.81	57.50
CHG-08-245	619729.34	7114091	15.9	2.59	2.8	2.24	57.53
CHG-08-246	634946	7111255	17.2	4.02	2.02	1.9	57.55
CHG-08-247	584481.34	7110180	15.9	2.27	2.39	3.39	57.55
CHG-08-248	635152	7111614	18.3	4.24	2.4	1.69	57.57
CHG-08-249	634051	7111956	17.3	3.98	2.12	1.84	57.64
CHG-08-250	631773	7135198	17	3.31	2.04	2.88	57.64
CHG-08-251	609812	7130131	15.1	2.7	2.41	2.05	57.65
CHG-08-252	634248	7111608	16.6	3.67	2.25	1.68	57.65
CHG-08-253	585266.02	7165398.8	18.2	2.87	2.97	3	57.68
CHG-08-254	609547	7128605	15.2	3.16	2.2	1.63	57.73
CHG-08-255	610009	7130062	15	2.53	2.3	2.4	57.73
CHG-08-256	609856	7130010	15	2.61	2.32	2.23	57.75
CHG-08-257	633073	7135145	16.2	3.37	1.21	3.45	57.75
CHG-08-258	635441.85	7111615.6	18.1	3.9	2.41	2	57.79
CHG-08-259	609760	7129984	15.3	2.55	2.47	2.28	57.81
CHG-08-260	634650	7112061	18.4	3.66	2.23	2.87	57.81
CHG-08-261	635345	7111307	18.1	4.15	2.35	1.66	57.81
CHG-08-262	609807	7129979	15.2	2.67	2.37	2.16	57.81

CHG-08-263	609706	7130189	15.5	2.75	2.38	2.2	57.84
CHG-08-264	609989	7130136	15.5	2.62	2.36	2.44	57.86
CHG-08-266	634861	7111802	17.6	3.99	2.31	1.6	57.92
CHG-08-267	610110	7130230	15.7	2.77	2.47	2.13	57.92
CHG-08-268	610187	7130142	16.1	2.91	2.57	1.99	57.97
CHG-08-269	635451.66	7110562.3	19.1	3.48	3.11	2.21	57.99
CHG-08-270	609988	7130185	14.4	2.46	2.22	2.13	57.99
CHG-08-271	635052	7111455	17.5	3.82	2.48	1.52	58.00
CHG-08-272	624653.42	7124711.1	18.3	3.71	2.59	2.07	58.01
CHG-08-273	610207	7129837	15.3	2.52	2.38	2.38	58.01
CHG-08-274	602583	7144950	16.7	2.98	2.78	1.91	58.07
CHG-08-275	634752	7111155	16.1	3.59	1.87	1.86	58.09
CHG-08-276	634144	7111518	17.3	3.55	2.46	1.82	58.11
CHG-08-277	609861	7129957	16	2.71	2.52	2.26	58.14
CHG-08-278	609819.3	7099741.1	15.9	2.82	2.76	1.64	58.15
CHG-08-279	609810	7130283	16.3	2.94	2.42	2.22	58.15
CHG-08-280	609986	7130086	16.1	2.72	2.54	2.27	58.16
CHG-08-281	634049	7111906	17.1	3.93	1.81	2.01	58.17
CHG-08-282	609857	7130226	14.9	2.45	2.37	2.18	58.17
CHG-08-283	610188	7130386	15.8	2.64	2.5	2.26	58.18
CHG-08-284	590120.86	7100787.6	16.4	2.14	2.4	3.65	58.18
CHG-08-285	609717	7130085	15.6	2.61	2.45	2.25	58.18
CHG-08-286	633960	7110854	15.1	3.19	1.84	1.87	58.19
CHG-08-287	620983.69	7110323.9	15.3	2.21	2.58	2.5	58.24
CHG-08-288	589625.43	7110963.2	16.6	2.77	2.28	2.86	58.28
CHG-08-289	635351	7111403	17.1	3.74	2.3	1.53	58.28
CHG-08-290	634154	7111953	15.3	3.6	1.63	1.59	58.29
CHG-08-291	635260.26	7111451.2	18.6	4.05	2.53	1.64	58.31
CHG-08-292	634253	7112101	17.2	3.62	2.23	1.89	58.31
CHG-08-293	634546	7110858	17.4	4.11	1.61	2.07	58.46
CHG-08-294	634350	7111914	19	4.76	2.11	1.26	58.48
CHG-08-295	635548	7111408	16.8	3.4	2.2	1.96	58.49
CHG-08-297	590748.48	7119503.8	15.4	1.74	2.47	3.42	58.49
CHG-08-298	599387.27	7084742.2	18.7	3.07	2.96	2.6	58.50
CHG-08-299	610313	7130141	15.2	2.16	2.25	2.91	58.51
CHG-08-300	634357	7110505	16.6	3.94	1.6	1.82	58.52
CHG-08-301	609933	7130138	15.9	2.75	2.32	2.25	58.56
CHG-08-302	634845	7111204	15.5	3.3	1.83	1.8	58.58
CHG-08-303	609763	7129731	15.7	2.26	2.4	2.81	58.58
CHG-08-304	599992.38	7074951.6	16.9	2.82	2.79	2.06	58.58
CHG-08-305	635243.28	7111596.2	19.2	4.48	2.31	1.48	58.63
CHG-08-306	620940.64	7119421.2	16.2	2.69	2.49	2.24	58.67
CHG-08-307	610309	7130375	15.9	2.41	2.39	2.66	58.69
CHG-08-308	609714	7130233	16.2	2.68	2.4	2.38	58.70
CHG-08-309	610059	7130063	15.5	2.37	2.31	2.58	58.71
CHG-08-310	633964	7111847	14.3	3.2	1.6	1.48	58.72
CHG-08-311	610082	7130185	13.7	2.09	2.05	2.27	58.72
CHG-08-312	633959	7110801	18.6	4.23	1.64	2.48	58.72
CHG-08-313	634556	7111853	18.3	3.35	2.45	2.51	58.77
CHG-08-314	599534	7123946	15.1	2.45	2.32	2.14	58.78

CHG-08-315	609952	7130282	15.6	2.48	2.3	2.43	58.82
CHG-08-316	609938	7130235	15.5	2.38	2.36	2.44	58.82
CHG-08-317	594331.77	7100138.5	16	2.28	2.47	2.76	58.83
CHG-08-318	641165	7134437	17.3	2.44	2.37	3.48	58.84
CHG-08-319	634852	7111955	17.8	3.68	2.33	1.78	58.84
CHG-08-320	634551	7112059	17.9	3.42	2.26	2.37	58.88
CHG-08-321	634851	7111257	17.9	4.3	1.72	1.7	58.90
CHG-08-322	609809	7129838	16.3	2.38	2.41	2.84	58.92
CHG-08-323	634559	7110547	18.7	4.23	2	1.9	58.92
CHG-08-324	634952	7110760	18.3	4.6	1.89	1.17	58.96
CHG-08-325	595723.49	7115994.4	15.4	2.45	2.3	2.29	58.97
CHG-08-326	634049	7112056	17.8	3.53	2.23	2.12	58.98
CHG-08-327	634254	7111556	17	3.14	2.33	2.1	59.00
CHG-08-328	610255	7130369	16.1	2.48	2.44	2.46	59.00
CHG-08-329	610114	7130215	14.1	1.91	2.06	2.71	59.01
CHG-08-330	579774.6	7149834	18.1	2.33	3.13	2.94	59.02
CHG-08-331	634451	7112105	18	3.33	2.34	2.39	59.03
CHG-08-332	610157	7130183	14.6	2.17	2.15	2.44	59.05
CHG-08-333	610018	7130206	15.2	2.22	2.22	2.62	59.09
CHG-08-334	610209	7130282	15	2.26	2.22	2.42	59.10
CHG-08-335	632674	7135146	16.5	2.77	1.44	3.7	59.12
CHG-08-336	584885.03	7130736.8	17.3	2.48	2.77	2.66	59.15
CHG-08-337	634354	7111806	16.9	3.41	2.14	1.8	59.16
CHG-08-338	609713	7129734	16.6	2.26	2.44	3.08	59.17
CHG-08-340	634148	7112056	17.8	3.34	2.21	2.38	59.17
CHG-08-341	634143	7111412	17.2	3.3	2.19	2.07	59.22
CHG-08-342	631301	7154328	15.1	1.92	1.82	3.61	59.23
CHG-08-343	634649	7111903	19.4	4.49	1.95	1.82	59.25
CHG-08-344	609909	7130230	16.2	2.66	2.41	2.16	59.26
CHG-08-345	634060	7112111	17.9	3.34	1.98	2.75	59.26
CHG-08-346	634750	7111008	17.7	3.46	2.18	2.11	59.27
CHG-08-347	631277	7135343	17.2	3.1	1.9	2.8	59.32
CHG-08-348	641222	7129647	16.5	2.19	2.33	3.23	59.33
CHG-08-349	634351	7111662	16.3	3.33	1.97	1.73	59.34
CHG-08-350	609912	7130085	14.7	2.34	2.16	2.09	59.35
CHG-08-351	619779.14	7104522.1	16.2	2.6	2.33	2.34	59.36
CHG-08-352	634742	7111797	18.6	3.67	2.34	2.03	59.39
CHG-08-353	634056	7111359	17.4	3.29	2.28	2	59.39
CHG-08-354	634251	7112050	17.7	3.48	2.09	2.15	59.41
CHG-08-355	610134	7130231	15.5	2.38	2.25	2.36	59.42
CHG-08-356	610310	7130336	15.8	2.31	2.25	2.66	59.44
CHG-08-357	612028.3	7119510.2	15.7	2.35	2.45	2.22	59.46
CHG-08-358	610357	7130138	15.9	2.11	2.35	2.9	59.46
CHG-08-359	634754	7111617	17.9	3.33	2.5	1.88	59.46
CHG-08-360	609906	7130274	15.8	2.35	2.35	2.41	59.52
CHG-08-361	634352	7112003	18.1	3.67	2.24	1.79	59.55
CHG-08-362	609914	7130208	16.2	2.47	2.36	2.43	59.55
CHG-08-363	630867	7134950	14.7	2.44	1.48	2.87	59.57
CHG-08-364	632675	7135096	18.6	3.36	1.42	3.85	59.59
CHG-08-365	610005	7130378	15.8	2.39	2.25	2.46	59.60

CHG-08-366	635056	7111356	18.5	4.26	2.06	1.29	59.62
CHG-08-367	634049	7111766	15.9	3.06	1.98	1.8	59.62
CHG-08-368	610549	7129566	14.5	1.6	2.04	3.28	59.63
CHG-08-369	632281	7134895	17.8	3.11	1.37	3.82	59.64
CHG-08-370	611075.87	7129548	14.6	1.7	2.03	3.18	59.66
CHG-08-371	609959	7130065	16.1	2.3	2.3	2.69	59.68
CHG-08-372	630116.86	7103503.1	15.8	2.34	1.88	3.07	59.69
CHG-08-373	609962	7130330	14.9	2.08	2.18	2.48	59.71
CHG-08-374	622183.24	7140660.2	15.7	2.3	2.31	2.41	59.72
CHG-08-375	635200.68	7149575.4	15.5	2.65	1.55	2.84	59.75
CHG-08-376	634250	7111894	14.6	3.27	1.41	1.44	59.78
CHG-08-377	634471.45	7159888.4	15.8	2.2	1.99	3.09	59.81
CHG-08-378	634857	7111051	18.7	3.95	2.06	1.84	59.82
CHG-08-379	609806	7130036	15.4	2.29	2.15	2.44	59.82
CHG-08-380	610361	7129986	15.3	1.75	2.11	3.34	59.84
CHG-08-381	614832.88	7105907.6	15.6	2.45	2.26	2.1	59.89
CHG-08-382	630973	7134949	15.4	2.34	1.63	3.11	59.92
CHG-08-383	610155	7130379	16.2	2.43	2.38	2.31	59.92
CHG-08-384	609880	7129991	15.8	2.24	2.18	2.68	59.94
CHG-08-385	633973	7110947	17.4	3.38	1.88	2.19	59.98
CHG-08-386	580751.76	7109459.3	16.2	1.89	2.14	3.55	60.00
CHG-08-387	609886	7130161	15.4	2.14	2.11	2.68	60.01
CHG-08-388	634252	7111003	16.6	3.12	1.98	1.97	60.01
CHG-08-389	631469	7135105	16.2	2.56	1.69	3.09	60.05
CHG-08-390	634144	7110906	16	3.41	1.6	1.67	60.06
CHG-08-391	633980	7110546	17.5	3.24	2.19	1.97	60.08
CHG-08-392	610163	7130161	15.2	2.26	2.27	2.08	60.09
CHG-08-393	632778	7135196	16.7	2.47	1.7	3.51	60.10
CHG-08-394	610107	7129729	15.8	1.81	2.22	3.27	60.12
CHG-08-395	634353	7111705	16.1	2.86	1.97	2.07	60.12
CHG-08-396	634169	7111916	18	3.22	2.16	2.34	60.12
CHG-08-397	610259	7129836	16	1.85	2.17	3.4	60.12
CHG-08-398	580070.44	7130223.3	20	2.5	2.42	4.37	60.14
CHG-08-399	608476	7130617	15.7	2.15	2.15	2.73	60.15
CHG-08-400	634750	7112108	18.7	3.64	2.09	2.14	60.18
CHG-08-401	634549	7111762	18.8	3.59	2.26	2.02	60.20
CHG-08-402	634248	7111306	17.4	3.13	2.08	2.21	60.20
CHG-08-403	604092	7124730	14.8	1.8	2	2.97	60.22
CHG-08-404	641767	7123788	16.9	2.74	1.87	2.86	60.24
CHG-08-405	610354	7129887	16.7	2.08	2.14	3.43	60.26
CHG-08-406	630971	7135097	16.6	2.69	1.78	2.89	60.26
CHG-08-407	632373	7134898	19	3.15	1.42	4.12	60.27
CHG-08-408	610212	7129787	15.3	1.72	2.09	3.25	60.28
CHG-08-409	634643	7110967	15.7	3.23	1.65	1.62	60.29
CHG-08-410	610258	7129985	15.8	1.85	2.09	3.33	60.29
CHG-08-411	634353	7111603	17.7	3.23	1.99	2.32	60.29
CHG-08-412	634852	7111666	18.9	3.6	2.32	1.92	60.31
CHG-08-414	634047	7111465	18	3.02	2.4	2.22	60.32
CHG-08-415	610009	7130185	15.2	2.17	2.13	2.35	60.33
CHG-08-416	610263	7129784	15.4	1.68	2.13	3.29	60.35

CHG-08-417	610063	7130282	16.7	2.41	2.23	2.7	60.35
CHG-08-418	609855	7129910	16	1.96	2.19	3.09	60.35
CHG-08-419	610161	7130089	15.2	2.02	2.05	2.71	60.37
CHG-08-420	609714	7130036	16	2.37	2.29	2.23	60.40
CHG-08-421	610975.89	7159778.2	12.2	1.23	0.98	3.83	60.41
CHG-08-422	634655	7110855	17.8	3.61	1.95	1.74	60.43
CHG-08-423	610362	7130292	16.5	2.25	2.25	2.78	60.44
CHG-08-424	610206	7129734	15.6	1.74	2.07	3.36	60.45
CHG-08-425	610114	7130134	14.6	1.7	2.08	2.8	60.47
CHG-08-426	610062	7129736	16.3	1.89	2.28	3.2	60.48
CHG-08-427	616878.1	7114223.1	14.5	2.05	1.84	2.51	60.49
CHG-08-428	609717	7129878	16	1.96	2.18	3.04	60.51
CHG-08-429	610310	7129838	16.3	1.75	2.21	3.52	60.53
CHG-08-430	634650	7110759	17.9	3.67	2.01	1.56	60.54
CHG-08-431	634154	7111608	14.8	2.68	1.96	1.43	60.54
CHG-08-432	634753	7112009	18.3	3.14	2.19	2.41	60.55
CHG-08-433	594685.54	7089646.2	16.6	1.99	2.47	2.89	60.56
CHG-08-434	609856	7130138	15.9	2.17	2.14	2.66	60.58
CHG-08-435	610113	7129782	16.4	1.92	2.29	3.15	60.59
CHG-08-436	609987	7129963	16.4	1.92	2.24	3.22	60.60
CHG-08-437	580893.22	7134527.6	18.3	1.48	2.7	4.4	60.61
CHG-08-438	632572	7135064	16.7	2.85	1.08	3.6	60.61
CHG-08-439	634055	7111602	19.5	3.64	2.39	1.96	60.61
CHG-08-440	634053	7111860	15.3	3.18	1.44	1.65	60.63
CHG-08-441	633967	7111098	17.6	3.22	1.83	2.37	60.63
CHG-08-442	610038	7129963	16	2.16	2.09	2.79	60.64
CHG-08-443	609806	7129935	16.6	2.01	2.22	3.2	60.65
CHG-08-444	634556	7110660	16.8	3.48	1.66	1.7	60.65
CHG-08-445	632777	7135142	18.3	3.24	1.2	3.7	60.66
CHG-08-446	634252	7110957	17.6	3.22	2.08	1.97	60.67
CHG-08-447	633958	7111948	17	3.15	1.99	1.86	60.68
CHG-08-448	610307	7129883	15.6	1.73	2.06	3.3	60.69
CHG-08-449	610086	7130230	15.8	2.15	2.08	2.68	60.69
CHG-08-450	604221	7119505	15.4	2.67	1.99	1.7	60.71
CHG-08-451	610010	7129783	16.2	1.68	2.2	3.52	60.71
CHG-08-452	610040	7129935	16.1	1.77	2.17	3.35	60.72
CHG-08-453	632868	7135143	17.7	2.86	1.23	3.9	60.73
CHG-08-454	634358	7111749	16.4	3.16	1.92	1.57	60.73
CHG-08-455	634748	7111649	17.8	2.98	2.5	1.79	60.82
CHG-08-456	609862	7130184	15.8	2.22	2.1	2.48	60.83
CHG-08-457	634752	7111860	19.4	3.87	2.15	1.77	60.84
CHG-08-458	633976	7110487	17.9	3.25	2.1	1.99	60.85
CHG-08-459	594317.9	7134185.4	14.3	3.07	1.57	0.95	60.87
CHG-08-460	634946	7111505	17.2	3.23	1.92	1.87	60.87
CHG-08-461	630972	7135000	17.3	2.82	1.72	2.92	60.88
CHG-08-462	634849	7110801	18.3	3.87	1.9	1.47	60.89
CHG-08-463	610127	7130104	15.7	1.93	2.2	2.73	60.89
CHG-08-464	580163.05	7115665.4	16	1.68	1.98	3.66	60.90
CHG-08-465	634252	7111999	16.9	3.66	1.53	1.55	60.90
CHG-08-466	595446.45	7084741.3	16.3	1.79	2.28	3.19	60.92

CHG-08-467	610260	7129886	16.2	1.81	2.08	3.4	60.92
CHG-08-468	609988	7129884	15.8	1.75	2.09	3.24	60.94
CHG-08-469	634553	7110611	16.8	3.29	1.78	1.71	60.96
CHG-08-470	610132	7130058	15.5	1.74	2.08	3.08	60.98
CHG-08-471	609910	7129832	16.8	2.06	2.27	3.02	60.98
CHG-08-472	610208	7130237	15.3	1.87	2.02	2.83	60.99
CHG-08-473	609712	7129940	16.8	2.03	2.27	3.06	61.01
CHG-08-474	635350	7111603	19.1	3.69	2.19	1.75	61.01
CHG-08-475	589990.53	7114924.1	16.4	1.82	2.03	3.53	61.04
CHG-08-476	634047	7112003	18.3	3.38	2.04	2.01	61.05
CHG-08-477	632474	7134943	18.5	3.14	0.96	4.17	61.05
CHG-08-478	633977	7110999	17.8	3.25	1.68	2.47	61.07
CHG-08-479	609910	7129890	16.6	2.01	2.19	3.07	61.07
CHG-08-480	634156	7112098	17.9	3.04	2.02	2.36	61.08
CHG-08-481	609892	7129918	16.6	2.02	2.18	3.06	61.09
CHG-08-482	584490.15	7115262.4	15.6	1.7	1.88	3.46	61.11
CHG-08-483	634649	7111808	13.3	1.56	1.11	3.51	61.12
CHG-08-484	634860	7111302	17.6	3.38	1.88	1.78	61.19
CHG-08-485	609862	7130159	16.6	2.33	2.22	2.43	61.21
CHG-08-486	610365	7130336	16	2.06	2.05	2.79	61.21
CHG-08-487	609989	7130207	16.7	2.26	2.19	2.65	61.22
CHG-08-488	609909	7130381	16.7	2.22	2.2	2.7	61.22
CHG-08-489	632276	7134742	17.9	3.08	1.03	3.73	61.23
CHG-08-490	610159	7130334	14.3	1.89	1.82	2.42	61.24
CHG-08-491	610316	7129983	16.2	1.68	2	3.61	61.24
CHG-08-492	610558.99	7124774.9	15	2.15	2.05	2.04	61.25
CHG-08-493	634149	7112009	17.8	3.29	1.94	1.92	61.27
CHG-08-500	634956	7111653	17.5	3.22	1.98	1.8	61.27
CHG-08-501	610257	7130284	14.5	1.56	1.81	3.09	61.29
CHG-08-502	635349	7111457	18.7	4.11	1.54	1.66	61.31
CHG-08-503	610041	7129886	16.4	1.86	2.19	3.11	61.31
CHG-08-504	634548	7111954	17.3	3.29	1.94	1.61	61.31
CHG-08-505	634542	7110708	15.3	3.05	1.52	1.48	61.33
CHG-08-506	609883	7130181	16	2.14	2.06	2.59	61.34
CHG-08-507	609883	7129891	16.8	1.96	2.17	3.19	61.34
CHG-08-508	609885	7129936	17	1.9	2.2	3.36	61.35
CHG-08-509	584758.1	7125056.4	15.8	1.62	2.06	3.34	61.36
CHG-08-510	610139	7130131	16	1.75	2.11	3.16	61.36
CHG-08-511	631972	7134847	16.6	2.2	1.55	3.59	61.40
CHG-08-512	610013	7129840	16.6	1.76	2.19	3.35	61.42
CHG-08-513	634054	7111410	17.5	2.98	2.21	1.79	61.42
CHG-08-514	633959	7111154	17.4	3.08	1.74	2.27	61.44
CHG-08-515	632774	7135394	16.8	2.2	1.82	3.27	61.46
CHG-08-516	632373	7134849	18.7	2.88	1.2	4.16	61.49
CHG-08-517	634044	7111551	16.2	2.89	2	1.48	61.49
CHG-08-518	610267	7129933	17	1.74	2.04	3.81	61.50
CHG-08-519	610366	7129733	15.5	1.63	1.99	3.2	61.50
CHG-08-520	584736.24	7119325.3	16.3	1.63	2.03	3.6	61.51
CHG-08-521	609917	7129931	16.7	1.73	2.16	3.46	61.52
CHG-08-522	631771	7135092	16.3	2.11	1.64	3.38	61.53

CHG-08-550	609862	7129838	17.2	1.93	2.22	3.31	61.55
CHG-08-551	632066	7134853	16.6	2.04	1.56	3.78	61.56
CHG-08-552	609961	7130089	16	1.97	2.06	2.79	61.56
CHG-08-553	609864	7129886	16.4	1.8	2.07	3.29	61.56
CHR-08-001	610132	7130080	15.1	1.89	1.93	2.6	61.57
CHR-08-002	633951	7111202	17.5	3.19	1.79	2.01	61.58
CHR-08-003	634045	7111801	15.3	3.15	1.42	1.37	61.58
CHR-08-004	634942	7111710	17.1	3.26	1.77	1.69	61.58
CHR-08-005	620023.83	7135420.1	14.8	1.75	1.98	2.58	61.58
CHR-08-006	634144	7111362	17.5	3.02	1.89	2.13	61.61
CHR-08-007	610359	7130034	16.6	1.63	2.05	3.7	61.62
CHR-08-008	609865	7129930	16.4	1.62	2.08	3.55	61.63
CHR-08-009	609886	7130040	15.8	1.93	1.99	2.82	61.63
CHR-08-010	634050	7111005	19.4	3.24	2.1	2.52	61.64
CHR-08-011	634748	7111759	19	3.46	2.1	1.92	61.64
CHR-08-012	610207	7130329	15.5	1.97	1.94	2.65	61.65
CHR-08-013	634051	7110658	17.1	2.81	1.55	2.75	61.65
CHR-08-014	609937	7129914	16.2	1.79	2.06	3.17	61.66
CHR-08-015	610310	7129936	16.5	1.69	2	3.6	61.66
CHR-08-016	609964	7130239	17	2.22	2.22	2.66	61.67
CHR-08-017	610056	7129783	16.2	1.64	2.15	3.28	61.67
CHS-08-001	634159	7111219	18.6	3.15	2.16	2.1	61.68
CHS-08-002	634553	7112005	18	3.43	1.84	1.77	61.69
CHS-08-003	609858	7130107	16.8	2.2	2.16	2.66	61.69
CHS-08-004	609937	7130088	16.2	2.26	2.07	2.35	61.69
CHS-08-005	610112	7129840	16.8	1.9	2.23	3.05	61.71
CHS-08-006	610363	7130082	16	1.68	2.02	3.28	61.71
CHS-08-007	610007	7129935	16.3	1.71	2.08	3.31	61.71
CHS-08-008	610259	7130040	16.3	1.65	2	3.53	61.72
CHS-08-009	634249	7111104	16.1	2.77	1.7	1.99	61.72
CHS-08-010	630969	7135199	16.1	2.26	1.54	3.08	61.74
CHS-08-011	610087	7130068	16.6	1.95	2.2	2.88	61.75
CHS-08-012	620234.71	7125111.7	16.7	2.09	2.16	2.76	61.76
CHS-08-013	634451	7111250	14.6	3.19	1.06	1.38	61.77
CHS-08-014	634146	7111462	16.7	2.66	1.89	2.2	61.79
CHS-08-015	609814	7129749	16.2	1.8	2.08	3.07	61.79
CHS-08-016	616187.96	7119397.4	15.3	1.58	2.07	2.94	61.79
CHS-08-017	610307	7129732	15.8	1.56	1.97	3.41	61.80
CHS-08-018	609889	7130138	16.3	2.12	2.01	2.68	61.83
CHS-08-019	632768	7135442	17.2	2.32	1.58	3.51	61.83
CHS-08-020	631767	7135245	18.3	2.78	1.76	3.09	61.84
CHS-08-021	610215	7129943	15.7	1.66	1.87	3.32	61.84
CHS-08-022	590247.41	7159610.6	17	1.66	2.31	3.39	61.85
CHS-08-023	610212	7130132	15.6	1.74	1.91	3.06	61.86
CHS-08-024	631069	7135193	17.6	2.49	1.77	3.15	61.87
CHS-08-025	609937	7129961	16.3	1.76	2.05	3.21	61.87
CHS-08-026	579958.27	7125100.7	17.2	1.91	2.22	3.21	61.87
CHS-08-027	610015	7129917	16.8	1.83	2.07	3.34	61.88
CHS-08-028	596204.78	7079817.7	18.2	2.16	2.67	2.67	61.88
CHS-08-029	610057	7130229	16.7	2.05	2.1	2.85	61.93

CHS-08-030	609962	7129788	16.6	1.69	2.14	3.33	61.95
CHS-08-031	610356	7130237	15.8	1.76	2.01	2.94	61.99
CHS-08-032	610088	7129916	15.6	1.66	1.94	3.1	61.99
CHS-08-033	610013	7130168	16.3	1.97	2.06	2.79	62.00
CHS-08-034	632272	7134843	18.4	3.23	1	3.47	62.01
CHS-08-035	609812	7130184	15.3	1.91	1.85	2.64	62.01
CHS-08-036	579874.67	7119565.5	15.8	1.54	1.8	3.62	62.01
CHS-08-037	633965	7111708	18.6	3.26	1.94	2.1	62.02
CHS-08-038	604884.19	7074313.7	17.9	2.25	2.43	2.65	62.03
CHS-08-039	609910	7130340	15.3	1.81	1.92	2.69	62.04
CHS-08-040	634049	7111510	18.2	2.99	2.08	2.1	62.05
CHS-08-041	610214	7130211	16.1	1.74	1.98	3.16	62.06
CHS-08-042	609910	7129981	15.6	1.61	1.97	3.11	62.07
CHS-08-043	634859	7110859	18.7	3.88	1.79	1.32	62.07
CHS-08-044	609912	7130165	16.5	2.12	2.1	2.56	62.08
CHS-08-045	634749	7111110	17.4	3.22	1.63	1.91	62.13
CHS-08-046	634547	7111905	18.2	3.08	2.1	1.88	62.14
CHS-08-047	610185	7130085	15.5	1.74	1.9	2.91	62.15
CHS-08-048	634458	7110854	16.8	3.43	1.44	1.5	62.16
CHS-08-049	631970	7135398	16.1	1.88	1.61	3.44	62.19
CHS-08-050	610164	7129988	15.5	1.88	1.94	2.6	62.19
CHS-08-051	630867	7135003	15.2	1.87	1.53	3.07	62.19
CHS-08-052	610211	7130158	16.5	1.93	2.08	2.86	62.20
CHS-08-053	610161	7129737	16.4	1.46	2.01	3.69	62.23
CHS-08-054	609962	7129960	16.5	1.69	2.06	3.28	62.24
CHS-08-055	610064	7129834	16.7	1.62	2.02	3.57	62.24
CHS-08-056	634851	7111461	18.2	3.35	1.89	1.7	62.24
CHS-08-057	609886	7129961	17.2	1.84	2.15	3.28	62.24
CHS-08-058	609962	7129887	16.7	1.73	2.1	3.26	62.25
CHS-08-059	610039	7129917	16.2	1.6	1.96	3.4	62.27
CHS-08-060	610059	7129935	16.5	1.59	2.01	3.5	62.30
CHS-08-061	611513	7128617	16.4	2.15	1.98	2.54	62.32
CHS-08-062	633953	7111538	14.3	2.1	1.53	2.13	62.33
CHS-08-063	610083	7130110	14.7	1.47	1.8	3	62.34
CHS-08-064	610060	7130108	15.7	1.68	1.92	3.02	62.35
CHS-08-065	610051	7130375	16.8	2.1	2.07	2.7	62.35
CHS-08-066	634649	7111008	17.3	2.95	1.66	2.17	62.36
CHS-08-067	633955	7112063	17.3	2.85	1.96	1.87	62.39
CHS-08-068	633970	7111046	17.3	2.84	1.56	2.49	62.40
CHS-08-069	633963	7111397	17.5	2.84	2.02	1.9	62.40
CHS-08-070	610309	7129785	16.4	1.51	1.96	3.61	62.41
CHS-08-071	610258	7129728	15.8	1.47	1.9	3.43	62.42
CHS-08-072	632172	7134747	16.7	2.16	1.26	3.74	62.43
CHS-08-073	634747	7110958	19.6	4	1.63	1.69	62.45
CHS-08-074	610159	7129782	16.3	1.5	1.95	3.57	62.45
CHS-08-075	610210	7129987	16.1	1.54	1.89	3.48	62.46
CHS-08-076	632574	7135147	18.6	2.55	1.55	3.67	62.50
CHS-08-077	634460	7110804	15.6	3.15	1.22	1.5	62.50
CHS-08-078	609962	7129915	16.8	1.68	2.02	3.41	62.53
CHS-08-079	632973	7135195	18.1	2.6	1.27	3.72	62.54

CHS-08-080	610258	7130333	15.8	1.86	1.86	2.79	62.55
CHS-08-081	632774	7135095	18.2	2.54	1.16	4.03	62.57
CHS-08-082	630970	7135148	17	2.22	1.68	3.11	62.58
CHS-08-083	610112	7130085	16	1.75	1.96	2.92	62.58
CHS-08-084	610061	7129887	16	1.5	1.97	3.32	62.59
CHS-08-085	610166	7130131	16.5	1.83	2.06	2.89	62.63
CHS-08-086	610363	7129834	17.2	1.6	2.11	3.58	62.65
CHS-08-087	630866	7134849	15.1	1.7	1.44	3.27	62.66
CHS-08-088	610314	7130037	17	1.6	1.96	3.69	62.67
CHS-08-089	633957	7111356	18.8	2.89	2.18	2.17	62.69
CHS-08-090	630864	7135158	17.5	2.15	1.72	3.39	62.71
CHS-08-091	610062	7129908	16.1	1.53	1.93	3.34	62.71
CHS-08-092	634143	7110860	19	3.08	1.98	2.25	62.72
CHS-08-093	609960	7129832	17.3	1.7	2.13	3.4	62.74
CHS-08-094	634450	7110558	18.2	3.57	1.63	1.5	62.77
CHS-08-095	634250	7110807	17	2.76	1.13	2.96	62.77
CHS-08-096	609860	7130035	16.3	1.76	1.93	3.04	62.78
CHS-08-097	632376	7134995	18.6	2.76	1.08	3.91	62.78
CHS-08-098	610071	7130207	16.2	1.59	1.96	3.22	62.79
CHS-08-099	610111	7130037	15.6	1.69	1.86	2.87	62.80
CHS-08-101	610136	7130164	16.2	1.77	1.94	2.94	62.81
CHS-08-102	634750	7111904	19.5	3.76	1.76	1.67	62.82
CHS-08-103	634053	7111055	19.4	3.17	2.02	2.21	62.83
CHS-08-104	631874	7134891	17	2.14	1.3	3.71	62.86
CHS-08-105	644863	7137058	19.2	2.03	1.93	4.13	62.88
CHS-08-106	634049	7110510	18.6	3.59	1.68	1.56	62.88
CHS-08-107	610011	7129959	16.4	1.58	1.92	3.37	62.89
CHS-08-108	610184	7129987	16.7	1.68	1.85	3.47	62.89
CHS-08-109	631471	7135055	16.9	2.17	1.46	3.34	62.91
CHS-08-110	634852	7111403	16	2.95	1.42	1.6	62.91
CHS-08-111	632777	7134993	18.4	2.5	1.05	4.22	62.93
CHS-08-112	610110	7129935	16.9	1.8	2	3.13	62.94
CHS-08-113	610031	7130112	16	1.76	1.89	2.86	62.98
CHS-08-114	609915	7129912	17.2	1.7	2.06	3.34	63.01
CHS-08-115	634452	7111614	16.2	2.77	1.67	1.59	63.02
CHS-08-116	633963	7111454	18.5	3.31	1.66	1.94	63.03
CHS-08-117	632566	7134999	16.1	2.12	1	3.64	63.04
CHS-08-118	610135	7130037	16.6	1.76	1.91	3.13	63.05
CHS-08-119	634045	7111155	18.6	3.16	1.68	2.21	63.05
CHS-08-120	609940	7130066	17.2	1.85	1.92	3.28	63.07
CHS-08-121	630968	7135298	18	2.4	1.67	3.16	63.09
CHS-08-122	610187	7129882	16.7	1.52	1.87	3.63	63.09
CHS-08-123	634454	7110609	16.8	3.16	1.58	1.37	63.09
CHS-08-124	633963	7110657	17.8	2.73	1.62	2.57	63.10
CHS-08-125	610313	7130086	16.9	1.46	1.94	3.73	63.10
CHS-08-126	609986	7130164	15.8	1.66	1.86	2.92	63.10
CHS-08-127	632275	7135239	15.2	1.82	1.06	3.54	63.11
CHS-08-128	610185	7129905	16.3	1.45	1.81	3.61	63.13
CHS-08-129	632779	7135045	18.3	2.48	1.11	4.02	63.13
CHS-08-130	610182	7130235	16.6	1.9	1.95	2.8	63.13

CHS-08-131	609935	7130181	16	1.91	1.89	2.55	63.14
CHS-08-132	632862	7135505	17	2.01	1.66	3.27	63.14
CHS-08-133	609863	7129982	16.6	1.68	1.96	3.15	63.15
CHS-08-134	610008	7129889	16.8	1.53	1.94	3.54	63.15
CHS-08-135	609962	7129741	17.2	1.67	2.08	3.3	63.17
CHS-08-136	609886	7130227	16.7	1.93	1.94	2.8	63.18
CHS-08-137	610186	7130037	17.4	2.08	2.03	2.78	63.20
CHS-08-138	609811	7129888	17	1.58	2	3.45	63.20
CHS-08-139	630976	7135350	16.9	2.22	1.54	3.02	63.20
CHS-08-140	609984	7129910	17.1	1.6	1.96	3.53	63.21
CHS-08-141	634256	7111644	15.8	2.44	1.84	1.6	63.21
CHS-08-142	610044	7130208	17	1.84	2	3	63.24
CHS-08-143	609915	7129964	17.5	1.71	2.07	3.38	63.24
CHS-08-144	610060	7130326	16.3	2.01	1.88	2.52	63.24
CHS-08-145	634849	7111558	16.4	2.82	1.43	1.89	63.26
CHS-08-146	610133	7130185	15.8	1.58	1.79	3.1	63.27
CHS-08-147	610187	7129937	16.5	1.62	1.85	3.3	63.31
CHS-08-148	634854	7111359	16.7	2.99	1.45	1.71	63.32
CHS-08-149	634452	7110509	21.6	4.38	1.44	2.01	63.33
CHS-08-150	610209	7130035	16.9	1.76	1.91	3.18	63.33
CHS-08-151	610038	7130188	15.4	1.63	1.77	2.8	63.36
CHS-08-152	610258	7130085	16.5	1.52	1.73	3.63	63.37
CHS-08-153	633071	7135440	16.6	1.82	1.66	3.28	63.38
CHS-08-154	610187	7129961	16.4	1.56	1.81	3.38	63.39
CHS-08-155	632970	7135439	17.6	2.06	1.67	3.39	63.40
CHS-08-156	609953	7130117	16.5	1.88	1.93	2.71	63.40
CHS-08-157	610011	7130111	16.8	1.95	1.93	2.75	63.40
CHS-08-158	631872	7135245	17.7	2	1.51	3.78	63.41
CHS-08-159	609912	7130186	16.9	1.96	1.99	2.69	63.42
CHS-08-160	609850	7130337	16.5	1.79	1.94	2.83	63.44
CHS-08-161	631875	7134751	17.4	2.01	1.39	3.77	63.45
CHS-08-162	631872	7135347	18.4	2.14	1.66	3.67	63.46
CHS-08-163	609758	7129937	17.1	1.63	1.98	3.34	63.48
CHS-08-164	610038	7130228	16	1.55	1.84	3.09	63.52
CHS-08-165	610365	7129932	17.4	1.48	1.84	3.94	63.54
CHS-08-166	634156	7110614	14.6	3.09	0.88	1.21	63.55
CHS-08-167	610214	7130014	16.5	1.51	1.76	3.53	63.55
CHS-08-168	610305	7130183	17.1	1.76	1.92	3.18	63.57
CHS-08-169	609856	7130210	17.1	1.93	1.98	2.8	63.58
CHS-08-170	633952	7111259	18.8	2.83	1.99	2.17	63.58
CHS-08-171	611543	7130657	15.1	1.64	1.76	2.56	63.58
CHS-08-172	631868	7134846	17.8	1.66	1.7	4.04	63.60
CHS-08-173	630968	7135048	17.9	2.21	1.62	3.29	63.60
CHS-08-174	610118	7130160	16	1.57	1.87	2.98	63.60
CHS-08-175	634054	7111206	18	2.91	1.86	1.8	63.61
CHS-08-176	631262	7134909	17.4	2.02	1.54	3.46	63.62
CHS-08-177	632674	7135246	19.4	2.22	1.61	4.06	63.65
CHS-08-178	585367.49	7160438.5	20.2	2.39	2.46	2.9	63.66
CHS-08-179	610135	7129961	16.5	1.68	1.84	3.08	63.67
CHS-08-180	634252	7111455	18.1	2.57	1.74	2.58	63.67

CHS-08-181	631171	7135498	18.3	2.05	1.66	3.68	63.67
CHS-08-182	632269	7135191	18.4	2.26	1.11	4.21	63.68
CHS-08-183	610210	7129913	16.8	1.44	1.83	3.65	63.69
CHS-08-184	610167	7130010	16.6	1.84	1.78	2.94	63.71
CHS-08-185	609959	7129935	16.7	1.48	1.89	3.43	63.71
CHS-08-186	634249	7111405	18.2	2.71	1.7	2.44	63.71
CHS-08-188	610062	7130183	15.4	1.46	1.73	3.02	63.72
CHS-08-190	609762	7130029	17.1	1.85	1.97	2.88	63.75
CHS-08-191	634549	7111707	17.6	2.76	1.96	1.6	63.83
CHS-08-192	632876	7135297	18.2	2.18	1.4	3.73	63.85
CHS-08-193	610141	7129918	16.5	1.84	1.85	2.72	63.87
CHS-08-194	609937	7129941	18	1.53	2.01	3.77	63.90
CHS-08-195	610260	7130136	16.6	1.44	1.7	3.66	63.90
CHS-08-196	610113	7130330	16.3	1.83	1.81	2.68	63.91
CHS-08-197	632870	7135336	17.8	2.13	1.34	3.66	63.94
CHS-08-198	609881	7130064	16.6	1.71	1.82	3.01	63.94
CHS-08-199	624829.83	7099964	16.7	1.75	2.17	2.46	63.95
CHS-08-200	633955	7112127	16.8	2.86	0.99	2.44	63.95
CHS-08-201	630774	7135051	15.1	1.39	1.32	3.52	63.96
CHS-08-202	580381.75	7170024.4	18.2	2.03	2.08	2.9	63.97
CHS-08-203	609982	7130110	16.8	1.81	1.9	2.81	63.98
CHS-08-204	610108	7130182	15.5	1.46	1.69	3.04	63.98
CHS-08-205	632175	7135486	17.3	1.83	1.52	3.61	63.99
CHS-08-206	621402.87	7099688.6	16.6	1.49	1.87	3.27	64.03
CHS-08-207	632975	7135145	18.2	2.4	1.07	3.78	64.05
CHS-08-208	635054	7111161	18.7	3.55	1.66	1.21	64.05
CHS-08-209	610210	7129962	16.8	1.5	1.81	3.44	64.05
CHS-08-210	631169	7135546	17.5	2.25	1.56	2.92	64.06
CHS-08-211	630870	7134905	15.5	1.45	1.43	3.42	64.07
CHS-08-212	610214	7129885	16.8	1.42	1.74	3.67	64.08
CHS-08-213	630968	7134896	17.9	2.19	1.46	3.37	64.09
CHS-08-214	610062	7130134	15.4	1.47	1.7	2.92	64.09
CHS-08-215	634748	7111407	18.2	2.98	1.74	1.77	64.09
CHS-08-216	632969	7135488	17.3	1.93	1.6	3.27	64.12
CHS-08-217	633960	7111304	18.2	2.61	1.97	2.03	64.12
CHS-08-218	610135	7129936	17	1.62	1.85	3.25	64.13
CHS-08-219	610036	7130136	16	1.58	1.77	2.92	64.14
CHS-08-220	634651	7111663	18.2	2.8	1.82	1.93	64.14
CHS-08-221	609911	7130036	16.4	1.69	1.77	2.94	64.15
CHS-08-222	631673	7134760	14.6	1.54	1.21	3.11	64.16
CHS-08-223	609966	7130131	16.7	1.75	1.88	2.82	64.16
CHS-08-224	633959	7110706	18.7	2.9	1.8	2.04	64.17
CHS-08-225	631378	7134797	16.2	1.64	1.38	3.5	64.18
CHS-08-226	630973	7134743	15.2	1.44	1.3	3.44	64.19
CHS-08-227	634052	7110606	18.1	2.84	1.77	1.86	64.21
CHS-08-228	632573	7135193	18.2	1.89	1.51	3.9	64.22
CHS-08-229	610087	7130084	16.8	1.65	1.9	2.98	64.24
CHS-08-230	609808	7130232	17.2	2.06	1.91	2.48	64.25
CHS-08-231	610361	7130188	17.1	1.47	1.87	3.48	64.25
CHS-08-232	632672	7135441	18	1.86	1.59	3.71	64.25

CHS-08-233	631771	7135048	16.6	1.82	1.4	3.34	64.27
CHS-08-234	610161	7130212	39.2	3.62	4.2	7.66	64.28
CHS-08-235	632671	7135339	19.3	2.2	1.52	3.9	64.29
CHS-08-236	634653	7111106	18.6	3.01	1.69	1.92	64.29
CHS-08-237	634166	7111258	19.2	2.92	1.95	1.98	64.30
CHS-08-238	610158	7130107	17.6	1.87	1.99	2.86	64.30
CHS-08-239	634349	7110706	15.3	2.41	1.49	1.53	64.31
CHS-08-240	634142	7110762	18.4	2.92	1.32	2.52	64.32
CHS-08-241	610011	7129730	17.3	1.52	1.95	3.35	64.32
CHS-08-242	615776.15	7125057.7	16.9	1.53	2.03	3	64.34
CHS-08-243	634551	7110761	19.3	3.65	1.4	1.62	64.35
CHS-08-244	634655	7111168	17.8	3.04	1.39	1.89	64.35
CHS-08-245	632672	7135298	18.7	2.1	1.48	3.78	64.38
CHS-08-246	633953	7111789	17.2	3.18	1.36	1.38	64.39
CHS-08-247	632677	7135193	19.4	2.03	1.58	4.1	64.39
CHS-08-248	634852	7111604	16.8	2.67	1.66	1.57	64.41
CHS-08-249	634751	7111504	17.4	2.94	1.44	1.75	64.42
CHS-08-250	632473	7134845	18.7	2.33	1.06	4	64.46
CHS-08-251	633070	7135243	17.3	1.85	1.28	3.75	64.48
CHS-08-252	631167	7134947	18	1.99	1.5	3.52	64.53
CHS-08-253	609816	7130073	15.9	1.5	1.68	3	64.53
CHS-08-254	610161	7129961	16.9	1.58	1.79	3.2	64.55
CHS-08-255	634457	7110761	16.2	3.21	0.99	1.32	64.56
CHS-08-256	609936	7129892	17.3	1.5	1.91	3.35	64.56
CHS-08-257	632675	7134996	18.7	2.16	1.06	4.24	64.57
CHS-08-258	631467	7134997	17.4	1.92	1.35	3.54	64.58
CHS-08-259	609860	7130063	18.5	1.87	2.03	3.14	64.60
CHS-08-260	632071	7134753	19	2.15	1.12	4.3	64.61
CHS-08-261	634052	7110953	19.1	3.06	1.64	2.03	64.62
CHS-08-262	631671	7135051	18	2.06	1.41	3.5	64.62
CHS-08-263	633955	7111743	18.1	2.85	1.58	1.96	64.64
CHS-08-264	634352	7110760	14	2.32	1.21	1.34	64.64
CHS-08-265	610314	7130289	17.8	1.81	1.93	3.02	64.65
CHS-08-266	634248	7110764	15.8	2.64	1.26	1.62	64.68
CHS-08-267	634751	7111256	17.4	2.79	1.52	1.77	64.71
CHS-08-268	610062	7130085	16.6	1.56	1.83	2.96	64.71
CHS-08-269	610161	7130058	15.5	1.32	1.75	2.93	64.72
CHS-08-270	610191	7130162	17.3	1.73	1.86	2.98	64.72
CHS-08-271	634150	7111061	16.6	2.19	1.47	2.44	64.74
CHS-08-272	610115	7130018	16.2	1.5	1.75	2.97	64.75
CHS-08-273	590573.95	7154926.9	21.1	2.26	2.86	2.47	64.75
CHS-08-274	634144	7110960	16.4	2.16	1.49	2.35	64.77
CHS-08-275	630872	7134816	15.1	1.63	1.24	2.96	64.79
CHS-08-276	625292	7105023	16.4	2.09	1.91	1.82	64.79
CHS-08-277	632371	7134946	19.7	2.04	1.42	4.3	64.80
CHS-08-278	609934	7129984	17.3	1.6	1.87	3.15	64.81
CHS-08-279	610038	7130088	16	1.68	1.75	2.54	64.82
CHS-08-280	610158	7130279	17.4	1.9	1.81	2.78	64.83
CHS-08-281	634749	7111357	18	2.88	1.69	1.61	64.84
CHS-08-282	634553	7110809	19.6	3.18	1.71	1.87	64.86

CHS-08-283	609986	7129935	17.3	1.41	1.86	3.46	64.87
CHS-08-284	632375	7135044	19.2	1.92	1.48	4.13	64.87
CHS-08-285	632072	7135494	17.7	1.73	1.59	3.52	64.90
CHS-08-286	610160	7130035	16.8	1.54	1.78	3.1	64.91
CHS-08-287	610190	7130203	16.2	1.49	1.69	3.02	64.91
CHS-08-288	609910	7130135	15.6	1.58	1.51	2.84	64.92
CHS-08-289	635260.84	7111251.2	20	3.18	1.97	1.65	64.92
CHS-08-301	610092	7130016	15.9	1.51	1.69	2.83	64.93
CHS-08-302	632476	7135092	18.6	1.83	1.51	3.91	64.94
CHS-08-303	634251	7111255	18.6	2.62	1.85	2.06	64.95
CHS-08-304	634055	7111308	18.4	2.63	1.72	2.14	64.95
CHS-08-305	610108	7130061	17.2	1.54	1.84	3.19	64.95
CHS-08-306	610086	7129885	17.1	1.49	1.8	3.28	64.97
CHS-08-307	634147	7111310	18.6	2.78	1.74	1.95	64.97
CHS-08-308	610213	7130114	17.3	1.56	1.78	3.28	65.00
CHS-08-309	632475	7135144	18.8	1.76	1.6	3.96	65.01
CHS-08-310	634142	7111012	20.1	2.94	1.95	2.09	65.02
CHS-08-311	632272	7135044	19.8	2.04	1.47	4.17	65.04
CHS-08-312	632272	7134948	19.4	1.88	1.37	4.39	65.05
CHS-08-313	634252	7111202	18.1	2.82	1.64	1.75	65.06
CHS-08-314	608548	7131596	16	1.46	1.78	2.76	65.12
CHS-08-315	610091	7130161	16.3	1.63	1.74	2.68	65.13
CHS-08-316	610473	7131628	15	1.24	1.59	2.92	65.13
CHS-08-317	610015	7130010	17	1.67	1.75	2.94	65.14
CHS-08-318	631972	7135349	16.9	1.68	1.42	3.37	65.15
CHS-08-319	632874	7135235	18.2	1.92	1.28	3.82	65.16
CHS-08-320	632378	7135098	19.5	1.93	1.52	4.08	65.16
CHS-08-321	632565	7134953	18.3	2.05	0.94	4.16	65.18
CHS-08-322	634553	7112106	19.5	2.73	1.7	2.45	65.19
CHS-08-323	632373	7135145	20.6	2.13	1.43	4.39	65.24
CHS-08-324	634552	7111452	17.1	2.72	1.38	1.75	65.24
CHS-08-325	631872	7135296	18.5	1.68	1.45	4.07	65.27
CHS-08-326	631673	7135099	16.9	1.57	1.27	3.74	65.27
CHS-08-327	610263	7130183	15.7	1.36	1.55	3.07	65.29
CHS-08-328	610085	7129936	16.4	1.44	1.68	3.08	65.30
CHS-08-329	632273	7134998	19	1.75	1.45	4.18	65.31
CHS-08-330	634053	7110911	19.4	2.86	1.61	2.26	65.33
CHS-08-331	634651	7111053	17.3	2.61	1.34	2.06	65.33
CHS-08-332	634454	7111567	18.3	2.63	1.8	1.8	65.38
CHS-08-333	632866	7135398	19	2.14	1.42	3.53	65.41
CHS-08-334	610186	7130111	16.9	1.56	1.74	2.99	65.41
CHS-08-335	610213	7130086	16.9	1.7	1.69	2.83	65.42
CHS-08-336	610013	7129983	16.5	1.5	1.69	2.97	65.42
CHS-08-337	634253	7111154	18.8	2.83	1.66	1.9	65.43
CHS-08-338	355951	7142556	17.2	1.48	1.34	3.87	65.44
CHS-08-339	631472	7134800	16.3	1.37	1.32	3.64	65.46
CHS-08-340	634651	7111509	17	2.6	1.48	1.67	65.46
CHS-08-341	610085	7130037	17.3	1.67	1.84	2.83	65.46
CHS-08-342	634353	7111457	17.8	2.67	1.28	2.24	65.48
CHS-08-343	632470	7134751	16.8	1.38	1.22	4.01	65.48

CHS-08-344	634552	7111306	18.4	2.64	1.84	1.73	65.48
CHS-08-345	632770	7135338	18.3	1.9	1.44	3.53	65.49
CHS-08-346	631171	7134899	17.1	1.7	1.32	3.46	65.50
CHS-08-347	634657	7111556	17.6	2.64	1.52	1.82	65.50
CHS-08-348	631268	7135004	18.6	2.22	1.42	3.16	65.51
CHS-08-349	633170	7135453	17.8	1.83	1.44	3.39	65.52
CHS-08-350	610138	7129986	16.6	1.44	1.64	3.15	65.55
CHS-08-351	610054	7130157	16.5	1.5	1.73	2.86	65.56
CHS-08-352	632669	7135491	19.3	1.83	1.56	3.92	65.56
CHS-08-353	632071	7134902	19	1.6	1.52	4.22	65.57
CHS-08-354	610310	7130241	16.8	1.43	1.65	3.24	65.57
CHS-08-355	634353	7111364	17.9	2.69	1.13	2.43	65.62
CHS-08-356	634358	7111555	18.7	2.97	1.23	2.19	65.63
CHS-08-357	634644	7110904	19.4	2.62	1.3	3.01	65.63
CHS-08-358	634457	7111462	16.5	2.52	1.17	1.97	65.63
CHS-08-359	609960	7129985	16.6	1.34	1.69	3.21	65.64
CHS-08-360	631972	7134902	16.6	1.5	1.28	3.56	65.65
CHS-08-361	634351	7111055	18.3	2.74	1.66	1.7	65.70
CHS-08-362	631570	7135047	18.8	1.96	1.36	3.7	65.72
CHS-08-363	634053	7111106	19.3	2.8	1.63	2.1	65.77
CHS-08-364	634251	7111362	18.2	2.55	1.52	2.15	65.79
CHS-08-365	632769	7135245	18.7	1.79	1.33	3.95	65.80
CHS-08-366	610007	7130230	17.2	1.52	1.8	2.96	65.83
CHS-08-367	634257	7111498	18.5	2.42	1.76	2.13	65.83
CHS-08-368	634556	7111108	17.8	2.69	1.49	1.74	65.86
CHS-08-369	632773	7135490	19.2	1.84	1.42	3.92	65.92
CHS-08-370	634344	7111407	18.7	2.48	1.3	2.78	65.94
CHS-08-371	632971	7135251	18.2	1.86	1.35	3.5	65.96
CHS-08-400	631971	7134999	18.3	1.56	1.31	4.11	65.97
CHS-08-401	631875	7135192	18.1	1.48	1.36	4.04	66.06
CHS-08-402	632474	7135186	18.6	1.65	1.38	3.96	66.06
CHS-08-403	631071	7134944	17.4	1.53	1.4	3.56	66.06
CHS-08-404	610165	7129936	17.2	1.41	1.52	3.48	66.07
CHS-08-405	634745	7111307	17.7	2.74	1.41	1.65	66.08
CHS-08-406	631169	7135302	17.1	1.67	1.28	3.35	66.10
CHS-08-407	610259	7130235	17.3	1.41	1.66	3.3	66.11
CHS-08-408	632580	7134858	19	1.91	0.86	4.48	66.12
CHS-08-409	610057	7130034	16.8	1.5	1.64	2.94	66.12
CHS-08-410	634446	7111505	15.7	2.17	1.35	1.73	66.14
CHS-08-411	631270	7135393	17.1	1.43	1.36	3.62	66.14
CHS-08-412	634554	7111559	18	2.62	1.56	1.74	66.14
CHS-08-413	632271	7135508	18.5	1.91	1.52	3.22	66.17
CHS-08-414	634149	7110708	17.1	2.47	1.32	1.92	66.17
CHS-08-415	631170	7134997	17.4	1.89	1.27	3.11	66.18
CHS-08-416	634051	7110853	19.1	2.59	1.76	1.99	66.18
CHS-08-417	609987	7129988	16.8	1.36	1.6	3.21	66.20
CHS-08-418	609876	7130111	17.7	1.62	1.71	3.03	66.20
CHS-08-419	630774	7135393	18.5	1.77	1.52	3.44	66.21
CHS-08-420	609908	7130063	17	1.44	1.66	3.07	66.22
CHS-08-421	632781	7135296	18.7	1.93	1.32	3.56	66.23

CHS-08-422	610160	7129837	16.7	1.13	1.4	3.84	66.23
CHS-08-423	631262	7135108	17.8	1.58	1.28	3.77	66.27
CHS-08-424	632071	7135004	18.6	1.53	1.37	4.09	66.28
CHS-08-425	610037	7130164	17	1.42	1.67	3.06	66.30
CHS-08-426	631573	7134998	17.7	1.76	1.24	3.47	66.30
CHS-08-427	634253	7110518	16.3	2.24	1	2.36	66.33
CHS-08-428	631078	7135249	18.2	1.77	1.4	3.43	66.34
CHS-08-429	634751	7111455	16.9	2.34	1.5	1.71	66.34
CHS-08-430	641032	7139661	18.1	1.37	1.34	4.14	66.36
CHS-08-431	610109	7129963	16.9	1.41	1.55	3.19	66.36
CHS-08-432	632871	7135042	18.5	1.7	1.04	4.22	66.38
CHS-08-433	631770	7134794	18	1.86	1.13	3.58	66.38
CHS-08-434	632171	7135097	17.5	1.37	1.39	3.77	66.39
CHS-08-435	609904	7130113	17.6	1.46	1.64	3.28	66.41
CHS-08-436	632670	7135392	19.4	1.62	1.33	4.32	66.42
CHS-08-437	634135	7110814	19.2	2.6	1.48	2.34	66.45
CHS-08-438	630866	7135059	17.1	1.56	1.47	3.12	66.45
CHS-08-439	632562	7135248	18.4	1.46	1.4	4	66.46
CHS-08-440	634558	7110909	17.8	2.6	1.19	2.12	66.47
CHS-08-441	632564	7135450	16.9	1.31	1.31	3.68	66.48
CHS-08-442	632864	7135431	17.3	1.4	1.35	3.64	66.52
CHS-08-443	634649	7111306	16.3	2.32	1.46	1.46	66.53
CHS-08-445	632267	7135441	18.4	1.62	1.36	3.76	66.54
CHS-08-446	633957	7110761	21.5	3	1.92	2.02	66.56
CHS-08-447	609435	7131557	16.1	1.18	1.63	3.01	66.57
CHS-08-448	634653	7111455	17.4	2.48	1.41	1.75	66.61
CHS-08-449	630975	7134802	16.8	1.58	1.34	3.09	66.61
CHS-08-450	634348	7110603	17.7	2.67	1.4	1.58	66.62
CHS-08-452	609990	7130013	17.7	1.46	1.63	3.26	66.63
CHS-08-453	631374	7134751	16.3	1.25	1.25	3.54	66.64
CHS-08-454	631069	7134893	17	1.4	1.27	3.58	66.64
CHS-08-455	611584	7131569	16.7	1.34	1.62	3.01	66.64
CHS-08-456	630872	7135107	17.1	1.4	1.32	3.55	66.64
CHS-08-457	634548	7111161	18	2.43	1.55	1.87	66.69
CHS-08-458	631174	7134850	17.5	1.47	1.29	3.64	66.70
CHS-08-459	631971	7134749	19.1	1.75	1.17	4.08	66.73
CHS-08-460	634252	7111057	17.4	2.15	1.35	2.34	66.76
CHS-08-461	630971	7134849	16.2	1.38	1.25	3.23	66.77
CHS-08-462	634347	7111309	16	2.92	0.76	1.29	66.79
CHS-08-463	609958	7130039	17.7	1.4	1.53	3.45	66.80
CHS-08-464	632470	7135291	18.8	1.49	1.31	4.11	66.87
CHS-08-465	634752	7111714	20.2	3.12	1.43	1.82	66.90
CHS-08-466	632376	7134793	19.6	1.88	0.98	4.31	66.90
CHS-08-467	632170	7134898	17.6	1.48	1.46	3.33	66.93
CHS-08-468	632073	7134947	19	1.44	1.42	4.08	66.97
CHS-08-469	609940	7130010	16.9	1.38	1.46	3.16	66.98
CHS-08-470	633167	7134948	18.4	1.24	1.29	4.33	67.00
CHS-08-471	630775	7134799	13.3	1.03	1.09	2.66	67.02
CHS-08-472	610141	7130008	17.2	1.53	1.61	2.8	67.03
CHS-08-473	609962	7130010	16.7	1.28	1.44	3.25	67.03

CHS-08-474	632563	7135302	19	1.36	1.45	4.14	67.04
CHS-08-475	634044	7111248	18.8	2.54	1.47	2.03	67.06
CHS-08-476	632374	7134744	19.4	1.46	1.57	3.96	67.07
CHS-08-477	634546	7111009	18.6	2.77	1.18	1.98	67.10
CHS-08-478	632374	7135198	20.5	1.65	1.43	4.34	67.10
CHS-08-479	630772	7135302	17.6	1.38	1.43	3.48	67.10
CHS-08-480	631874	7135140	19	1.49	1.42	3.94	67.11
CHS-08-481	632558	7134808	19.2	1.54	1.45	3.9	67.12
CHS-08-482	631768	7134853	17.8	1.51	1.21	3.68	67.12
CHS-08-483	634250	7110857	18.4	2.72	0.88	2.42	67.12
CHS-08-484	632872	7135092	18.6	1.43	0.95	4.57	67.12
CHS-08-485	632472	7135237	18.7	1.31	1.27	4.32	67.15
CHS-08-486	634054	7111655	19.2	2.42	1.54	2.27	67.15
CHS-08-487	634052	7110806	19.5	2.48	1.64	2.14	67.19
CHS-08-488	580013.78	7145210.5	19.8	2.51	2.04	1.6	67.23
CHS-08-489	634647	7111218	14.8	2.24	1.12	1.2	67.23
CHS-08-490	634450	7111414	18	2.32	1.48	1.95	67.26
CHS-08-491	630860	7135252	16.3	1.21	1.26	3.38	67.27
CHS-08-492	630774	7135200	16.6	1.23	1.26	3.48	67.27
CHS-08-493	634349	7111109	18	2.46	1.54	1.61	67.29
CHS-08-494	634554	7111508	17	2.43	1.31	1.56	67.29
CHS-08-495	634248	7110904	18.3	2.36	1.33	2.23	67.30
CHS-08-496	634589.71	7130430	19.5	1.17	1.86	3.95	67.33
CHS-08-497	631079	7135139	16.7	1.31	1.23	3.41	67.35
CHS-08-498	630974	7135400	18.3	1.47	1.33	3.7	67.36
CHS-08-499	631770	7135146	18.2	1.56	1.24	3.64	67.37
CHS-08-500	632072	7135441	18.5	1.5	1.32	3.75	67.38
CHS-08-501	609888	7130008	17.3	1.46	1.6	2.85	67.39
CHS-08-502	632971	7135346	18.6	1.58	1.41	3.51	67.41
CHS-08-503	634340	7111510	19.1	2.33	1.26	2.7	67.42
CHS-08-504	634646	7111706	18.4	2.41	1.37	2.08	67.43
CHS-08-505	631772	7135300	17.9	1.32	1.32	3.76	67.44
CHS-08-506	634554	7111602	17.8	2.54	1.27	1.74	67.45
CHS-08-507	632171	7134949	19.6	1.54	1.52	3.84	67.45
CHS-08-508	634345	7111211	20.4	3.34	0.81	2.25	67.46
CHS-08-509	631171	7135599	17.7	1.43	1.33	3.46	67.47
CHS-08-510	634650	7111758	20.3	3.27	0.95	2.1	67.48
CHS-08-511	631262	7134855	18.2	1.29	1.33	3.91	67.49
CHS-08-512	632671	7134939	18.8	1.46	1.06	4.3	67.50
CHS-08-513	633069	7135295	18.5	1.52	1.18	3.88	67.51
CHS-08-514	634345	7110955	18.1	2.49	1.33	1.83	67.55
CHS-08-515	635254.2	7111551.8	20.2	3.12	1.51	1.43	67.55
CHS-08-516	631170	7135197	18.2	1.47	1.19	3.8	67.55
CHS-08-517	631077	7134995	17.6	1.37	1.17	3.72	67.58
CHS-08-518	631464	7135196	15	0.8	0.98	3.81	67.60
CHS-08-519	630770	7135249	17.2	1.28	1.3	3.49	67.60
CHS-08-520	634453	7111358	17.8	2.67	1.23	1.52	67.62
CHS-08-521	631770	7134746	18.7	1.66	1.16	3.72	67.62
CHS-08-522	631170	7135446	18.6	1.45	1.39	3.67	67.65
CHS-08-523	634153	7111109	19.8	2.87	1.27	1.99	67.67

CHS-08-524	634649	7111407	18.2	2.42	1.48	1.72	67.67
CHS-08-525	632271	7135092	19.8	1.29	1.37	4.49	67.67
CHS-08-526	610161	7129884	17.1	1.04	1.25	3.9	67.67
CHS-08-527	609990	7130056	16.9	1.29	1.42	3.12	67.71
CHS-08-528	632970	7135393	18.7	1.51	1.34	3.66	67.73
CHS-08-529	634450	7111304	18.9	2.84	1.19	1.74	67.73
CHS-08-530	634448	7110913	18.5	3.05	0.98	1.53	67.73
CHS-08-531	631569	7134849	17.1	1.1	1.16	3.9	67.78
CHS-08-532	609882	7130087	17.7	1.37	1.59	3.05	67.80
CHS-08-533	631770	7134999	17.8	1.42	1.14	3.69	67.81
CHS-08-534	631264	7135252	17.8	1.18	1.24	3.94	67.81
CHS-08-535	634146	7110504	16.4	2.23	1.24	1.56	67.82
CHS-08-536	631279	7134755	18.9	1.34	1.45	3.83	67.82
CHS-08-537	632674	7135046	18.8	1.46	0.96	4.32	67.85
CHS-08-538	631374	7134898	17.8	1.44	1.16	3.61	67.85
CHS-08-539	632172	7135442	18.4	1.34	1.25	3.9	67.86
CHS-08-540	630869	7135346	17.9	1.26	1.29	3.75	67.87
CHS-08-541	633071	7134898	18.5	1.11	1.2	4.4	67.88
CHS-08-543	632777	7134946	18.8	1.41	0.95	4.4	67.90
CHS-08-544	632973	7135096	18.3	1.41	0.9	4.24	67.94
CHS-08-545	632371	7135343	19.1	1.34	1.42	3.91	67.96
CHS-08-546	631962	7135493	18.7	1.3	1.34	3.92	67.97
CHS-08-547	631168	7135098	17.4	1.31	1.12	3.67	67.98
CHS-08-548	634551	7111406	17	2.27	1.28	1.64	67.98
CHS-08-549	634751	7111204	17.2	2.36	1.29	1.56	67.98
CHS-08-550	634657	7111359	17.5	2.45	1.25	1.6	67.98
CHS-08-551	610158	7130232	18.4	1.45	1.61	3.12	67.99
CHS-08-552	631074	7134847	18.5	1.4	1.22	3.84	67.99
CHS-08-553	632567	7135491	19	1.6	1.27	3.64	68.01
CHS-08-554	631064	7135407	16.9	0.88	1.18	4.07	68.02
CHS-08-555	631270	7134953	19.4	1.62	1.29	3.74	68.03
CHS-08-556	632072	7134799	20	1.59	1.17	4.23	68.04
CHS-08-557	631471	7135391	16	1.18	1.19	3.15	68.05
CHS-08-558	631875	7134948	18.9	1.5	1.13	3.96	68.05
CHS-08-559	633956	7111503	16.5	1.79	1.25	2.24	68.08
CHS-08-560	631473	7134847	19.2	1.26	1.3	4.22	68.09
CHS-08-561	631972	7134797	19.8	1.5	1.25	4.15	68.10
CHS-08-562	631574	7134796	18.2	1.48	1.15	3.62	68.16
CHS-08-563	634050	7110709	19.3	2.14	1.21	2.88	68.20
CHS-08-564	634547	7110959	18.3	2.33	1.25	2.06	68.23
CHS-08-565	631470	7134953	17.8	1.45	1.14	3.49	68.23
CHS-08-566	631375	7134943	18.9	1.48	1.2	3.82	68.23
CHS-08-567	632567	7135393	18.3	1.14	1.25	4.04	68.28
CHS-08-568	630882	7134762	16.4	1.08	1.16	3.46	68.28
CHS-08-569	632370	7135490	18.8	1.19	1.3	4.08	68.32
CHS-08-570	632167	7134805	19.4	1.42	1.08	4.28	68.33
CHS-08-571	634359	7111154	18	2.35	1.18	1.94	68.40
CHS-08-572	631973	7135297	18.5	1.25	1.23	3.92	68.42
CHS-08-574	579688.95	7139874.9	20.1	1.32	1.77	3.66	68.43
CHS-08-575	631768	7134899	17.5	1.07	1.12	3.95	68.46

CHS-08-576	610036	7130037	16.8	1.28	1.61	2.55	68.47
CHS-08-577	632165	7134852	20.7	1.38	1.37	4.4	68.48
CHS-08-578	634359	7110860	18	2.37	1.33	1.65	68.48
CHS-08-579	634451	7111155	15.8	2.09	0.99	1.7	68.49
CHS-08-580	632372	7135298	19.7	1.2	1.34	4.32	68.49
CHS-08-583	631169	7135049	17.9	1.39	1.08	3.63	68.50
CHS-08-584	632973	7134797	18	1	1.11	4.28	68.50
CHS-08-585	609935	7130105	17.2	1.33	1.37	2.99	68.50
CHS-08-586	630775	7135352	19	1.52	1.34	3.48	68.51
CHS-08-587	633167	7135345	19.1	1.44	1.18	3.9	68.51
CHS-08-588	634047	7110558	19	2.29	1.16	2.46	68.51
CHS-08-589	631470	7134749	18.4	1.32	1.12	3.89	68.52
CHS-08-590	631076	7136200	17.7	1.28	1.24	3.47	68.54
CHS-08-591	632974	7134843	19.3	0.99	1.22	4.66	68.56
CHS-08-592	632674	7134895	19.2	1.41	0.91	4.38	68.57
CHS-08-593	631972	7134948	19.5	1.5	1.15	3.98	68.60
CHS-08-594	610034	7129985	16.4	1.21	1.34	2.86	68.62
CHS-08-595	631473	7134900	18.6	1.22	1.2	3.98	68.63
CHS-08-596	631171	7136098	16.3	0.86	1.36	3.37	68.64
CHS-08-597	632169	7135197	19.3	1.21	1.16	4.35	68.64
CHS-08-598	610113	7129914	17.5	1.48	1.47	2.66	68.66
CHS-08-599	630872	7135546	18.3	1.2	1.29	3.74	68.66
CHS-08-601	634346	7110908	17	2.17	1.33	1.5	68.67
CHS-08-602	633146	7135396	14.9	0.91	0.95	3.3	68.70
CHS-08-603	632471	7135488	19.2	1.2	1.29	4.1	68.71
CHS-08-604	631473	7135495	17.6	0.85	1.47	3.74	68.72
CHS-08-605	634551	7111636	18.4	2.37	1.31	1.75	68.76
CHS-08-606	632069	7135051	19.4	1.11	1.33	4.25	68.78
CHS-08-607	634051	7110756	20.5	2.39	1.56	2.21	68.78
CHS-08-608	630865	7135205	17.8	1.23	1.27	3.46	68.80
CHS-08-609	631372	7135099	18.6	1.4	1.11	3.75	68.81
CHS-08-610	610088	7129961	18.1	1.28	1.41	3.28	68.83
CHS-08-611	632073	7135094	19.1	1.05	1.25	4.32	68.85
CHS-08-612	631875	7134798	20.2	1.58	1.15	4.04	68.85
CHS-08-613	630855.11	7129017.9	20.1	1.36	2.08	2.95	68.86
CHS-08-614	629839.03	7100155.1	19.8	1.13	2.13	3.13	68.88
CHS-08-615	632369	7135444	19.6	1.14	1.28	4.32	68.88
CHS-08-616	631768	7134944	17.8	1.16	1.02	3.92	68.91
CHS-08-617	632171	7135045	19.6	1.15	1.36	4.17	68.91
CHS-08-618	632370	7135393	19.5	1.2	1.35	4.05	68.94
CHS-08-619	630773	7135150	17.8	1.12	1.2	3.7	68.95
CHS-08-620	631971	7135251	19.4	1.2	1.19	4.24	68.97
CHS-08-621	631078	7135092	18.4	1.2	1.31	3.63	69.00
CHS-08-622	610135	7129885	17.3	1.25	1.44	2.89	69.01
CHS-08-623	632974	7135299	18.8	1.34	1.12	3.84	69.03
CHS-08-624	634459	7111014	14.9	1.82	0.81	1.88	69.06
CHS-08-625	631572	7135338	18.4	1.16	1.11	3.98	69.06
CHS-08-626	632073	7135198	18.6	0.96	1.14	4.35	69.07
CHS-08-627	633161	7135071	18.5	0.86	1.15	4.45	69.10
CHS-08-628	631169	7135145	18.3	1.12	1.22	3.81	69.14

CHS-08-629	631365	7135444	17.8	0.95	1.49	3.47	69.17
CHS-08-630	633155	7135003	18.8	0.85	1.18	4.52	69.17
CHS-08-631	634347	7110655	18.2	2.43	0.98	1.91	69.21
CHS-08-632	630768	7135553	16.9	1	1.12	3.56	69.22
CHS-08-633	605903.48	7094457	18.9	1.61	2.07	1.9	69.26
CHS-08-634	631670	7134952	17.8	1.07	1.1	3.83	69.26
CHS-08-635	634548	7111062	19	2.56	1.02	1.94	69.26
CHS-08-636	634553	7111255	18.3	2.13	1.38	1.82	69.28
CHS-08-637	633064	7135485	20.1	1.54	1.39	3.51	69.34
CHS-08-638	631672	7134799	18.7	1.26	1.06	3.91	69.34
CHS-08-639	610214	7130055	17.6	1.12	1.26	3.38	69.38
CHS-08-640	631870	7135093	18.5	1.07	1.12	4.01	69.47
CHS-08-641	631079	7134797	18.4	1.22	1.3	3.44	69.49
CHS-08-642	632468	7135432	18.8	1.1	1.17	3.99	69.52
CHS-08-643	634343	7111014	18.7	2.24	1.33	1.79	69.52
CHS-08-644	632470	7135329	19.4	1.17	1.23	4.02	69.53
CHS-08-645	632468	7135384	18.7	1.12	1.15	3.94	69.53
CHS-08-646	631170	7134796	19.4	1.2	1.34	3.8	69.54
CHS-08-647	632374	7135245	20.6	0.95	1.26	4.82	69.55
CHS-08-648	631666	7135005	19.1	1.28	1.14	3.84	69.56
CHS-08-649	634248	7110659	17.3	2.39	1.24	1.09	69.57
CHS-08-650	633072	7135047	18.4	0.79	1.01	4.57	69.58
CHS-08-651	632172	7134996	19.7	1.15	1.36	3.95	69.60
CHS-08-652	633162	7134804	18.8	0.86	1.16	4.37	69.62
CHS-08-653	632268	7135387	18.1	0.95	1.05	4.1	69.64
CHS-08-654	634659	7111257	17.7	2.22	1.25	1.5	69.64
CHS-08-655	610163	7129911	17.7	1.08	1.22	3.46	69.64
CHS-08-656	632571	7135343	19.3	1.02	1.2	4.23	69.66
CHS-08-657	631666	7134905	17.6	0.99	1	3.9	69.66
CHS-08-658	630971	7135798	17.3	0.73	1.23	3.86	69.68
CHS-08-659	630774	7135452	18.8	1.18	1.28	3.63	69.68
CHS-08-660	631873	7135049	18.7	1.03	1.05	4.19	69.68
CHS-08-661	610081	7129982	17.5	1.13	1.35	3.08	69.70
CHS-08-662	631364	7135488	18.4	1.21	1.44	3.17	69.70
CHS-08-663	630767	7136194	19	1.01	1.49	3.67	69.70
CHS-08-664	633196	7134903	19.2	0.86	1.09	4.61	69.70
CHS-08-665	632071	7135343	18	0.94	1.07	4.02	69.71
CHS-08-666	610009	7130039	17.3	1.45	1.3	2.53	69.72
CHS-08-667	633069	7134797	19.7	0.97	1.21	4.43	69.74
CHS-08-668	634145	7110565	17	2.23	1.15	1.32	69.74
CHS-08-669	632973	7134899	18.8	0.75	1.05	4.66	69.80
CHS-08-670	630972	7136093	16.3	0.72	1.08	3.66	69.81
CHS-08-671	631279	7134805	18.7	1.07	1.21	3.83	69.82
CHS-08-672	633072	7134996	19	0.84	1.12	4.47	69.83
CHS-08-673	609936	7130036	17.8	1.16	1.28	3.21	69.83
CHS-08-674	630772	7135493	19.6	1.35	1.22	3.7	69.83
CHS-08-675	631870	7134994	18.9	0.94	1.01	4.42	69.86
CHS-08-676	633069	7135341	19.5	1.23	1.11	4.02	69.86
CHS-08-677	631374	7135048	19.2	1.31	1.04	3.86	69.89
CHS-08-678	631872	7135392	18.6	0.93	1.14	4.09	69.94

CHS-08-679	633167	7134745	19.2	0.78	1.14	4.58	69.94
CHS-08-680	631172	7136000	17.2	0.8	1.24	3.6	69.94
CHS-08-681	634152	7111161	19.3	2.32	1.39	1.64	69.98
CHS-08-682	631975	7135097	18.7	0.97	1.03	4.21	70.00
CHS-08-683	632075	7135391	18.8	1.08	1.14	3.89	70.02
CHS-08-684	624808.1	7129944.6	19.4	0.88	1.45	3.99	70.03
CHS-08-685	631072	7135301	18.6	1.04	1.25	3.7	70.05
CHS-08-686	631573	7134951	19.3	1.35	1.08	3.71	70.06
CHS-08-687	632174	7135145	20	1.03	1.15	4.41	70.08
CHS-08-688	631972	7135200	19.2	1.1	1.11	4.03	70.10
CHS-08-689	630871	7135495	18.6	0.98	1.29	3.71	70.14
CHS-08-690	631571	7134899	18.2	1.08	1.01	3.81	70.14
CHS-08-700	630970	7135544	17.3	0.79	1.18	3.67	70.18
CHS-08-701	632779	7134744	19.3	0.87	1.06	4.5	70.19
CHS-08-702	632873	7134785	19	0.82	0.94	4.64	70.21
CHS-08-703	634553	7111356	17.6	2.12	1.29	1.37	70.23
CHS-08-704	634246	7110559	15.2	2.12	0.87	1.05	70.30
CHS-08-705	631062	7135652	16.7	0.66	0.96	3.95	70.30
CHS-08-706	610186	7130017	18.3	1.09	1.23	3.44	70.31
CHS-08-707	634457	7110659	12.7	1.4	0.87	1.28	70.31
CHS-08-708	631175	7136048	17.7	0.85	1.26	3.56	70.32
CHS-08-709	630971	7135249	19.2	1.12	1.13	3.88	70.34
CHS-08-710	631977	7135453	18.7	0.89	1.15	4.04	70.35
CHS-08-711	633072	7134944	19.1	0.74	0.99	4.69	70.35
CHS-08-712	632072	7135251	18.7	0.84	1.02	4.32	70.35
CHS-08-713	633071	7135092	19.6	0.85	1.12	4.5	70.35
CHS-08-714	631871	7135486	18.3	0.84	1.1	4.04	70.36
CHS-08-715	634450	7111108	19.3	2.43	1.11	1.74	70.37
CHS-08-716	632067	7135295	18.2	0.78	0.95	4.32	70.39
CHS-08-717	631061	7136143	17.6	0.82	1.14	3.73	70.39
CHS-08-718	632876	7134738	19.1	0.73	0.89	4.84	70.40
CHS-08-719	610059	7129985	17.7	1.3	1.42	2.53	70.41
CHS-08-720	630775	7134898	18.3	1.17	1.1	3.46	70.43
CHS-08-721	630875	7136148	18.6	0.9	1.41	3.55	70.46
CHS-08-722	631469	7135151	18	0.88	0.9	4.12	70.48
CHS-08-723	634453	7111204	18.1	1.76	1.18	2.25	70.49
CHS-08-724	632174	7135239	19.9	0.95	1.13	4.38	70.50
CHS-08-725	631074	7134745	19.1	1.04	1.27	3.7	70.52
CHS-08-726	632172	7135300	19.3	0.87	1.02	4.44	70.53
CHS-08-727	632975	7134746	19.6	0.87	1.06	4.49	70.54
CHS-08-728	632275	7135148	20.7	0.91	1.11	4.77	70.54
CHS-08-729	632276	7135343	19.8	1.05	1.14	4.14	70.55
CHS-08-730	632073	7135154	19.6	0.84	1.04	4.55	70.60
CHS-08-731	632973	7135045	18.6	0.94	0.89	4.22	70.61
CHS-08-732	632973	7134945	19.3	0.77	0.98	4.61	70.69
CHS-08-733	631771	7135392	18.2	0.82	0.93	4.18	70.69
CHS-08-734	631670	7135253	18.7	0.77	1.02	4.31	70.72
CHS-08-735	632171	7135401	18.7	0.97	0.97	4.04	70.75
CHS-08-736	631463	7135298	16.5	0.97	1	3.15	70.76
CHS-08-737	630977	7135750	17.8	0.65	1.1	4.03	70.77

CHS-08-738	633069	7134739	19.8	0.8	1.16	4.45	70.77
CHS-08-739	630769	7134745	17.7	0.89	1.02	3.71	70.77
CHS-08-740	631071	7136001	17	0.72	1.17	3.5	70.77
CHS-08-741	631171	7135245	19.1	1.03	1.11	3.87	70.77
CHS-08-742	634165	7110665	18.4	2.37	1.11	1.35	70.78
CHS-08-743	610039	7130066	17.8	1.15	1.34	2.82	70.78
CHS-08-744	631468	7135251	16.3	0.9	1	3.17	70.83
CHS-08-745	633160	7135257	19.3	1.02	0.96	4.17	70.83
CHS-08-746	610037	7130037	16.9	1.03	1.26	2.78	70.85
CHS-08-747	631570	7135446	18	0.8	1.11	3.81	70.85
CHS-08-748	634459	7110703	14.9	1.95	0.7	1.32	70.86
CHS-08-749	631668	7135153	18.7	0.84	1.02	4.13	70.90
CHS-08-750	631772	7135493	18.4	0.87	1	3.99	70.92
CHS-08-751	631064	7135803	17.9	0.67	1.12	3.95	70.93
CHS-08-753	633068	7135394	19.2	0.72	0.98	4.57	70.93
CHS-08-754	630971	7135849	17.7	0.71	1.17	3.73	70.93
CHS-08-755	632172	7135344	19.2	0.88	0.98	4.3	70.94
CHS-08-756	609912	7130016	18	0.97	1.19	3.36	70.98
CHS-08-757	631371	7135147	16.8	1.02	0.94	3.2	70.99
CHS-08-758	631572	7135096	18.9	1.06	0.98	3.86	71.01
CHS-08-759	610037	7130011	17.8	1.17	1.31	2.75	71.03
CHS-08-760	630872	7135451	19.3	0.9	1.26	3.84	71.05
CHS-08-761	630973	7136143	18.1	0.76	1.17	3.76	71.05
CHS-08-762	631076	7135952	17.6	0.75	1.22	3.51	71.05
CHS-08-763	630871	7135901	15.7	0.57	0.95	3.5	71.08
CHS-08-764	631579	7134743	19.3	1.12	1.06	3.76	71.09
CHS-08-765	609989	7130038	17.4	1.04	1.21	2.95	71.09
CHS-08-766	631472	7135342	16.3	0.99	0.94	3.03	71.10
CHS-08-767	631975	7135152	19.4	0.91	1.04	4.16	71.14
CHS-08-768	631669	7135205	20.2	0.74	1.09	4.66	71.17
CHS-08-769	630871	7136098	17.2	0.69	1.05	3.68	71.18
CHS-08-770	631772	7135444	18.6	0.69	0.95	4.35	71.19
CHS-08-771	630973	7135647	18.6	0.7	1.09	4.12	71.19
CHS-08-772	630972	7135600	17.9	0.69	1.07	3.9	71.21
CHS-08-773	631265	7135058	18.1	0.81	0.94	3.97	71.21
CHS-08-774	634245	7110613	18.3	2.2	1.12	1.42	71.26
CHS-08-775	630873	7135599	19.3	0.77	1.16	4.12	71.30
CHS-08-776	631470	7135443	19	1.11	1.13	3.48	71.31
CHS-08-777	631772	7135340	19.1	0.85	1.04	4.09	71.31
CHS-08-778	630871	7136194	18.7	0.88	1.34	3.43	71.33
CHS-08-779	631074	7136050	16.1	0.61	0.97	3.48	71.33
CHS-08-780	631573	7135391	17.5	0.7	0.86	4.01	71.35
CHS-08-781	631071	7135856	17.1	0.64	1.06	3.65	71.37
CHS-08-782	633067	7134850	20.1	0.9	1.05	4.34	71.37
CHS-08-783	630780	7135797	17.6	0.62	0.9	4.11	71.38
CHS-08-784	630772	7134954	17.9	0.99	1.02	3.41	71.40
CHS-08-785	631374	7134998	19.1	1.07	0.94	3.83	71.43
CHS-08-786	631380	7134850	19.1	1.06	0.95	3.83	71.44
CHS-08-787	630975	7135946	15.8	0.56	0.93	3.48	71.44
CHS-08-788	633160	7135492	18.7	0.94	1.01	3.79	71.45

CHS-08-789	631576	7135147	18.7	0.77	0.96	4.15	71.45
CHS-08-800	609863	7130091	17.8	0.97	1.13	3.21	71.49
CHS-08-801	632675	7134846	20.4	0.98	0.89	4.5	71.54
CHS-08-802	630873	7135851	16.5	0.67	1.03	3.37	71.55
CHS-08-803	631667	7135484	19.5	0.8	1.14	4.08	71.57
CHS-08-804	630774	7136097	15.8	0.58	0.83	3.56	71.58
CHS-08-805	599750.35	7080164.8	20	1.67	1.81	1.78	71.58
CHS-08-806	634354	7110561	18.6	2.19	1.06	1.53	71.59
CHS-08-807	632774	7134791	19.4	0.69	0.88	4.61	71.61
CHS-08-808	630771	7135847	16.6	0.54	0.87	3.85	71.61
CHS-08-809	631174	7136148	18.8	0.78	1.22	3.7	71.67
CHS-08-810	633167	7135200	18.7	0.69	0.93	4.25	71.69
CHS-08-811	610089	7129876	17	0.84	1.28	2.84	71.71
CHS-08-812	631073	7136103	17.4	0.67	0.99	3.71	71.72
CHS-08-813	631375	7135342	19.3	0.97	0.95	3.95	71.74
CHS-08-814	630968	7136047	17.5	0.63	0.98	3.82	71.74
CHS-08-815	632672	7134745	20.8	0.78	1.05	4.64	71.80
CHS-08-816	631075	7135348	18.4	0.86	1.07	3.6	71.82
CHS-08-817	632774	7134847	20.8	0.82	1.01	4.61	71.87
CHS-08-818	632878	7134836	20	0.67	0.89	4.75	71.88
CHS-08-819	631270	7135439	17.7	0.58	0.87	4.1	71.88
CHS-08-820	631072	7135752	18.7	0.6	0.92	4.35	71.89
CHS-08-821	634553	7111806	20	1.96	1.37	1.84	71.92
CHS-08-822	631068	7135504	17.5	0.55	0.86	4.08	71.92
CHS-08-823	631170	7136199	18.3	0.76	1.13	3.57	72.03
CHS-08-824	631376	7135193	18.7	0.75	0.9	4.07	72.06
CHS-08-825	630875	7135651	19.4	0.6	0.98	4.45	72.07
CHS-08-826	633071	7135191	19.5	0.84	0.76	4.4	72.11
CHS-08-827	633172	7135143	18.7	0.57	0.88	4.38	72.13
CHS-08-828	631173	7135949	17.7	0.66	1.09	3.52	72.23
CHS-08-829	631070	7135700	18.3	0.54	0.81	4.36	72.24
CHS-08-830	634448	7110947	19.3	2.08	1.12	1.64	72.29
CHS-08-831	631368	7135396	19	0.72	0.97	4.04	72.30
CHS-08-832	631971	7135045	19.3	0.63	0.86	4.46	72.32
CHS-08-833	630971	7135999	16.6	0.56	0.86	3.61	72.36
CHS-08-834	630771	7135002	19.3	1.1	1.04	3.37	72.40
CHS-08-835	631067	7135451	18.4	0.57	0.87	4.19	72.43
CHS-08-836	631372	7135250	18.2	0.8	0.85	3.76	72.44
CHS-08-837	631269	7135156	18.7	0.66	0.78	4.27	72.47
CHS-08-838	631869	7135440	18.7	0.67	0.88	4.08	72.53
CHS-08-839	610062	7129961	17.2	0.95	1.06	2.81	72.53
CHS-08-840	610109	7129884	19.3	1.1	1.36	2.83	72.55
CHS-08-841	631067	7135908	16.8	0.64	0.99	3.29	72.56
CHS-08-842	632280	7135299	17.8	0.73	0.85	3.7	72.56
CHS-08-843	630973	7135495	18	0.66	0.96	3.72	72.56
CHS-08-844	631171	7135897	17.3	0.64	1.06	3.35	72.59
CHS-08-845	631172	7135850	17.8	0.7	0.95	3.59	72.59
CHS-08-846	631575	7135495	18.6	0.67	0.93	3.92	72.68
CHS-08-847	632678	7134795	20.7	0.77	0.89	4.54	72.69
CHS-08-848	631373	7135303	18.9	0.86	0.74	3.99	72.69

CHS-08-849	631172	7135652	18.3	0.61	0.88	3.98	72.72
CHS-08-850	630863	7135301	19.7	0.98	1.02	3.62	72.75
CHS-08-851	630874	7135800	17.7	0.65	0.97	3.55	72.78
CHS-08-852	632572	7134749	20.2	0.72	0.84	4.49	72.79
CHS-08-853	632973	7134994	19.7	0.7	0.85	4.33	72.81
CHS-08-854	630775	7136151	19.1	0.7	1.17	3.62	72.86
CHS-08-855	631273	7135196	18.7	0.62	0.75	4.18	73.09
CHS-08-856	631173	7135748	17.6	0.56	0.78	3.84	73.16
CHS-08-857	630973	7135699	19.4	0.6	0.93	4.13	73.23
CHS-08-858	631669	7135303	18.5	0.52	0.78	4.16	73.32
CHS-08-859	630969	7135894	18.1	0.59	1.02	3.52	73.40
CHS-08-860	630771	7136045	15.6	0.5	0.79	3.18	73.41
CHS-08-861	634247	7110709	18.5	1.95	1.06	1.24	73.61
CHS-08-862	634357	7110809	18.5	2.08	0.83	1.37	73.62
CHS-08-863	631057.38	7134367.1	18.6	1.05	0.77	3.22	73.63
CHS-08-864	630778	7135590	18.6	0.57	0.76	4.02	73.70
CHS-08-865	632877	7134998	20.5	0.62	0.58	4.83	73.72
CHS-08-866	632875	7134890	20.4	0.58	0.75	4.6	73.73
CHS-08-867	631172	7135802	19.3	0.59	0.94	3.92	73.77
CHS-08-868	632876	7134947	20.2	0.64	0.67	4.51	73.86
CHS-08-869	631070	7135550	18.7	0.5	0.8	4.03	73.95
CHS-08-870	630872	7135702	17.2	0.42	0.67	3.86	74.00
CHS-08-871	631572	7135245	18.8	0.51	0.7	4.18	74.01
CHS-08-872	631671	7135438	19.4	0.42	0.73	4.48	74.01
CHS-08-873	630771	7135703	18.8	0.52	0.7	4.14	74.08
CHS-08-874	630872	7136001	18.4	0.46	0.79	3.97	74.09
CHS-08-875	630777	7135938	18.7	0.47	0.77	4.08	74.10
CHS-08-876	631675	7135389	19.1	0.51	0.78	4.11	74.15
CHS-08-900	630873	7135750	17.7	0.43	0.68	3.86	74.44
CHS-08-901	630772	7135653	18.8	0.46	0.66	4.14	74.59
CHS-08-902	630872	7136050	17.5	0.48	0.71	3.62	74.60
CHS-08-903	631570	7135195	19.7	0.51	0.68	4.28	74.68
CHS-08-904	633162	7135312	21	0.76	0.81	3.99	74.91
CHS-08-905	630874	7135398	21.6	0.79	0.99	3.84	74.94
CHS-08-906	593452.4	7149579.4	18.7	0.6	0.74	3.61	75.05
CHS-08-907	630770	7135097	19	0.68	0.81	3.46	75.06
CHS-08-908	630772	7136000	18.2	0.42	0.67	3.82	75.20
CHS-08-909	632776	7134895	21.1	0.61	0.64	4.38	75.35
CHS-08-910	630777	7135748	19.2	0.4	0.61	4.19	75.39
CHS-08-911	631671	7135344	19.4	0.38	0.61	4.28	75.41
CHS-08-989	631170	7135698	18.2	0.37	0.62	3.89	75.51
CHW-08-494	630976	7136199	21.1	0.48	0.78	4.21	75.86
CHW-08-495	630970	7135445	18.8	0.45	0.65	3.77	75.90
CHW-08-496	631575	7135297	18.9	0.36	0.51	4.15	75.95
CHW-08-497	630779	7135896	18.6	0.3	0.61	3.85	76.49
CHW-08-498	630871	7135942	20.3	0.32	0.66	4.09	76.91
CHW-08-499	631075	7135597	18.2	0.15	0.32	3.62	79.41

Appendix F: Publications from the thesis work

Johnson, C.L., Ross, M., Grunsky, E., and Hodder, T.J. Fingerprinting Glacial Processes for Diamond Exploration on Baffin Island. Poster presentation. Presented at Yellowknife Geoforum 2012. Yellowknife, Northwest Territories. 13-15 November

Johnson, C. L. and Ross, M. 2012. Glacial landscape evolution on Hall Peninsula, Baffin Island, since the Last Glacial Maximum: insights into switching glacial dynamics and thermo-mechanical conditions. Abstract EP53D-1071. Presented at 2012 Fall Meeting, AGU. San Francisco, California., 3-7 December

Johnson, C.L., Ross, M., Hodder, T., Tremblay, T., Gosse, J., 2013. Evidence of shifting subglacial dynamics and thermomechanical conditions from the Quaternary record of north central, Hall Peninsula, Baffin Island. Abstract in section CCIS 1-140. Presented at 2013 CANQUA meeting. Edmonton, Alberta. 18-22 August.

Johnson, C.L., Ross, M. and Tremblay, T. 2013. Glacial geomorphology of north-central Hall Peninsula, Southern Baffin Island. Geological Survey of Canada, Open File 7413.

Tremblay, T., Leblanc-Dumas, J., Allard, M., Ross, M. and Johnson, C., in press: Surficial geology of central Hall Peninsula, Baffin Island, Nunavut: summary of the 2013 field season; *in* Summary of Activities 2013, Canada-Nunavut Geoscience Office.